Phytochemical Studies of *Mimusops elengi* and *Pometia pinnata* Leaf Extracts

with Anti-HIV-1 Integrase Activity

Areerat   Suedee

A Thesis Submitted in Fulfillment of the Requirements for the Degree of

Doctor of Philosophy in Pharmaceutical Sciences

Prince of Songkla University

2012

Thesis Title   Phytochemical Studies of *Mimusops elengi* and *Pometia pinnata* Leaf Extracts with Anti-HIV-1 Integrase Activity

Author   Miss Areerat Suedee

Major Program   Pharmaceutical Sciences

Major Advisor: **Examinig Committee:**

……………………………………........… …………………………………......Chairperson

(Assoc. Prof. Dr. Pharkphoom Panichayupakaranant) (Assoc. Prof. Dr. Sunibhond Pummangura)

Co-Advisor: ..………………………………....……….…..…

(Assoc. Prof. Dr. Supinya Tewtrakul)

………………………………………....... ..………………………………....……….…..…

(Assoc. Prof. Dr. Supinya Tewtrakul)   (Asst. Prof. Dr. Chatchai Wattanapiromsakul)

..………………………………....………....

(Assoc. Prof. Dr. Pharkphoom Panichayupakaranant)

The Graduated School, Prince of Songkla University, has approved this thesis as fulfillment of the requirements for the Doctor of Philosophy Degree in Pharmaceutical Sciences

………………………………………

(Prof. Dr. Amornrat Phongdara)

Dean of Graduated School

This is to certify that the work here submitted is the result of the candidate's own investigations. Due acknowledgement has been made of any assistance received.

_____ Signature

(Assoc. Prof. Dr. Pharkphoom Panichayupakaranant)

Major Advisor

_____ Signature

(Miss Areerat Suedee)

Candidate

I hereby certify that this work has not already been accepted in substance for any degree, and is not being concurrently submitted in candidature for any degree.

_____ Signature

(Miss Areerat Suedee)

Candidate

ชื่อวิทยานิพนธ์   การศึกษาพฤกษเคมีของสารสกัดจากใบพิกุลและใบแดงน้ำที่มีฤทธิ์ยับยั้ง HIV-1
                     integrase

ผู้เขียน   นางสาว อารีรัตน์ ซื่อดี

สาขาวิชา   เภสัชศาสตร์

ปีการศึกษา   2555

บทคัดย่อ

        การทดสอบฤทธิ์ยับยั้งเอนไซม์ HIV-1 integrase ของสารสกัดหยาบด้วยเอทานอลจาก
สมุนไพรไทย 16 ชนิด ได้แก่ มะเฟือง , กะหล่ำปลี, ตำลึง, ผักกูด, ชะมวง, โป๊ยกั๊ก, ปีบ, พิกุล, ยอป่า,
มะรุม, แก้ว, ใบเตย, แดงน้ำ, ผักหวานบ้าน, ย่านาง และ ถั่วฝักยาว โดยใช้วิธี multiplate integration
assay (MIA) พบว่าสารสกัดจากใบแดงน้ำและสารสกัดจากใบพิกุลมีฤทธิ์ยับยั้งเอนไซม์ HIV-1
integrase ได้ดีที่สุดโดยให้ค่า IC_{50} เท่ากับ 8.8 และ 62.1 μg/mL ตามลำดับ การแยกสารสำคัญจากใบ
พิกุลโดยวิธี bioassay-guided isolation ได้สารสำคัญเป็นสารผสมระหว่าง gallocatechin กับ
epigallocatechin ซึ่งสารนี้มีฤทธิ์ยับยั้งเอนไซม์ HIV-1 integrase โดยมีค่า IC_{50} เท่ากับ 35.0 μM
นอกจากนี้ยังแยกได้สาร mearnsitrin ซึ่งเป็นสารในกลุ่ม flavonol glycoside แต่พบว่า mearnsitrin
ไม่มีฤทธิ์ยับยั้งเอนไซม์ HIV-1 integrase ที่ความเข้มข้น 100 μM

        การแยกสารสำคัญที่มีฤทธิ์ยับยั้งเอนไซม์ HIV-1 integrase โดยวิธี bioassay-guided
isolation จากสารสกัดใบแดงน้ำ สามารถแยกสารสำคัญซึ่งมีฤทธิ์ยับยั้งเอนไซม์ HIV-1 integrase ได้
หนึ่งสาร proanthocyanidin A2 โดยมีค่า IC_{50} เท่ากับ 30.1 μM นอกจากนั้นยังสามารถแยกสารอื่นๆ
ได้อีก ได้แก่ สารในกลุ่ม flavonoids คือ epicatechin, kaempferol-3-*O*-rhamnoside, และ quercetin-
3-*O*-rhamnoside, สารในกลุ่ม glycolipid คือ 1-*O*-palmitoyl-3-*O*-[α-D-galactopyranosyl-(1→6)-β-
D-galactopyranosyl]-*sn*-glycerol, สารในกลุ่ม steroidal glycoside คือ stigmasterol-3-*O*-glucoside
และสารในกลุ่ม pentacyclic triterpenoid saponin คือ 3-*O*-α-L-arabinofuranosy(1→3)-α-L-
rhamnopyranosyl(1→2)]-α-L-arabino-pyranosyl hederagenin   และ 3- *O*-(5-*O*-acetyl-α-L-
arabinofuranosyl-(1→3)-α-L-rhamnopyranosyl (1→2)]-α-L-arabinopyranosyl hederagenin ซึ่ง
สารดังกล่าวนี้ไม่มีฤทธิ์ยับยั้งเอนไซม์ HIV-1 integrase ที่ความเข้มข้น 100 μM

        สารสำคัญ epigallocatechin และ proanthocyanidin A2 ที่แยกได้สามารถนำมาใช้เป็นสาร
มาตรฐานในการพัฒนาวิธีการวิเคราะห์ปริมาณสารสำคัญด้วยเทคนิค HPLC เพื่อการควบคุมคุณภาพ
ของสารสกัดจากใบพิกุลและใบแดงน้ำตามลำดับ โดยใช้ระบบ   reversed-phase HPLC ในการ

วิเคราะห์ปริมาณสาร epigallocatechin จากสารสกัดใบพิกุล และวิเคราะห์ปริมาณส าร proantho-cyanidin A2 จากสารสกัดใบแดงน้ำ สำหรับสาร epigallocatechin วิเคราะห์โดยใช้คอลัมน์ชนิด Phenominex® Luna 5u Hilic (ขนาดอนุภาค 5 µm, ความกว้าง 4.6 □ ยาว 150mm) และใช้เฟส เคลื่อนที่เป็นน้ำบริสุทธิ์ อัตราการไหลของ เฟสเคลื่อนที่เท่ากับ 1.0 mL/min และตรวจวัดสัญญาณที่ ความยาวคลื่น 210 nm การประเมินความถูกต้องของวิธีการวิเคราะห์ (method validation) ประกอบด้วยการประเมิน linearity, repeatability, reproducibility, accuracy, specificity และ sensitivity พบว่าค่า % recovery ของการวิเคราะห์สาร epigallocatechin อยู่ในช่วง 99-103% กราฟ มาตรฐานของสารมาตรฐานมี linearity ที่ดี โดยมีค่า r^2 มากกว่าหรือเท่ากับ 0.9998 ระบบดังกล่าวมี ความเที่ยงตรงสูง (% RSD ทั้ง repeatability และ reproducibility น้อยกว่า 5%) และมีค่า limit of detection (LOD) และ limit of quantification (LOQ) เท่ากับ 0.10 และ 0.25 µg/mL ตามลำดับ จาก การศึกษาวิธีการสกัดสารพบว่าการสกัดด้วยไมโครเวฟเป็นวิธีการที่ดีที่สุดในการสกัดสาร epigallo-catechin จากใบพิกุล โดยวิธีการนี้สามารถเพิ่มปริมาณสาร epigallocatechin ในสารสกัดจากใบพิกุล ได้สูงถึง 5.15 %w/w

การวิเคราะห์ปริมาณสาร proanthocyanidin A2 ในสารสกัดใบแดงน้ำ วิเคราะห์โดยใช้ คอลัมน์ชนิด Phenominex® Luna 5u Hilic และใช้เฟสเคลื่อนที่เป็น 2% กรดอะซิติกในน้ำ กับ อะซิ โตรไนไตรล์ (โดย ใช้ระบบการชะสารดังนี้ ที่ช่วงเวลา 0-4 นาที อัตราส่วนเป็น 5:95 , ช่วงเวลา 5-9 นาที อัตราส่วนเป็น 10:90 , ช่วงเวลา 10-14 นาที อัตราส่วนเป็น 20:80 และช่วงเวลา 15-20 นาที อัตราส่วนเป็น 0:100 โดยปริมาตร) อัตราการไหลของ เฟสเคลื่อนที่เท่ากับ 1.0 mL/min และตรวจวัด สัญญาณที่ความยาวคลื่น 280 nm การประเมินความถูกต้องของวิธีการวิเคราะห์ด้วยวิธีการประเมิน linearity, repeatability, reproducibility, accuracy, specificity และ sensitivity พบว่าค่า % recovery ของการวิเคราะห์สาร proanthocyanidin A2 อยู่ในช่วง 96-98% กราฟมาตรฐานของสาร มาตรฐานมี linearity ที่ดี โดยมีค่า r^2 มากกว่าหรือเท่ากับ 0.9999 ระบบดังกล่าวมีความเที่ยงตรงสูง (% RSD ทั้ง repeatability และ reproducibility น้อยกว่า 5%) และมีค่า LOD และ LOQ เท่ากับ 1.25 และ 2.50 µg/mL ตามลำดับ การศึกษาวิธีการสกัดสารพบว่า การสกัดสารด้วยไมโครเวฟเป็นวิธีการที่ดีที่สุดใน การสกัดสาร proanthocyanidin A2 จากใบแดงน้ำโดยวิธีการนี้สามารถเพิ่มปริมาณสาร proantho-cyanidin A2 ในสารสกัดจากใบแดงน้ำได้สูงถึง 36.58 %w/w

Thesis Title Phytochemical Studies of *Mimusops elengi* and *Pometia pinnata* Leaf Extracts with Anti‑HIV‑1 Integrase Activity

Author Miss Areerat Suedee

Major Program Pharmaceutical Sciences

Academic Year 2012

ABSTRACT

Ethanol extracts of sixteen Thai medicinal plants, including *Averrhoa carambola, Brassica oleracea, Coccinia grandis, Diplazium esculentum, Garcinia cowa, Illicium verum, Millingtonia hortensis, Mimusops elengi, Morinda coreia, Moringa oleifera, Murraya paniculata, Pandanus amaryllifolius, Pometia pinnata, Sauropus androgynus, Tiliacora triandra* and *Vigna unguiculata* were investigated for their inhibitory effect against human immunodeficiency virus type 1 integrase (HIV‑1 IN) inhibitory activity using the multiplate integration assay (MIA). The result revealed that leaf extracts from *P. pinnata* and *M. elengi* had the strongest anti‑HIV‑1 IN activity with IC_{50} values of 8.8 and 62.1 µg/mL, respectively. A bioassay‑guided isolation of the active compounds from *M. elengi* leaf extract resulted in the isolation of active compounds, identified as a mixture of gallocatechin and epigallocatechin. This mixture of gallocatechin and epigallocatechin showed satisfactory anti‑HIV‑1 IN activity with an IC_{50} value of 35.0 µM. A flavanol glycoside, mearnsitrin was also isolated but was inactive at a concentration of 100 µM.

An anti‑HIV‑1 IN assay‑guided isolation of the active compounds from a leaf extract of *P. pinnata* resulted in the isolation of one active compound, identified as proanthocyanidin A2. This compound showed satisfactory anti‑HIV‑1 IN activity with an IC_{50} value of 30.1 µM. Three flavonoids, epicatechin, kaempferol‑3‑*O*‑rhamnoside, quercetin‑3‑*O*‑rhamnoside; a glycolipid, 1‑*O*‑palmitoyl‑3‑*O*‑[α‑D‑galactopyranosyl‑(1$\longrightarrow$6)‑β‑D‑galactopyranosyl]‑*sn*‑glycerol; a steroidal glycoside; stigmasterol‑3‑*O*‑glucoside; and a pentacyclic triterpenoid saponin, 3‑*O*‑α‑L‑arabinofuranosyl‑(1$\longrightarrow$3)‑α‑L‑rhamnopyranosyl‑(1$\longrightarrow$2)]‑α‑L‑arabinopyranosyl hederagenin and 3‑*O*‑(5‑*O*‑acetyl‑α‑L‑arabinofuranosyl‑(1$\longrightarrow$3)‑α‑L‑rhamnopyranosyl(1$\longrightarrow$2)]‑α‑L‑arabinopyra‑nosyl hederagenin were also isolated but were inactive at a concentration of 100 µM.

The obtained active compounds, epigallocatechin and proanthocyanidin A2 were used as standard markers for development of validated quantitative HPLC analytical methods for quality control of *M. elengi* and *P. pinnata* leaf extracts, respectively. A reversed-phase HPLC method was described for quantitative analysis of epigallocatechin in *M. elengi*, and proanthocyanidin A2 in *P. pinnata* leaf extracts. For epigallocatechin, the method utilized a Phenominex® Luna 5u Hilic column (5 μm, 4.6 × 150 mm) with 100% milli-Q water as the mobile phase at a flow rate of 1.0 mL/min, and UV detection at 210 nm. The parameters of linearity, precision, accuracy, specificity and sensitivity of the method were evaluated. The recovery of the method was 99-103% with good linearity ($r^2 \geq 0.9998$) for epigallocatechin. A high degree of specific as well as repeatability and reproducibility (RSD values less than 5%) were also achieved. The limits of detection and quantification were 0.10 and 0.25 μg/mL, respectively. Microwave-assisted extraction (MAE) was selected as the best extraction method for epigallocatechin. The optimized MAE method was capable of increasing epigallocatechin in the dried leaf extract up to 5.15 %w/w.

The method for determination of proanthocyanidin A2 in *P. pinnata* leaf extracts utilized a Phenominex® Luna 5u Hilic column with the mixture of 2% acetic acid and acetonitrile (gradient elution as follows: 0-4 min, 5:95; 5-9 min, 10:90; 10-14 min, 20:80; 15-20 min, 0:100 v/v) as mobile phase at a flow rate of 1 mL/min and UV detection at 280 nm. The parameters of linearity, precision, accuracy, specificity and sensitivity of the method were evaluated. The recovery of the method was 96-98% with good linearity ($r^2 \geq 0.9999$) for proanthocyanidin A2. A high degree of specific as well as repeatability and reproducibility (RSD values less than 5%) were also achieved. The limits of detection and quantification were 1.25 and 2.50 μg/mL, respectively. Microwave-assisted extraction (MAE) was selected as the best extraction method for proanthocyanidin A2. The optimized MAE method was capable of increasing proanthocyanidin A2 in the dried leaf extract up to 36.58 %w/w.

CONTENTS

CONTENTS (continued)

CONTENTS (continued)

CONTENTS (continued)

LIST OF TABLES

LIST OF TABLES (continued)

LIST OF TABLES (continued)

LIST OF FIGURES

LIST OF FIGURES (continued)

LIST OF FIGURES (continued)

LIST OF FIGURES (continued)

LIST OF SCHEMES

CHAPTER 1

INTRODUCTION

1.1 Rational and background for investigation

Acquired immunodeficiency syndrome (AIDS) is a disease of the human immune system caused by the human immunodeficiency virus (HIV), which causes profound immune suppression. It is a serious life threatening health problem, and one of the most quickly spreading diseases known to man. HIV is now a leading cause of death, worldwide. HIV-1 is the cause of the worldwide epidemic and is most commonly referred to as HIV. A very high proportion of men and women infected with HIV virus are in their active reproductive ages and around half of the people who acquire HIV become infected before they turn 25. A greater concern is the possibility of infected mothers transferring the disease to their babies (Singh *et al.*, 2005). Symptoms that may indicate HIV infection are of the following: rapid weight loss and loss of appetite, dry or productive cough, recurring fever or profuse night sweats, profound and unexplained fatigue, swollen lymph glands (armpits, groin, or neck), diarrhea at least for more than a week, white spots or unusual blemishes on the tongue, in the mouth, or in the throat, shortness of breath and red, brown, pink, or purplish blotches on or under the skin or inside the mouth, nose, or eyelids, memory loss, depression, and other neurological disorders, or a condition that is characterized by low $CD4^+$ cells (below 200 cells/mL or below 14% of total lymphocytes). This growing health epidemic has focused the energies of many research organizations on identifying new HIV molecular targets and their inhibitors.

The main steps in the viral entry process are attachment of the viral gp120 to the CD4 T cell receptor, binding of the gp120 to CCR5 or CXCR4 co-receptors and fusion of the viral and cellular membranes (Briz, *et al.*, 2006). The HIV genome encodes three enzymes essential to its replication, including reverse transcriptase (RT), protease (PR) and integrase (IN). HIV reverse transcriptase is crucial for viral replication. HIV protease processes viral polyproteins into functional enzymes and structural proteins, thereby facilitating maturation and infectivity of the viral particles (Ng *et al.*, 1997). HIV integrase is one of the three HIV-1 enzymes that together with a reverse transcriptase (RT) and protease (PR) allow the virus to reproduce itself after infecting the host cells. HIV-1 IN is the enzyme responsible for inserting the HIV proviral DNA

into the host DNA. This enzyme functions in a two-step manner, it initially removes a dinucleotide unit from the 3' ends of the proviral DNA (termed ''3'-processing''), then the 3'-processed strands are transferred from the cytoplasm to the host nucleus, where they are introduced into the host DNA (termed ''strand-transfer'' or ''integration''). Therefore, affecting the mechanism of action of this enzyme selectively would be a significant contribution towards discovering novel therapeutics for treatment of HIV/AIDS (Ovenden *et al*., 2004). Over 20 antiretroviral drugs (ARVs) have been licensed for the treatment of HIV-1 infection in the past 25 years. These has significantly improved the prognosis of HIV-infected individuals and reduced the mortality and morbidity rates worldwide. Whilst anti-HIV-1 drugs target the different steps of the virus life cycle. Currently, drugs for HIV treatment are approved by the Food and Drug Administration (FDA) of the U.S.A. They can be classified into four different groups: fusion or entry inhibitors (FI), reverse transcriptase inhibitors, integrase inhibitors (IN), and protease inhibitors (PI). Nucleoside reverse transcriptase inhibitors (NRTIs) are nucleoside analogs that inhibit DNA synthesis by acting as chain terminators. Subsequently, further classes of ARVs with different inhibitory mechanisms and/or targets were approved for use against HIV-1, these being non-NRTIs and protease inhibitors (PIs). All three classes target viral enzymes required for HIV-1 viral replication, namely reverse transcriptase and protease. Therefore, it is not surprising that drug-resistant variants eventually emerge against these agents due to HIV's high mutation rate and lack of a proofreading mechanism. The occurrence of drug resistance was a particular problem in the early years of ARV therapy when the drugs were used separately. This led to the idea of using no less than three different drugs belonging to at least two different classes to increase the genetic barrier to resistance development in what is termed highly active antiretroviral therapy (HAART) (Hupfeld and Efferth, 2009., Mbisa *et al.*, 2011).

Nonetheless, the emergence of drug-resistant HIV-1 variants in patients undergoing HAART remains a major reason for treatment failure in HIV-1 therapy. Several factors contribute to treatment failure in the era of HAART, and these include poor adherence due to adverse effects associated with the drugs, high pill burden, or irregular supply of the ARVs particularly in resource-poor countries. In addition, the transmission of drug-resistant viral strains can compromise and limit the effectiveness of first-line treatment regimens. Currently, second-generation ARVs have been introduced i.e., fusion inhibitors, entry inhibitors, and integrase (IN)

inhibitors (Mbisa *et al.*, 2011). The effective and durable chemotherapy of this disease require the use of innovative combinations of drugs having diverse mechanisms of anti-HIV-1 activity (Bedoya *et al.*, 2001). An increasing number of patients with HIV infection cannot use the currently approved anti-HIV drugs, including the reverse transcriptase and protease inhibitors, due to their adverse effects and the emergence of drug resistance. Many antiviral compounds presently in clinical use have a narrow spectrum of activity and limited therapeutic usefulness (Asres et al., 2005). Thus, there is an urgent need, globally for new anti-HIV drugs. HIV-1 integrase (IN) is another key enzyme involved in the replication cycle of the retrovirus. It catalyzes the integration of the reverse transcribed viral DNA into the chromosomal DNA. Integration of the HIV-1 DNA ensures the stable maintenance of the viral genome and perpetuation of the virus in the host (Mouscadet and Desmaële, 2010). Any new knowledge on inhibitors of this enzyme could provide essential clues for the development of anti-HIV drugs.

Nowadays, there is only one HIV-1 IN inhibitor, Raltegravir that is available commercially and approved for clinical use. Raltegravir has been one of the ARVs chosen for intensification therapy partially because it has been documented to produce an accelerated decay of HIV-1 RNA in infected individuals. This is believed to result from improved distribution of raltegravir to less accessible sites and cells capable of producing HIV-1 particles, such as in the cerebrospinal fluid. However, preliminary results have proved disappointing with unsustainable reductions of residual HIV-1 viremia and no eradication of the virus. In the future, intensification treatments could involve the use of raltegravir or novel IN inhibitors with or without more potent inducers of HIV-1 expression (Mbisa *et al.*, 2011). Other investigate used of raltegravir include prevention of perinatal infection and postexposure prophylaxis. Thus, searching for alternative HIV-1 IN inhibitors from natural sources can serve as a target of an effective with less side-effect of first-line ARVs. Over the past decade, substantial progress has been made in research on the natural products possessing anti-HIV-1 IN activity. Bioassay-guided isolations of crude herbal extracts have provided lead molecules for discovery of anti-HIV-1 IN drug candidates (Singh *et al.*, 2005; Artan *et al.*, 2008). It has been reported that an ethanol extract of *Smilax corbularia* exhibited a potent anti-HIV-1 IN activity (IC_{50} 1.9 μg/mL) (Tewtrakul *et al.*, 2006). Several flavonoids isolated from plants also exhibited anti-HIV-1 IN activity, such as orobol from *Eclipta prostata* (Tewtrakul *et al.*, 2007), luteolin from *Coleus parvifolius* (Tewtrakul *et al.*, 2003), gal[2]-

^{1}glc-sinapoyl and gal^2-^{1}glc-feruloyl from *Thevetia peruviana* (Tewtrakul *et al.*, 2002), with IC$_{50}$ values of 8.1, 11.0, 7.0 and 5.0 μM, respectively. Natural occurring lignan also showed anti-HIV-1 IN activity, such as globoidnan isolated from *Eucalyptus globoidea* possessed HIV-1 IN inhibitory activity with an IC$_{50}$ of 0.64 μM (Ovenden *et al.*, 2004). In addition, MAP30 and GAP31, the proteins isolated from *Momordica charantia* and *Gelonium multiflorum*, respectively showed anti-HIV-1 IN activity (Huang *et al.*, 1990, Huang *et al.*, 1995).

Our preliminary screening for anti-HIV-1 IN activity from sixteen Thai medicinal plants, including *Averrhoa carambola, Brassica oleracea, Coccinia grandis, Diplazium esculentum, Garcinia cowa, Illicium verum, Millingtonia hortensis, Mimusops elengi, Morinda coreia, Moringa oleifera, Murraya paniculata, Pandanus amaryllifolius, Pometia pinnata, Sauropus androgynus, Tiliacora triandra* and *Vigna unguiculata* were investigated for their inhibitory effect against human immunodeficiency virus type 1 integrase (HIV-1 IN) inhibitory activity using the multiplate integration assay (MIA). The result revealed that leaf extracts from *P. pinnata* and *M. elengi* had the strongest anti-HIV-1 IN activity with IC$_{50}$ values of 8.8 and 62.1 μg/mL, respectively (Suedee *et al.*, 2011). Thus, our interest is to focus on these two plants to isolate, elucidate and establish HPLC methods for the quantitative analysis of their active compounds. The results can provide an alternative therapy or combination of drugs therapy for HIV-1 treatment to minimize resistant and potential side effect usually observed in currently available ARVs.

1.2 Occurring of AIDS and epidemic

AIDS occurring from retrovirus called human immunodeficiency virus or "HIV". There are two types which are HIV-1 (Figure 1-1) and HIV-2. The most occurring type is HIV-1 and it is found that South Africa has the largest number of HIV patients in the world. UN AIDS and WHO estimate the AIDS has killed nearly 30 million people since it was first recognized in 1981 (U.S. Global Health Policy. 2011). Thailand is the third worst affected and it has reported that there are 372,874 AIDS patients in Thailand (ศูนย์ข้อมูลทางระบาดวิทยา สำนักระบาดวิทยา กองควบคุมโรค, 2554).

1.3 Immune system related to HIV

An immune system is a system of biological structures and processes within an organism that protects against disease by identifying and killing pathogens and tumor cells. It detects a wide variety of agents, from viruses to parasitic worms, and needs to distinguish them from the organism's own healthy cells and tissues in order to function properly. Detection is complicated since pathogens can evolve rapid, producing adaptations that avoid the immune system and allow the pathogens to successfully infect their hosts. When HIV virus infects the host cell, they destroy an immune system. Then pathogens (bacteria, virus, fungi, or protozoa) can infect AIDS patients easily. HIV leads to immunosuppression that allows opportunistic pathogens to cause disease and death in AIDS patients such as tuberculosis and pneumonia. In the previous reports found that the Western Cape region of South Africa has one of the highest recorded incidence rates of tuberculosis (TB) that it has related with the number of AIDS patients in rate 1600/100,000 (Rangaka *et al.*, 2007).
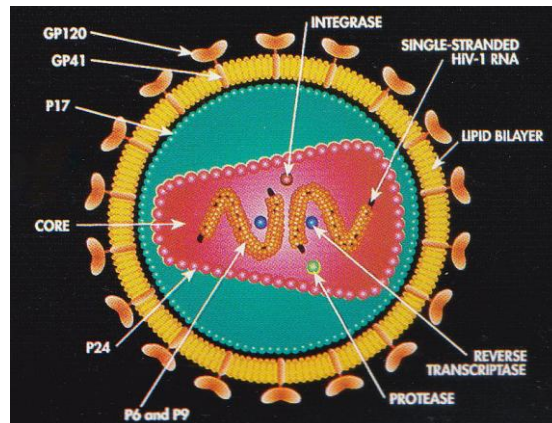
Figure 1-1 HIV-virus (Nittayananta, W. 2001)

1.4 HIV-1 life cycle

HIV life cycle consists of five steps to infect T-helper cells. Firstly, HIV binds and fuses to T-helper cells and release its RNA to T-cell cytoplasm. Then, viral RNA converts to viral DNA using reverse transcriptase enzyme. After that, viral DNA enters host nucleus and integrates into host chromosomal DNA using assembly. Finally, newly made HIV virus is released and ready to infect other cells (Figure 1-2).
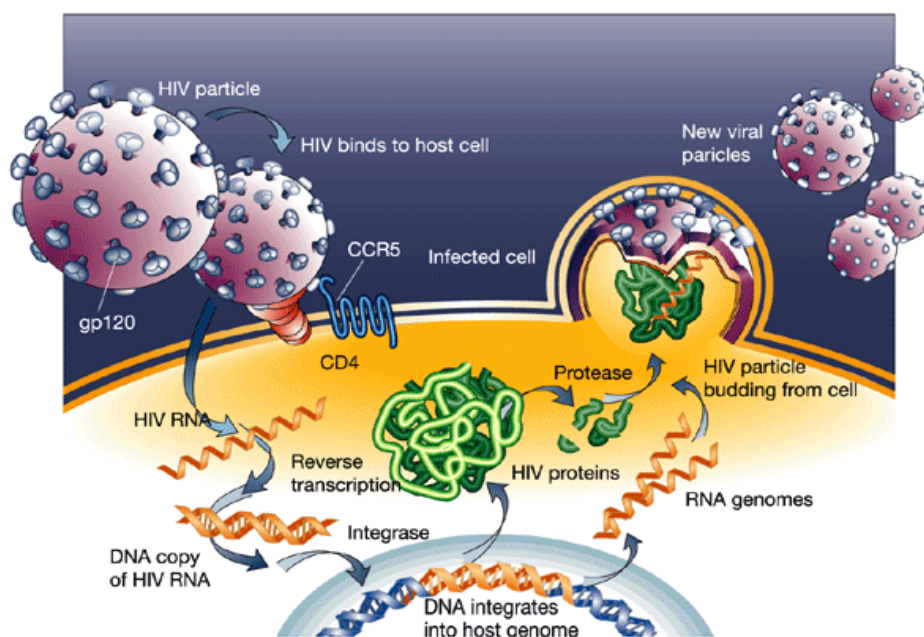
Figure 1-2 HIV-1 life cycle (Weiss, R.A. 2003)

1.5 HIV-1 IN structure

HIV-1 IN consists of 288 amino acids which is 32 KD of protein and it functions as a dimer. HIV‑IN contains three domains protein (Figures 1‑3 and 1‑4), which contains conserved amino acid sequence motifs in both the N-terminus (HHCC) and core domain (D, D-35-E). Structural analysis of the core domain revealed that integrase is structurally related to a diverse superfamily of polynucleotidyl transferases. The isolated C‑terminal domain, which can bind DNA, adopts a SH3 domain topology in solution The structure of the isolated N-terminal domain, bound with zinc, is similar to that of a helix–turn–helix DNA‑binding domain, such as the Trp repressor. All three domains are required for integration activity (Katz and Skalka, 1994; Jenkins *et al*., 1997).
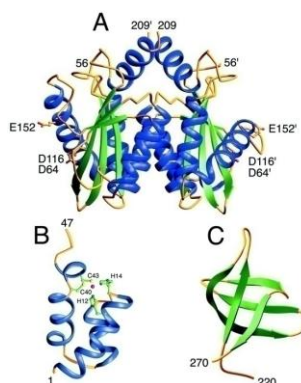
Figure 1‑3 Three domains of HIV‑1 integrase shown as ribbon diagrams (Craigie, 2001)
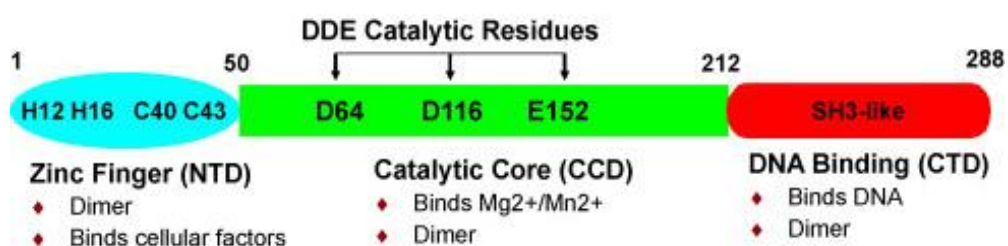
Figure 1‑4 HIV‑1 integrase of structure (McColl and Chen, 2010)

1.6 Function of HIV‑1 integrase enzyme

The integration step of the HIV lifecycle requires two steps mediated by the integrase enzyme, $3'$-end processing ($3'$-EP) and strand transfer reaction. The $3'$-EP reaction occurs in the cytoplasm following completion of viral DNA synthesis by reverse transcriptase. The $3'$-EP reaction is an endonucleolytic cleavage of the viral DNA and occurs immediately $3'$ of a conserved CA dinucleotide motif. This produces a reactive $3'$ hydroxyl at each end of the viral DNA. Integrase remains bound to the ends of the viral DNA which remain in close proximity to one another. This complex of viral DNA, integrase multimers and associated cellular factors form the preintegration complex (PIC). The PIC is transported across the nuclear membrane and is then targeted to chromatinized host genomic DNA via LEDGF (lens epithelium‑derived growth factor). The second reaction catalyzed by integrase, the STF reaction then takes place. STF is $3'$-end joining. Each of the $3'$ hydroxyl ends of the viral DNA are coordinated to attack the phosphodiester bond on the host chromosomal DNA and then ligated to the ends of the nicked chromosomal DNA. The $3'$ ends of the viral DNA are positioned such that they attack the host chromosomal DNA across a span of 5 base pair along the major groove. The STF reaction results

in a 5 base pair, single stranded gap at the join between the viral and chromosomal DNA and a 2 base pair "flap" at the end of the 5′end of the viral DNA. Cellular repair enzymes then fill the gap, resulting in production of the mature integrated pro- virus from which viral transcription can be initiated (McColl and Chen, 2010) (Figure 1-5).
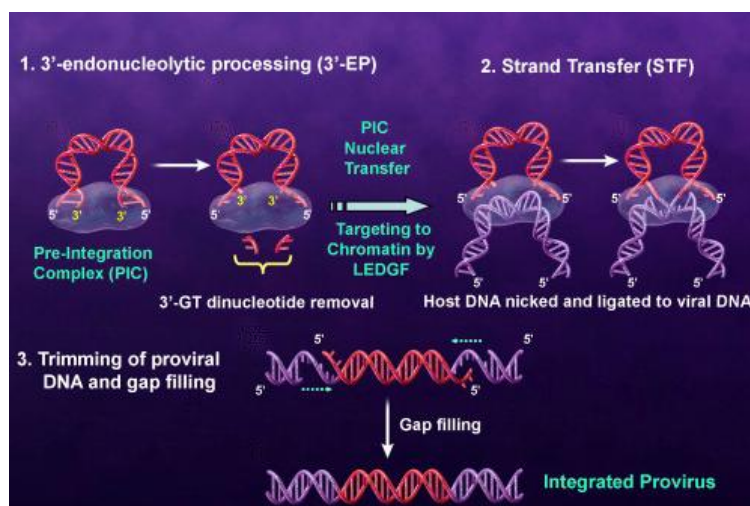
Figure 1-5 Function of HIV-1 integrase enzyme (McColl and Chen, 2010)

1.7 Example of radio-labelled assay for integrase inhibitor screening

The radio-labelled assay used for screening integrase inhibitor is as follow; the 21-mer oligodeoxynucleotide is radio-labelled with ^{32}P at the 5′-terminus. Recombinant integrase catalyzes the last two oligonucleotide from 3′-end. Release of GT dinucleotide at the 3′-end of the radio-labelled strand generates 19-mer oligonucleotide that can be readily separated from the 21-mer substrate using gel electrophoresis. Figure 1.6 showed differential effect of 3′-processing and strand-transfer inhibitors (Figure 1-6 part I and II). This method is used for anti-HIV-1 integrase activity assay from *Salvia miltiorrhiza* (Ibrahim *et al.*, 2002) and is used to detect both 3′-processing and 3′-joining (Pommier *et al.*, 2005).
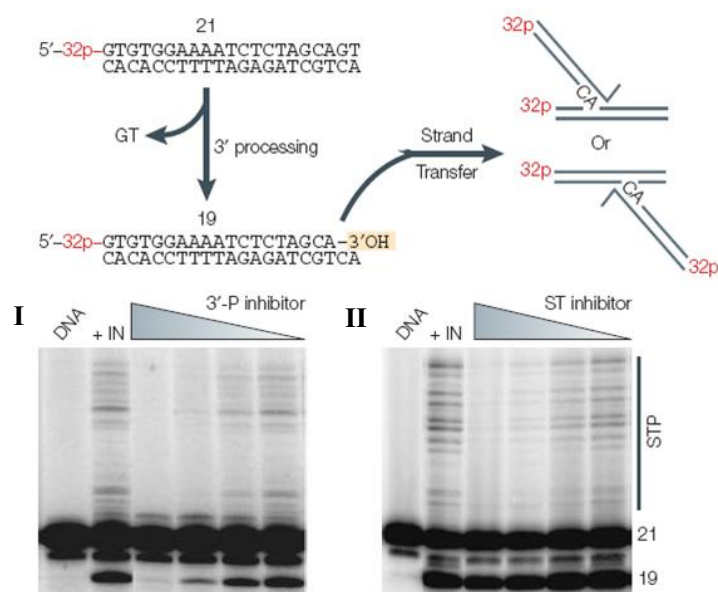
Figure 1-6 Radio-labelled assay for integrase inhibitor screening (Pommier *et al*., 2005)

The donor DNA (generally derived from the U5-LTR) is immobilized on a micro-titre well plate or bound to a magnetic bead (Dynabead). Integrase 3′-processing is required to activate the donor DNA, which is then able to react with biotin-labelled target DNA. Integration can be detected after isolation of the bound donor DNA. Inhibition is measured as signal extinction (Figure 1-7). Pre-integration complex (PIC) assays detect the inhibition of integrase within PICs isolated from infected cell extracts. Such assays are generally cumbersome and use biological materials from HIV-infected cells (Pommier *et al*., 2005).
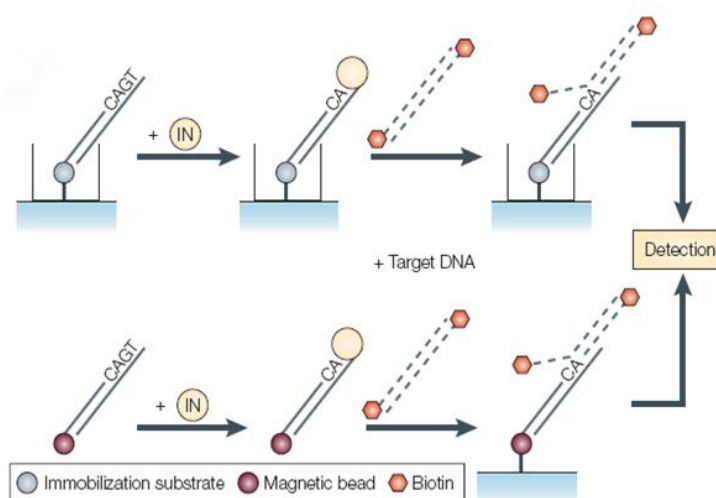
Figure 1-7 Illusstrate high-throughput assay (Pommier *et al*., 2005)

Recently, there have been several reports on anti‑HIV‑1 IN assay using isotope‑labelled substrate and denaturing gel separation of products (Ibrahim *et al*., 2002). However, they are inconvenient and time consuming, especially when screening inhibitors from many samples. Lately, an assay for HIV‑1 IN activity using DNA‑coated plates has been reported in a few reports (Chang *et al*., 1996; Hazuda *et al*., 1994; Pommier *et al*., 2005; Vink *et al*., 1994). It is a non‑radioisotopic technique and can be used for screening the inhibitory activity of plant extracts or any compounds against HIV‑1 IN. In this method, 96 well plates were used for the screening test called a multiple integration assay (MIA). It is sample, convenient and accurate and does not require the centrifugation, electrophoresis or other DNA denaturation steps. This assay screens for both 3′‑processing and 3′‑strand transfer and be used without any exposure to radioisotopes. In this study, we therefore used this assay method for screening the HIV‑1 IN inhibitor substances. MIA is the method to measure the incorporation of digoxigenin‑labelled target DNA in to long terminal repeat (LTR) donor DNA. For this assay, a biotin‑labelled donor DNA is add into each well, which strong bind with a streptavidin coated‑well plate, followed by addition of digoxigenin‑labelled target DNA, integrase enzyme and sample solution. After intergration process, the ligated two double‑stranded DNA is immobilized on streptavidin‑coated wells and subsequently bound with an alkaline phosphate (AP)‑labelled anti‑digoxigenin antibody. Finally, it is colorized by adding *p*‑nitrophenylphosphate as a substrate, In basic solution (pH 9.5), AP hydrolyzes *p*‑nitrophenylphosphate to *p*‑nitrophenol which exhibits a yellow color (Bunluepuech, 2010).

CHAPTER 2

LITERATURE REVIEW

2.1 Thai medicinal plants used for AIDS treatment

Screening of medicinal plants for anti-HIV-1 activity has been a promising approach to search for compounds that act as anti-HIV-1 agents. There are several plants showing anti-HIV, anti-HIV-RT and anti-HIV-PR activities. They are listed in Table 2-1 (เย็นจิตร เตชะดำรงสิน และ คณะ, 2546; Bunluepuech, 2010)

Table 2-1 Thai medicinal plants used for AIDS treatment

Botanical name	Family	Part used / Extract	Anti-HIV			Anti-HIV-RT			Anti-HIV-PR		
			Conc. (μg/mL)	% Inhi-bition	IC_{50} (μg/mL)	Conc. (μg/mL)	% Inhi-bition	IC_{50} (μg/mL)	Conc. (μg/mL)	% Inhi-bition	IC_{50} (μg/mL)
Alpinia galangal (L.) Willd. (ข่า)	Zingiberaceae	Fresh and dry rhizome / EtOH and H_2O	ND			250	NA	ND	ND		
Annona reticulata L. (น้อยโหน่ง)	Annonaceae	Fresh leaf / EtOH	ND			250	NA	ND	40	60	ND
Clinnacanthus siamensis Bremek. (ลิ้นงูเห่า)	Acanthaceae	Fresh leaf / EtOH	ND			250	NA	ND	18.2	65	ND
Excoecaria cochinchinensis Lour. var. *cochinchinensis* (กระบือเจ็ดตัว)	Euphorbiaceae	Fresh leaf / EtOH	ND			250	23.8	ND	ND		
		Fresh branch/ EtOH	ND			250	NA	ND	ND		
		Dry leaf and branch / H_2O	ND			250	NA	ND	ND		

EtOH = ethanol; ND = not determine; NA = not active

Table 2-1 Thai medicinal plants used for AIDS treatment (continued)

Botanical name	Family	Part used / Extract	Anti-HIV			Anti-HIV-RT			Anti-HIV-PR		
			Conc. (µg/mL)	% Inhi-bition	IC$_{50}$ (µg/mL)	Conc. (µg/mL)	% Inhi-bition	IC$_{50}$ (µg/mL)	Conc. (µg/mL)	% Inhi-bition	IC$_{50}$ (µg/mL)
Imperata cylindrical (L.) P. Beauv. (หญ้าคา)	Gramineae	Fresh rhizome / EtOH	ND			250	NA	ND	66.7	98	ND
		Fresh rhizome / H$_2$O	ND			250	NA	ND	100	60	ND
		Dry rhizome / EtOH	ND			250	NA	ND	66.7	30	ND
Jatropha gossypifolia L. (สบู่แดง)	Euphorbiaceae	Stems and leaves /EtOH	ND			250	NA	ND	200	16.7	ND
		Stems and leaves /H$_2$O	ND			250	21.6	ND	200	22.2	ND
Jatropha integerrima Jacq. (ปัตตาเวีย)	Euphorbiaceae	Leaves/ EtOH	ND			250	NA	ND	66.7	100	ND
		Leaves/ H$_2$O	ND			250	50.6	ND	200	NA	ND
Melaleuca cajuputi Powell (เสม็ด)	Myrtaceae	Oil from Leaves	250	14.3	NA	250	68.9	111.1	18.2	ND	ND
		Leaves/ EtOH	250	45.5	NA	250	48.7	ND	18.2	ND	ND
		Leaves/ CHCl$_3$	250	ND	ND	250	75.6	74.7	18.2	ND	ND
		Leaves/ CHCl$_3$	250	ND	ND	250	63	ND	18.2	55	ND

EtOH = ethanol; ND = not determine; NA = not active

Table 2-1 Thai medicinal plants used for AIDS treatment (continued)

Botanical name	Family	Part used / Extract	Anti-HIV			Anti-HIV-RT			Anti-HIV-PR		
			Conc. (µg/mL)	% Inhi-bition	IC$_{50}$ (µg/mL)	Conc. (µg/mL)	% Inhi-bition	IC$_{50}$ (µg/mL)	Conc. (µg/mL)	% Inhi-bition	IC$_{50}$ (µg/mL)
Merremia vitifolia (Burm.f.) Hallier f. (จิงจ้อขน)	Convolvulaceae	Stems/ EtOH	62.5	93	30	ND			ND		
		Stems/ EtOH	166.7	96	71.5	ND			ND		
		Stems/ H$_2$O	60	96	17.6	ND			ND		
Moringa oleifera Lam. (มะรุม)	Moringaceae	Leaves/ EtOH	166.7	NA	ND	250	NA	ND	66.7	66.7	ND
		Young pods / EtOH	10.0	NA	ND	250	NA	ND	66.7	86.7	ND
		Leaves/ 50% EtOH	125	78	125	250	43.7	ND	100	33.3	ND
		Young pods / 50% EtOH	125	NA	ND	250	NA	ND	100	NA	ND
		Leaves/ H$_2$O	125	NA	ND	250	41.8	ND	200	NA	ND
		Old pods/ EtOH	166.7	NA	ND	250	NA	ND	66.7	50	ND
		Old pods/ 50% EtOH	125	78	125	250	41.3	ND	100	NA	ND
		Old pods / H$_2$O	250	78	250	250	41.3	ND	200	100	ND
Murraya paniculata (L.) Jack (แก้ว)	Rutaceae	Fresh leaf and branch/ EtOH	7.5	93	3.5	250	11.4	ND	ND		
		Dry leaf and branch/ EtOH	30	NA	ND	250	8	ND	ND		

EtOH = ethanol; ND = not determine; NA = not active

Table 2-1 Thai medicinal plants used for AIDS treatment (continued)

Botanical name	Family	Part used / Extract	Anti-HIV			Anti-HIV-RT			Anti-HIV-PR		
			Conc. (μg/mL)	% Inhibition	IC$_{50}$ (μg/mL)	Conc. (μg/mL)	% Inhibition	IC$_{50}$ (μg/mL)	Conc. (μg/mL)	% Inhibition	IC$_{50}$ (μg/mL)
Murraya paniculata (L.) Jack (แก้ว)	Rutaceae	Fresh leaf and branch / H$_2$O	125	NA	ND	250	20.4	ND	ND		
Panicum repens L. (หญ้าชันกาด)	Gramineae	Rhizome/ EtOH	ND			250	NA	ND	66.7	NA	ND
		Rhizome/ H$_2$O	ND			250	NA	ND	200	50	ND
Petunia hybrida (พิทูเนีย)	Solanaceae	Aerial part/ EtOH	ND			250	NA	ND	66.7	33.3	ND
		Aerial part/ H$_2$O	ND			250	NA	ND	200	NA	ND
Plantago major L. (หญ้าเอ็นยืด)	Plantaginaceae	Whole plant / EtOH	ND			250	30	ND	40	0	ND
Plumeria obtuse L. (ลั่นทมขาว)	Apocynaceae	Branch/ EtOH and H$_2$O	ND			250	NA	ND	ND		
Spathodea campanulata (แคแสด)	Bignoniaceae	Bark/ EtOH	ND			250	NA	ND	66.7	88.7	ND
		Bark/ H$_2$O	ND			250	52.2	242	200	85	ND
		Leaves/ EtOH	ND			250	NA	ND	66.7	88.3	ND
		Leaves/ H$_2$O	ND			250	53.9	236	200	96	ND

EtOH = ethanol; ND = not determine; NA = not active

Table 2-1 Thai medicinal plants used for AIDS treatment (continued)

Botanical name	Family	Part used / Extract	Anti-HIV			Anti-HIV-RT			Anti-HIV-PR		
			Conc. (µg/mL)	% Inhi-bition	IC$_{50}$ (µg/mL)	Conc. (µg/mL)	% Inhi-bition	IC$_{50}$ (µg/mL)	Conc. (µg/mL)	% Inhi-bition	IC$_{50}$ (µg/mL)
Stephania venosa (Bl.) Spreng. (สบู่เลือด)	Menispermaceae	Tuber (orange)/ H$_2$O	250	87.4	ND	50	39.3	103.8	ND		
		Tuber (yellow)/ H$_2$O	250	68.8	ND	50	20.6	170.3	ND		
Streblus asper Lour. (ข่อย)	Moraceae	Bark/EtOH	ND			250	7.8	ND	ND		
		Bark/ H$_2$O	ND			250	34	ND	ND		
Suregada multiflorum (A.Juss.) Baill. (ขันทอง-พยาบาท)	Euphorbiaceae	Seeds and fruits/ EtOH	ND			250	NA	ND	ND		
		Seeds and fruits/ H$_2$O	ND			250	NA	ND	ND		
Thevetia peruviana (Pers.) K.Schum. (รำเพย)	Apocynaceae	Leaves/ EtOH	7.5	NA	ND	50	70	ND	250	ND	ND
		Leaves/ H$_2$O	30.0	NA	ND	200	100	ND	250	NA	ND
		Leaves/ EtOH	7.5	NA	ND	50	70	ND	250	ND	ND
		Leaves/ H$_2$O	30.0	NA	ND	200	NA	ND	250	ND	ND

EtOH = ethanol; ND = not determine; NA = not active

2.2 Thai medicinal plants showing anti HIV-1 IN activity

Anti-HIV-1 IN activity of some Thai medicinal plant extracts and anti HIV-1 IN compounds have been reported as shown in Table 2-2 and Table 2-3, respectively.

Table 2-2 Anti-HIV-1 IN activity of some Thai medicinal plants.

Plants	Family	Part used	Extract	IC$_{50}$ (µg/mL)	References
Acacia concinna DC.	Mimosaceae	Leaves	Ethanol	3.8	Tewtrakul *et al*., 2003
Adhatoda vasica Nees.	Acanthaceae	Leaves	Ethanol	12.0	Tewtrakul *et al*., 2003
Albizia procera Benth.	Mimosaceae	Barks	Ethanol	19.5	Bunluepuech and Tewtrakul, 2011
			Water	5.9	Bunluepuech and Tewtrakul, 2011
Andrographis paniculata Wall ex. Ness.	Acanthaceae	Leaves	Ethanol	12.0	Tewtrakul *et al*., 2003
			Water	1.5	Tewtrakul *et al*., 2003
Areca catechu Linn.	Palmaceae	Fruits	Ethanol	3.2	Bunluepuech and Tewtrakul, 2011
			Water	15.7	Bunluepuech and Tewtrakul, 2011
Artocarpus heterrophyllus Lam.	Moraceae	Woods	Ethanol	80.2	Bunluepuech and Tewtrakul, 2011
			Water	32.1	Bunluepuech and Tewtrakul, 2011
Baleria lupulina Lindl.	Acanthaceae	Leaves	Ethanol	10.0	Tewtrakul *et al*., 2003
			Water	10.0	Tewtrakul *et al*., 2003
Bauhinia strychnifolia Craib.	Fabaceae	Vines	Ethanol	6.4	Bunluepuech and Tewtrakul, 2011
			Water	11.2	Bunluepuech and Tewtrakul, 2011

Table 2-2 Anti-HIV-1 IN activity of some Thai medicinal plants (continued).

Plants	Family	Part used	Extract	IC$_{50}$ (µg/mL)	References
Betula alnoides Buch.-Ham. ex G.Don.	Betulaceae	Woods	Ethanol	20.1	Bunluepuech and Tewtrakul, 2011
			Water	10.2	Bunluepuech and Tewtrakul, 2011
Bixa orellana Linn.	Bixaceae	Seeds	Ethanol	2.2	Tewtrakul *et al*., 2003
			Water	0.7	Tewtrakul *et al*., 2003
Blumea balsamifera Linn.	Compositae	Leaves	Water	7.8	Bunluepuech and Tewtrakul, 2011
Calophyllum inophyllum Linn.	Guttiferae	Leaves	Ethanol	4.5	Tewtrakul *et al*., 2003
			Water	4.0	Tewtrakul *et al*., 2003
Caesalpinia sappan Linn.	Caesalpiniaceae	Woods	Ethanol	31.0	Bunluepuech and Tewtrakul, 2011
			Water	27.7	Bunluepuech and Tewtrakul, 2011
Cassia angustifolia Vahl.	Caesalpiniaceae	Leaves	Ethanol	4.9	Tewtrakul *et al*., 2003
Cassia fistula Linn.	Caesalpiniaceae	Fruits	Ethanol	10.0	Tewtrakul *et al*., 2003
			Water	0.8	Tewtrakul *et al*., 2003
Cassia garrettiana Craib.	Caesalpiniaceae	Woods	Ethanol	3.0	Bunluepuech and Tewtrakul, 2011
			Water	5.2	Bunluepuech and Tewtrakul, 2011
Clinacanthus nutans Lindau.	Acanthaceae	Leaves	Ethanol	2.8	Tewtrakul *et al*., 2003
			Water	2.0	Tewtrakul *et al*., 2003
Clerodendron indicum (L.) Kuntze	Verbenaceae	Whole plants	Water	43.5	Bunluepuech, 2010

Table 2-2 Anti-HIV-1 IN activity of some Thai medicinal plants (continued).

Plants	Family	Part used	Extract	IC$_{50}$ (µg/mL)	References
Coleus parvifolius Benth.	Libiatae	Arial parts	Ethanol	9.2	Tewtrakul *et al*., 2003
			Water	2.0	Tewtrakul *et al*., 2003
Combretum quadrangulare Kutz.	Combretaceae	Leaves	Ethanol	2.5	Tewtrakul *et al*., 2003
			Water	2.9	Tewtrakul *et al*., 2003
Croton sublyranthus Kurz.	Euphorbiaceae	Leaves	Ethanol	3.0	Tewtrakul *et al*., 2003
Cyperus rotundus Linn.	Cyperaceae	Rhizomes	Water	58.0	Bunluepuech and Tewtrakul, 2011
Derris scandens Benth.	Papilionaceae	Leaves	Ethanol	13.9	Tewtrakul *et al*., 2003
			Water	10.0	Tewtrakul *et al*., 2003
Diospyros decandra Lour.	Ebenaceae	Woods	Ethanol	69.9	Bunluepuech, 2010
			Water	27.8	Bunluepuech, 2010
Dracaena loureiri Gagnep.	Agavaceae	Woods	Ethanol	28.0	Bunluepuech, 2010
			Water	22.1	Bunluepuech, 2010
Fagraea fragrans Roxb.	Gentianaceae	Leaves	Water	94.3	Bunluepuech and Tewtrakul, 2011
Ficus glomerata Roxb.	Moraceae	Woods	Ethanol	7.8	Bunluepuech, 2010
			Water	29.5	Bunluepuech, 2010
Ficus foveolata Wall.	Moraceae	Vines	Water	40.1	Bunluepuech and Tewtrakul, 2011
Harrisonia perforata (Blanco) Merr.	Simaroubaceae	Woods	Water	2.3	Bunluepuech, 2010
Hisbiscus sabdariffa Linn.	Malvaceae	Flowers	Water	1.4	Tewtrakul *et al*., 2003

Table 2-2 Anti-HIV-1 IN activity of some Thai medicinal plants (continued).

Plants	Family	Part used	Extract	IC$_{50}$ (µg/mL)	References
Lawsonia inermis Linn.	Lythraceae	Leaves	Ethanol	2.1	Tewtrakul *et al.*, 2003
			Water	3.3	Tewtrakul *et al.*, 2003
Morinda citrifolia Linn.	Rubiaceae	Leaves	Ethanol	1.2	Tewtrakul *et al.*, 2003
			Water	6.0	Tewtrakul *et al.*, 2003
Myristica fragrans Linn.	Myristicaceae	Leaves	Ethanol	3.0	Tewtrakul *et al.*, 2003
			Water	2.3	Tewtrakul *et al.*, 2003
Ocimum basilicum Linn.	Labiatae	Leaves	Water	6.0	Tewtrakul *et al.*, 2003
Ocimum canum Sims.	Labiatae	Leaves	Ethanol	1.6	Tewtrakul *et al.*, 2003
Piper betle Linn.	Piperaceae	Leaves	Ethanol	4.0	Tewtrakul *et al.*, 2003
Piper nigrum Linn.	Piperaceae	Fruits	Water	8.0	Tewtrakul *et al.*, 2003
Piper ribesoides Wall. (A)	Piperaceae	Stems	Water	0.9	Tewtrakul *et al.*, 2003
Piper ribesoides Wall. (A)	Piperaceae	Leaves	Ethanol	0.6	Tewtrakul *et al.*, 2003
			Water	0.5	Tewtrakul *et al.*, 2003
Piper ribesoides Wall. (B)	Piperaceae	Stems	Water	0.4	Tewtrakul *et al.*, 2003
Piper ribesoides Wall. (B)	Piperaceae	Leaves	Ethanol	0.1	Tewtrakul *et al.*, 2003
			Water	4.1	Tewtrakul *et al.*, 2003
Piper sarmentosum Roxb.	Piperaceae	Leaves	Ethanol	1.2	Tewtrakul *et al.*, 2003
Plumbago indica Linn.	Plumbaginaceae	Leaves	Ethanol	6.0	Tewtrakul *et al.*, 2003
			Water	2.9	Tewtrakul *et al.*, 2003
Psidium guajava Linn.	Myrtaceae	Leaves	Ethanol	2.5	Tewtrakul *et al.*, 2003
			Water	1.7	Tewtrakul *et al.*, 2003
Quisqualis indica Linn.	Combretaceae	Leaves	Ethanol	2.0	Tewtrakul *et al.*, 2003
			Water	1.2	Tewtrakul *et al.*, 2003

A = lanceolate shaped leaf; B = cordate shape leaf

Table 2-2 Anti-HIV-1 IN activity of some Thai medicinal plants (continued).

Plants	Family	Part used	Extract	IC$_{50}$ (µg/mL)	References
Rhinacanthus nasutus Kurz.	Acanthaceae	Leaves	Ethanol	0.8	Tewtrakul *et al.*, 2003
			Water	0.7	Tewtrakul *et al.*, 2003
Stephania pierrei Diels.	Menispermaceae	Tubers	Water	97.2	Bunluepuech and Tewtrakul, 2011
Stephania venosa Diels.	Menispermaceae	Tubers	Ethanol	9.3	Bunluepuech and Tewtrakul, 2011
			Water	41.2	Bunluepuech and Tewtrakul, 2011
Terminalia citrina Roxb. Ex. Flemming.	Combretaceae	Fruits	Ethanol	2.7	Tewtrakul *et al.*, 2003
			Water	0.3	Tewtrakul *et al.*, 2003
Theobroma cacao Linn.	Sterculiaceae	Leaves	Ethanol	8.0	Tewtrakul *et al.*, 2003
			Water	2.5	Tewtrakul *et al.*, 2003
Thevetia peruviana (Pers.) K. Schum.	Apocyanaceae	Leaves	Water	8.8	Tewtrakul *et al.*, 2003
Thunbergia laurifolia Linn.	Thunbergiaceae	Arial parts	Ethanol	3.0	Tewtrakul *et al.*, 2003
Tribulus terristris Linn.	Zygophyllaceae	Arial parts	Water	2.8	Tewtrakul *et al.*, 2003
			Ethanol	8.0	Tewtrakul *et al.*, 2003
Zingiber officinale Roscoe.	Zingiberaceae	Rhizomes	Ethanol	4.0	Tewtrakul *et al.*, 2003
			Water	1.8	Tewtrakul *et al.*, 2003
Zingiber zerumbet Smith.	Zingiberaceae	Rhizomes	Water	2.8	Tewtrakul *et al.*, 2003

Table 2-3 Anti-HIV-1 integrase compounds isolated from some Thai medicinal plants.

Plants	Compounds	IC$_{50}$ (µM)	References
Acer okamotoanum Nakai.	Quercetin 3-*O*-(2″-galloyl)-α-L-arabinopyranoside	18,100	Kim *et al*., 1998; Kejik, 2008
	Quercetin 3-*O*-(2″,6″-O-digalloyl)-β-D-galactopyranoside	24,200	Kim *et al*., 1998; Kejik, 2008
Agastache rugosa (Fisch. & C.A.Mey.) Kuntze	Rosmarinic acid	10,000	Kim *et al*., 1999; Kejik, 2008
Chysanthemum morifolium Ramat.	Apigenin-7-*O*-β-D-(4″-caffeoyl)-glucuronide	7,200	Lee *et al*., 2003; Kejik, 2008
Coleus parvifolius Benth.	5 *O*-β-D-glucopyranosyl-luteolin-7-methyl ether	70.0	Tewtrakul *et al*., 2003
	Luteolin	11.0	Tewtrakul *et al*., 2003
	Luteolin-5 *O*-β-D-glucopyranoside	58.0	Tewtrakul *et al*., 2003
	Luteolin-5 *O*-β-D-glucuronide	20.0	Tewtrakul *et al*., 2003
	Luteolin-7-methyl ether	11.0	Tewtrakul *et al*., 2003
	Rosmarinic acid	5.9	Tewtrakul *et al*., 2003
	Rosmarinic acid-methyl ether	3.1	Tewtrakul *et al*., 2003
Eclipta prostrate Linn.	Orobol	8.1	Tewtrakul *et al*., 2007
	Wedelolactone	4.0	Tewtrakul *et al*., 2007
Lindera chunii Merr.	Hernandonine	16.3	Zhang *et al*., 2002
	Laurolistine	7.7	Zhang *et al*., 2002
	Lindechunine A	21.1	Zhang *et al*., 2002
	7-Oxohernangerine	18.2	Zhang *et al*., 2002
Paeonia suffruticosa Andrews	(methanol extract)	15,000	Au *et al*., 2001; Kejik, 2008

Table 2-3 Anti-HIV-1 integrase activity of compounds from the plants (continued)

Plants	Compounds	IC$_{50}$ (µM)	References
Prunella vulgaris Linn.	(aqueous extract)	45,000	Au *et al.*, 2001; Kejik, 2008
Salvia miltiorrhiza Bunge	Lithospermic acid	0.83	Abd-Elazem *et al.*, 2002; Kejik, 2008
	Lithospermic acid B	0.48	Abd-Elazem *et al.*, 2002; Kejik, 2008
Thevetia peruviana (Pers.) K. Schum.	Kaempferol	40	Tewtrakul *et al.*, 2002
	Kaempferol-3-*O*-[β-D-gluco-pyranosyl-(1→2)-[β-D-glucopyranoside	59	Tewtrakul *et al.*, 2002
	Kaempferol-3-*O*-[(6-*O*-feru-loyl)-β-D-glucopyranosyl-(1→2)-[β-D-galactopyranoside	31	Tewtrakul *et al.*, 2002
	Kaempferol-3-*O*-[(6-*O*-sinapoyl)-β-D-glucopyranosyl-(1→2)-[β-D-galactopyranoside	30	Tewtrakul *et al.*, 2002
	Kaempferol-3-*O*-[β-D-glucopy-ranosyl-(1→2)-[α-L-rhamno-pyranosyl-(1→6)]-β-D-galac-topyranoside	43	Tewtrakul *et al.*, 2002
	Quercetin	15	Tewtrakul *et al.*, 2002
	Quercetin-3-*O*-)-β-D-glucopyra-nosyl-(1→2)-[β-D-glucopyra-noside	45	Tewtrakul *et al.*, 2002

Table 2-3 Anti-HIV-1 integrase activity of compounds from the plants (continued)

Plants	Compounds	IC$_{50}$ (μM)	References
Thevetia peruviana (Pers.) K. Schum.	Quercetin-3-*O*-[(6-*O*-feruloyl)-β-D-glucopyranosyl-(1→2)-[β-D-galactopyranoside	5	Tewtrakul *et al.*, 2002
	Quercetin-3-*O*-[(6-*O*-sinapoyl)-β-D-glucopyranosyl-(1→2)-[β-D-galactopyranoside	7	Tewtrakul *et al.*, 2002

2.3 *Mimusops elengi* Linn.

M. elengi is a small to large evergreen tree belonging to Sapotaceae (Figure 2-1). The bark is mostly fissured, thick, tough and heavy. It is brownish black or grayish black in color on the exterior and dark red inside. The trunk is straight with spreading branches and the canopy is very dense. The leaves are small, narrow, pointed, glossy, thick, dark green, oval in shape, and wavy at margin. They are about 5-16 cm in length and 3-7 cm in width. The heart wood is deep red in color, very hard and an excellent timber. The heartwood is a valuable wood and is in great demand for carving intricate designs. The tree flowers once in a year and in India it is normally during the months of March to June. The flowers are star-shaped, small, yellowish white in color, hairy and occur in small clusters or in solitaire. The flowers are woven in to the form of a garland and offered in temples and shrines. They are powerfully scented and the fragrance is retained even when the flowers are completely dried. The process of fruiting takes about eight to ten weeks and the fruits are ovoid and 2-2.5 cm long. When raw the fruits are green in color and become yellow, golden orange to bright red-orange when fully ripe. The fruits contain one to two seeds and are ovoid, shiny, compressed and grayish brown in color (Baliga *et al*., 2011).

Figure 2-1 *Mimusops elengi* Linn. (Sapotaceae)

The bark is used as a gargle for odontopathy, ulitis, and ulemorrhagia. The fruit is used as astringent, coolant, anthelmintic. The tender stems are used as tooth brushes and in cystorrhea, diarrhea and dysentery. The flowers' lotion is used for wounds and ulcers. The unripe fruits are astringent, while the ripen fruits are sweet and edible. The seeds are used for treatment of constipation, and mimusopic acid isolated from the seeds showed mild anti-HIV reverse transcriptase activity. The scientific studies, especially on the pharmacological activities of *M. elengi* are still limited. The leaf extracts are well known for their analgesic and antipyretic activities (Sehgal *et al*., 2011; Gami *et al*., 2012) and showed good inhibitory activity against *Bacillus subtilis* and *Trichoderma viride* (Sahu, 1996; Ali *et al*., 2008), and antioxidant activity (Saha *et al*., 2008). Other pharmacological activities of *M. elengi* are shown in Table 2-4 (Baliga *et al*., 2011).

Table 2-4 Pharmacological activities of *M. elengi*.

Phamacological activities	Plant parts	Extracts/Compounds
Antibacterial	Leaves	Aqueous and ethanol extracts
	Bark, fruits and leaves	Petroleum ether, ethyl acetate and methanol extracts
	Seeds	2,3-dihydro-3,3′4′5,7-pentahydroxyflavone and 3,3′,4′,5,7-pentahydroxyflavone
Anti-cariogenic	Bark	Petroleum ether, acetone, methanol and aqueous extracts
Antidiabetic	Bark	Aqueous extract
	Stem bark	Methanol extract
Antifungal	Bark, fruits and leaves	Petroleum ether, ethyl acetate and methanol extracts
Anti-inflammatory	Bark	Ethanol extract
Antioxidant	Leaves	Methanol extract
	Stem bark	Methanol extract

Table 2-4 Pharmacological activities of *M. elengi* (continued).

Phamacological activities	Plant parts	Extracts/Compounds
Diuretic	Bark	Ethyl acetate, ethanol, methanol and aqueous extracts
Gastroprotective	Bark	Ethyl acetate extract
Hypotensive	Bark	Methanol extract

Several compounds isolated from various parts of this plant are shown in Table 2-5 with the corresponding structures shown in Figure 2-2.

Table 2-5 Compounds isolated from various parts of *M. elengi*

Group of compounds	Plant parts	Chemical names	References
Flavonoids	Seeds	2,3-Dihydro-3,3′,4′,5,7-pentahydroxyflavone **(1)**	Hazra *et al*., 2007
		3,3′,4′,5,7-Pentahydroxyl-flavone **(2)**	Hazra *et al*., 2007; Sahu, 1996
Triterpenoids	Stem barks	Betulinic acid **(3)**	Ng *et al*., 1997; Baliga, *et al*., 2011
		Mimusopfarnanol **(4)**	Akhtar *et al*., 2009
		Lupeol **(5)**	Baliga, *et al*., 2011
		3β-hydroxy-lup-20(29)-ene-23,28-dioic acid **(6)**	Jahan, *et al*., 1995
		Ursolic acid **(7)**	Misra and Mitra, 1968; Baliga, *et al*., 2011
Triterpenoids	Seeds	Mimusopgenone **(8)**	Sen *et al*., 1995; Baliga, *et al*., 2011
		Mimugenone **(9)**	Sen *et al*., 1995; Baliga, *et al*., 2011

Table 2-5 Compounds isolated from various parts of *M. elengi* (continued)

Group of compounds	Plant parts	Chemical name	References
Triterpenoid saponins	Bark and seeds	Bassic acid **(10)**	Hazra *et al*., 2007; Sahu, *et al*., 1995; Sahu, 1996; Akhtar *et al*., 2009
		Mimusopic acid **(11)**	Sahu, 1996
		Mimusopsic acid **(12)**	Sahu, 1996
		3-*O*-β-D-glucuronopyranoside **(13)**	Sahu, *et al*., 1995
		Mimusopside A **(14)**	Sahu, 1996; Baliga, *et al*., 2011
		Mimusopside B **(15)**	Sahu, 1996; Baliga, *et al*., 2011
		Protobassic acid **(16)**	Sahu, 1996; Baliga, *et al*., 2011
		Mi-glycoside **(17)**	Sahu, 1996; Baliga, *et al*., 2011
		Methyl ester of mi-glycoside **(18)**	Sahu, 1996
		Prosapogenin **(19)**	Sahu, 1996
		Mi-saponin A **(20)**	Sahu, *et al*., 1995; Lavaud, *et al*., 1996; Sahu, *et al*., 1997; Eskander *et al*., 2006; Baliga, *et al*., 2011
		16α-Hydroxy-mi-saponin A **(21)**	Lavaud, *et al*., 1996; Sahu, *et al*., 1997; Baliga, *et al*., 2011
		Arganine C **(22)**	Lavaud, *et al*., 1996
		Butyroside C **(23)**	Lavaud, *et al*., 1996
		Tieghemelin A **(24)**	Lavaud, *et al*., 1996; Sahu, *et al*., 1996; Baliga, *et al*., 2011

Table 2-5 Compounds isolated from various parts of *M. elengi* (continued)

Group of compounds	Plant parts	Chemical name	References
Triterpenoid saponins	Bark and seeds	Mimusopin **(25)**	Sahu, *et al.*, 1995; Lavaud, *et al.*, 1996; Sahu, *et al.*, 1996; Baliga, *et al.*, 2011
		Mimusopsin **(26)**	Sahu, *et al.*, 1995; Lavaud, *et al.*, 1996; Sahu, *et al.*, 1996; Sahu, *et al.*, 1997; Baliga, *et al.*, 2011
		Mimusin **(27)**	Sahu, *et al.*, 1997; Baliga, *et al.*, 2011
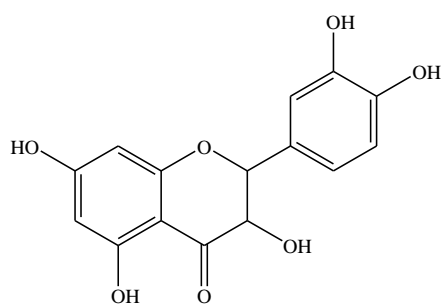
2,3-Dihydro-3,3′,4′,5,7-pentahydroxyflavone **(1)**
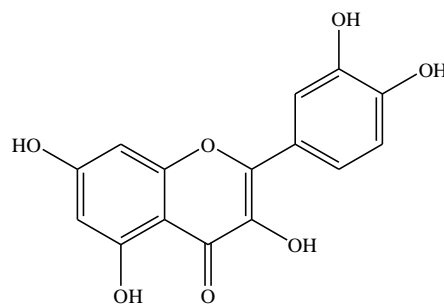
3,3′,4′,5,7-Pentahydroxyflavone **(2)**
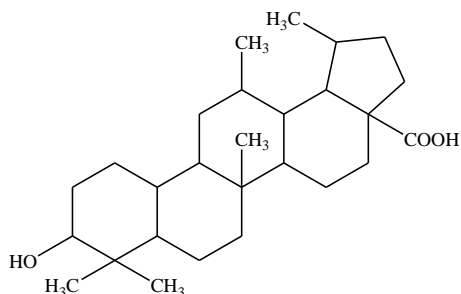
Betulinic acid **(3)**
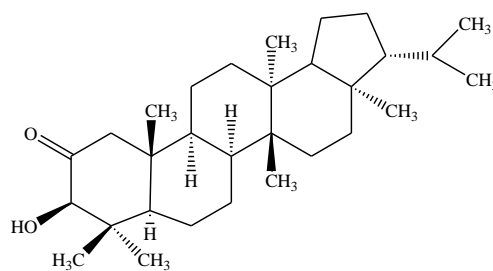
Mimusopfarnanol **(4)**
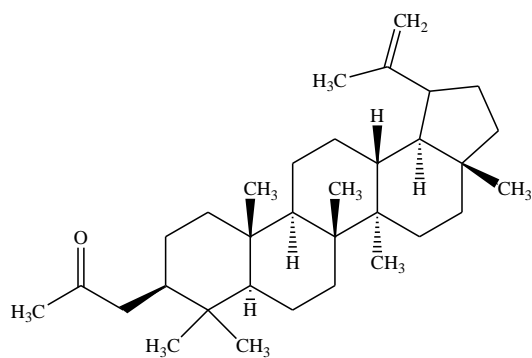
Lupeol **(5)**
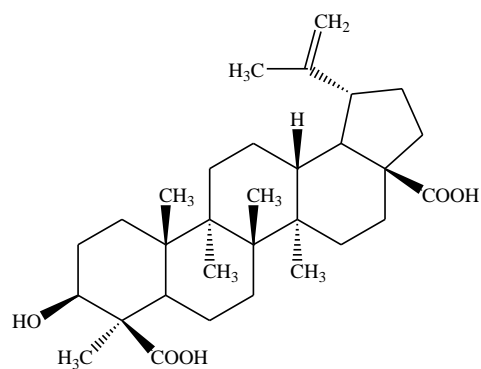
3β-Hydroxy-lup-20(29)-ene-23,28-dioic acid **(6)**
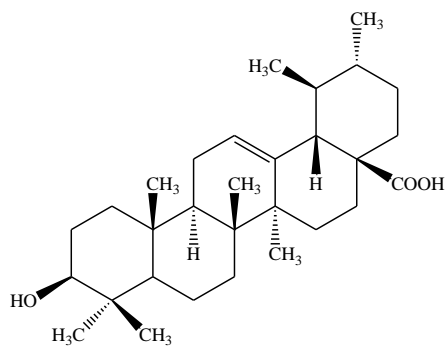
Ursolic acid **(7)**
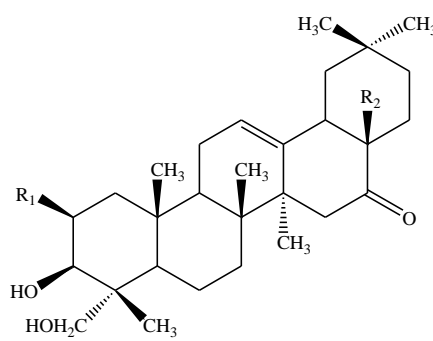
R_1= OH, R_2= H   :   Mimusopgenone **(8)**

R_1= H, R_2= CH_3 :   Mimugenone **(9)**

Figure 2-2 Chemical structures of the compounds shown in Table 2-5

Bassic acid (10)

Mimusopic acid (11)

Mimusopsic acid (12)

3-*O*-β-D-glucuronopyranoside (13)
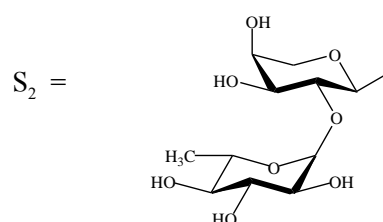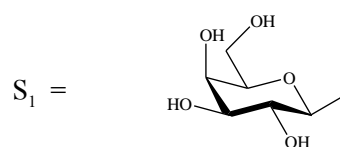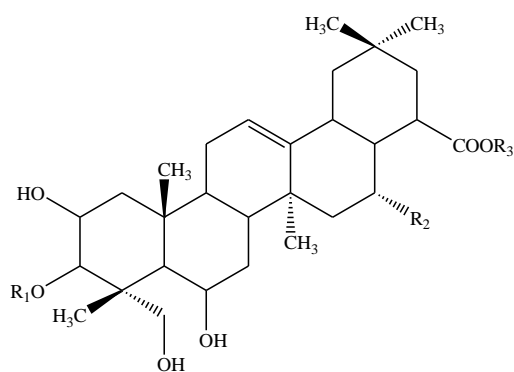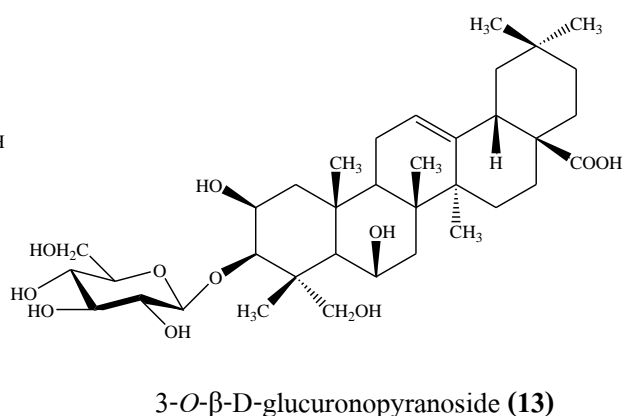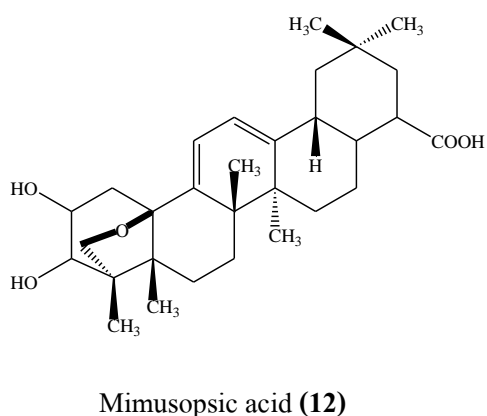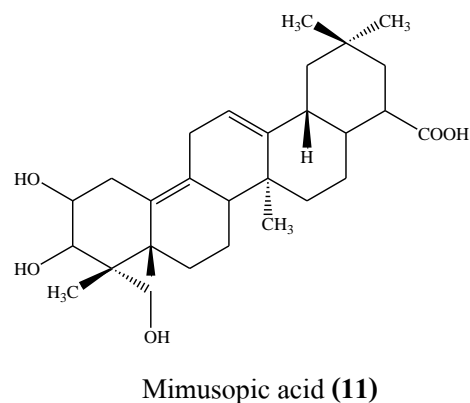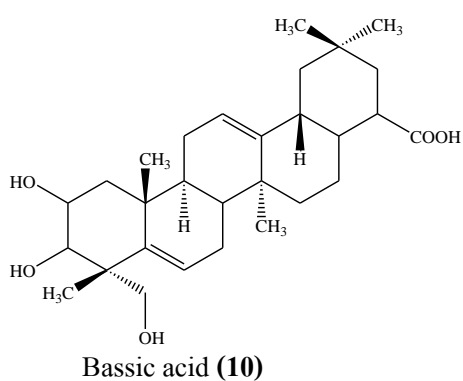
$R_1= S_1$,	$R_2= H$,	$R_3= S_2$	: Mimusopside A (14)
$R_1= S_1$,	$R_2= OH$,	$R_3= S_2$	: Mimusopside B (15)
$R_1= H$,	$R_2= H$,	$R_3= H$	: Protobassic acid (16)
$R_1= S_1$,	$R_2= H$,	$R_3= H$	: Mi-glycoside (17)
$R_1= S_1$,	$R_2= H$,	$R_3= CH_3$	: Methyl ester of mi-glycoside (18)
$R_1= S_1$,	$R_2= OH$,	$R_3= H$	: Prosapogenin (19)

Figure 2-2 Chemical structures of the compounds shown in Table 2-5 (continued)
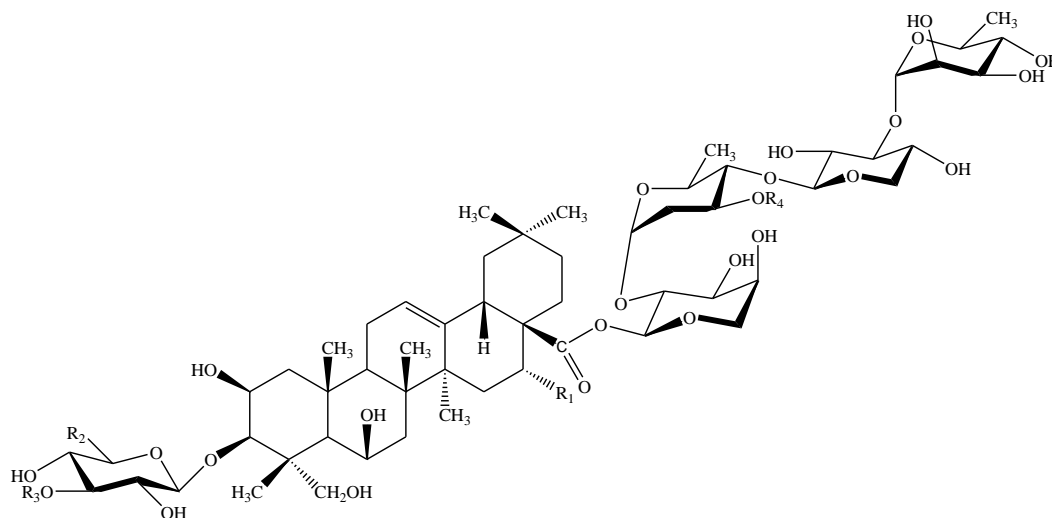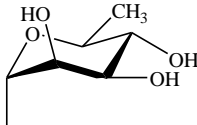
R₁= H,   R₂= CH₂OH,   R₃= H,   R₄= H : Mi-saponin A **(20)**
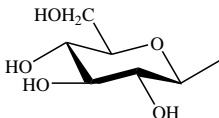
R₁= OH, R₂= CH₂OH,   R₃= H,   R₄= H : 16α-Hydroxy-mi-saponin A **(21)**

R₁= OH, R₂= CH₂OH,   R₃= H,   R₄= H : Arganine **C (22)**

R₁= H,   R₂= COOH,   R₃= H,   R₄= H : Butyroside **C (23)**

R₁= OH, R₂= COOH,   R₃= H,   R₄= H : Tieghemelin A **(24)**

R₁= H,   R₂= COOH,   R₃= H,   R₄=   : Mimusopin **(25)**

R₁= H,   R₂= CH₂OH,   R₃=   , R₄= H : Mimusopsin **(26)**
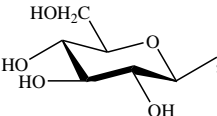
R₁= H,   R₂=   ,   R₃= H   , R₄= H : Mimusin **(27)**

Figure 2-2 Chemical structures of the compounds shown in Table 2-5 (continued)

There have been several reports on chemical constituents isolated from other *Mimusops* spp. The compounds are shown in Table 2-6 with the corresponding structures shown in Figure 2-3.

Table 2-6 Compounds isolated from various parts of other *Mimusops* spp.

Plants / Group of compounds	Plant parts	Chemical names	References
M. hexandra / Long-chain hydrocarbon	Leaves	Hentriacontane **(28)**	Misra and Mitra, 1968
M. hexandra / Phenolic acid	Leaves	Cinnamic acid **(29)**	Misra and Mitra, 1968
M. manilkara / Flavonoids	Seeds	Dihydroquercetin **(30)**	Misra and Mitra, 1969
		Quercetin **(31)**	Misra and Mitra, 1969
M. hexandra, *M. manilkara* / Triterpenoid saponins	Barks, fruits and roots	α-Spinasterol **(32)**	Misra and Mitra, 1966; Misra and Mitra, 1968; Misra and Mitra, 1969
	Fruits and roots	β-Amyrin **(33)**	Misra and Mitra, 1968; Misra and Mitra, 1969
		α-Amyrin **(34)**	Misra and Mitra, 1968; Misra and Mitra, 1969
M. hexandra / Triterpenoid saponins	Barks and root	Taraxerol **(35)**	Misra and Mitra, 1966; Misra and Mitra, 1968
	Barks	Taraxeryl acetate **(36)**	Misra and Mitra, 1966
		α-Amyrin cinnamate **(37)**	Misra and Mitra, 1966
	Roots	Quercitol	Misra and Mitra, 1968
M. hexandra / Triterpenoid acid	Mesocarp	Ursolic acid	Misra and Mitra, 1968; Baliga, *et al*., 2011
M. hexandra, *M. manilkara* / Triterpenoid saponins	Fruits and roots	β-Sitosterol-β-D-glucoside **(38)**	Misra and Mitra, 1968; Misra and Mitra, 1969

Table 2-6 Compounds isolated from various parts of other *Mimusops* spp. (continued)

Plants / Group of compounds	Plant parts	Chemical names	References
M. hexandra, *M. manilkara* / Triterpenoid saponins	Seeds	β-D-xylopyranosyl(1→4) [α-L-rhamnopyranosyl- (1→3)] α-l-rhamnopyranosyl(1→2) α-L-arabino- pyranosyl) protobassic acid	Lavaud *et al*., 1996
		3-*O*-(β-D-glucuronopyranosly)-28-*O*-(α-L-rhamnopyra-nosyl(1→3) β-D-xylopyranosyl(1→4) α-L-rhamnopyranosyl (1→2) α-L-arabinopyranosyl)16-α-hydroxy protobassic acid	Lavaud *et al*., 1996
		3-*O*-(β-D-glucopyranosyl(1→3)-β-D-glucopyranosyl)-28-*O*-(α-L-rhamnopyranosyl(1→3)-β-D-xylopyranosyl-(1→4) α-L-rhamnopyranosyl (1→2)-α-L-arabinopyranosyl protobassic acid	Lavaud *et al*., 1996
M. laurifolia / Triterpenoid saponins	Seeds	Arganine A **(39)**	Eskander *et al*., 2006
		Arganine C	Lavaud *et al*., 1996; Eskander *et al*., 2006
		Arganine D **(40)**	Eskander *et al*., 2006
		Butyroside C	Lavaud *et al*., 1996; Eskander *et al*., 2006
		Mi-saponin A	Eskander *et al*., 2006
		Tieghemelin A	Eskander *et al*., 2006
		3-*O*-(β-D-apiofuranosyl-(1→3)-β-D-glucuronopyranosyl)-28-*O*-(α -L-rhamnopyranosyl-(1→ 3)-β-D-xylopyranosyl-(1→4)-α-L-rhamnopyranosyl-(1→2)-α- Larabinopyranosyl)-16-α-hydroxyprotobassic acid **(41)**	Eskander *et al*., 2006

Table 2-6 Compounds isolated from various parts of other *Mimusops* spp. (continued)

Plants / Group of compounds	Plant parts	Chemical names	References
M. laurifolia / Triterpenoid saponins	Seeds	3-*O*-(β-D-glucopyranosyl-(1⟶3)-β -D-glucopyranosyl)-28-*O*-(α-L-rhamnopyranosyl-(1⟶3)-β-D-xylopyranosyl-(1⟶4)-α-L-rhamnopyranosyl-(1⟶2)-α-L-arabinopyranosyl)-16-α-hydroxyprotobassic acid **(42)**	Eskander *et al.*, 2006
		3-*O*-(β-D-glucopyranosyl-(1⟶6)-β-D-glucopyranosyl-(1⟶6)-β-D-glucopyranosyl)-28-*O*-(α-L-rhamnopyranosyl-(1⟶ 3)-β-D-xylopyranosyl-(1⟶4)-α-L-rhamnopyranosyl-(1⟶2)-α-L-arabinopyranosyl)-16-α-hydroxyprotobassic acid **(43)**	Eskander *et al.*, 2006

Hentriacontane (28)

Cinnamic acid **(29)**   Dihydroquercetin **(30)**

Quercetin **(31)**   α-Spinasterol **(32)**

β-Amyrin **(33)**   α-Amyrin **(34)**

Taraxerol **(35)**   Taraxeryl acetate **(36)**

Figure 2-3 Chemical structures of the compounds shown in Table 2-6

α-Amyrin cinnamate **(37)**   β-Sitosterol-β-D-glucoside **(38)**
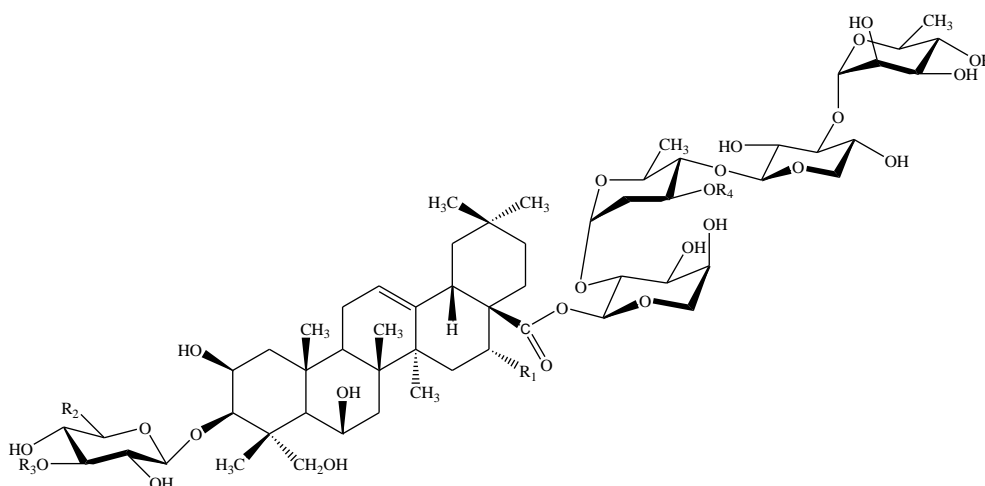
R_1= OH, R_2= CH$_2$O-β-D-glucose, R_3= H, R_4= H : Arganine **A (39)**

R_1= H, R_2= CH$_2$O-β-D-glucose, R_3= H, R_4= H : Arganine **D (40)**

R_1= OH, R_2= COOH, R_3= β-D-apiose, R_4= H : 3-*O*-(β-D-apiofuranosyl-(1→3)-β-D-glucuronopyranosyl)-28-*O*-(α -L-rhamnopyranosyl-(1→ 3)-β-D-xylopyranosyl-(1→4)-α-L-rhamnopyranosyl-(1→2)-α -L-arabinopyranosyl)-16-α–hydroxylprotobassic acid **(41)**

R_1= OH, R_2= C H$_2$OH, R_3= β-D-glucose, R_4= H : 3-*O*-(β-D-glucopyranosyl-(1→3)-β-D-glucupyranosyl)-28-*O*-(α-L-rhamnopyranosyl-(1→ 3)-β-D-xylopyranosyl-(1→4)-α-L-rhamnopyranosyl-(1→2)-α-L-arabinopyranosyl)-16-α-hydroxylprotobassic acid **(42)**

R_1= OH, R_2= CH$_2$O-β-D-glucose(6→1)β-D-glucose, R_3= H, R_4= H : 3-*O*-(β-D-glucopyranosyl-(1→6)-β-D-glucopyranosyl-(1→6)-β-D-glucopyranosyl)-28-*O*-(α-L-rhamno-pyranosyl-(1→3)-β-D-xylopyranosyl-(1→4)-α-L-rhamnopyranosyl-(1→2)-α-L-arabinopyra-nosyl)-16-α-hydroxyprotobassic acid **(43)**

Figure 2-3 Chemical structures of the compounds shown in Table 2-6 (continued)

2.4 *Pometia pinnata* J. R. Forst. & G. Forst.

Pometia pinnata is a small to very large tree up to 50 m belonging to family Sapindaceae (Figure 2-4). The leaves are paripinnate, the rachis up to 1 m long, or rarely longer, with 4–8 subopposite pairs of sub-sessile leaflets. Leaflets are firmly herbaceous to coriaceous, asymmetrical to symmetrical, variably shaped (oblong/lanceolate/ovate). The floral inflorescences are highly variable. They include clusters of terminal, sub-terminal, or rarely axillary panicles, conspicuously projecting beyond the foliage, from stiff to hanging, 15–70 cm long main branches, simple or with secondary branching. The fruits are highly variable, indehiscent (not splitting), round to elliptical, sometimes paired, and often with one or more vestigial ovary lobes at the base, 1.5–5 cm long by 1–4.5 cm diameter, the skin or pericarp smooth and variously colored (greenish-yellow, yellow, red, purple, blackish or brown) with a gelatinous, sweet, white to slightly pinkish, translucent pulp (mesocarp) partially encasing a single large seed. The seeds are large, to 2.5 cm long by 1.5 cm across, flattened and rounded on the ends, and brown (Thomson and Thaman, 2006).

Figure 2-4 *Pometia pinnata* J. R. Forst. & G. Forst. (Sapindaceae)

The leaves and barks are used for treatment of fever. *P. pinnata* is also used in as traditional medicines in the South Pacific Kingdom of Tonga for the treatment of mouth infections, abdominal ailments, unclosed fontanel, obstetric and gynaecological complaints. It has been reported that saponins isolated from *P. eximia* exhibited molluscicidal, insecticidal, antifungal, and antibacterial activities (Jayasinghe *et al.*, 1995, Voutquenne *et al.*, 2003). Until now, there have been very few studies on the chemical composition and pharmacological activities of this plant. There is only one report on the isolation of a new triterpenoidal saponin, namely pometin (Figure 2-5) from the stem bark of *P. pinnata* (Mohammad *et al.*, 2010). In addition, it has been reported that the leaf extracts of *P. pinnata* possessed antifungal activity against *Phytophthora infestans* (Suprapta *et al.*, 2002), and wood and bark extracts showed antioxidant and antifungal activities against *Gleophyllum trabeum* and *Pycnoporus sanguineus* (Kawamura *et al.*, 2010).
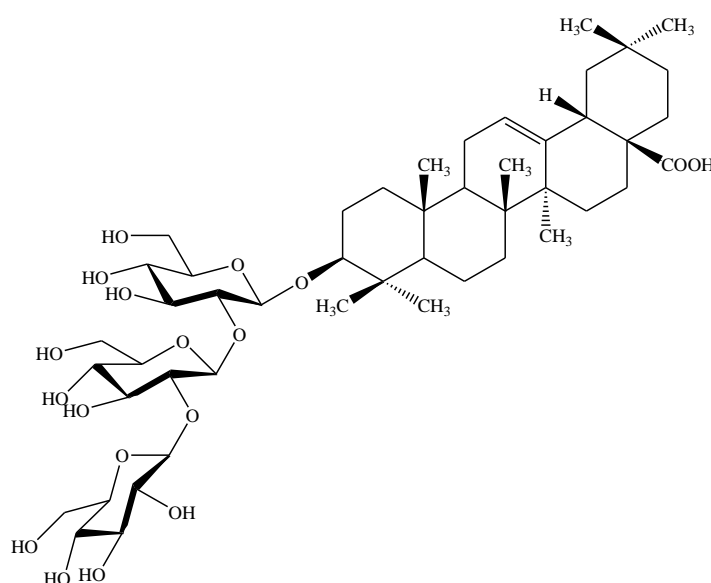
Figure 2-5 Chemical structure of pometin

There have been several reports on chemical constituents isolated from other *Pometia* spp.

The compounds are shown in Table 2-7 with corresponding structures shown in Figure   2-6.

Table 2-7 Compounds isolated from various parts of other *Pometia* spp.

Plants / Group of compounds	Plant parts	Chemical names	References
P. eximia / Triterpenoid glycoside	Stems	Hederagenin **(1)**	Jayasinghe *et al*., 1995
		3-*O*-α-L-arabinopyranosyl **(2)**	Jayasinghe *et al*., 1995
		3-*O*-β-D-xylopyranosyl-(1⟶3)-α-L-arabinopyrano-syl hederagenin **(3)**	Jayasinghe *et al*., 1995
		3-*O*-α-L-arabinofuranosyl-(1⟶3)-[α-L-rhamnopyra-nosyl-(1⟶2)]-β-D-xylopyranosyl hederagenin **(4)**	Jayasinghe *et al*., 1995
		3-*O*-β-D-apinosyl-(1⟶3)-[α-L-rhamnopyranosyl-(1⟶2)]-β-D-glucopyranosyl hederagenin **(5)**	Jayasinghe *et al*., 1995
		3-*O*-α-L-arabinofuranosyl-(1⟶3)-[α-L-rhamnopyra-nosyl-(1⟶2)]-β-L-arabinopyranosyl hederagenin **(6)**	Jayasinghe *et al*., 1995
		3-*O*-α-D-xylopyranosyl-(1⟶3)-[α-L-rhamnopyra-nosyl-(1⟶2)]-α-L-arabinopyranosyl hederagenin **(7)**	Jayasinghe *et al*., 1995
		3-*O*-β-D-xylopyranosyl-(1⟶3)-[α-L-rhamnopyra-nosyl-(1⟶2)]-β-D-glucopyranosyl hederagenin **(8)**	Jayasinghe *et al*., 1995
		3-*O*-β-D-galactopyranosyl-(1⟶3)-[α-L-rhamnopyra-nosyl-(1⟶2)]-β-D-glucopyranosyl hederagenin **(9)**	Jayasinghe *et al*., 1995
		28-*O*-β-D-apinosyl-(1⟶2)-β-D-glucopyranosyl hederagenin **(10)**	Jayasinghe *et al*., 1995
P. ridleyi / Saponins	Barks	Acutoside A	Voutquenne *et al*., 2003
		Calenduloside C	Voutquenne *et al*., 2003
P. ridleyi / Triterpenoid saponins	Barks	3-*O*-β-D-glucopyranosyl-(1⟶2)-β-D-glucopyrano-syl oleanoic **(11)**	Voutquenne *et al*., 2003

Table 2-7 Compounds isolated from various parts of other *Pometia* spp. (continued)

Plants / Group of compounds	Plant parts	Chemical names	References
P. ridleyi / Triterpenoid saponins	Barks	3-*O*-β-D-apifuranosyl-(1⟶3)-[β-D-glucopyranosyl-(1⟶2)]-β-D-glucopyranosyl oleanoic acid **(12)**	Voutquenne *et al*., 2003
		3-*O*-β-D-apifuranosyl-(1⟶3)-α-L-arabinopyranosyl-(1⟶3)-[β-D-glucopyranosyl-(1⟶2)]-β-D-gluco-pyranosyl oleanoic acid **(13)**	Voutquenne *et al*., 2003
		3-*O*-β-D-galactopyranosyl-(1⟶3)-[β-D-glucopyra-nosyl-(1⟶2)]-β-D-glucopyranosyl oleanoic acid **(14)**	Voutquenne *et al*., 2003
		3-*O*-β-D-apifuranosyl-(1⟶3)-β-D-galactopyranosyl (1⟶3)-[β-D-glucopyranosyl-(1⟶2)]-β-D-glucopy-ranosyl oleanoic acid **(15)**	Voutquenne *et al*., 2003
		3-*O*-α-L-arabinofuranosyl-(1⟶3)-[β-D-glucopyrano-syl-(1⟶2)]-α-L-arabinopyranosyloleanoic acid **(16)**	Voutquenne *et al*., 2003
		3-*O*-β-D-galactopyranosyl-(1⟶3)-[β-D-glucopyra-nosyl-(1⟶2)]-α-L-arabinopyranosyl oleanoic acid **(17)**	Voutquenne *et al*., 2003
		3-*O*-β-D-arabinofuranosyl (1⟶3)-β-D-galactopyra-nosyl-(1⟶3)-[β-D-glucopyranosyl(1⟶2)]-α-L-arabinopyranosyl oleanoic acid **(18)**	Voutquenne *et al*., 2003

R= H Hederagenin **(1)**

R= Ara— 3-*O*-α-L-arabinopyranosyl **(2)**

R= Xyl—Ara— 3-*O*-β-D-xylopyranosyl-(1⟶3)-α-L-arabinopyranosyl hederagenin **(3)**

R= Rha—Xyl— 3-*O*-α-L-arabinofuranosyl-(1⟶3)-[α-L-rhamnopyranosyl (1⟶2)]-β-D-
|
Ara(*f*) xylopyranosyl hederagenin **(4)**

R= Rha—Glu — 3-*O*-β-D-apinosyl-(1⟶3)-[α-L-rhamnopyranosyl-(1⟶2)]-β-D-
|
Api glucopyranosyl hederagenin **(5)**

R= Rha—Ara*— 3-*O*-α-L-arabinofuranosyl-(1⟶3)-[α-L-rhamnopyranosyl-(1⟶2)]-β-L-
|
Ara(*f*) arabinopyranosyl hederagenin **(6)**

R= Rha—Ara— 3-*O*-α-D-xylopyranosyl-(1⟶3)-[α-L-rhamnopyranosyl-(1⟶2)]-α-L-
|
Xyl arabinopyranosyl hederagenin **(7)**

R= Rha—Glu— 3-*O*-β-D-xylopyranosyl-(1⟶3)-[α-L-rhamnopyranosyl (1⟶2)]-β-D-
|
Xyl glucopyranosyl hederagenin **(8)**

R= Rha—Glu— 3-*O*-β-D-galactopyranosyl-(1⟶3)-[α-L-rhamnopyranosyl-(1⟶2)]-β-D-
|
Gal glucopyranosyl hederagenin **(9)**

Figure 2-6 Chemical structures of the compounds shown in Table 2-7
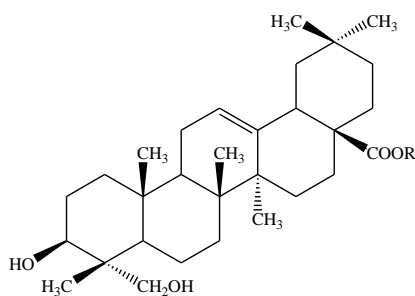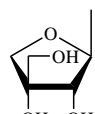
R= Api—Glu—   28-*O*-β-D-apinosyl-(1→2)-β-D-glucopyranosyl hederagenin **(10)**
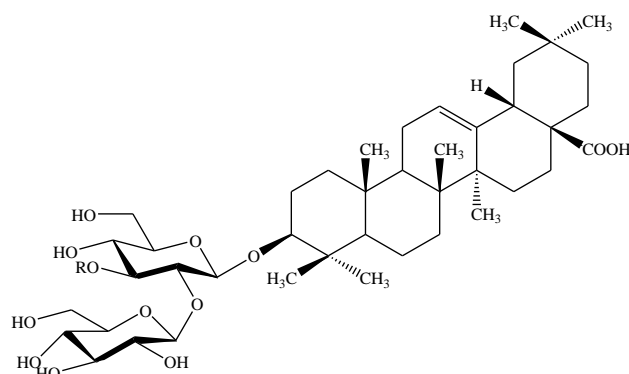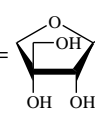
R = H   3-*O*-β-D-glucopyranosyl-(1→2)-β-D-glucopyranosyl oleanoic acid **(11)**
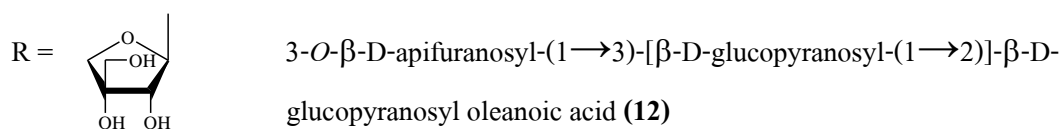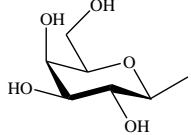
R =   3-*O*-β-D-apifuranosyl-(1→3)-[β-D-glucopyranosyl-(1→2)]-β-D-

glucopyranosyl oleanoic acid **(12)**
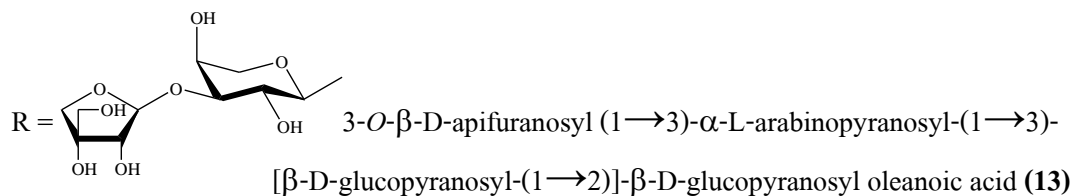
R =   3-*O*-β-D-apifuranosyl (1→3)-α-L-arabinopyranosyl-(1→3)-

[β-D-glucopyranosyl-(1→2)]-β-D-glucopyranosyl oleanoic acid **(13)**
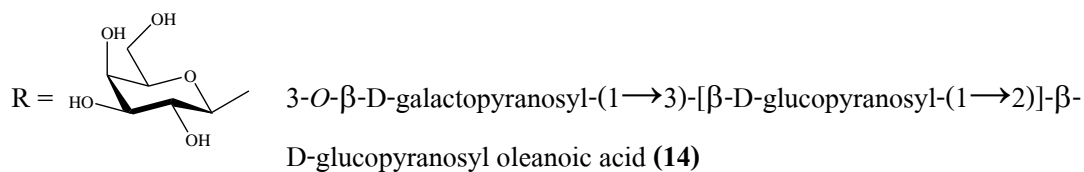
R =   3-*O*-β-D-galactopyranosyl-(1→3)-[β-D-glucopyranosyl-(1→2)]-β-
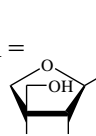
D-glucopyranosyl oleanoic acid **(14)**
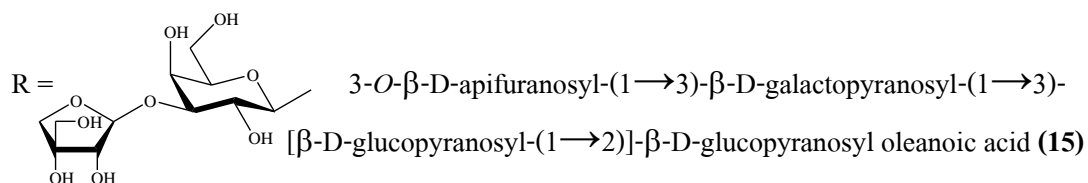
R =   3-*O*-β-D-apifuranosyl-(1→3)-β-D-galactopyranosyl-(1→3)-

[β-D-glucopyranosyl-(1→2)]-β-D-glucopyranosyl oleanoic acid **(15)**

Figure 2-6 Chemical structures of the compounds shown in Table 2-7 (continued)

R =   3-*O*-α-L-arabinofuranosyl-(1⟶3)-[β-D-glucopyranosyl-(1⟶2)]-α-L-arabinopyranosyl oleanoic acid **(16)**

R =   3-*O*-β-D-galactopyranosyl-(1⟶3)-[β-D-glucopyranosyl-(1⟶2)]-α-L-arabinopyranosyl oleanoic acid **(17)**

R =   3-*O*-β-D-arabinofuranosyl-(1⟶3)-β-D-galactopyranosyl-(1⟶3)-[β-D-glucopyranosyl(1⟶2)]-α-L-arabinopyra-nosyl oleanoic acid **(18)**
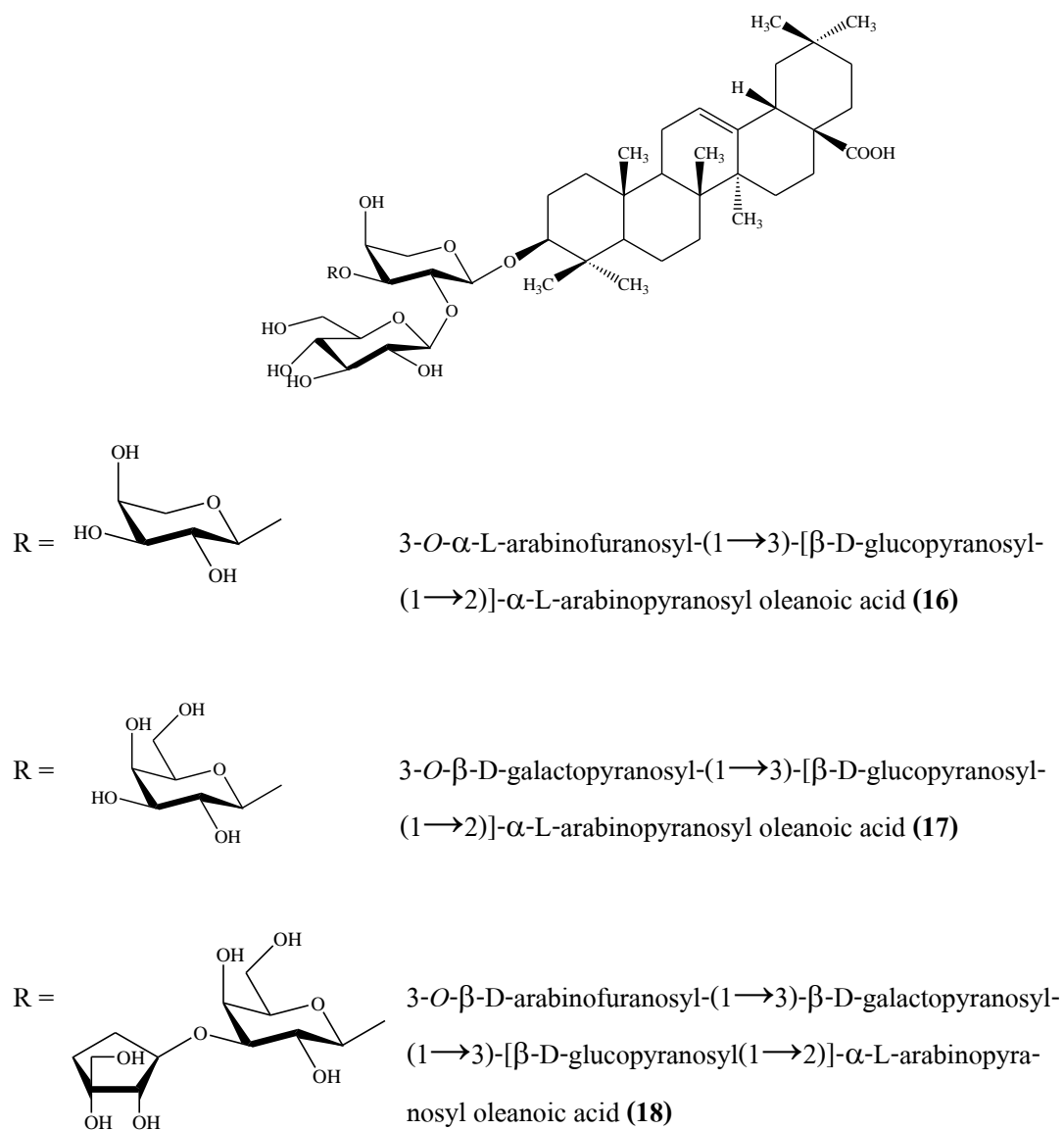
Figure 2-6 Chemical structures of the compounds shown in Table 2-7 (continued)

CHAPTER 3

MATERIALS AND METHODS

3.1 Instruments

The equipments used in this study were listed in Table 3-1.

Table 3-1 General information of equipments

Equipments	Company, Country
Autoclave	Model HA-3D, Hirayama, Japan
Balance	Explorer, OHAUS Corp, USA
Hot air oven	Memmert, Schwubuch, Germany
HPLC spectrophotometer	Agilent 1100 series Photodiode-array detector, International Equipment Trading Ltd., USA.
HPLC analytical column	Phenomenex® Luna Hilic column 5 μm, 4.6 mm × 15 cm, Phenomenex, USA
IR spectrophotometer	JASCO-IR-810, Japan Spectroscopic, Japan
Mass spectrometer	MAT95 XL MS, Thermofinigan , Egelsbach, Germany
Melting point apparatus	Buchi 520, Switzerland
Microfilter	0.45 μm, 0.22 μm, Whatman, GE healthcare, UK
Microplate reader	Biotek Power-x BioTex Instruments, USA
Micropipette	Socorex, Switzerland; Pipetman, France
Microwave ovens	LG Electronics Inc., Thailand
NMR spectrometer	Fourier Transform NMR spectrometer 500 MHz, Unity Inova, Varian, German
Refrigerator	(4˚C) Sanden Intercool, Thailand; (-20˚C) Whirlpool, Thailand
Rotary evapporator	Aspirator A-3S, EYELA, Tokyo, Japan
Sonicator	Crest Ultrasonic Corporation, USA
TLC- plate silica gel GF$_{254}$	Merck, Germany

Table 3-1 General information of equipments (continued)

Equipments	Company, Country
TLC- plate RP-18 F$_{254s}$	Merck, Germany
UV-VIS spectrophotometer	Genesis-6, Thermo scientific, USA
Vacuum pump	Vacuubrand, Wertheim, Germany
Vortex	Vortex-Genie 2TM, USA

3.2 Chemicals

The chemicals used in this study were listed in Table 3-2 to Table 3-4.

Table 3-2 For extraction and purification

Chemicals	Company, Country
Acetone, commercial grade	Lab-scan Asia Co., Ltd., Bangkok, Thailand
Anisaldehyde	Fluka, Biochemica, Switzerland
Chloroform, commercial grade	Lab-scan Asia Co., Ltd., Bangkok, Thailand
Ethanol (95% v/v)	MAT95 XL MS, Thermofinigan
Ethyl acetate, commercial grade	Lab-scan Asia Co., Ltd., Bangkok, Thailand
Hexane, commercial grade	Lab-scan Asia Co., Ltd., Bangkok, Thailand
Methanol, commercial grade	Lab-scan Asia Co., Ltd., Bangkok, Thailand
Silica gel 60 (SiO$_2$ 60, 230-400 mesh)	Merck, Germany

*All commercial grade organic solvents were distilled before used.

Table 3-3 For anti-HIV-1 IN activity

Chemicals	Company, Country
Alkaline phosphatase (AP) labelled anti-digoxigenin antibody	Lab-scan Asia Co., Ltd., Bangkok, Thailand
Bovine serum albumin	Fluka, Biochemica, Switzerland
Dithiothritol (DTT)	Nacalai Tesque, Inc. Kyoto, Japan
Dimethyl sulfoxide (DMSO)	Lab-scan Asia Co., Ltd., Bangkok, Thailand

Table 3-3 For anti-HIV-1 IN activity (continued)

Chemicals	Company, Country
Ethylenediaminetetraacetate disodium salt (EDTA, 2Na)	Nacalai Tesque, Inc. Kyoto, Japan
Glycerol	Sigma-Aldrich Co., USA
Integrase enzyme	National Institute of Health, Bethesda, Maryland, USA.
Magnesium chloride ($MgCl_2$)	Nacalai Tesque, Inc. Kyoto, Japan
2-Mercaptoethanol (β-mercaptoethanol)	Sigma-Aldrich Co., USA
Monoclonal anti-digoxin-alkaline phosphatase	Sigma-Aldrich Co., USA
3-*(N*-morpholino) propane sulfonic acid (MOPS)	Sigma-Aldrich Co., USA
Nonidet-P 40 (NP-40) or Igepal CA-630	Sigma-Aldrich Co., USA
p-nitrophenyl phosphate	Sigma-Aldrich Co., UK
Potassium chloride (KCl)	Nacalai Tesque, Inc. Kyoto, Japan
Sodium carbonate (Na_2CO_3)	Nacalai Tesque, Inc. Kyoto, Japan
Sodium hydrogen carbonate ($NaHCO_3$)	Nacalai Tesque, Inc. Kyoto, Japan
Sodium chloride (NaCl)	Lab-scan Asia Co., Ltd., Bangkok, Thailand
skim milk	Difco, Becton Dickinson and company, USA
Sulfuric acid	Lab-scan Asia Co., Ltd., Bangkok, Thailand
Streptavidin	Invitrogen, USA
Suramin	Sigma-Aldrich Co., USA
Tris-HCl	Sigma-Aldrich Co., USA
Tween 20	Sigma-Aldrich Co., USA
Urea	Nacalai Tesque, INC. Kyoto, Japan

Table 3-4 For HPLC analysis

Chemicals	Company, Country
Acetic acid, glacial	Lab-scan Asia Co., Ltd., Bangkok, Thailand
Acetonitrile, HPLC grade	Lab-scan Asia Co., Ltd., Bangkok, Thailand
Epigallocatechin	Sigma-Aldrich Co., USA
Gallocatechin	Sigma-Aldrich Co., USA
Mill-Q grade water was purified in a Mill-Q system	Milipore, Bedford, USA
Methanol, HPLC grade	Lab-scan Asia Co., Ltd., Bangkok, Thailand

3.3 Plants materials

Sixteen plants (Table 4-1) were collected from the Hat-Yai District, Songkhla Province, Thailand, in August 2010. Voucher specimens were deposited in the herbarium of the Faculty of Pharmaceutical Sciences, Prince of Songkla University, Thailand. These plants were dried at 50 $^{\circ}$C for 24 hours in a hot air oven and were reduced to coarse powders using a grinder.

3.4 Preparation of the plant extract for screening HIV-1 IN inhibitory activity of Thai plants

Plant material were dried at 50 $^{\circ}$C, powdered (10 g) were separately extracted with ethanol (100 ml) under reflux conditions for 30 min (×2). The pooled ethanol extracts were evaporated under reduced pressure to give dried crude ethanol extracts and dissolved in 50% DMSO for bioassay. Sample solutions of these extracts were prepared in the concentration ranging from 1-100 µg/mL.

3.5 Assay of HIV-1 IN inhibitory activity

3.5.1 Enzyme

The HIV-1 IN protein was kindly provided by Dr.Robert Craigie, National Institute of Health, Bethesda, Maryland, USA. This enzyme was expressed in *Escherichia coli* and purified according to the method described in (Goldgur *et al.*,1999), and stored at -80°C before use.

3.5.2 Oligonucleotide substrates

Oligonucleotides of long terminal repeat donor DNA (LTR-D) and target substrate (TS) DNA were purchased from QIAGEN Operon, USA and stored at -25°C before use. The sequence of biotinylated LTR donor DNA and its unlabelled complement were 5'-biotin-ACC-CTTTTAGTCAGTGTGGAAAATCTCTAGCAGT-3' (LTR-D1) and 3'-GAAAATCAGTCAC-ACCTTTTAGAGATCGTCA-5' (LTR-D2), respectively. Those of the target substrate DNA (digoxigeninlabelled target DNA, TS-1) and its 3'-labelled complement were 5'-TGACCAAGGGCTAATTCACT-digoxigenin and digoxigenin-ACTGGTTCCCGATTAAGTG-A-5' (TS-2), respectively.

3.5.3 Annealing of the substrate DNA

The anti-HIV-1 IN assay was carried out following the procedure described by Tewtrakul *et al.* (2001). Two separate solutions, the first containing LTR-D1 and LTR-D2, and the second containing TS-1 and TS-2 were made to concentrations of 2 pmol/µL and 5 pmol/µL, respectively, by dilution with a buffer solution [containing 10 mM Tris-HCl (pH 8.0), 1 mM EDTA and 100 mM KCl]. The LTR- and TS solutions were heated at 85°C for 15 min in an incubator. After heating, each solution was gradually cooled down to room temperature. Both solutions were then stored at -20°C until use.

3.5.4 Multiplate integration assay (MIA) procedure

3.5.4.1 Principle of MIA

MIA is the method to measure the incorporation of digoxigenin-labelled target DNA into long terminal repeat (LTR) donor DNA. For this assay, a biotin- labeled donor DNA is added into each well, which strongly bind with a streptavidin coated-well plate, followed by addition of digoxigenin-labelled target DNA, integrase enzyme and sample solution. After intergration process, the ligated two double-stranded DNA is immobilized on streptavidin coated-well and subsequently bound with an alkaline phosphatase (AP)-labeled anti-digoxigenin antibody. Finally, it is colorized by adding *p*-nitrophenyl- phosphate as a substrate. In basic solution (pH 9.5) AP hydrolyzes *p*-nitrophenol which exhibits a yellow color.

3.5.4.2 Pretreatment of the multiplate (microplate)

A 96 well plate was coated overnight with 50 µL of streptavidin solution containing 40 µg/mL streptavidin, 90 mM Na_2CO_3, and 10 mM KCl. After discarding the streptavidin coating solution, each of the coated plates was washed twice with sterilized water (270 µL) and twice with PBS solution (270 µL). The blocking buffer (270 µL) containing 1% skim milk in PBS was then added into each well, and the plate was kept at room temperature for 30 min. After discarding the blocking buffer, each well was washed three times with PBS solution (270 µL). A biotinylated - LTR donor DNA (50 µL) solution containing 10 mM Tris-HCl (pH 8.0), 1 mM NaCl, and 40 fmol/µL of LTR donor DNA was added into each well and kept at room temperature for 60 min. After discarding the LTR donor solution, the microplate was washed three times with PBS solution (270 µL) and then each well filled with 270 µL of PBS solution. Just before the integration reaction, the PBS solution of each well was discarded and each well again rinsed three times with 270 µL of distilled water.

3.5.4.3 Integration reaction

A mixture (45 µl) composed of 12 µL of IN buffer [containing 150 mM 3-*(N*-morpholino) propane sulfonic acid, pH 7.2 (MOPS), 75 mM $MnCl_2$, 5 mM dithiothritol (DTT), 25% glycerol, and 500 µg/ml bovine serum albumin], 1 µL of 5 pmol/µL digoxigenin-labelled target DNA and 32 µL of sterilized water were added into each well of the 96-well plate. Subsequently, 6 µL of plant extract sample solution and 9 µL of 1/5 dilution of the integrase enzyme was added to the plates and incubated at 37°C for 80 min. After washing the wells three times with 270 mL PBS, 100 µL of 500 mU/mL alkaline phosphatase (AP) labelled anti-digoxigenin antibody were added and incubated at 37°C for 1 h. The plates were washed again three times with 270 mL washing buffer containing 0.05% tween 20 in PBS and there after another three times with 270 mL PBS. Then, an AP buffer (150 µL) containing 100 mM Tris-HCl (pH 9.5), 100 mM NaCl, 5 mM $MgCl_2$ and 10 mM *p*-nitrophenyl phosphate was added to each well and incubated at 37°C for 1 h. Finally, the absorbance in each well was measured with a microplate reader under a wavelength of 405 nm (Figure 3-1). A control composed of a reaction mixture, 50% DMSO and integrase enzyme, while a blank was buffer-E containing 20 mM MOPS (pH 7.2), 400 mM potassium glutamate, 1 mM ethylenediaminetetraacetate disodium salt (EDTA, 2Na) 0.1% Nonidet-P 40

(NP-40), 20% glycerol, 1mM DTT, and 4 M urea without the integrase enzyme (Tewtrakul *et al.*, 2002). Suramin, an HIV‑1 IN inhibitor, was used as a positive control.

$$\% \text{ Inhibition against HIV-1 IN} = \text{OD}_{control} - \text{OD}_{sample} / \text{OD}_{control} \times 100$$

Where OD is the absorbance detected from each well at 405 nm.

3.5.4.4 Statistics

For statistical analysis, the values are expressed as mean ± S.D. of four determinations. The IC_{50} values were calculated using the Microsoft Excel program.
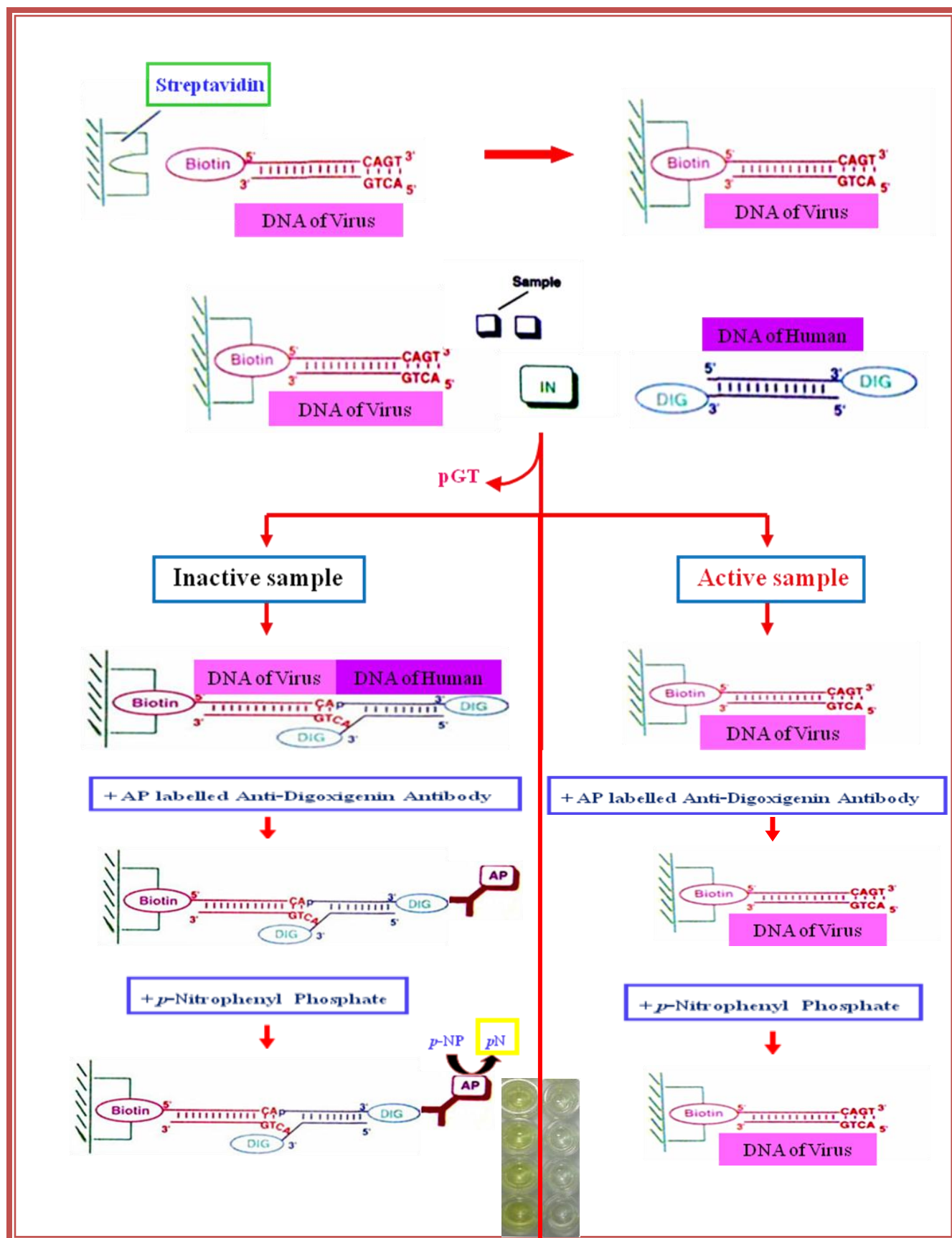
Figure 3 Diagram of the multiplate integration assay (MIA) using the 96 well plate

3.5.5 Bioassay-guided isolation

The dried plants were extracted with ethanol under reflux conditions. The dried crude ethanol extract was tested using a non-radioisotropic technique bioassay. The extract was subjected to fractionation using silica gel vacuum chromatography, sephadex LH-20 column and HPLC. The fractions that continue to demonstrate anti-HIV-1 IN activity were further purified until pure compounds with anti-HIV-1 IN activity were obtained.

3.5.6 Purification of compounds

Fractions of *M. elengi* and *P. pinnata* were purified using chromatography techniques such as silica gel column chromatography, Sephadex LH-20. After that, compounds were tested for their purification using thin layer chromatography (TLC), and the structures were interpreted using spectroscopic techniques.

3.5.6.1 Extraction and isolation of *Mimusops elengi*

The dried leaf powder of *M. elengi* (500 g) was extracted with ethanol (2.5 L × 4), under reflux conditions for 1 h, to obtain (after solvent evaporation) a greenish-brown extract (120.7 g). The crude ethanol extract was partitioned between water and ethyl acetate. The ethyl acetate fraction, was pre-adsorbed in silica gel, then applied to the top of a silica gel column (13 cm in diameter and 6 cm in height), and the column was subsequently eluted with 500 mL of solvent with the aid of a vacuum pump. Mixtures of hexane and ethyl acetate were used for column elution, using a step-gradient elution starting from 100% v/v hexane and moving towards 100% v/v ethyl acetate, followed by mixtures of ethyl acetate and methanol, from 10 to 20% v/v methanol. Based on TLC chromatograms of each fraction, eight pooled fractions (ME 1-8) were obtained. The fractions were then tested for anti-HIV-1 IN activity. The anti-HIV-1 IN active fraction (ME 7) was further purified by silica gel column chromatography (1 g extract per 40 g silica gel) eluted with mixtures of chloroform and methanol (from 9.7:0.3 to 8:2, v/v, 50 mL each) to give five pooled fractions (ME 9-13). The fractions ME12 (639 mg) and ME13 (158 mg) were further re-chromatographed on silica gel (2.5 × 35 cm) with $CHCl_3$ and MeOH (from 9.5:0.5 to 8:2, v/v, 30 mL each) to give four pooled fractions of each fractions as ME14-17 and 18-21. The fractions ME17 (399 mg) was chromatographed further using a sephadex LH-20 column (1 × 35 cm) with 100% MeOH to afford compound **1.1** and compound **1.2** (180 mg, 0.08 % yield of dried leaves weight) and fraction ME20 (109 mg) was chromatographed further using a sephadex LH-20 column

(1 × 20 cm) with 100% MeOH to afford compound **2** (69 mg, 0.014 % yield of dried leaves weight) (Scheme 3-1).

Mimusops elengi dried powered leaves 500 g

↓ Refluxed with EtOH

EtOH extract (120.7 g)

↓ Partitioned between EtOAc and water

EtOAc extract (25.5 g)

Silica gel column chromatography | Hexane:EtOAc (10-100%)⟶ EtOAc:MeOH (10-20%)

ME1	ME2	ME3	ME4	ME5	ME6	**ME7**	ME8
(1.6 g)	(4 g)	(1.8 g)	(1.3 g)	(2.1 g)	(0.3 g)	**(1.3 g)**	(1.4 g)

CHCl$_3$: MeOH (9.7: 0.3⟶ 8: 2)

ME9	ME10	ME11	**ME12**	**ME13**
(4 mg)	(5.7 mg)	(47 mg)	**(639 mg)**	**(158 mg)**

CHCl$_3$: MeOH (9.5: 0.5⟶ 8: 2) | CHCl$_3$: MeOH (9.5: 0.5⟶ 8: 2)

ME14	ME15	ME16	**ME17**	ME18	ME19	**ME20**	ME21
(4 mg)	(10.2 mg)	(43 mg)	**(399 mg)**	(4.3 mg)	(18.3 mg)	**(109 mg)**	(22.2 mg)

Sephadex (MeOH) | Sephadex (MeOH)

ME22	ME23	**ME24**	ME25	ME26	ME27	**ME28**	ME29	ME30	ME31
(27 mg)	(151 mg)	**(180 mg)**	(13 mg)	(9.6 mg)	(5.2 mg)	**(69 mg)**	(2 mg)	(1.8 mg)	(2.8 mg)
		Compound 1				**Compound 2**			

Scheme 3-1 The procedure of *Mimusops elengi* extraction

3.5.6.2 Extraction and isolation of *Pometia pinnata*

The dried leaf powder of *P. pinnata* (500 g) was extracted with ethanol (2.5 L × 4), under reflux conditions for 1 h, to obtain (after solvent evaporation) a greenish-brown extract (105 g). The crude ethanol extract was partitioned between water and ethyl acetate. The ethyl acetate fraction, was pre-adsorbed in silica gel, then applied to the top of a silica gel column (13 cm in diameter and 6 cm in height), and the column was subsequently eluted with 500 ml of solvent with the aid of a vacuum pump. Mixtures of hexane and ethyl acetate were used for column elution, using a step-gradient elution starting from 100% v/v hexane and moving towards 100% v/v ethyl acetate, and followed by mixtures of ethyl acetate and methanol, from 10 to 20% v/v methanol. Based on TLC chromatograms of each fraction (500 ml), four pooled fractions (PP1-PP5) were obtained. The fractions were then tested for anti-HIV-1 IN activity. Fractions (PP2-PP5) possessed anti-HIV-1 IN activity.

Fraction PP2 (4.6 g) was further purified by silica gel column (5.5 × 80 cm) (1 g extract per 50 g silica gel) eluted with a mixture of $CHCl_3$ and MeOH (9.8:0.2 to 8:2, v/v, 50 ml each) to give seven pooled fractions (PP6-PP12). Fractions PP11 (398 mg) and PP12 (2.7 g) were further re-chromatographed on silica gel (4.5 × 20 cm) with $CHCl_3$ and MeOH (9.5:0.5 to 8:2) to give four pooled fractions each of fractions as PP13-PP16 and PP17-PP20. The fractions PP13 (400 mg) was further purified by column chromatography (CC) with $CHCl_3$ and MeOH (9.5:0.5 to 8:2) to give two pooled fractions (PP17-PP18). Fractions PP17 (164 mg) and PP18 (186 mg) were chromatographed further using a sephadex LH-20 column (2 × 120 cm) with 100% MeOH to afford compound **3** (40 mg, 0.008 % yield of dried leaves weight) and compound **4** (10 mg, 0.002 % yield of dried leaves weight), respectively. The fraction PP27 (128 mg) was further purified by column chromatography (CC) with EtOAc and acetone (9: 1) to afford compound **5** (74 mg, 0.015 % yield of dried leaves weight).

Fraction PP3 (5.4 g) was further purified by silica gel column (5.5 × 100 cm) (1 g extract per 50 g silica gel) eluted with a mixture of hexane and EtOAC (4:6, v/v, 100 ml each) to give five pooled fractions (PP34-PP38). The fraction PP37 (4.9 g) was further purified by column chromatography (CC) with $CHCl_3$ and MeOH (9.5:0.5 to 8:2) to give six pooled fractions (PP39-PP44), fraction (PP42) 500 mg was chromatographed on silica gel (1 × 40 cm) with $CHCl_3$ and MeOH (9:1 to 8:2) to give four pooled fractions (PP45-PP48), fractions PP48 (400 mg) was further re-chromatographed on silica gel (1 × 40 cm) with $CHCl_3$ and MeOH (9.5:0.5 to 8:2) to give five

pooled fractions (PP49-PP53). The fraction PP52 (114 mg) was further chromatographed on silica gel (1.0 × 20 cm) with $CHCl_3$: acetone (4:6 v/v, 50 ml each) to afford compound **6** (13 mg, 0.003 % yield of dried leaves weight) and fraction 13 (373 mg) was further purified by column chromatography (CC) with $CHCl_3$ and acetone (1:9) to afford compound **7** (49 mg, 0.01 % yield of dried leaves weight).

Fraction PP4 (3 g) was further purified by silica gel column (4.5 × 80 cm) (1 g extract per 50 g silica gel) eluted with a mixture of EtOAC and MeOH (9.8:0.2 to 7.5:2.5, v/v, 100 ml each) to give four pooled fractions (PP60-PP63). The fraction PP62 (1.7 g) was further chromatographed with $CHCl_3$ and MeOH (9:1 to 8:2) to give five pooled fractions (PP64-PP68), fractions PP65 (444 mg) and PP67 (979 mg) were further using a sephadex LH-20 column (1 × 50 cm) with 100% MeOH to give each of pooled fractions as fractions PP69-PP71 and fractions PA77-PA79, respectively. The fraction PP69 (295 mg) and PP79 (750 mg) were further purified by crystallization with MeOH to afford compound **8** (20 mg, 0.004 % yield of dried leaves weight) and compound **9** (11 mg, 0.022 % yield of dried leaves weight), respectively.

Fraction PP5 (10 g) was chromatographed on silica gel (5 × 34 cm) with $CHCl_3$ and MeOH (9.5:0.5 to 8:2) to give five pooled fractions (PP84-PP88), fraction PP87 (3.5 g) was further purified by further re-chromatography (CC) with $CHCl_3$ and MeOH (9.5:0.5 to 8:2) to give seven pooled fractions (PP89-PP95). The fraction PP91 (323 mg) was chromatographed further using a sephadex LH-20 column (1 × 40 cm) with 100% MeOH to afford compound **10** (97 mg, 0.019 % yield of dried leaves weight) (Scheme 3-2).

Pometia pinnata dried powered leaves 500 g

Refluxed with EtOH

EtOH extract (105 g)

Partitioned between EtOAc and water

EtOAc extract (61 g)

Silica gel column chromatography | Hexane: EtOAc (10-100%) → EtOAc : MeOH (10-20%)

PP1 (16 g)　　CC; $CHCl_3$: MeOH (9.8: 0.2 → 8: 2)　**PP2** (4.6 g)　　CC; Hexane: EtOAc (4 : 6 → 0 : 10)　**PP3** (5.4 g)　　CC; EtOAc: MeOH (9.5 : 0.5 → 7.5 :2.5)　**PP4** (3 g)　　CC; $CHCl_3$: MeOH (9.5 : 0.5 → 8 : 2)　**PP5** (10 g)

PP6 (24 mg)　PP7 (54 mg)　PP8 (17 mg)　PP9 (178 mg)　PP10 (292 mg)　PP11 (398 mg)　**PP12** (2.7 g)

PP34 (17 mg)　PP35 (7.1 mg)　PP36 (238 mg)　**PP37** (4.9 mg)　PP38 (148 mg)

PP60 (3.5 mg)　PP61 (72 mg)　**PP62** (1.7 g)　PP63 (213 mg)

PP84 (189 mg)　PP85 (2.1 g)　PP86 (1.3 g)　**PP87** (3.5 g)　PP88 (1.5 g)

$CHCl_3$: MeOH (9.5: 0.5 → 8: 2)

PP27 (128 mg)　PP28 (189 mg)　PP29 (45 mg)　PP30 (3.7 mg)　**PP13** (400 mg)　PP14 (996 mg)　PP15 (204 mg)　PP16 (172 mg)

$CHCl_3$: MeOH (9.5: 0.5 → 8: 2)

PP39 (5.2 mg)　**PP40** (373 g)　PP41 (5.1 mg)　**PP42** (500 mg)　PP43 (27 mg)　PP44 (3 g)

$CHCl_3$: MeOH (9: 1 → 8: 2)

PP64 (32 mg)　**PP65** (444 mg)　PP66 (51 mg)　**PP67** (979 mg)　PP68 (63 mg)

$CHCl_3$: MeOH (9.5: 0.5 → 8: 2)

PP89 (3 g)　PP90 (239 mg)　**PP91** (323 mg)　PP92 (82 mg)　PP93 (18 mg)　PP94 (51 mg)　PP95 (404 mg)

EtOAc: Acetone (9:1)

PP31 (16 mg)　**PP32** (74 mg)　PP33 (10 mg)

$CHCl_3$: MeOH (9.8: 0.2 → 8: 2)

PP17 (164 mg)　**PP18** (186 mg)

$CHCl_3$: acetone (1: 9)

PP58 (49 mg)　PP59 (303 mg)

$CHCl_3$: MeOH (9: 1 → 8: 2)

PP45 (5.4 mg)　PP46 (1.3 mg)　PP47 (63 mg)　**PP48** (400 mg)

Sephadex (MeOH)

PP69 (295 mg)　PP70 (64 mg)　PP71 (22 mg)

Sephadex (MeOH)

PP77 (37 mg)　**PP78** (750 mg)　PP79 (143 mg)

Sephadex (MeOH)

PP96 (1.7 mg)　**PP97** (97 mg)　PP98 (252 mg)　PP99 (1.2 mg)

Compound **5**

Compound **7**

Compound **10**

Sephadex (MeOH)

PP19 (6.6 mg)　**PP20** (40 mg)　PP21 (78 mg)

Compound **3**

$CHCl_3$: MeOH (9.5: 0.5 → 8: 2)

PP49 (27 mg)　PP50 (119 mg)　PP51 (7.5 mg)　**PP52** (114 mg)　PP53 (22 mg)

Crytallization (MeOH)

PP72 (5.7 mg)　PP73 (57 mg)　**PP74** (20 mg)　PP75 (28 mg)　PP76 (128 mg)

Compound **8**

$CHCl_3$: MeOH (9.8: 0.2 → 8: 2)

PP22 (10 mg)　PP23 (23 mg)　PP24 (5.7 mg)　PP25 (20 mg)　PP26 (6.6 mg)

Compound **4**

$CHCl_3$: acetone (4: 6)

PP54 (34 mg)　PP55 (33 mg)　**PP56** (13 mg)　PP57 (25 mg)

Compound **6**

$CHCl_3$: acetone (1: 9)

PP80 (7.8 mg)　PP81 (232 mg)　**PP82** (11 mg)　PP83 (183 mg)

Compound **9**

Scheme 3-2 The procedure of *Pometia pinnata* extraction

3.5.7 Structure elucidation

The structures of the isolated compounds were mainly determined using a combination of spectroscopic techniques, including ultraviolet (UV) spectroscopy, infrared (IR) spectroscopy, nuclear magnetic resonance (NMR) spectroscopy and mass spectrometry. Ultraviolet spectroscopy is the molecular absorption of ultraviolet radiation, resulting in the excitation of electrons from ground to exited states. The absorption roughly informs the pharmacophores in the molecule. Infrared spectroscopy determines the absorption of infrared radiation, which causes molecular bond vibrations and bond rotations. The absorption frequencies indicate the types of inter-atomic bonds, i.e., the functional groups. Nuclear magnetic resonance spectroscopy, both ^{1}H and ^{13}C NMR, analyzes the magnetic properties of the atomic nuclei to determine the different electronic local environments. The technique provides information of the correlations between nuclei, leading to the atomic connectivity. Mass spectrometry (MS), was employs chemical fragmentation of the molecule into charged particles. In addition to the molecular mass, the chemical structures, projected via the fragmentation, can also be confirmed.

3.5.7.1 Compound 1

Gallocatechin (1.1): white amorphous powder; UV (MeOH) λ_{max} (log ε) 221 (4.70), 269 (3.70), 321 (3.03) nm; IR (KBr) ν_{max} 3400, 1629, 1016 cm^{-1}; ^{1}H NMR (CD$_3$OD, 500 MHz) δ 2.50 (1H, *dd*, *J* = 7.78, 16.00 Hz, H-4α), 2.85 (1H, *dd*, *J* = 5.48, 16.92 Hz, H-4β), 3.96 (1H, *m*, H-3), 4.53 (1H, *d*, *J* = 7.32 Hz, H-2), 5.91 (1H, *d*, *J* = 2.29 Hz, H-8), 5.94 (1H, *d*, *J* = 2.29 Hz, H-6), 6.51 (1H, *s*, H-2′, 6′). ^{13}C NMR (CD$_3$OD, 125 MHz) δ 28.05 (C-4), 68.73 (C-3), 82.83 (C-2), 95.91 (C-8), 96.31 (C-6), 100.76 (C-10), 107.24 (C-2′, 6′), 131.58 (C-1′), 134.00 (C-4′), 146.84 (C-3′, 5′), 156.81 (C-5), 157.63 (C-7), 157.78 (C-9). EIMS *m/z* (%): 306 [M]$^{+}$ (28), 138 (100), 281 (20), 264 (10), 168 (32), 126 (33), 112 (23), 98 (22), 72 (98).

Epigallocatechin (1.2): white amorphous powder; UV (MeOH) λ_{max} (log ε) 221 (4.70), 269 (3.70), 321 (3.03) nm; IR (KBr) ν_{max} 3400, 1629, 1016 cm^{-1}; ^{1}H NMR (CD$_3$OD, 500 MHz) δ 2.71 (1H, *dd*, *J* = 3.20, 16.69 Hz, H-4α), 2.82 (1H, *dd*, *J* = 4.12, 16.92 Hz, H-4β), 4.16 (1H, *m*, H-3), 4.75 (1H, *s*, H-2), 5.86 (1H, *d*, *J* = 2.29 Hz, H-8), 5.92 (1H, *d*, *J* = 2.28 Hz, H-6), 6.40 (1H, *s*, H-2′, 6′). (CD$_3$OD, 125 MHz) 29.10 (C-4), 67.48 (C-3), 79.87 (C-2), 95.55 (C-8), 96.43 (C-6), 100.13 (C-10), 107.03 (C-2′, 6′), 131.53 (C-1′), 133.60 (C-4′), 146.66 (C-3′, 5′), 157.28 (C-5), 157.55 (C-7), 157.93 (C-9). EIMS *m/z* (%): 306 [M]$^{+}$ (28), 138 (100), 281 (20), 264 (10), 168 (32), 126 (33), 112 (23), 98 (22), 72 (98).

3.5.7.2 Compound 2

Mearnsitrin (2): yellow needles; UV (MeOH) λ_{max} (log ε) 202 (4.99), 263 (4.32), 337 (4.11) nm; IR (KBr) ν_{max} 3417, 1634, 1022 cm^{-1}; ^{1}H NMR (CD$_3$OD, 500 MHz) δ 0.95 (3H, *d*, *J* = 5.50 Hz, Me-6″), 3.33 (1H, *m*, H-4″, 5″), 3.72 (1H, *dd*, *J* = 3.21, 8.69 Hz, H-3″), 3.87 (3H, *s*, OMe-4), 4.22 (1H, *d*, *J* = 1.83 Hz, H-2″), 5.37 (1H, *d*, *J* = 1.38 Hz, H-1″), 6.20 (1H, *d*, *J* = 2.0 Hz, H-6), 6.36 (1H, *d*, *J* = 2.0 Hz, H-8), 6.88 (1H, *s*, H-2′, 6′). ^{13}C NMR (CD$_3$OD, 125 MHz) δ 17.71 (Me-6″), 60.93 (OMe-4), 71.90 (C-5″), 72.05 (C-2″), 72.13 (C-3″), 73.26 (C-4″), 94.79 (C-8), 99.93 (C-6), 103.71 (C-1″), 106.03 (C-10), 109.92 (C-2′, 6′), 127.02 (C-1′), 136.76 (C-3), 139.43 (C-4′), 151.92 (C-3′, 5′), 158.62 (C-9), 159.07 (C-2), 163.27 (C-5), 166.06 (C-7), 179.72 (C-4). EIMS *m/z* (%): 332 (100), 317 (85), 262 (25), 234 (7), 205 (7), 153 (15), 136 (10), 69 (25).

3.5.7.3 Compound 3

Proanthocyanidin A2 (3): pale brown amorphous powder; UV (MeOH) λ_{max} (log ε) 213 (4.65), 280 (3.96), 322 (2.94) nm; IR (KBr) ν_{max} 3411, 1616 cm^{-1}; ^{1}H NMR (CD$_3$OD, 500 MHz) δ 2.75 (1H, *dd*, *J* = 2.06, 17.21 Hz, H-4′α), 2.94 (1H, *dd*, *J* = 4.91, 17.10 Hz, H-4′β), 4.05 (1H, *d*, *J* = 3.43 Hz, H-3), 4.24 (1H, *br s*, H-3′), 4.40 (1H, *d*, *J* = 3.43 Hz, H-4), 4.92 (1H, *br s*, H-2′), 6.00 (1H, *d*, *J* = 2.40 Hz, H-6), 6.09 (1H, *s*, H-6′), 6.06 (1H, *d*, *J* = 2.34 Hz, H-8), 6.97 (1H, *dd*, *J* = 2.06, 8.17 Hz, H-14′), 6.80 (1H, *dd*, *J* = 1.82, 8.29 Hz, H-13′), 6.81 (1H, *dd*, *J* = 1.72, 8.29 Hz, H-13), 7.02 (1H, *dd*, *J* = 2.17, 8.28 Hz, H-14), 7.13 (1H, *d*, *J* = 2.17 Hz, H-10), 7.15 (1H, *d*, *J* = 2.06 Hz, H-10′). ^{13}C NMR (CD$_3$OD, 125 MHz) δ 29.28 (C-4), 29.89 (C-4′), 66.98 (C-3′), 68.09 (C-3), 81.79 (C-2′), 96.55 (C-6′), 96.66 (C-8), 98.35 (C-6), 100.21 (C-2), 102.46 (C-4a′), 104.29 (C-4a), 107.24 (C-8′), 115.97 (C-10), 115.65 (C-13), 115.69 (C-13′), 116.07 (C-10′), 119.80 (C-14), 120.40 (C-14′), 131.20 (C-9′), 132.47 (C-9), 145.67 (C-11), 146.01 (C-11′), 146.32 (C-12′), 146.78 (C-12), 152.13 (C-8a′), 152.30 (C-7′), 154.26 (C-8a), 156.60 (C-5′), 157.00 (C-5), 158.14 (C-7). EIMS *m/z* (%): 288 (5), 264 (8), 238 (7), 126 (22), 83 (18), 72 (100).

3.5.7.4 Compound 4

Epicatechin (4): orange needles; UV (MeOH) λ_{max} (log ε) 211 (4.43), 280 (3.54), 315 (2.85) nm; IR (KBr) ν_{max} 3436, 1631, 1097 cm^{-1}; ^{1}H NMR (CD$_3$OD, 500 MHz) δ 2.73 (1H, *dd*, *J* = 2.75, 16.80 Hz, H-4β), 2.85 (1H, *dd*, *J* = 4.57, 16.69 Hz, H-4α), 4.17 (1H, *m*, H-3), 4.81 (1H, *s*, H-2),

5.90 (1H, *d*, *J* = 2.29 Hz, H-8), 5.93 (1H, *d*, *J* = 2.52 Hz, H-6), 6.75 (1H, *d*, *J* = 8.23 Hz, H-5′), 6.79 (1H, *dd*, *J* = 2.05, 8.23 Hz, H-6′), 6.96 (1H, *d*, *J* = 2.06 Hz, H-2′). ^{13}C NMR (CD$_3$OD, 125 MHz) δ 29.07 (C-4), 67.49 (C-3), 79.88 (C-2), 95.86 (C-8), 96.35 (C-6), 100.45 (C-10), 115.30 (C-2′), 115.87 (C-5′), 119.37 (C-6′), 132.28 (C-1′), 145.78 (C-4′), 145.95 (C-3′), 157.37 (C-9), 157.67 (C-7), 158.02 (C-5). EIMS *m/z* (%): 290 [M]$^+$ (35), 272 (2), 167 (5), 152 (40), 139 (100), 123 (36), 110 (3).

3.5.7.5 Compound 5

Kaempferol-3-O-rhamnoside (5): amorphous yellow powder; UV (MeOH) λ$_{max}$ (log ε) 203 (4.67), 265 (4.21), 343 (4.03) nm; IR (KBr) ν$_{max}$ 3422, 1634, 1018 cm^{-1}; ^{1}H NMR (CD$_3$OD, 500 MHz) δ 0.95 (3H, *d*, *J* = 5.50, Me-6″), 3.33 (1H, *m*, H-4″, 5″), 3.72 (1H, *dd*, *J* = 3.21, 8.69 Hz, H-3″), 4.22 (1H, *d*, *J* = 1.83 Hz, H-2″), 5.37 (1H, *d*, *J* = 1.38 Hz, H-1″), 6.19 (1H, *d*, *J* = 1.70 Hz, H-6), 6.36 (1H, *d*, *J* = 1.80 Hz, H-8), 6.92 (1H, *d*, *J* = 8.69 Hz, H-3′, 5′), 7.76 (1H, *d*, *J* = 8.69 Hz, H-2′, 6′). ^{13}C NMR (CD$_3$OD, 125 MHz) δ 17.64 (Me-6″), 71.93 (C-5″), 72.02 (C-3″), 72.16 (C-2″), 73.23 (C-4″), 94.77 (C-8), 99.85 (C-6), 103.51 (C-1″), 105.96 (C-10), 116.53 (C-3′, 5′), 122.67 (C-1′), 131.89 (C-2′, 6′), 136.24 (C-3), 158.56 (C-2), 159.29 (C-9), 161.56 (C-4′), 163.21 (C-5), 165.85 (C-7), 179.63 (C-4). EIMS *m/z* (%): 432 [M]$^+$ (1), 286 (100), 258 (9), 229 (8), 213 (5), 121 (10), 128 (5), 93 (3).

3.5.7.6 Compound 6

Quercetin-3-O-rhamnoside (6): amorphous yellow powder; UV (MeOH) λ$_{max}$ (log ε) 202 (4.94), 255 (4.41), 350 (4.25) nm; IR (KBr) ν$_{max}$ 3417, 1656 cm^{-1}; ^{1}H NMR (CD$_3$OD, 500 MHz) δ 0.95 (3H, *d*, *J* = 6.17 Hz, Me-6″), 3.34 (1H, *dd*, *J* = 6.86, 9.60 Hz, H-4″), 3.43 (1H, *m*, H-5″), 3.74 (1H, *dd*, *J* = 3.20, 9.49 Hz, H-3″), 4.21 (1H, *dd*, *J* = 1.83, 3.13 Hz, H-2″), 5.34 (1H, *d*, *J* = 1.60 Hz, H-1″), 6.19 (1H, *d*, *J* = 2.29 Hz, H-6), 6.34 (1H, *d*, *J* = 2.05 Hz, H-8), 6.90 (1H, *d*, *J* = 8.24 Hz, H-5′), 7.30 (1H, *dd*, *J* = 1.90, 8.35 Hz, H-6′), 7.33 (1H, *d*, *J* = 2.28 Hz, H-2′). ^{13}C NMR (CD$_3$OD, 125 MHz) δ 17.65 (Me-6″), 71.89 (C-5″), 72.03 (C-3″), 72.09 (C-2″), 73.23 (C-4″), 94.70 (C-8), 99.81 (C-6), 122.94 (C-1′), 103.58 (C-1″), 105.87 (C-10), 116.36 (C-5′), 116.90 (C-2′), 122.86 (C-6′), 136.22 (C-3), 146.41 (C-3′), 149.80 (C-4′), 158.52 (C-2), 159.31 (C-9), 163.21 (C-5), 165.90 (C-7), 179.63 (C-4). EIMS *m/z* (%): 301 (100), 272 (9), 245 (5), 229 (6), 216 (3), 153 (7), 128 (10), 108 (3).

3.5.7.7 Compound 7

1-O-palmitoyl-3-O-[α-D-galactopyranosyl-(1→6)-β-D-galactopyranosyl]-sn-glycerol (7): colourless semisolid; IR (KBr) ν_{max} 3391, 2854, 1733 cm^{-1}; ^{1}H NMR (CD$_3$OD, 500 MHz) δ 0.90 (3H, *t*, *J* = 6.90 Hz, Me-16‴), 1.30 (2H, *br s*, H-4‴-15‴), 1.61 (2H, *d*, *J* = 5.49 Hz, H-3‴), 2.35 (2H, *d*, *J* = 7.31 Hz, H-2‴), 3.46 (1H, *dd*, *J* = 3.20, 10.06 Hz, H-3′), 3.57 (1H, *dd*, *J* = 7.32, 10.06 Hz, H-2′), 3.64 (1H, *dd*, *J* = 6.40, 10.52 Hz, H-6″α), 3.67 (1H, *dd*, *J* = 4.12, 10.06 Hz, H-3α, 6′α), 3.68 (1H, *dd*, *J* = 4.12, 10.20 Hz, H-6″β), 3.73 (1H, *m*, H-5′, 2″), 3.74 (1H, *m*, H-3″), 3.84 (1H, *t*, *J* = 5.94 Hz, H-4′, 5″), 3.85 (1H, *m*, H-4″), 3.88 (1H, *dd*, *J* = 6.40, 10.06 Hz, H-3β, 6′β), 3.98 (1H, *m*, H-2), 4.22 (1H, *dd*, *J* = 6.40, 11.85 Hz, H-1β), 4.31 (1H, *d*, *J* = 7.32 Hz, H-1′), 4.42 (1H, *dd*, *J* = 3.21, 12.00 Hz, H-1α), 4.84 (1H, *d*, *J* = 3.65 Hz, H-1″). ^{13}C NMR (CD$_3$OD, 125 MHz) δ 14.48 (C-16‴), 23.70-35.00 (C-4‴-15‴), 26.03 (C-3‴), 34.94 (C-2‴), 62.84 (C-6″), 63.99 (C-1), 67.78 (C-6′), 68.74 (C-2), 70.05 (C-4′), 70.21 (C-3″), 71.10 (C-4″), 71.45 (C-2″), 71.74 (C-3), 72.37 (C-5″), 72.54 (C-2′), 74.65 (C-3′), 74.57 (C-5′), 100.61 (C-1″), 105.30 (C-1′), 175.06 (C-1‴). EIMS *m/z* (%): 551 (3), 467 (3), 401 (3), 341 (25), 313 (35), 239 (32), 171 (21), 163 (44), 145 (42), 98 (58), 73 (100).

3.5.7.8 Compound 8

Stigmasterol-3-O-glucoside (8): amorphous white powder; IR (KBr) ν_{max} 3436, 1639, 1023 cm^{-1}; ^{1}H NMR (DMSO-d_6, 500 MHz) δ 0.65 (3H, s, Me-18), 0.77 (3H, *t*, *J* = 7.25 Hz, Me-29), 0.79 (3H, *d*, *J* = 6.47 Hz, Me-27), 0.81 (3H, *d*, *J* = 6.47 Hz, Me-26), 0.87 (1H, *m*, H-9), 0.90 (1H, *m*, H-24), 0.94 (3H, *s*, Me-19), 0.98 (3H, *d*, *J* = 6.73 Hz, Me-21), 1.02 (2H, *m*, H-15), 1.04 (1H, *m*, H-14), 1.05 (2H, *m*, H-28), 1.12 (2H, *m*, H-17), 1.14 (2H, *m*, H-4), 1.18 (2H, *m*, H-11), 1.21 (2H, *m*, H-20), 1.23 (2H, *m*, H-2), 1.35 (2H, *m*, H-12), 1.48 (2H, *m*, H-7), 1.50 (1H, *m*, H-8), 1.52 (1H, *m*, H-25), 1.80 (2H, *m*, H-16), 2.35 (2H, *m*, H-1), 2.85-3.65 (1H, *m*, H-Glc), 3.36 (1H, *m*, H-3), 4.89 (1H, *d*, *J* = 7.77 Hz, H-1′), 5.02 (1H, *dd*, *J* = 8.81, 15.03 Hz, H-23), 5.14 (1H, *dd*, *J* = 8.82, 15.28 Hz, H-22), 5.31 (1H, *br d*, *J* = 4.92 Hz, C-6) ^{13}C NMR (DMSO-d_6, 125 MHz) δ 12.00 (C-18), 12.25 (C-29), 19.01 (C-26), 19.25 (C-19), 20.74 (C-21), 21.07 (C-11), 21.27 (C-27), 24.03 (C-15), 25.00 (C-28), 28.62 (C-16), 29.43 (C-25), 31.47 (C-7), 31.58 (C-2), 31.95 (C-8), 36.39 (C-10), 36.99 (C-1), 38.49 (C-12), 40.20 (C-20), 40.30 (C-4), 41.91 (C-13), 49.80 (C-24), 50.74 (C-9), 55.52 (C-17), 56.67 (C-14), 61.28 (C-6′), 70.29 (C-4′), 73.64 (C-2′), 76.90 (C-3′), 76.94 (C-5′), 77.12 (C-3), 100.98 (C-1′),

121.30 (C-6), 129.00 (C-23), 138.17 (C-22), 140.64 (C-5). EIMS *m/z* (%): 412 (7), 394 (100), 382 (11), 351 (10), 255 (40), 213 (12), 161 (15), 145 (25), 83 (68).

3.5.7.9 Compound 9

3-O-α-L-arabinofuranosyl-(1→3)-[α-L-rhamnopyranosyl-(1→2)]-α-L-arabinopyranosyl hederagenin (9): colourless needles; IR (KBr) ν_{max} 3413, 1659, 1017 cm^{-1}; ^{1}H NMR (CD$_3$OD, 500 MHz) δ 0.69 (3H, *s*, Me-24), 0.80 (3H, *s*, Me-26), 0.90 (3H, *s*, Me-30), 0.94 (3H, *s*, Me-29), 0.96 (3H, *s*, Me-25), 1.17 (3H, *s*, Me-27), 1.23 (3H, *d*, *J* = 6.40 Hz, Me-6″), 2.84 (1H, *dd*, *J* = 3.7, 13.94 Hz, H-18), 3.38 (1H, *t*, *J* = 9.60, H-4″), 3.55 (1H, *dd*, *J* = 1.82, 11.43 Hz, H-5′β), 3.59 (2H, *d*, *J* = 10.0 Hz, H-23), 3.60 (1H, *dd*, *J* = 3.66, 9.60 Hz, H-3″), 3.62 (1H, *dd*, *J* = 5.49, 11.89 Hz, H-3), 3.63 (1H, *dd*, *J* = 5.49, 11.89 Hz, H-4‴), 3.66 (2H, *d*, *J* = 3.70 Hz, H-5‴), 3.70 (1H, *dd*, *J* = 3.66, 7.50 Hz, H-3′), 3.82 (1H, *m*, H-2′), 3.84 (1H, *m*, H-5′α), 3.85 (1H, *m*, H-3‴), 3.86 (1H, *m*, H-5″), 3.93 (1H, *dd*, *J* = 1.37, 3.20 Hz, H-2″), 3.98 (1H, *br s*, H-4′), 4.05 (1H, *br s*, H-2‴), 4.50 (1H, *d*, *J* = 6.41 Hz, H-1′), 5.05 (1H, *d*, *J* = 1.37 Hz, H-1‴), 5.10 (1H, *br s*, H-1″), 5.23 (1H, *t*, *J* = 3.66 Hz, H-12). ^{13}C NMR (CD$_3$OD, 125 MHz) δ 13.69 (C-24), 16.39 (C-25), 17.78 (C-26), 18.03 (C-6″), 18.78 (C-6), 23.98 (C-30), 24.06 (C-16), 24.52 (C-11), 26.46 (C-2), 26.63 (C-27), 28.83 (C-15), 31.61 (C-20), 33.39 (C-7), 33.58 (C-29), 33.83 (C-22), 34.89 (C-21), 37.62 (C-10), 39.67 (C-1), 40.50 (C-8), 42.74 (C-18), 42.97 (C-14), 43.97 (C-4), 47.24 (C-19), 47.66 (C-17), 48.05 (C-9), 49.63 (C-5), 63.24 (C-5‴), 64.42 (C-23), 65.65 (C-5′), 69.51 (C-4′), 70.66 (C-5″), 71.53 (C-2″), 71.99 (C-3″), 73.73 (C-4″), 75.82 (C-2′), 79.04 (C-3‴), 82.06 (C-3′), 82.40 (C-2‴), 82.90 (C-3), 86.90 (C-4‴), 102.52 (C-1″), 105.04 (C-1′), 110.68 (C-1‴), 123.60 (C-12), 145.26 (C-13), 182.09 (C-28). EIMS *m/z* (%): 604 (2), 471 (10), 281 (9), 126 (21), 95 (24), 87 (38), 72 (100).

3.5.7.10 Compound 10

3-O-(5-acetyl-α-L-arabinofuranosyl)-(1→3)-[α-L-rhamnopyranosyl-(1→2)]-α-L-arabinopyranosyl hederagenin (10): colourless needles; IR (KBr) ν_{max} 3413, 1659, 1017 cm^{-1}; ^{1}H NMR (CD$_3$OD, 500 MHz) δ 0.70 (3H, *s*, Me-24), 0.80 (3H, *s*, Me-26), 0.90 (3H, *s*, Me-30), 0.93 (3H, *s*, Me-29), 0.96 (3H, *s*, Me-25), 1.17 (3H, *s*, Me-27), 1.23 (3H, *d*, *J* = 6.4 Hz, Me-6″), 2.84 (1H, *dd*, *J* = 4.11, 13.72 Hz, H-18), 3.38 (1H, *t*, *J* = 9.6, H-4″), 3.55 (1H, *dd*, *J* = 1.83, 11.35 Hz, H-5′β), 3.51 (2H, *d*, *J* = 12.35 Hz, H-23), 3.68 (1H, *dd*, *J* = 3.20, 9.61 Hz, H-3″), 3.60 (1H, *dd*, *J* =

4.58, 11.89 Hz, H-3), 3.59 (1H, *d*, *J* = 11.89 Hz, H-4‴), 4.60 (2H, *br s*, H-5‴), 3.70 (1H, *dd*, *J* = 3.66, 7.50 Hz, H-3′), 3.83 (1H, *m*, H-2′), 3.82 (1H, *m*, H-5′α), 3.84 (1H, *m*, H-3‴), 3.85 (1H, *m*, H-5″), 3.93 (1H, *dd*, *J* = 1.83, 3.2 Hz, H-2″), 3.95 (1H, *br s*, H-4′), 4.14 (1H, *t*, *J* = 6.4 Hz, H-2‴), 4.50 (1H, *d*, *J* = 5.94 Hz, H-1′), 5.05 (1H, *d*, *J* = 1.37 Hz, H-1‴), 5.10 (1H, *br s*, H-1″), 5.23 (1H, *t*, *J* = 3.65 Hz, H-12). ^{13}C NMR (CD$_3$OD, 125 MHz) δ 13.68 (C-24), 16.39 (C-25), 17.77 (C-26), 18.23 (C-6″), 18.78 (C-6), 23.98 (C-30), 24.06 (C-16), 24.53 (C-11), 26.64 (C-2), 26.46 (C-27), 28.84 (C-15), 31.62 (C-20), 33.39 (C-7), 33.58 (C-29), 33.83 (C-22), 34.90 (C-21), 37.63 (C-10), 39.68 (C-1), 40.51 (C-8), 42.74 (C-18), 42.98 (C-14), 43.97 (C-4), 47.24 (C-19), 47.64 (C-17), 48.04 (C-9), 49.34 (C-5), 63.31 (C-5‴), 64.42 (C-23), 65.64 (C-5′), 69.58 (C-4′), 70.69 (C-5″), 71.52 (C-2″), 72.00 (C-3″), 73.73 (C-4″), 75.83 (C-2′), 79.40 (C-3‴), 82.95 (C-3′), 82.06 (C-2‴), 83.73 (C-3), 85.82 (C-4‴), 102.54 (C-1″), 105.05 (C-1′), 110.77 (C-1‴), 123.62 (C-12), 145.25 (C-13), 181.94 (C-28). EIMS *m/z* (%): 604 (2), 471 (10), 281 (9), 126 (21), 95 (24), 87 (38), 72 (100).

3.6 HPLC quantitative analysis

3.6.1 HPLC conditions

HPLC analysis was carried out using the Agilent 1100 series equipped with an Agilent 1100 series Photodiode-array detector (PDA) and autosampler. Data analysis was performed using Agilent Chemstation for LC 3D software. Separation was achieved at 25 ºC on a 150 × 4.6 mm i.d., Phenominex® Luna 5u Hilic column (USA). The mobile phase consisted of 100% Milli-Q water with pumped at a flow rate of 1 mL/min. The optimum ratio of the mobile phase and elution system were optimized for good resolution. The injection volume is 20 µL. The quantitation wavelength is set at 210 nm of epigallocatechin. Whlist, the mobile phase consisted of acetonitrile-water of proanthocyanidin A2 with pumped at a flow rate of 1 mL/min. The optimum ratio of the mobile phase and elution system were optimized for good resolution. The injection volume is 20 µL. The quantitation wavelength is set at 280 nm of proanthocyanidin A2.

3.6.2 Preparation of standard solutions

A stock solution of the reference standard, epigallocatechin and proanthocyanidin A2 were made in methanol and subsequently diluted to provide a series of the standard ranging containing 0.77-25 µg/mL of epigallocatechin and 7.7-250 µg/mL of proanthocyanidin A2, respectively. These solutions were subjected to HPLC analysis, and calibration curves constructed for epigallocatechin and proanthocyanidin A2 by plotting peak areas against concentrations.

3.6.3 Preparation of samples

The dried powder of plant samples (100 mg) were extracted with suitable solvent (20 mL) under reflux conditions for 20 min. The extracts were filtered and then concentrated under reduced pressure. The sample was reconstituted and the volume adjusted to 10 mL with methanol. Samples were analyzed immediately after extraction in order to avoid possible chemical degradation. The experiments were carried out in triplicate.

3.6.4 Method validation

For validation of the analytical method, the guidelines of the International Conference on Harmonization of Technical Requirement for the Registration of Pharmaceuticals for Human Use

were followed (ICH, 2005). Calculated data were checked for their linearity, accuracy, intra-day and inter-day precision specificity, LOD and LOQ to validate the HPLC method.

3.6.4.1 Limits of detection (LOD) and quantification (LOQ)

Serial dilutions of a reference standard were carried out with methanol and were then analyzed by the HPLC method. LOD and LOQ were the concentrations that give a signal to noise ratio equal to 3 and 10, respectively.

3.6.4.2 Calibration curve and linearity

The calibration curves were constructed on three consecutive days by analysis of a mixture containing each of the standard compounds at six concentrations and plotting peak areas against the concentration of each reference standard. The linearity of the detector response for the standards was determined by means of linear regression analysis. The calibration curve should show a coefficient of correlation $(r^2) \geq 0.999$.

3.6.4.3 Accuracy

The standard solutions were prepared at three different concentrations (25, 12.5 and 6.125 µg/mL of epigallocatechin and 250, 125 and 61.25 µg/mL of proanthocyanidin A2), and mixed with the leaf extracts containing a known amount of standard solutions at a ratio of 1:1 (v/v). Three injections for each concentration were performed per day over 3 different days (3 injections × 3 concentrations × 3 days) and the percentage recoveries of epigallocatechin and proanthocyanidin A2 were then calculated.

3.6.4.4 Precision

Precision experiments were conducted to ascertain any intra-day and inter-day variability. A solution of one dried leaf extracts was used to check intraday precision. Six separate injections of this sample were performed on the same day. The data was used to calculate % R.S.D. for intraday precision. The inter-day precision was validated by repeating the extraction procedure on the same sample. An aliquot of each extract was then injected and quantified. This parameter was evaluated by repeating the extraction in triplicate on 3 different days with freshly prepared mobile phase and samples. The data was used to calculate % R.S.D. for inter-day precision.

3.6.4.5 Specificity

Peak identification was carried out using authentic standards and scanning the UV spectrum of each peak using the photodiode-array detector. The UV spectra were taken at various points of the peaks to check peak homogeneity.

3.7 Determination of solvent for extraction

To optimize the solvent for extraction, *M. elengi* dried leaf powders (100 mg) were separately extracted with acetone, ethyl acetate, ethanol and methanol (2×20 mL) under reflux conditions for 20 min and *P. pinnata* dried leaf powders (100 mg) were separately extracted with hexane, chloroform, ethyl acetate and methanol (2×20 mL) under reflux conditions for 20 min, respectively. The extracts were then filtered through a whatman No.1 filter paper, and the solvents were evaporated to dryness under reduced pressure (40 ºC). The residues were dissolved in methanol, and the volume was adjusted to 10 mL, and subjected to HPLC analysis. All sample analyses were performed in triplicate.

3.8 Determination of extraction methods

M. elengi and *P. pinnata* dried leaf powders were separately extracted by extraction under reflux conditions (RE), sonication-assisted extraction (SAE) and microwave assisted extraction (MAE) in order to optimize the extraction method.

3.8.1 Extraction under reflux conditions

The dried leaf powders (100 mg) were extracted with methanol (20 mL) under reflux conditions for 20 min. The extracts was then filtered and concentrated under reduced pressure. The extracts were redissolved in methanol and the volume adjusted to 10 mL, and subjected to HPLC analysis. The experiments were performed in triplicate.

3.8.2 Microwave assisted extraction

MAE was carried out in a laboratory scale microwave extraction apparatus at atmospheric pressure with microwave frequency 2450 MHz and power 90 W. Methanol (20 mL) was added into 250 mL-beaker containing the dried leaf powders (100 mg). The beaker was removed and cooled to room temperature. Then again, placed back again in the microwave extractor to be exposed. The above steps were repeated until the duration of microwave radiation was summed to the designed value (Hao et al., 2002). The extracts were then filtered and concentrated under reduce pressure. The samples were adjusted to 10 mL with methanol and subject to HPLC analysis. The experiments were performed in triplicate.

3.8.3 Sonication extraction method

The dried leaf powders (100 mg) were extracted with methanol (20 mL) under sonicated conditions for 20 min. The extracts were then filtered and concentrated under reduced pressure. The extracts were redissolved in methanol and the volume adjusted to 10 mL, and subjected to HPLC analysis. The experiments were performed in triplicate.

3.9 Optimization of MAE condition

3.9.1 Effect of different irradiation period on the yield of plants

The dried leaf powders (100 mg) were placed into a flask. After adding 20 mL of solvent, the flasks are exposed for 15 sec, 30 sec, 60 sec and 120 sec in a microwave extractor. The extracts were then filtered and concentrated under reduce pressure. The samples were adjusted to 10 mL with methanol and subject to HPLC analysis. The experiments were performed in triplicate.

3.9.2 Effect of irradiation cycles on the yield of plants

The dried leaf powders (100 mg) were placed into a flask. After adding 20 mL of solvent, the flasks were exposed for 60 second, 1-5 cycles (1 cycle as 60 second power on and 15 second power off of epigallocatechin in *M. elengi*) and 30 second, 1-5 cycles (1 cycle as 30 second power on and 15 second power off of proanthocyanidin A2 in *P. pinnata*) in a microwave extractor. The extracts were then filtered and concentrated under reduce pressure. The samples were adjusted to 10 mL with methanol and subject to HPLC analysis. The experiments were performed in triplicate.

3.9.3 Effect of extraction times on the yield of plants

The dried leaf powders (100 mg) were placed into a flask. After adding 20 mL of solvent, the flasks was exposed for 60 second, 3 cycles of epigallocatechin in *M. elengi* and 30 second, 4 cycles of proanthocyanidin A2 in *P. pinnata*, 1-3 extraction times in a microwave extractor. The extracts was then filtered and concentrated under reduce pressure. The samples were adjusted to 10 mL with methanol and subject to HPLC analysis. The experiments were performed in triplicate.

3.10 Determination of suitable ratio of plants powder to solvent

Various amounts of the dried leaf powder (100, 300, 500, 700 and 1,000 mg) were used to optimize a suitable ratio of the plants powder to a fixed volume of methanol (20 mL) for extracting

using the optimized MAE conditions. The extracts were then filtered, and the solvent subsequently evaporated to dryness under reduced pressure (45 ºC). The residues were reconstituted, and the volume adjusted to 10 mL with methanol. These samples were filtered through a 0.45 μm membrane filter and analyzed immediately in order to avoid possible chemical degradation. All samples were analyzed in triplicate.

CHAPTER 4

RESULTS AND DISCUSSION

4.1 Structure elucidation of the isolated compounds

R_1	R_2	
H	OH	Gallocatechin
OH	H	Epigallocatechin
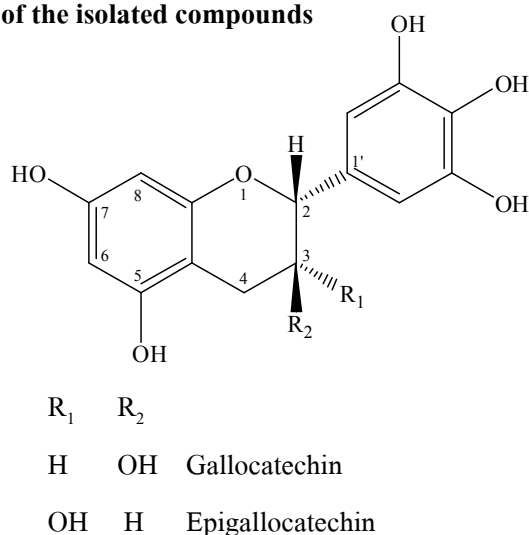
Figure 4-1 Chemical structure of gallocatechin and epigallocatechin

Compound **1** was obtained as a white amorphous powder (180 mg): mp 280-283 °C. The molecular formula was proposed to be $C_{30}H_{28}O_{14}$ determined by EI mass spectrum, which showed C_{15} flavonoid peak of mixture of compounds **1.1** and **1.2** were quite similar and showed their most abundant signals at m/z 305.8. UV spectrum showed absorption λ_{max} (MeOH) at 221, 269 nm. IR spectrum showed absorption band for hydroxyl (3400 cm^{-1}), C=C (1629 cm^{-1}) and C-O (1016 cm^{-1}). The ^{13}C NMR spectra data (Table 4-3) recorded in CD_3OD showed the existence of 30 signals for 30 carbon atoms in the molecule. This compound suggested the presence of 15 methine (δ 29.10, 67.48, 68.73, 79.87, 82.83, 95.55, 95.91, 96.31, 96.43, 107.03, 107.03, 107.24, 107.24, 156.81, 157.28 ppm), 1 methylene (δ 28.05 ppm) and 14 quaternary carbons (δ 100.13, 100.76, 131.53, 131.58, 133.60, 134.00, 146.66, 146.66, 146.84, 146.84, 157.55, 157.63, 157.78, 157.93 ppm). The ^{13}C NMR spectra of **1.1** and **1.2** showed similar carbon signals for the phloroglucinol A-ring and the pyrogallol B-ring, but differences in the signals for the pyran C-ring (Table 4-1 and 4-2). In contrast to **1.2** (δ 79.9 and δ 67.5 ppm), the C-2 and C-3 signals of **1.1** appeared downfield at δ 82.8 and δ 68.7 ppm.

The ^{1}H NMR spectra data (Table 4-1 and 4-2) recorded in CD$_3$OD displayed 8 aromatic protons at δ 5.91 ppm (*d*, *J* = 2.29 Hz, 1H-8), 5.94 ppm (*d*, *J* = 2.29 Hz, 1H-6), 6.51 ppm (*s*, 1H-2′), 6.51 ppm (*s*, 1H-6′) of **1.1** and 5.86 ppm (*d*, *J* = 2.29 Hz, 1H-8), 5.92 ppm (*d*, *J* = 2.28 Hz, 1H-6), 6.40 ppm (*s*, 1H-2′), 6.40 ppm (*s*, 1H-6′) of **1.2**. The large coupling observed for the H-2 to H-3 (δ 4.53 and δ 3.96 ppm, *d*, *J* =7.32 Hz) in the ^{1}H NMR spectrum indicated a 2, 3-trans-orientation in **1.1**. A 2, 3-cis-orientation between C-2 and C-3 in **1.2** was deduced from the singlet at δ 4.75 ppm corresponding to H-2. Thus on the basis of its spectroscopic data and compare with the previously reported data (Rösch *et al*., 2004 / Table 4-1 and 4-2). Compound **1.1** and **1.2** were identified as gallocatechin and epigallocatechin (Figure 4-1 and Figures 4-2 to 4-6).

Table 4-1 Spectral data of compound **1.1** (CD$_3$OD; 500 MHz for ^{1}H NMR, CD$_3$OD; 125 MHz for ^{13}C NMR) compare with gallocatechin (CD$_3$OD; 500 MHz for ^{1}H NMR, CD$_3$OD; 125 MHz for ^{13}C NMR)

Position	Type of C	δ_C / ppm		δ_H / ppm	
		Compound **1.1**	Gallocatechin	Compound **1.1**	Gallocatechin
1	-	-	-	-	-
2	CH	82.83	82.9	4.53, 1H, *d*, *J* = 7.32 Hz	4.58, 1H, *d*, *J* = 7.2 Hz
3	CH	68.73	68.8	3.96, 1H, *m*	4.02, 1H, *m*
4α	CH$_2$	28.05	28.1	2.50, 1H, *dd*, *J* = 7.78, 16.00 Hz	2.55, 1H, *dd*, *J* = 7.8, 16.2 Hz
4β	CH$_2$	28.05	28.1	2.85, 1H, *dd*, *J* = 5.48, 16.92 Hz	2.85, 1H, *dd*, *J* = 5.3, 16.1Hz
5	C	156.81	156.8	-	-
6	CH	96.31	96.2	5.94, 1H, *d*, *J* = 2.29 Hz	5.97, 1H, *d*, *J* = 2.2 Hz

Table 4-1 Spectral data of compound **1.1** (CD$_3$OD; 500 MHz for ^{1}H NMR, CD$_3$OD; 125 MHz for ^{13}C NMR) compare with gallocatechin (CD$_3$OD; 500 MHz for ^{1}H NMR, CD$_3$OD; 125 MHz for ^{13}C NMR) (continued)

Position	Type of C	δ_C / ppm		δ_H / ppm	
		Compound **1.1**	Gallocatechin	Compound **1.1**	Gallocatechin
7	C	157.63	157.6	-	-
8	CH	95.91	95.5	5.91, 1H, *d*, *J* = 2.29 Hz	5.91, 1H, *d*, *J* = 2.2 Hz
9	C	157.78	157.8	-	-
10	C	100.76	100.7	-	-
1′	C	131.58	131.5	-	-
2′, 6′	CH	107.24	107.2	6.51, 1H, *s*	6.45, 1H, *s*
3′	C	146.84	146.9	-	-
4′	C	134.00	134.0	-	-
5′	C	146.84	146.9	-	-

Table 4-2 Spectral data of compound **1.2** (CD$_3$OD; 500 MHz for ^{1}H NMR, CD$_3$OD; 125 MHz for ^{13}C NMR) compare with epigallocatechin (CD$_3$OD; 500 MHz for ^{1}H NMR, CD$_3$OD; 125 MHz for ^{13}C NMR) (continued)

Position	Type of C	δ$_C$ / ppm		δ$_H$ / ppm	
		Compound **1.2**	Epigallocatechin	Compound **1.2**	Epigallocatechin
1	-	-	-	-	-
2	CH	79.87	79.9	4.75, 1H, *s*	4.74, 1H, *s*
3	CH	67.48	67.5	4.16, 1H, *m*	4.16, 1H, *m*
4α	CH$_2$	29.10	29.2	2.71, 1H, *dd*, J = 3.20, 16.69 Hz	2.71, 1H, *dd*, J = 3.0, 16.7 Hz
4β	CH$_2$	29.10	29.2	2.82, 1H, *dd*, J = 4.12, 16.92 Hz	2.84, 1H, *dd*, J = 4.5, 16.7 Hz
5	C	157.28	157.3	-	-
6	CH	96.43	96.3	5.92, 1H, *d*, J = 2.28 Hz	5.92, 1H, *d*, J = 2.1 Hz
7	C	157.55	157.6	-	-
8	CH	95.55	95.5	5.86, 1H, *d*, J = 2.29 Hz	5.90, 1H, *d*, J = 2.3 Hz
9	C	157.93	158.0	-	-
10	C	100.13	100.1	-	-
1′	C	131.53	131.5	-	-
2′, 6′	CH	107.03	107.0	6.40, 1H, *s*	6.50, 1H, *s*
3′	C	146.66	146.7	-	-
4′	C	133.60	133.6	-	-
5′	C	146.66	146.7	-	-
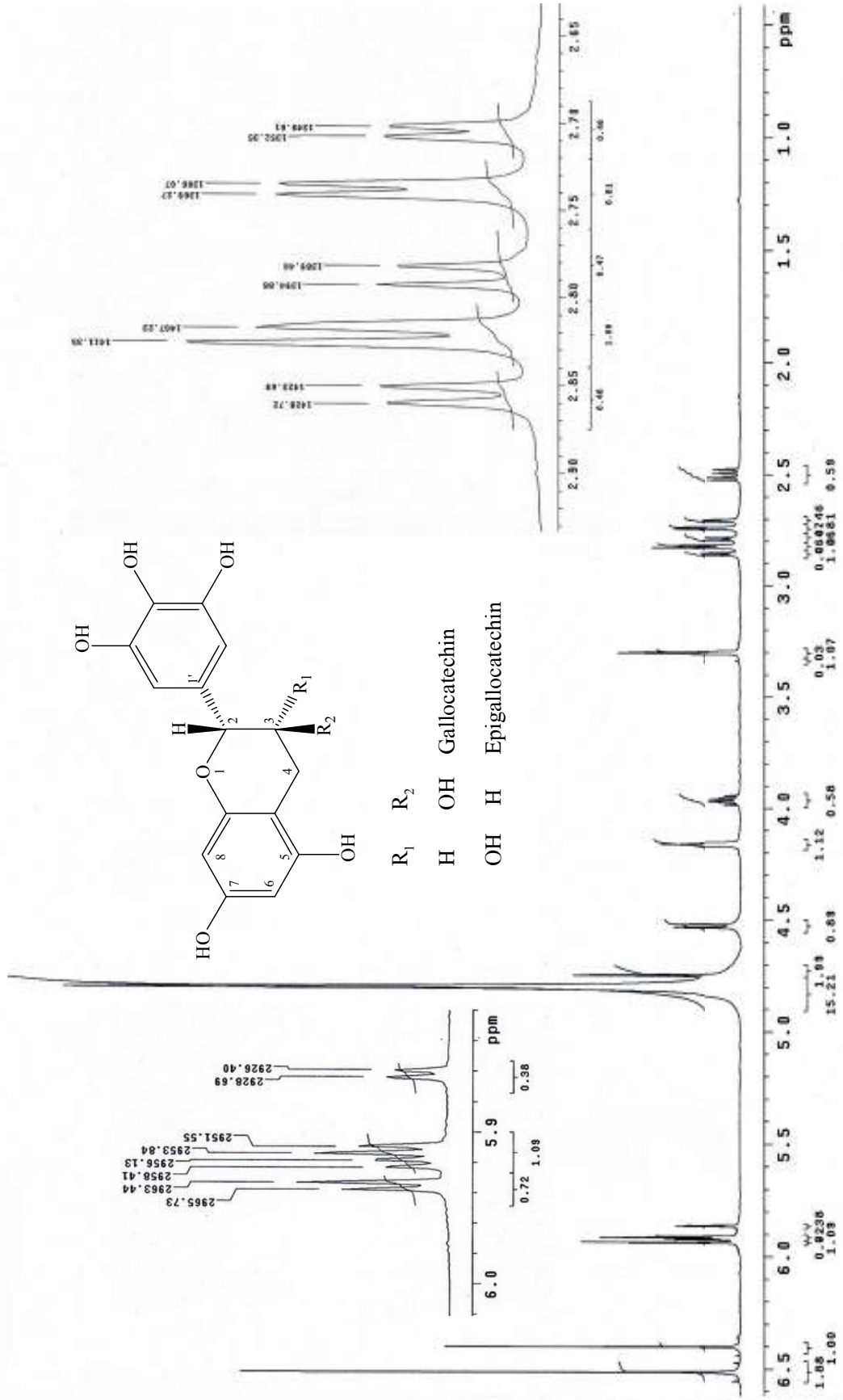
Figure 4-2 ^{1}H NMR spectrum of compound **1** in CD$_3$OD
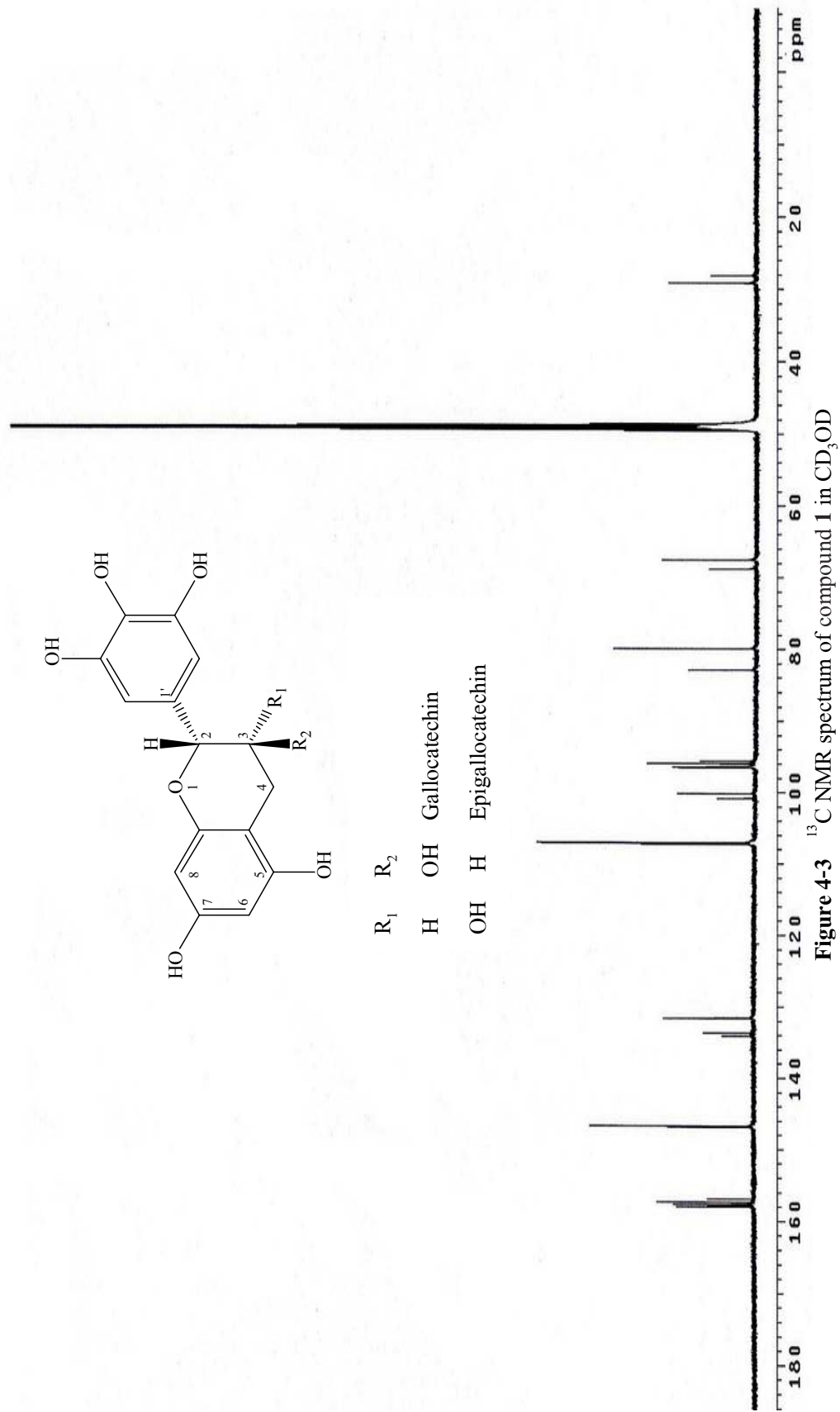
Figure 4-3 ^{13} C NMR spectrum of compound 1 in CD$_3$OD

	R$_1$	R$_2$	
	H	OH	Gallocatechin
	OH	H	Epigallocatechin

	R_1	R_2	
	H	OH	Gallocatechin
	OH	H	Epigallocatechin
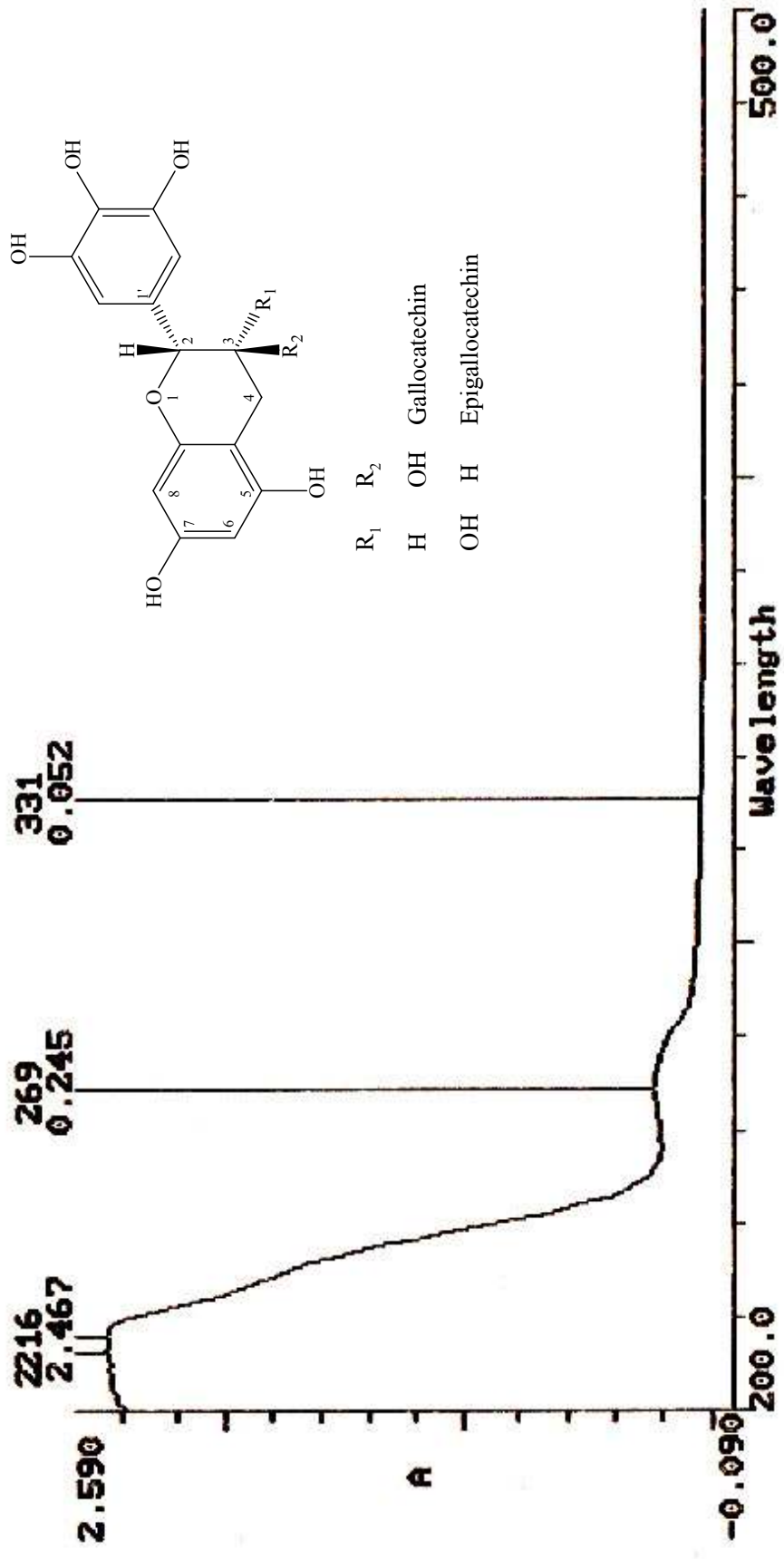
Figure 4-4 UV spectrum of mixture compound **1** in methanol
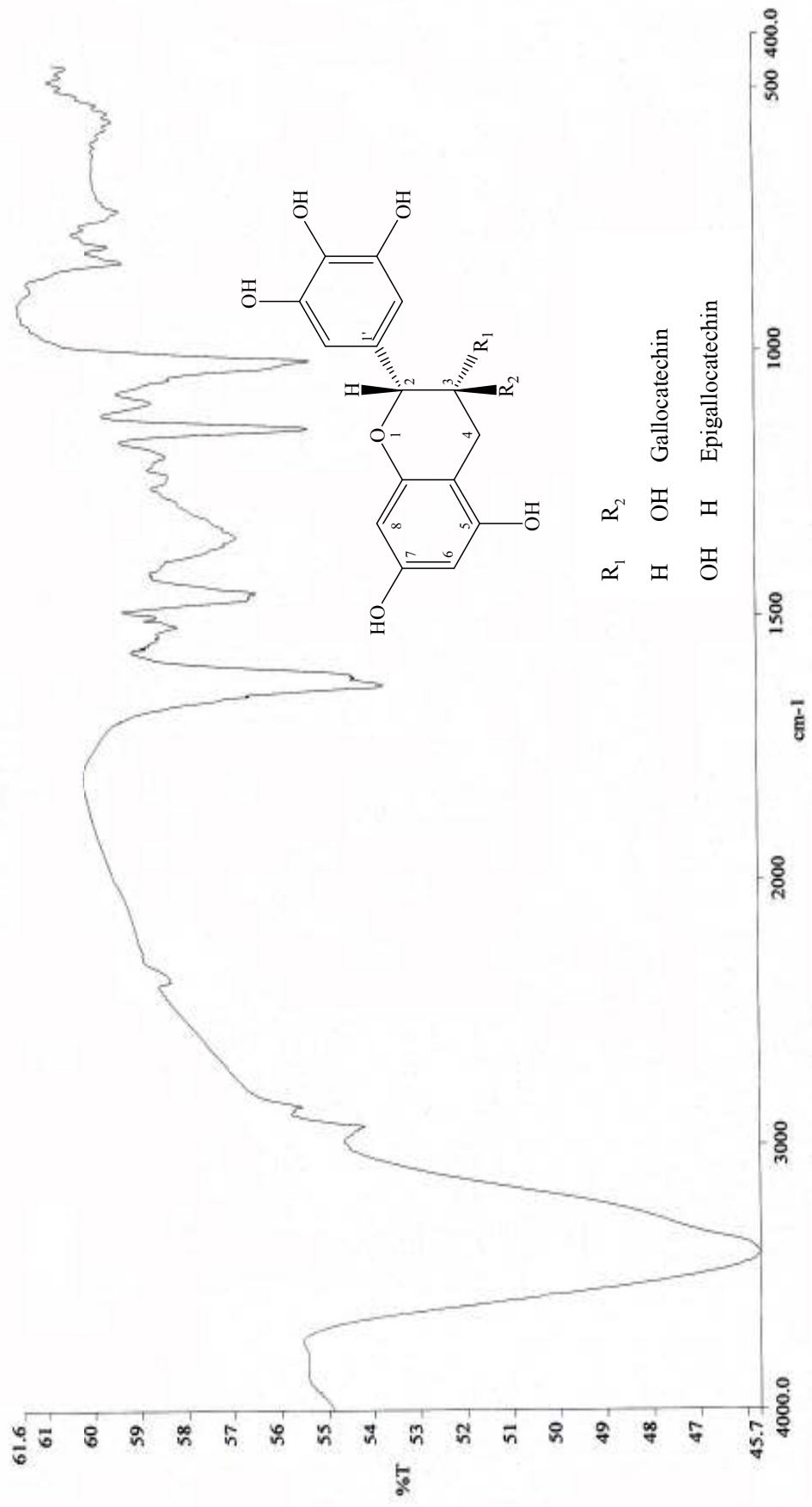
Figure 4-5 IR spectrum of compound **1**
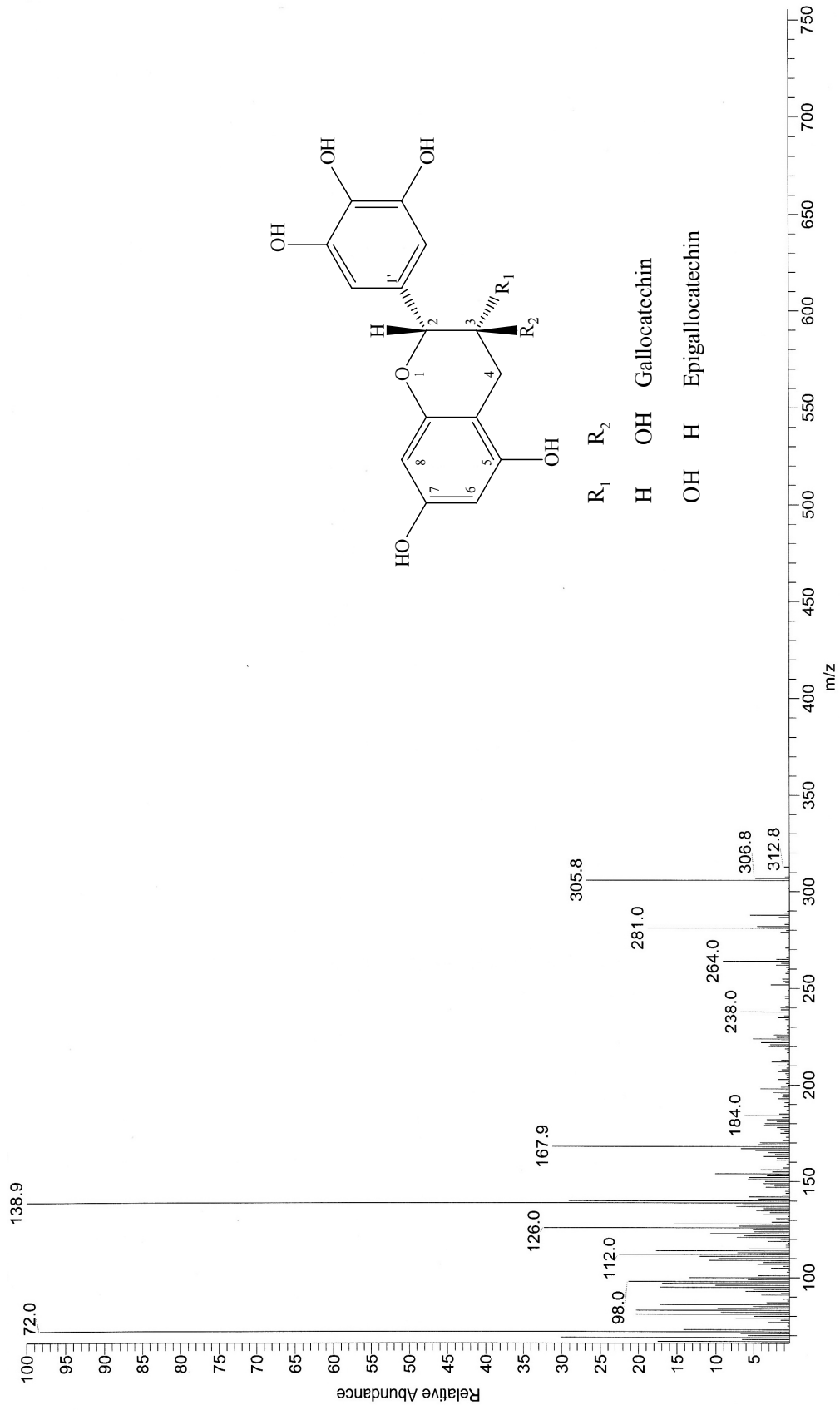
Figure 4-6 EI mass spectrum of compound

76
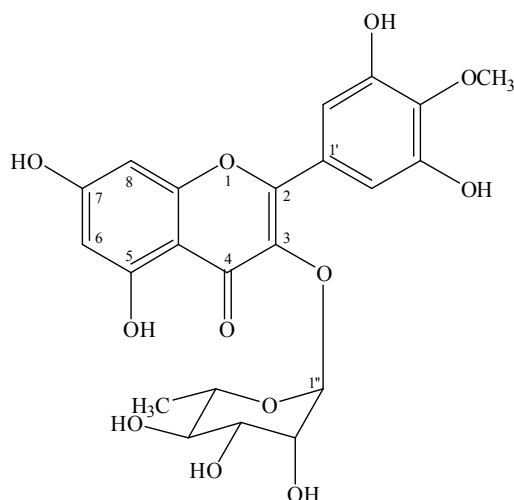
Figure 4-7   Chemical structure of mearnsitrin

Compound **2** was obtained as yellow needles (69 mg): mp 275-280 $^\circ$C. The molecular formula of 1 was proposed to be $C_{22}H_{22}O_{12}$ determined by EI mass spectrum, which showed C_{15} flavonoid peak at m/z 332.7. UV spectrum showed absorption λ_{max} (MeOH) at 202, 263, 337 nm. IR spectrum showed absorption band for hydroxyl (3417 cm^{-1}), C=C (1634 cm^{-1}) and C-O (1022 cm^{-1}). The ^{13}C NMR spectra data (Table 4-2) recorded in CD_3OD showed the existence of 22 signals for 22 carbon atoms in the molecule. This compound suggested the presence of 2 methyl (δ17.71, 60.93 ppm), 9 methine (δ 71.90, 72.05, 72.13, 73.26, 94.79, 99.93, 103.71, 109.92, 109.92 ppm), and 11 quaternary carbons (δ 106.03, 127.02, 136.76, 139.43, 151.92, 151.92, 158.62, 159.07, 163.27, 166.06, 179.72 ppm).

The ^{1}H NMR spectra data (Table 4-3) recorded in CD_3OD displayed a typical flavonol-α-L-rhamnopyranoside pattern having δ 0.95 ppm (*d*, *J* = 5.50 Hz, 3H-6″), 3.33 ppm (*m*, 1H-4″, 1H-5″), 3.72 ppm (*dd*, *J* = 3.21, 8.69 Hz, 1H-3″), 4.22 (*d*, *J* = 1.83 Hz, 1H-2″), and 5.37 ppm (*d*, *J* = 1.38 Hz, 1H-1″). Furthermore, one methoxyl signals at δ 3.87 ppm (*s*, 3H-4′) and 4 aromatic protons at δ 6.20 ppm (*d*, *J* = 2.0 Hz, 1H-6), 6.36 ppm (*d*, *J* = 2.0 Hz, 1H-8) and 6.88 ppm (*s*, 1H-2′, 1H-6′) were observed in the ^{1}H NMR spectrum. Thus on the basis of its spectroscopic data and compare with the previously reported data (Chung *et al*., 2004 / Table 4-3). Compound **2** was assigned as mearnsitrin (Figure 4-7 and Figures 4-8 to 4-12).

Table 4-3 Spectral data of compound **2** (CD$_3$OD; 500 MHz for ^{1}H NMR, CD$_3$OD; 125 MHz for ^{13}C NMR) compare with mearnsitrin (CD$_3$OD; 500 MHz for ^{1}H NMR, CD$_3$OD; 125 MHz for ^{13}C NMR) (continued)

Position	Type of C	δ_C / ppm		δ_H / ppm	
		Compound **2**	mearnsitrin	Compound **2**	mearnsitrin
1	-	-	-	-	-
2	C	159.07	159.48	-	-
3	C	136.76	136.98	-	-
4	C	179.72	179.80	-	-
4	OCH$_3$	60.93	60.93	3.87, 3H, *s*	3.88, 3H, *s*
5	C	163.27	163.27	-	-
6	CH	99.93	99.06	6.20, 1H, *d*, *J* = 2.00 Hz	6.32, 1H, *d*, *J* = 2.3 Hz
7	C	166.06	167.36	-	-
8	CH	94.79	93.17	6.36, 1H, *d*, *J* = 2.00 Hz	6.54, 1H, *d*, *J* = 2.3 Hz
9	C	158.62	158.45	-	-
10	C	106.03	106.85	-	-
1′	C	127.02	126.90	-	-
2′, 6′	CH	109.92	109.89	6.88, 1H, *s*	6.90, 1H, *s*
3′, 5′	C	151.92	151.90	-	-
4′	C	139.43	139.49	-	-
1″	CH	103.71	103.62	5.37, 1H, *d*, *J* = 1.38 Hz	5.33, 1H, *d*, *J* = 1.4 Hz
2″	CH	72.05	71.89	4.22, 1H, *d*, *J* = 1.83 Hz	4.24, 1H, *dd*, *J* = 3.4,1.4 Hz
3″	CH	72.13	72.07	3.72, 1H, *dd*, *J* = 3.21, 8.69 Hz	3.75, 1H, *dd*, *J* = 3.4, 9.2 Hz

Table 4-3 Spectral data of compound **2** (CD$_3$OD; 500 MHz for ^{1}H NMR, CD$_3$OD; 125 MHz for ^{13}C NMR) compare with mearnsitrin (CD$_3$OD; 500 MHz for ^{1}H NMR, CD$_3$OD; 125 MHz for ^{13}C NMR)

Position	Type of C	δ_C / ppm		δ_H / ppm	
		Compound **2**	mearnsitrin	Compound **2**	mearnsitrin
4″	CH	73.26	73.21	3.33, *m*	3.30-3.31, 1H, *m*
5″	CH	71.90	72.05	3.33, *m*	3.34-3.36, 1H, *m*
6″	CH$_3$	17.71	17.71	0.95, 3H, *d*, $J = 5.50$ Hz	0.95, 3H, *d*, $J = 5.50$ Hz
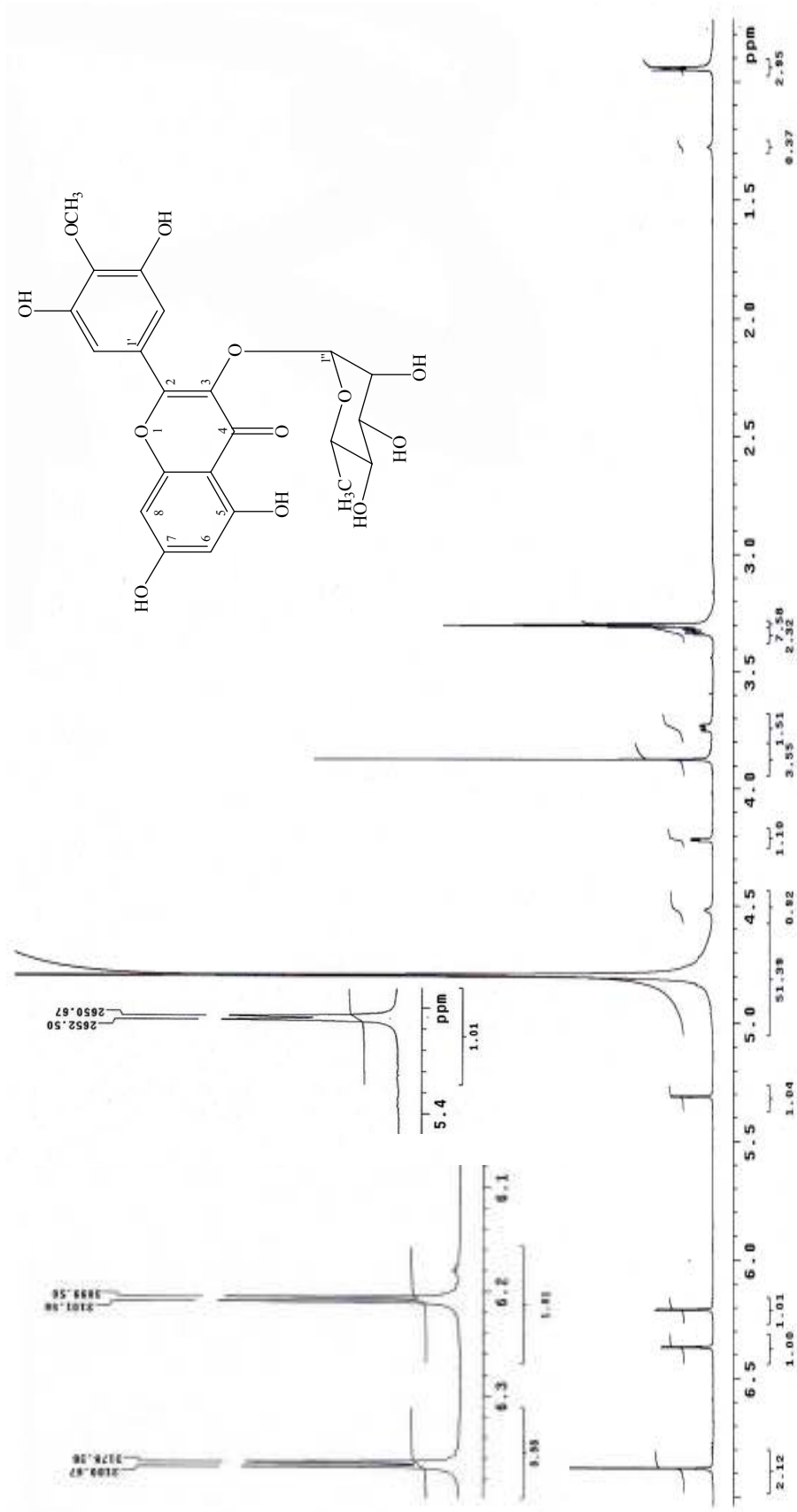
Figure 4-8 ^{1}H NMR spectrum of compound **2** in CD$_3$OD
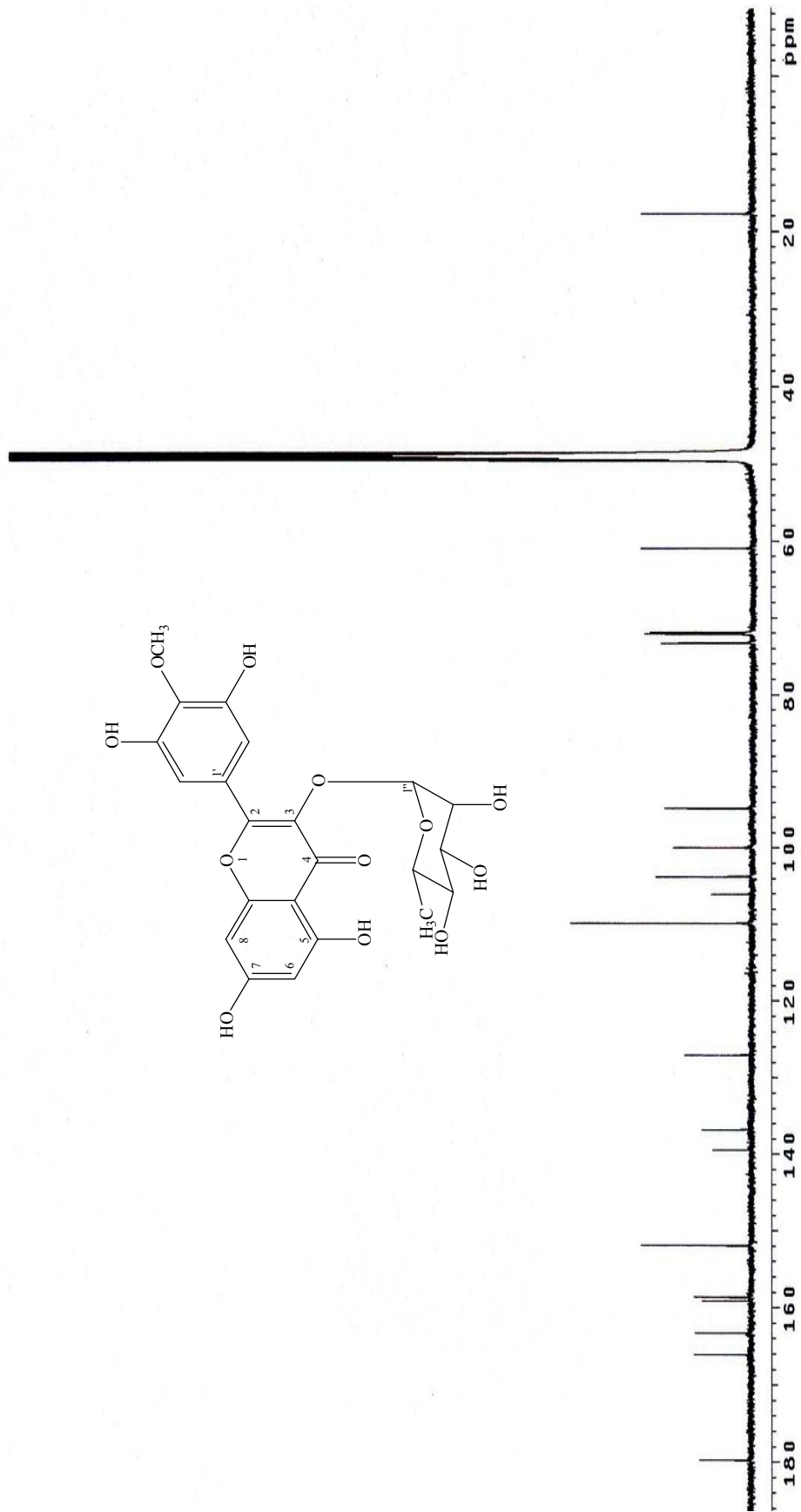
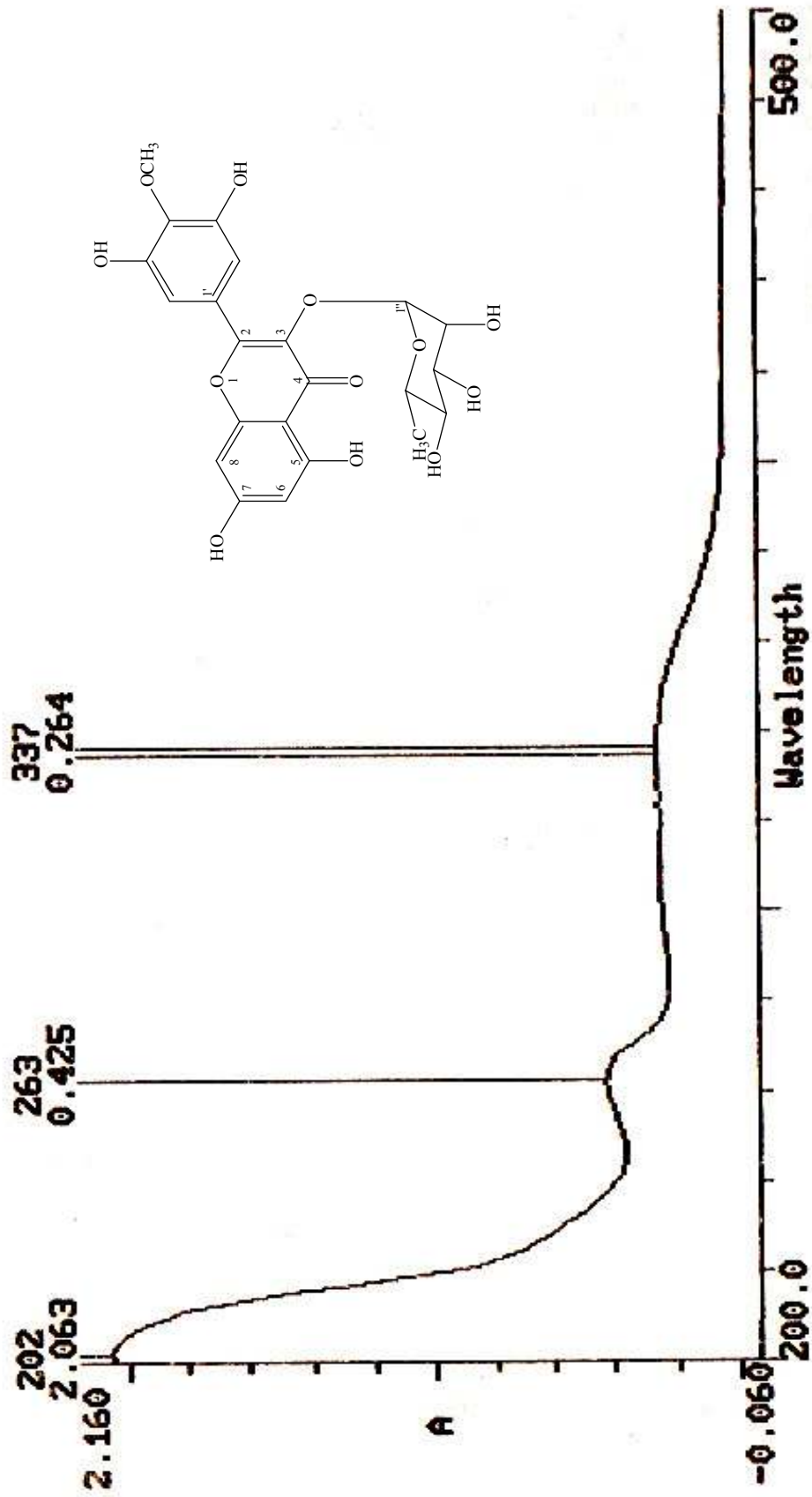**Figure 4-9** ^{13}C NMR spectrum of compound **2** in CD$_3$OD

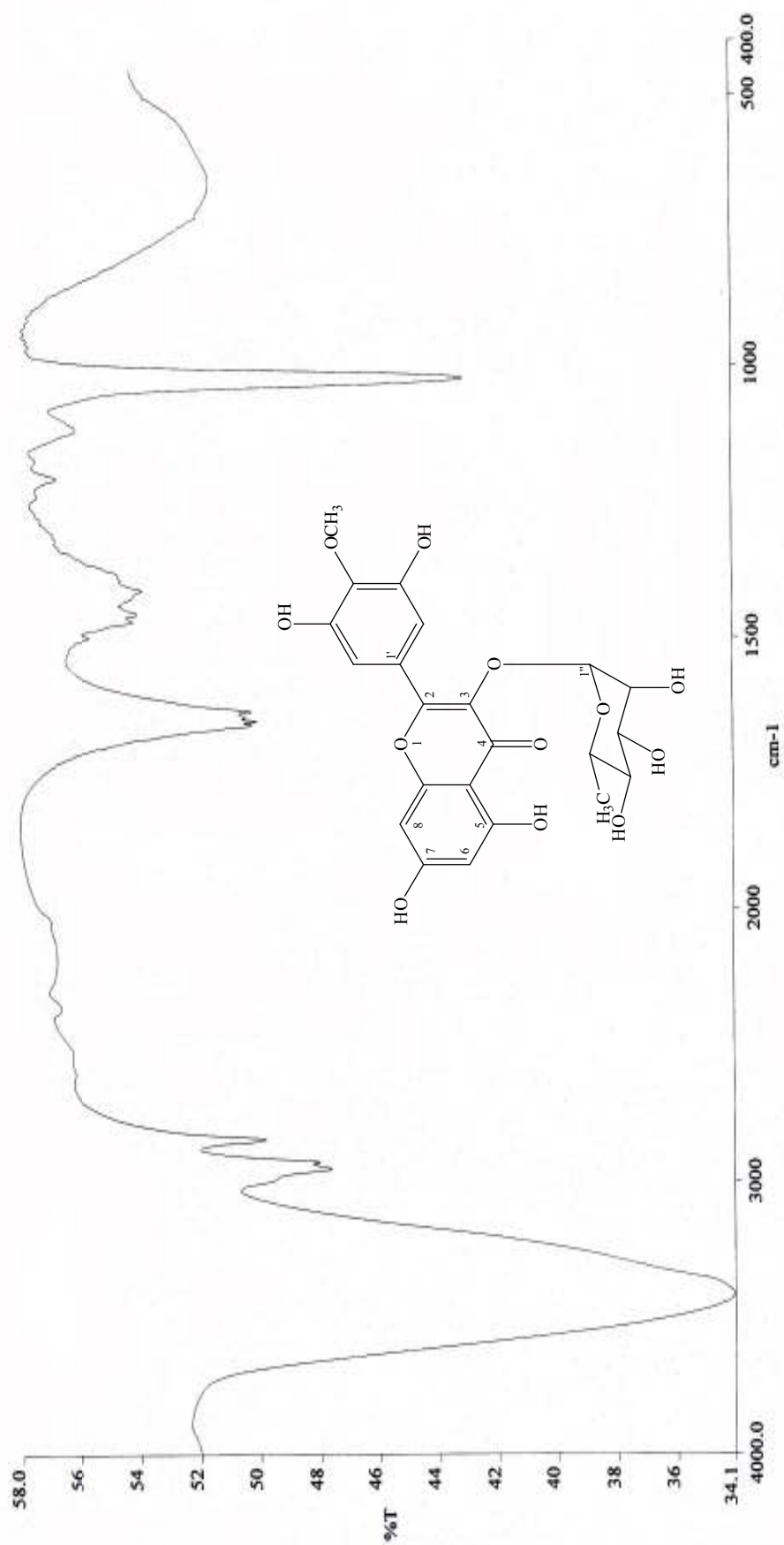**Figure 4-10** UV spectrum of compound **2** in methanol
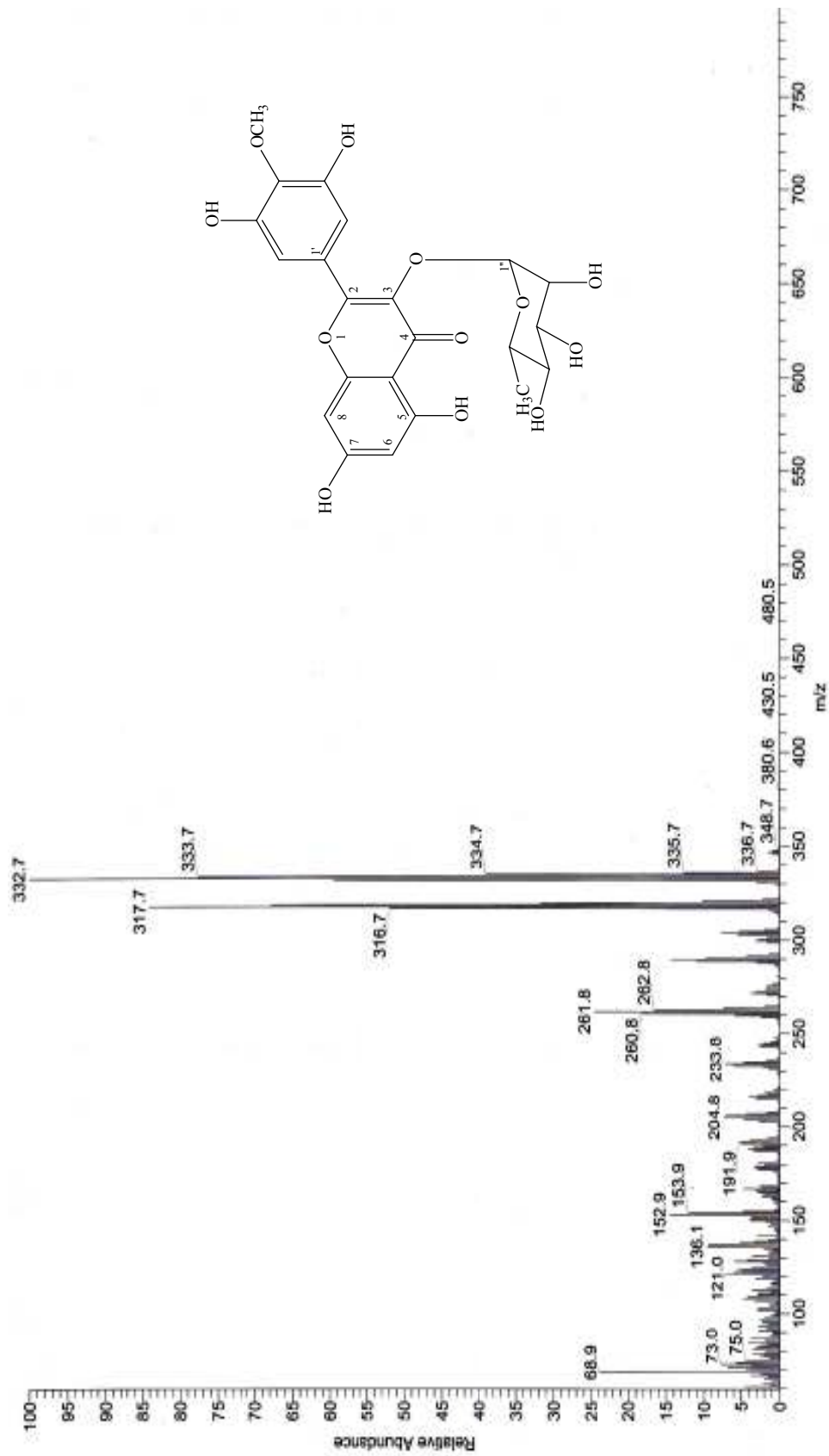
Figure 4-11 IR spectrum of compound **2**

Figure 4-12 EI mass spectrum of compound
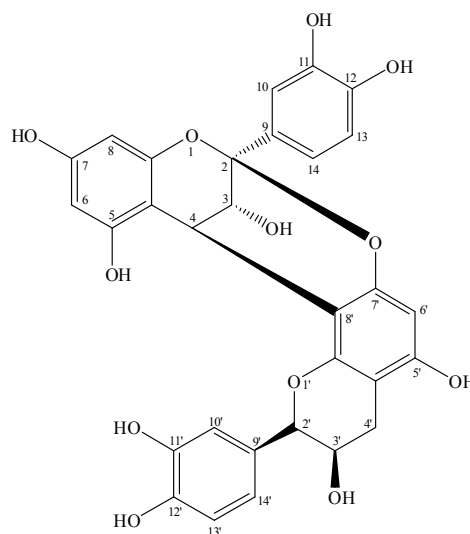
Figure 4-13 Chemical structure of proanthocyanidin A2

Compound **3** was obtained as a pale brown amorphous powder (40 mg): mp 185-190 $^{\circ}$C. The molecular formula of 4 was proposed to be $C_{30}H_{24}O_{12}$ determined by EI mass spectrum, which showed C_{15} flavonoid peak at m/z 287.0. UV spectrum showed absorption λ_{max} (MeOH) at 213, 280 nm. IR spectrum showed absorption band for hydroxyl (3411 cm^{-1}) and C=C (1616 cm^{-1}). The ^{13}C NMR spectra data (Table 4-4) recorded in CD$_3$OD showed the existence of 30 signals for 30 carbon atoms in the molecule. This compound suggested the presence of 1 methylene (δ 29.89 ppm), 15 methine (δ 29.28, 66.98, 68.09, 81.79, 96.55, 96.66, 98.35, 102.46, 104.29, 115.97, 115.65, 115.69, 116.07, 119.80, 120.40 ppm), and 14 quaternary carbons (δ 100.21, 107.24, 131.20, 132.47, 145.67, 146.01, 146.32, 146.78, 152.13, 152.30, 154.26, 156.60, 157.00, 158.14 ppm). The chemical shift of the ketal carbon (C-2) formed as a result of additional bond observed at 100.21 ppm provided further support for A-type linkage.

The ^{1}H NMR spectra data (Table 4-4) recorded in CD$_3$OD displayed 9 aromatic proton signals appeared at δ 6.00 ppm (*d*, *J* = 2.40 Hz, 1H-6), 6.06 ppm (*d*, *J* = 2.34 Hz, 1H-8), 6.09 ppm (*s*, 1H-6′), 6.81 ppm (*dd*, *J* = 1.72, 8.29 Hz, 1H-13), 6.81 ppm (*dd*, *J* = 1.82, 8.29 Hz, 1H-13′), 6.97 ppm (*dd*, *J* = 2.06, 8.17 Hz, 1H-14′), 7.02 ppm (*dd*, *J* = 2.17, 8.28 Hz, 1H-14), 7.13 ppm (*d*, *J* = 2.17 Hz, 1H-10), 7.15 ppm (*d*, *J* = 2.06 Hz, 1H-10′), corresponding to a biflavonoid structure and consistent with a proanthocyanidin A-type with a molecular weight of 576. The presence of the isolated AB coupling system at δ 4.05–4.40 ppm with $J_{3,4}$ = 3.43 Hz was described

as a diagnostic feature of the C-ring protons of A-type proanthocyanidins. Finally, the ^{1}H and ^{13}C NMR signals were in agreement with the data published and compare with the previously reported data (Hsieh *et al*., 2008 / Table 4-4). Compound **3** was assigned as proanthocyanidin A2 or epicatechin-(4β-8, 2β-*O*-7)-epicatechin (Figure 4-13 and Figures 4-14 to 4-18).

Table 4-4 Spectral data of compound **3** (CD₃OD; 500 MHz for ^{1}H NMR, CD₃OD; 125 MHz for ^{13}C NMR) compare with proanthocyanidin A2 (CD₃OD; 500 MHz for ^{1}H NMR, CD₃OD; 125 MHz for ^{13}C NMR)

Position	Type of C	δ_C / ppm		δ_H / ppm	
		Compound **3**	proanthocyanidin A2	Compound **3**	proanthocyanidin A2
1	-	-	-	-	-
1′	-	-	-	-	-
2	C	100.21	100.2	-	-
2′	CH	81.79	81.8	4.92, 1H, *br s*	4.92, 1H, *br s*
3	CH	68.09	68.1	4.05, 1H, *d*, $J = 3.43$ Hz	4.92, 1H, *d*, $J = 3.4$ Hz
3′	CH	66.98	67.0	4.24, 1H, *br s*	4.23, 1H, *br s*
4	CH	29.28	29.3	4.40, 1H, *d*, $J = 3.43$ Hz	4.40, 1H, *d*, $J = 3.4$ Hz
4′α	CH₂	29.89	29.9	2.75, 1H, *dd*, $J = 2.06, 17.21$ Hz	2.75, 1H, *dd*, $J = 2.1, 17.2$ Hz
4′β	CH₂	29.89	29.9	2.94, 1H, *dd*, $J = 4.91, 17.1$ Hz	2.94, 1H, *dd*, $J = 4.9, 17.2$ Hz
4a	C	104.29	104.3	-	-
4a′	C	102.46	102.4	-	-
5	C	157.00	157.0	-	-
5′	C	156.60	156.6	-	-
6	CH	98.35	98.3	6.00, 1H, *d*, $J = 2.40$ Hz	5.99, 1H, *d*, $J = 2.3$ Hz
6′	CH	96.55	96.5	6.09, 1H, *s*	6.09, 1H, *s*

Table 4-4 Spectral data of compound **3** (CD$_3$OD; 500 MHz for ^{1}H NMR, CD$_3$OD; 125 MHz for ^{13}C NMR) compare with proanthocyanidin A2 (CD$_3$OD; 500 MHz for ^{1}H NMR, CD$_3$OD; 125 MHz for ^{13}C NMR) (continued)

Position	Type of C	δ_C / ppm		δ_H / ppm	
		Compound **3**	proanthocyanidin A2	Compound **3**	proanthocyanidin A2
7	C	158.14	158.1	-	-
7′	C	152.30	152.3	-	-
4	CH	29.28	29.3	4.40, 1H, *d*, *J* = 3.43 Hz	4.40, 1H, *d*, *J* = 3.4 Hz
8	C	96.66	96.6	6.06, 1H, *d*, *J* = 2.34 Hz	6.06, 1H, *d*, *J* = 2.3 Hz
8′	C	107.24	107.2	-	-
8a	C	154.26	154.3	-	-
8a′	C	152.13	152.1	-	-
9	C	132.47	132.5	-	-
9′	C	131.20	131.2	-	-
10	CH	115.97	116.0	7.13, 1H, *d*, *J* = 2.17 Hz	7.13, 1H, *d*, *J* = 2.1 Hz
10′	CH	116.07	116.1	7.15, 1H, *d*, *J* = 2.06 Hz	7.15, 1H, *d*, *J* = 1.9 Hz
11	C	145.67	145.7	-	-
11′	C	146.01	146.0	-	-
12	C	146.78	146.8	-	-
12′	C	146.32	146.3	-	-
13	CH	115.65	115.7	6.81, 1H, *dd*, *J* = 1.72, 8.29 Hz	6.81, 1H, *d*, *J* = 8.2 Hz
13′	CH	115.69	115.6	6.80, 1H, *dd*, *J* = 1.82, 8.29 Hz	6.80, 1H, *d*, *J* = 8.2 Hz

Table 4-4 Spectral data of compound **3** (CD$_3$OD; 500 MHz for ^{1}H NMR, CD$_3$OD; 125 MHz for ^{13}C NMR) compare with proanthocyanidin A2 (CD$_3$OD; 500 MHz for ^{1}H NMR, CD$_3$OD; 125 MHz for ^{13}C NMR) (continued)

Position	Type of C	δ_C / ppm		δ_H / ppm	
		Compound **3**	proanthocyanidin A2	Compound **3**	proanthocyanidin A2
14	CH	119.80	119.8	7.02, 1H, *dd*, J = 2.17, 8.28 Hz	7.01, 1H, *dd*, J = 2.1, 8.2 Hz
14′	CH	120.40	120.4	6.97, 1H, *dd*, J = 2.06, 8.17 Hz	6.97, 1H, *dd*, J = 1.9, 8.2 Hz

Figure 4-14 ^{1}H NMR spectrum of compound **3** in CD$_3$OD
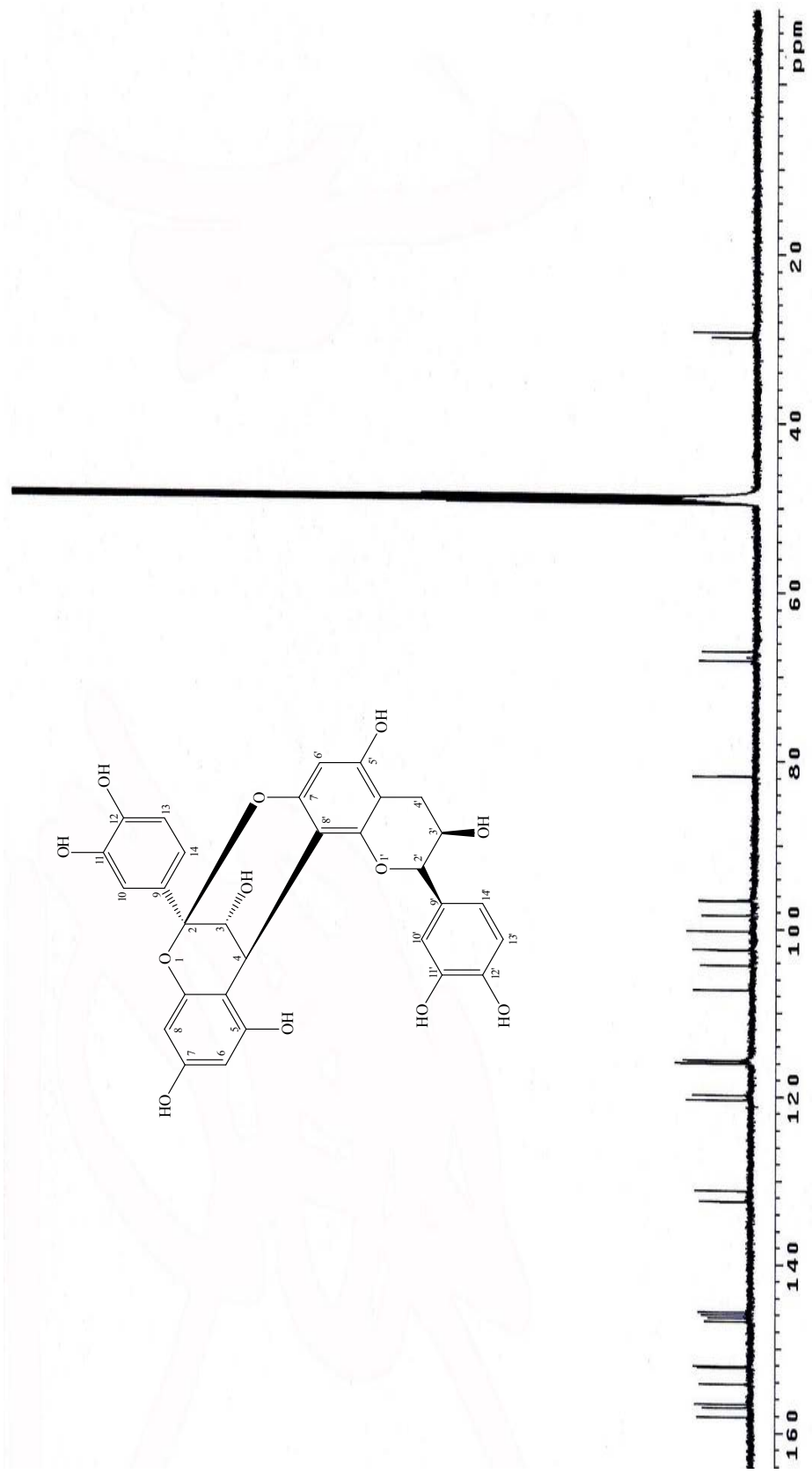
Figure 4-15 ^{13}C NMR spectrum of compound **3** in CD$_3$OD
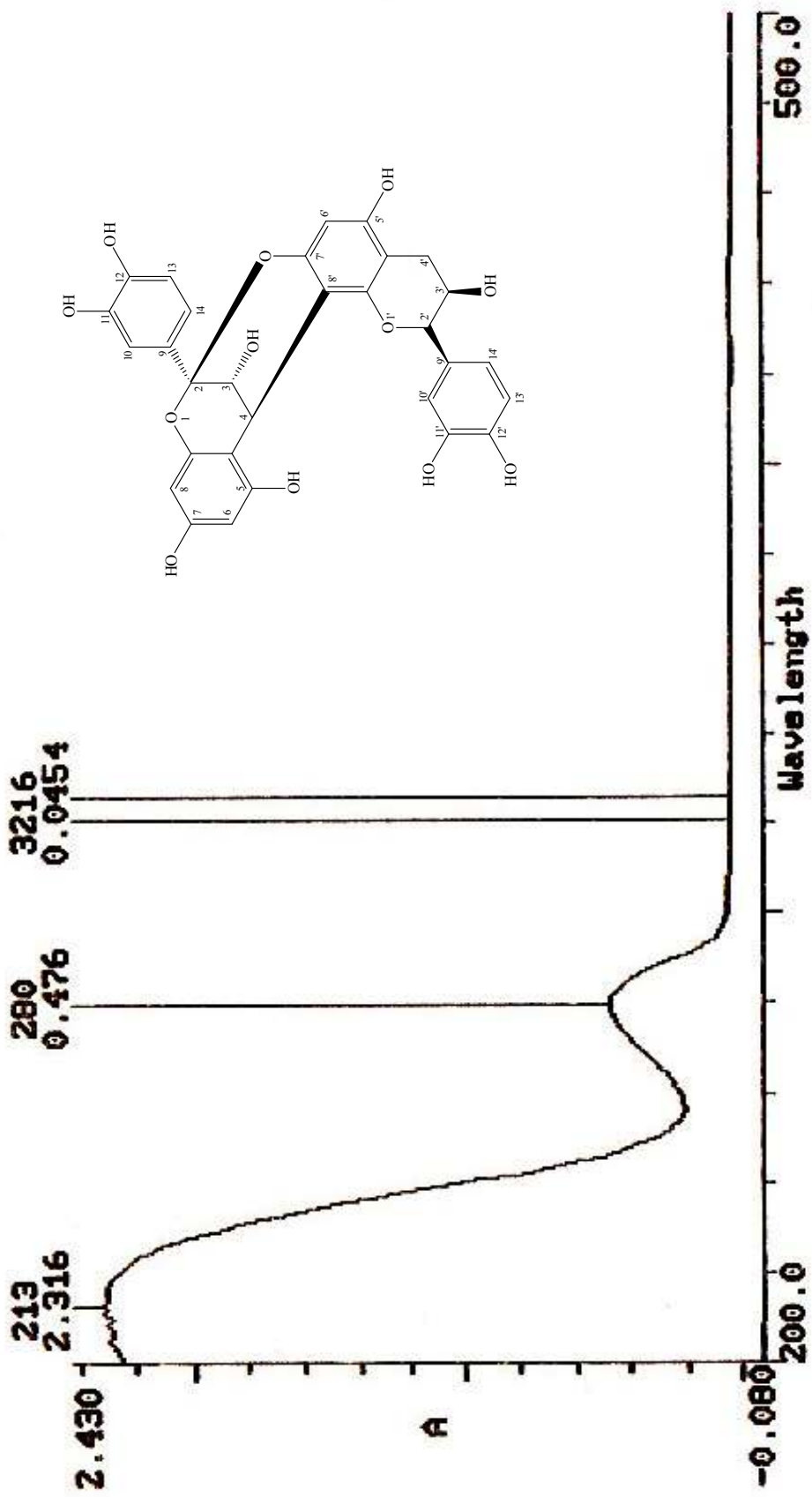
Figure 4-16 UV spectrum of compound **3** in methanol
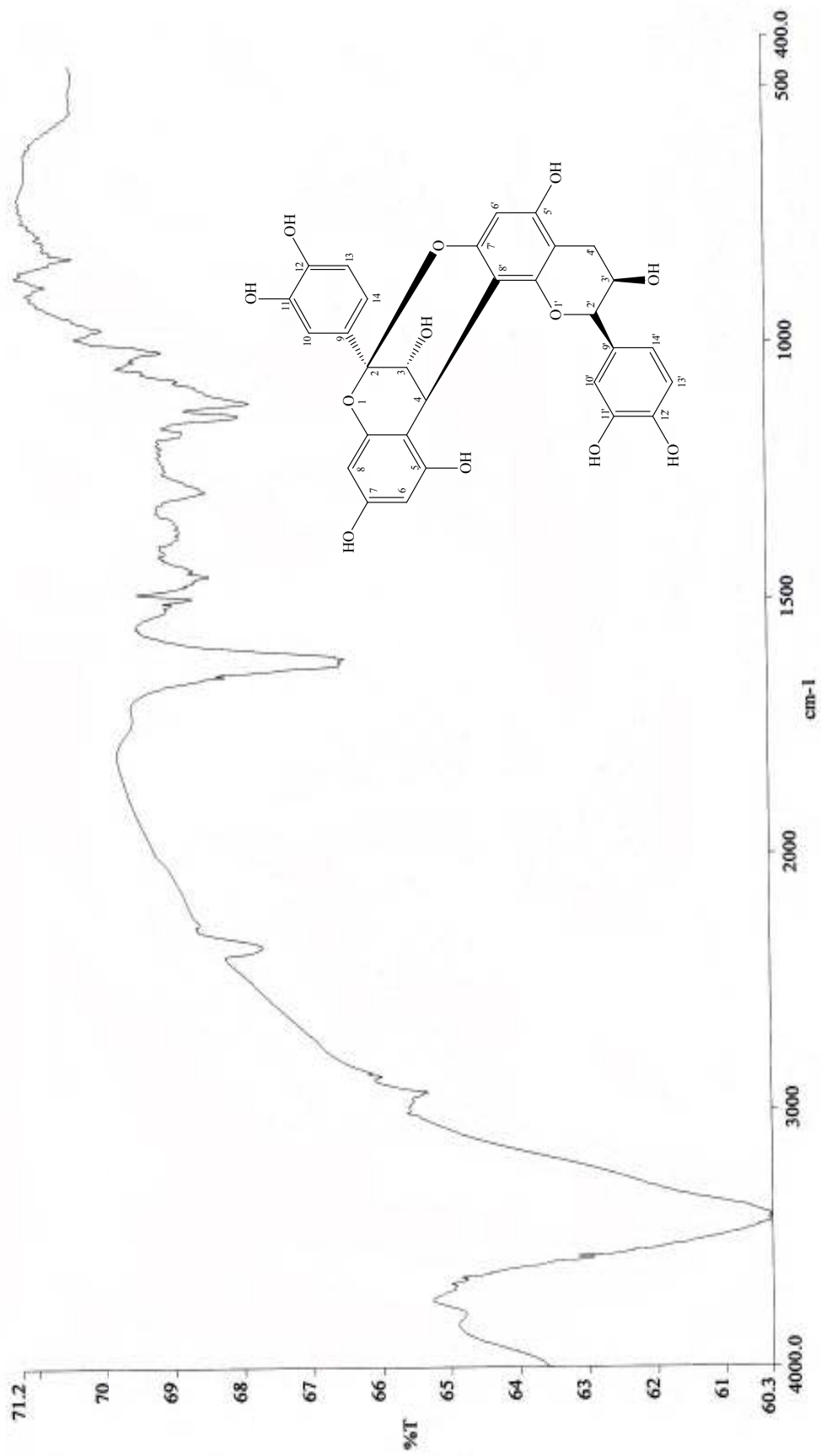
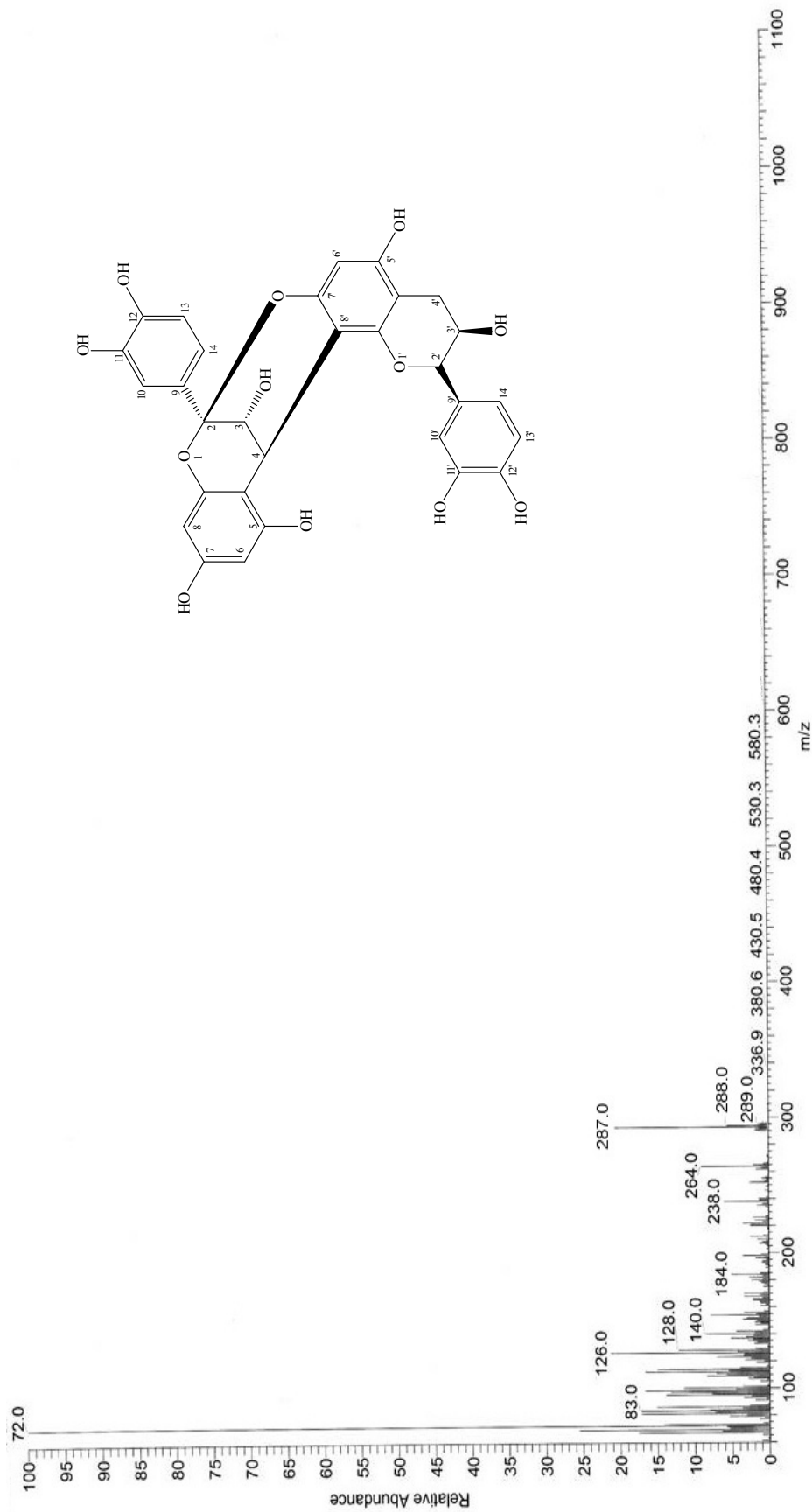**Figure 4-17** IR spectrum of compound **3**

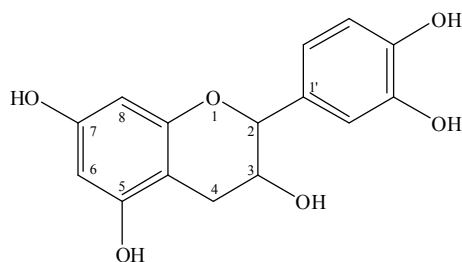**Figure 4-18** EI mass spectrum of compound **3**

Figure 4-19 Chemical structure of epicatechin

Compound **4** was obtained as orange needles (10 mg): mp 175-178 $^{\circ}$C. The molecular formula of 4 was proposed to be $C_{15}H_{14}O_6$ determined by EI mass spectrum, which showed C_{15} flavonoid peak at m/z 289.8. UV spectrum showed absorption λ_{max} (MeOH) at 211, 280 nm. IR spectrum showed absorption band for hydroxyl (3436 cm^{-1}), C=C (1631 cm^{-1}) and C-O (1097 cm^{-1}). The ^{13}C NMR spectra data (Table 4-5) recorded in CD$_3$OD showed the existence of 15 signals for 15 carbon atoms in the molecule. This compound suggested the presence of 1 methylene (δ 29.07 ppm), 7 methine (δ 67.49, 79.88, 95.86, 96.35, 115.30, 115.87, 119.37 ppm), and 7 quaternary carbons (δ 100.45, 132.28, 145.78, 145.95, 157.37, 157.67, 158.02 ppm).

The ^{1}H NMR spectra data (Table 4-5) recorded in CD$_3$OD displayed 5 aromatic proton signals appeared at δ 5.90 ppm (*d*, *J* = 2.29 Hz, 1H-8), 5.93 ppm (*d*, *J* = 2.52 Hz, 1H-6), 6.75 ppm (*d*, *J* = 8.23 Hz, 1H-5′), 6.79 ppm (*dd*, *J* = 2.05, 8.23 Hz, 1H-6′), 6.96 ppm (*d*, *J* = 2.06 Hz, 1H-2′) and as a pair of meta-coupled doublets at δ 5.93 (*d*, *J* = 2.29 Hz, H-6) and δ 5.90 (*d*, *J* = 2.29 Hz, H-8). The ^{1}H NMR spectrum of 2 showed two doublets of doublets at δ 2.73 and 2.85 assigned to the H-4 protons (coupled to each other with *J* = 16.80 Hz, and to H-3 with *J* = 4.57 and 2.75 Hz) and a singlet at δ 4.81 ppm (1H-2) and δ 4.17 ppm (*m*, 1H-3). Thus on the basis of its spectroscopic data and compare with the previously reported data (Qi *et al*., 2003 / Table 4-5). Compound **4** was assigned as epicatechin (Figure 4-19 and Figures 4-20 to 4-21).

Table 4-5 Spectral data of compound **4** (CD$_3$OD; 500 MHz for ^{1}H NMR, CD$_3$OD; 125 MHz for ^{13}C NMR) compare with epicatechin (CD$_3$OD; 500 MHz for ^{1}H NMR, CD$_3$OD; 125 MHz for ^{13}C NMR)

| Position	Type of C	δ_C / ppm		δ_H / ppm	
		Compound **4**	Epicatechin	Compound **4**	Epicatechin
1	-	-	-	-	-
2	CH	79.88	79.46	4.81, 1H, *s*	4.81, 1H, *s*
3	CH	67.49	66.97	4.17, 1H, *m*	4.18, 1H, *m*
4α	CH$_2$	29.07	29.01	2.85, 1H, *dd*, $J = 4.57, 16.69$ Hz	2.85, 1H, *dd*, $J = 5.4, 16.1$ Hz
4β	CH$_2$	29.07	29.01	2.73, 1H, *dd*, $J = 2.75, 16.80$ Hz	2.74, 1H, *dd*, $J = 2.7, 16.1$ Hz
5	C	158.02	157.61	-	-
6	CH	96.35	96.22	5.93, 1H, *d*, $J = 2.52$ Hz	5.95, 1H, *d*, $J = 1.8$ Hz
7	C	157.67	157.60	-	-
8	CH	95.86	95.75	5.90, 1H, *d*, $J = 2.29$ Hz	5.88, 1H, *d*, $J = 1.8$ Hz
9	C	157.37	157.19	-	-
10	C	100.45	99.85	-	-
1′	C	132.28	132.32	-	-
2′	CH	115.30	115.31	6.96, 1H, *d*, $J = 2.06$ Hz	6.97, 1H, *d*, $J = 1.8$ Hz
3′	C	145.95	145.42	-	-
4′	C	145.78	145.31	-	-
5′	CH	115.87	115.51	6.75, 1H, *d*, $J = 8.23$ Hz	6.72, 1H, *d*, $J = 8.0$ Hz
6′	CH	119.37	119.41	6.79, 1H, *dd*, $J = 2.05, 8.23$ Hz	6.81, 1H, *dd*, $J = 1.8, 8.0$ Hz
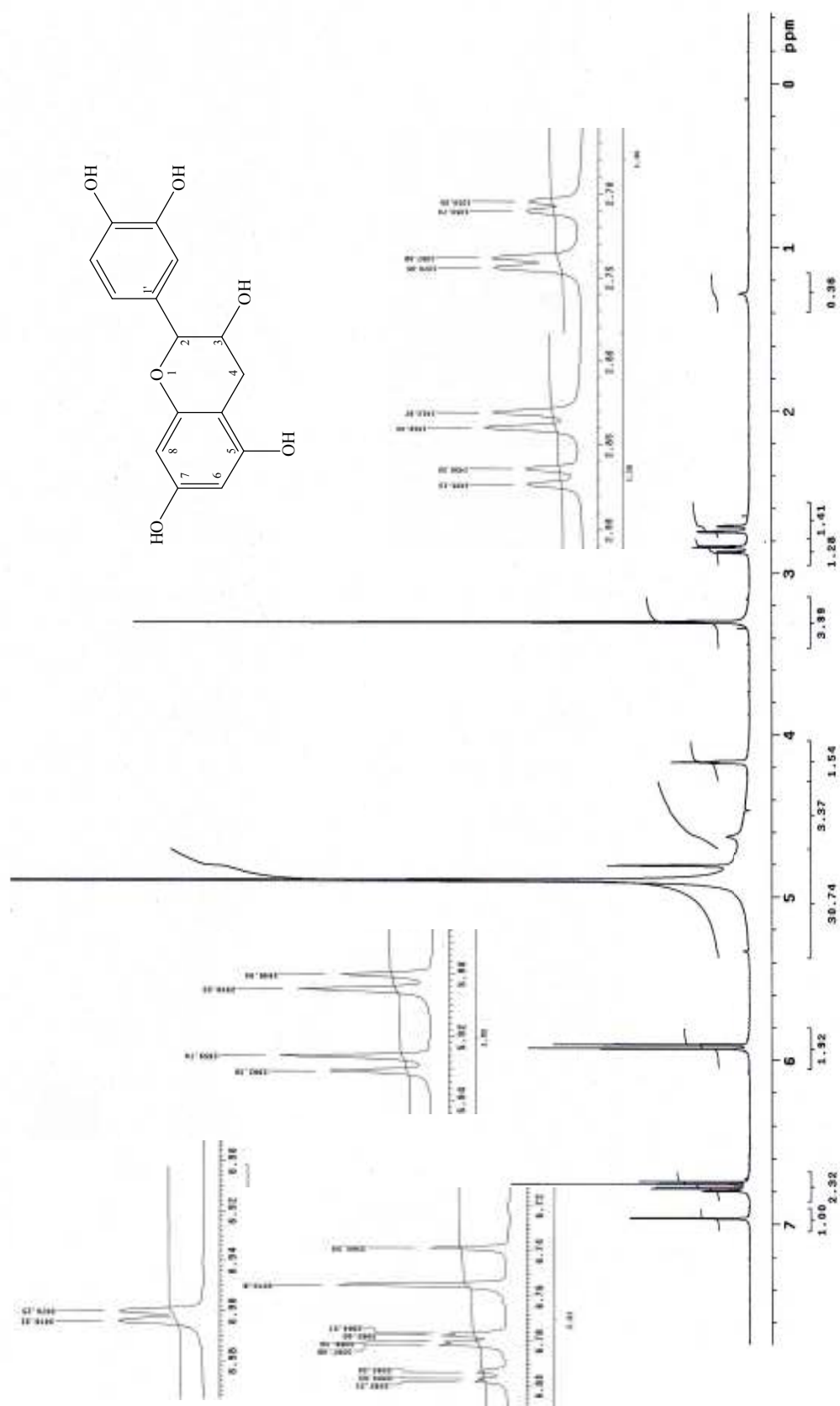
Figure 4-20 ^{1}H NMR spectrum of compound 4 in CD$_3$OD
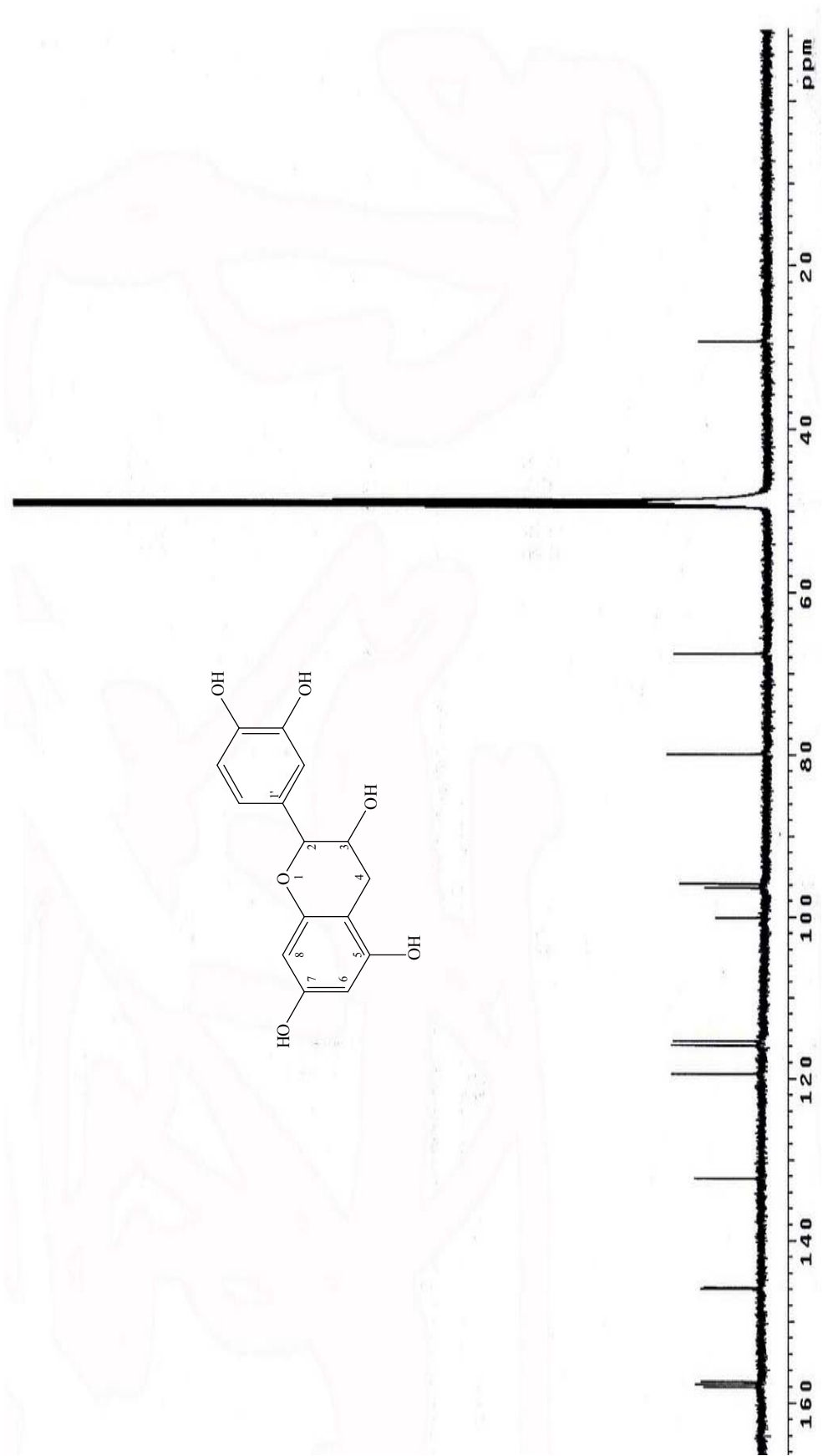
Figure 4-21 ^{13}C NMR spectrum of compound **4** in CD$_3$OD
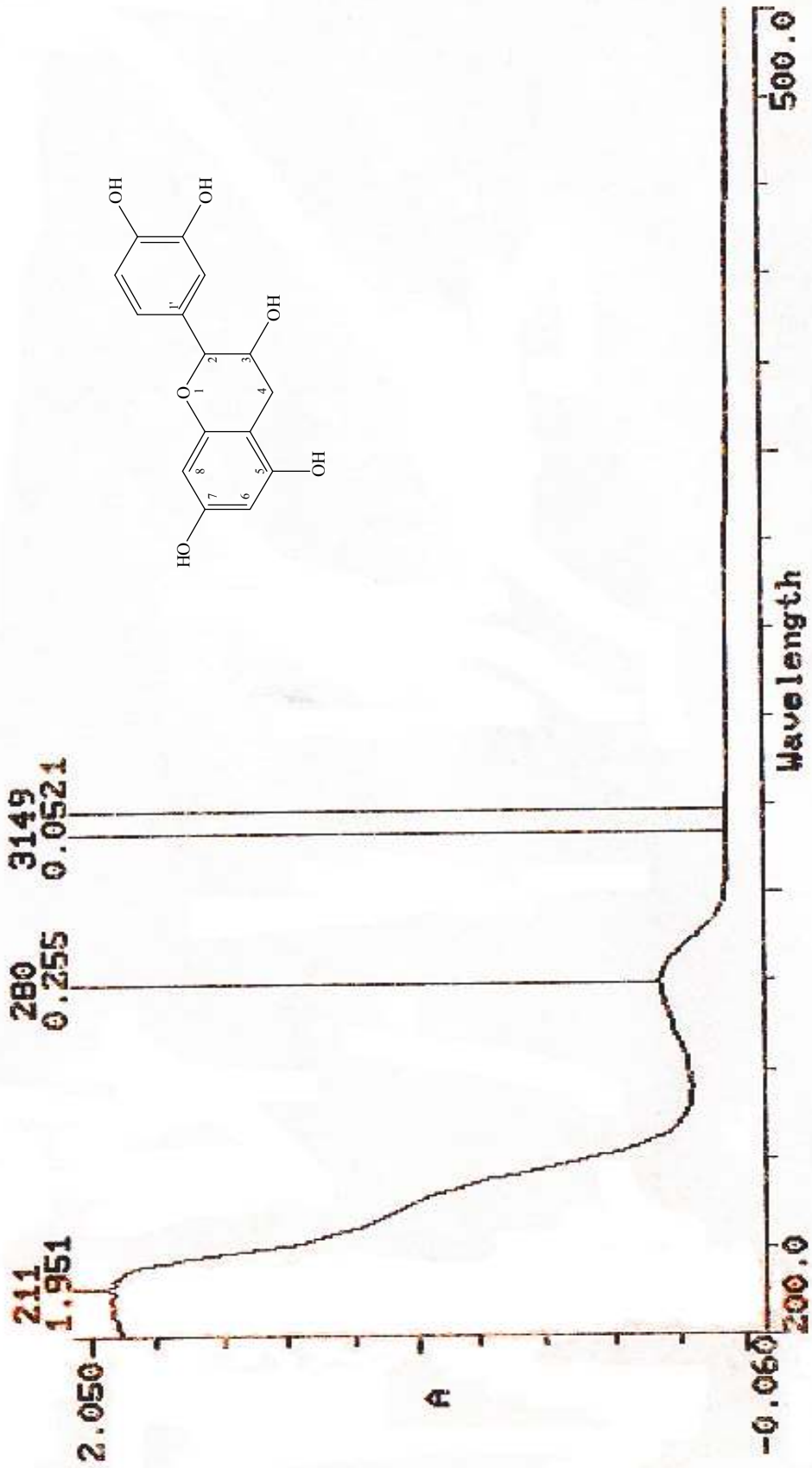
Figure 4-22 UV spectrum of compound 4 in methanol
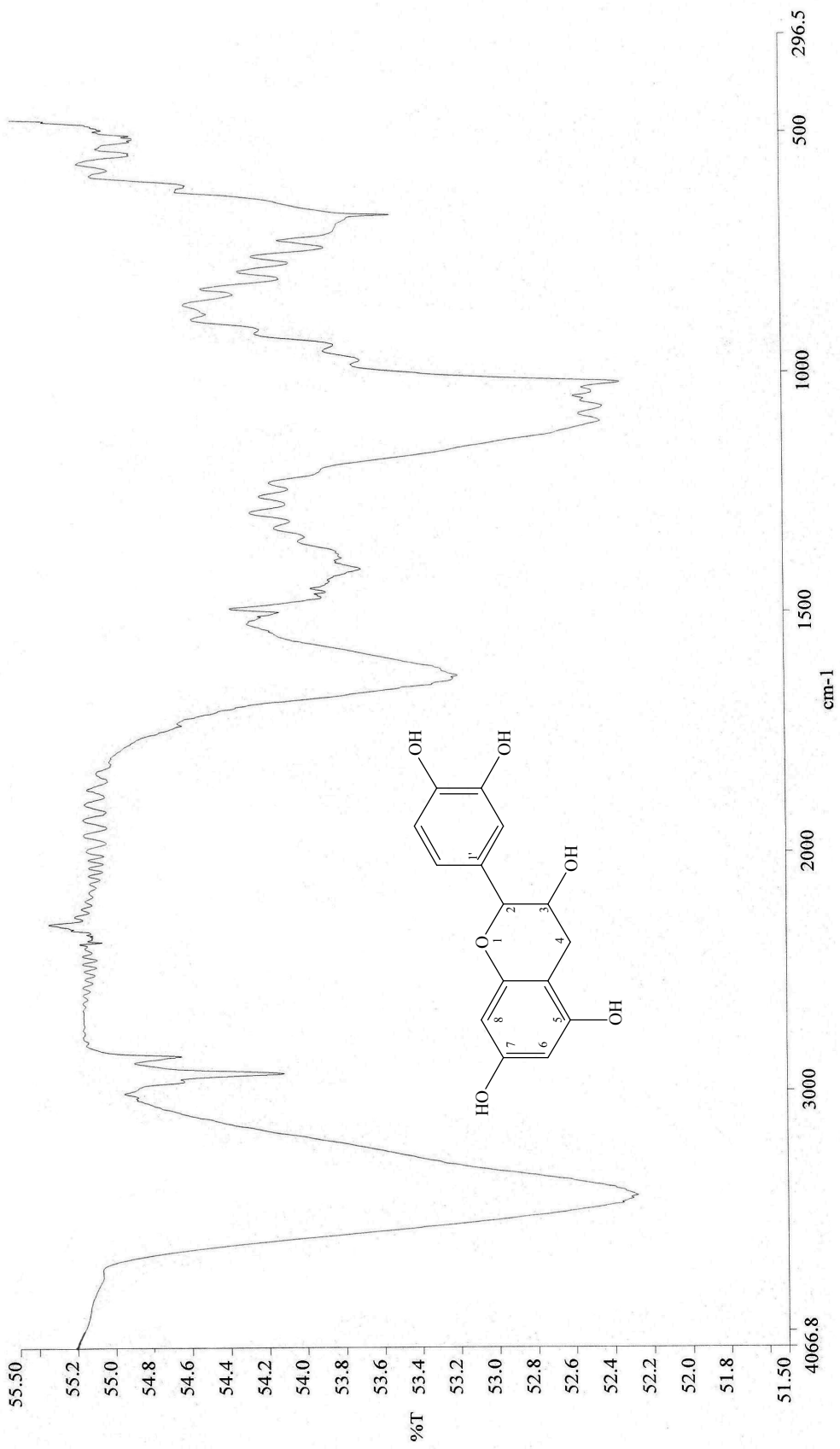
Figure 4-23 IR spectrum of compound **4**
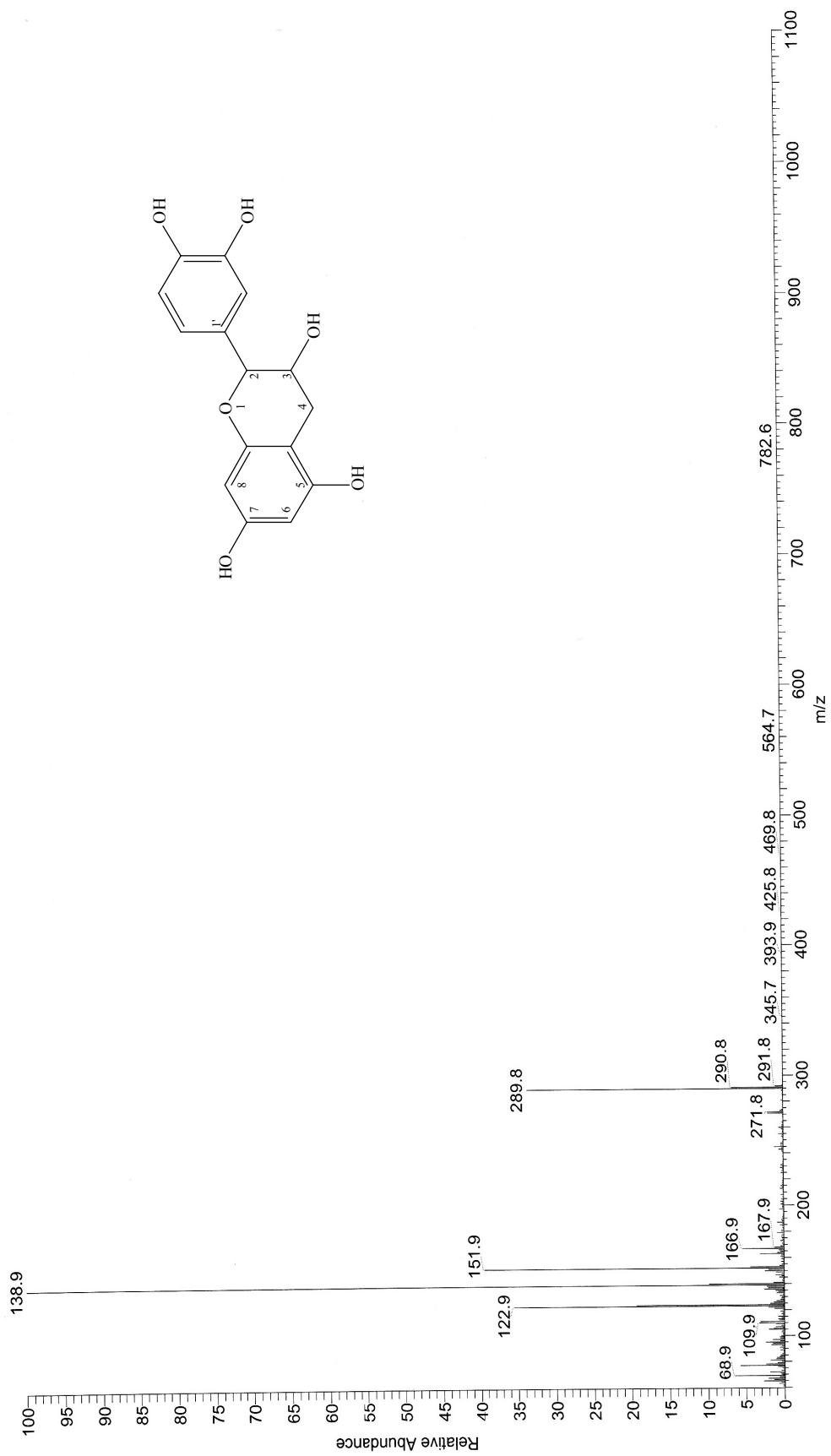
Figure 4-24 EI mass spectrum of compound **4**
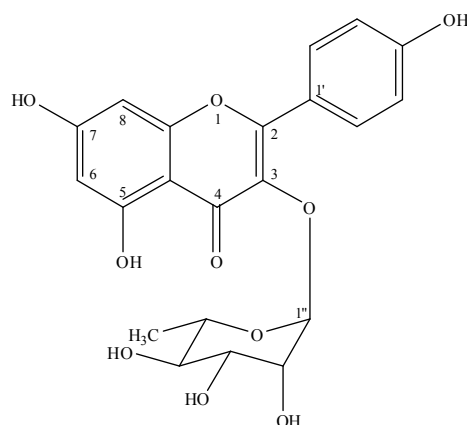
Figure 4-25 Chemical structure of kaempferol-3-*O*-rhamnoside

Compound **5** was obtained as yellow amorphous powder (74 mg): mp 285-295 °C. The molecular formula of 5 was proposed to be $C_{21}H_{20}O_{10}$ determined by EI mass spectrum, which showed C_{15} flavonoid peak at m/z 285.7. UV spectrum showed absorption λ_{max} (MeOH) at 203, 265, 343 nm. IR spectrum showed absorption band for hydroxyl (3422 cm^{-1}), C=C (1634 cm^{-1}) and C-O (1018 cm^{-1}). The ^{13}C NMR spectra data (Table 4-6) recorded in CD_3OD showed the existence of 21 signals for 21 carbon atoms in the molecule. This compound suggested the presence of 1 methyl (δ17.64 ppm), 11 methine (δ 71.93, 72.02, 72.16, 73.23, 94.77, 99.85, 103.51, 116.53, 116.53, 131.89, 131.89 ppm) and 9 quaternary carbons (δ 105.96, 122.67, 136.24, 158.56, 159.29, 161.56, 163.21, 165.85, 179.63 ppm).

The ^{1}H NMR spectra data (Table 4-6) recorded in CD_3OD displayed a typical flavonol-rhamnopyranoside pattern having δ 0.95 ppm (*d*, *J* = 5.50 Hz, 3H-6″), 3.33 ppm (*m*, 1H-4″, 1H-5″), 3.72 ppm (*dd*, *J* = 3.21, 8.69 Hz, 1H-3″), 4.22 (*d*, *J* = 1.83 Hz, 1H-2″), and 5.37 ppm (*d*, *J* = 1.38 Hz, 1H-1″). Furthermore, 6 aromatic protons at δ 6.19 ppm (*d*, *J* = 1.7 Hz, 1H-6), 6.36 ppm (*d*, *J* = 1.8 Hz, 1H-8), 6.92 ppm (*d*, *J* = 8.69 Hz, 1H-3′,1H-5′) and 7.76 ppm (*d*, *J* = 8.69 Hz, 1H-2′,1H-6′) were observed in the ^{1}H NMR spectrum. Thus on the basis of its spectroscopic data and compare with the previously reported data (Matsuda, *et al*., 2002; Chung, *et al*., 2004 / Table 4-6). Compound **5** was assigned as kaempferol-3-*O*-rhamnoside (Figure 4-25 and Figures 4-26 to 4-30).

Table 4-6 Spectral data of compound **5** (CD$_3$OD; 500 MHz for ^{1}H NMR, CD$_3$OD; 125 MHz for ^{13}C NMR) compare with kaempferol-3-*O*-rhamnoside (CD$_3$OD; 500 MHz for ^{1}H NMR, CD$_3$OD; 125 MHz for ^{13}C NMR)

Position	Type of C	δ_C / ppm		δ_H / ppm	
		Compound **5**	kaempferol-3-*O*-rhamnoside	Compound **5**	kaempferol-3-*O*-rhamnoside
1	-	-	-	-	-
2	C	158.56	158.8	-	-
3	C	136.24	136.2	-	-
4	C	179.63	179.1	-	-
5	C	163.21	163.0	-	-
6	CH	99.85	99.9	6.19, 1H, *d*, *J* = 1.70 Hz	6.20, 1H, *d*, *J* = 2.3 Hz
7	C	165.85	166.5	-	-
8	CH	94.77	94.8	6.36, 1H, *d*, *J* = 1.80 Hz	6.38, 1H, *d*, *J* = 2.3 Hz
9	C	159.29	158.4	-	-
10	C	105.96	105.5	-	-
1′	C	122.67	123.1	-	-
2′, 6′	CH	131.89	132.0	7.76, 1H, *d*, *J* = 8.69 Hz	7.77, 1H, *d*, *J* = 8.7 Hz
3′, 5′	CH	116.53	115.9	6.92, 1H, *d*, *J* = 8.69 Hz	6.87, 1H, *d*, *J* = 8.7 Hz
4′	C	161.56	161.2	-	-
1″	CH	103.51	103.5	5.37, 1H, *d*, *J* = 1.38 Hz	5.38, 1H, *d*, *J* = 1.8 Hz
2″	CH	72.16	71.9	4.22, 1H, *d*, *J* = 1.83 Hz	4.22, 1H, *dd*, *J* = 3.2,1.8 Hz

Table 4-6 Spectral data of compound **5** (CD$_3$OD; 500 MHz for ^{1}H NMR, CD$_3$OD; 125 MHz for ^{13}C NMR) compare with kaempferol-3-*O*-rhamnoside (CD$_3$OD; 500 MHz for ^{1}H NMR, CD$_3$OD; 125 MHz for ^{13}C NMR) (continued)

Position	Type of C	δ$_C$ / ppm		δ$_H$ / ppm	
		Compound **5**	kaempferol-3-*O*-rhamnoside	Compound **5**	kaempferol-3-*O*-rhamnoside
3″	CH	72.02	72.2	3.72, 1H, *dd*, *J* = 3.21, 8.69 Hz	3.71, 1H, *dd*, *J* = 3.2, 9.2 Hz
4″	CH	73.23	73.2	3.33, 1H, *m*	3.33, 1H, *m*
5″	CH	71.93	72.0	3.33, 1H, *m*	3.33, 1H, *m*
6″	CH$_3$	17.64	17.7	0.95, 3H, *d*, *J* = 5.50 Hz	0.92, 3H, *d*, *J* = 5.5 Hz
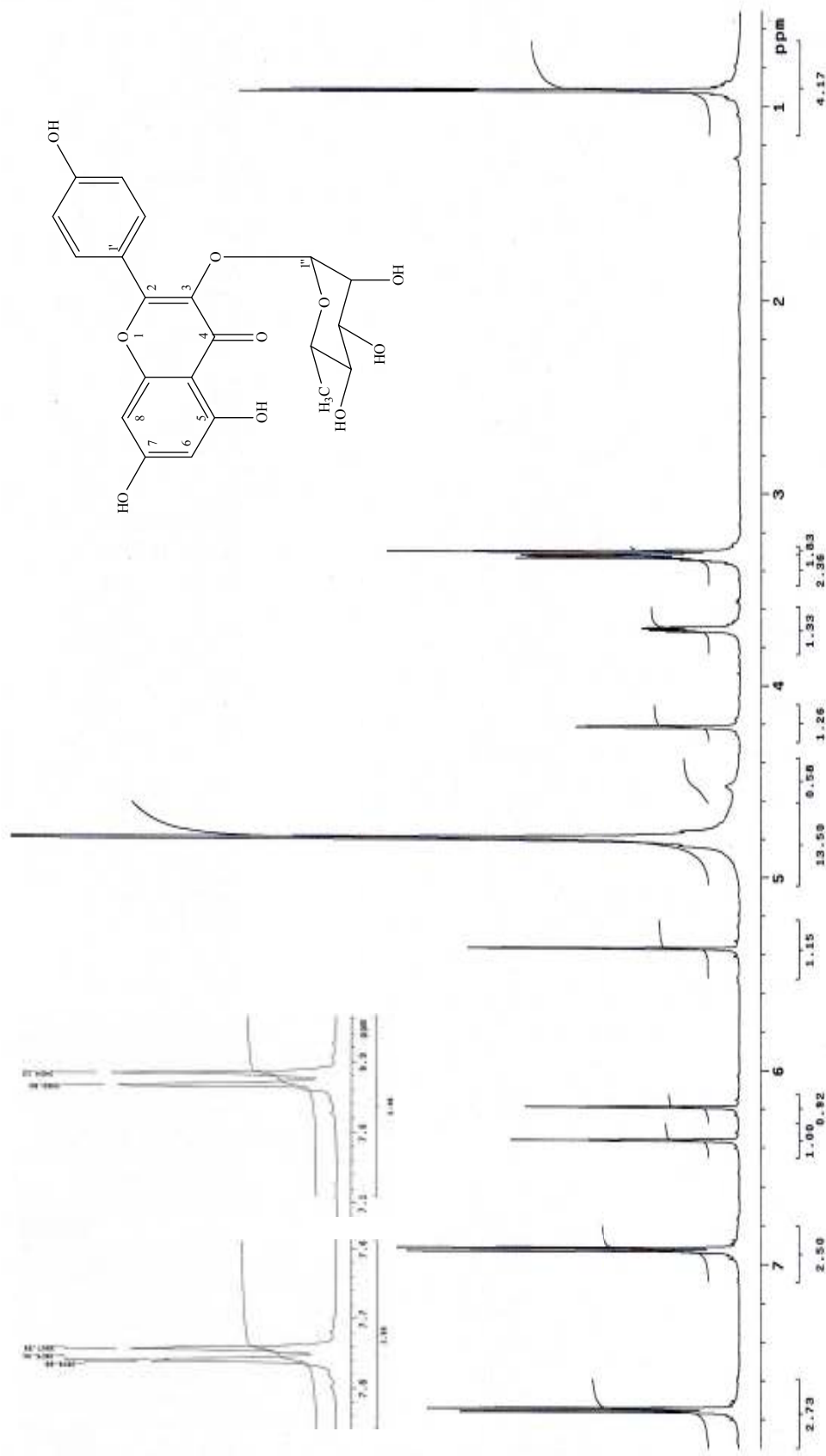
Figure 4-26 ^{1}H NMR spectrum of compound **5** in CD$_3$OD
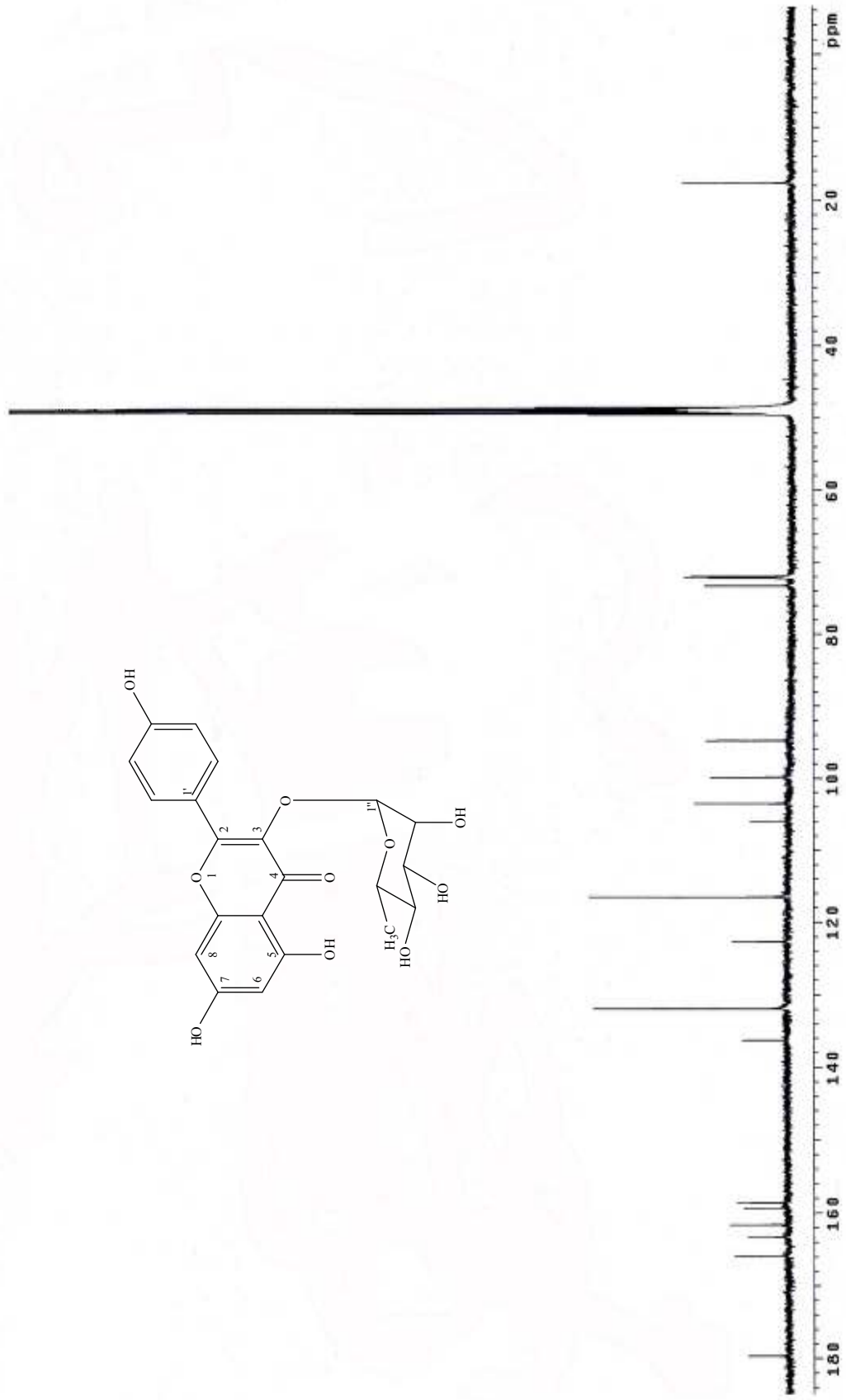
Figure 4-27 ^{13}C NMR spectrum of compound **5** in CD$_3$OD
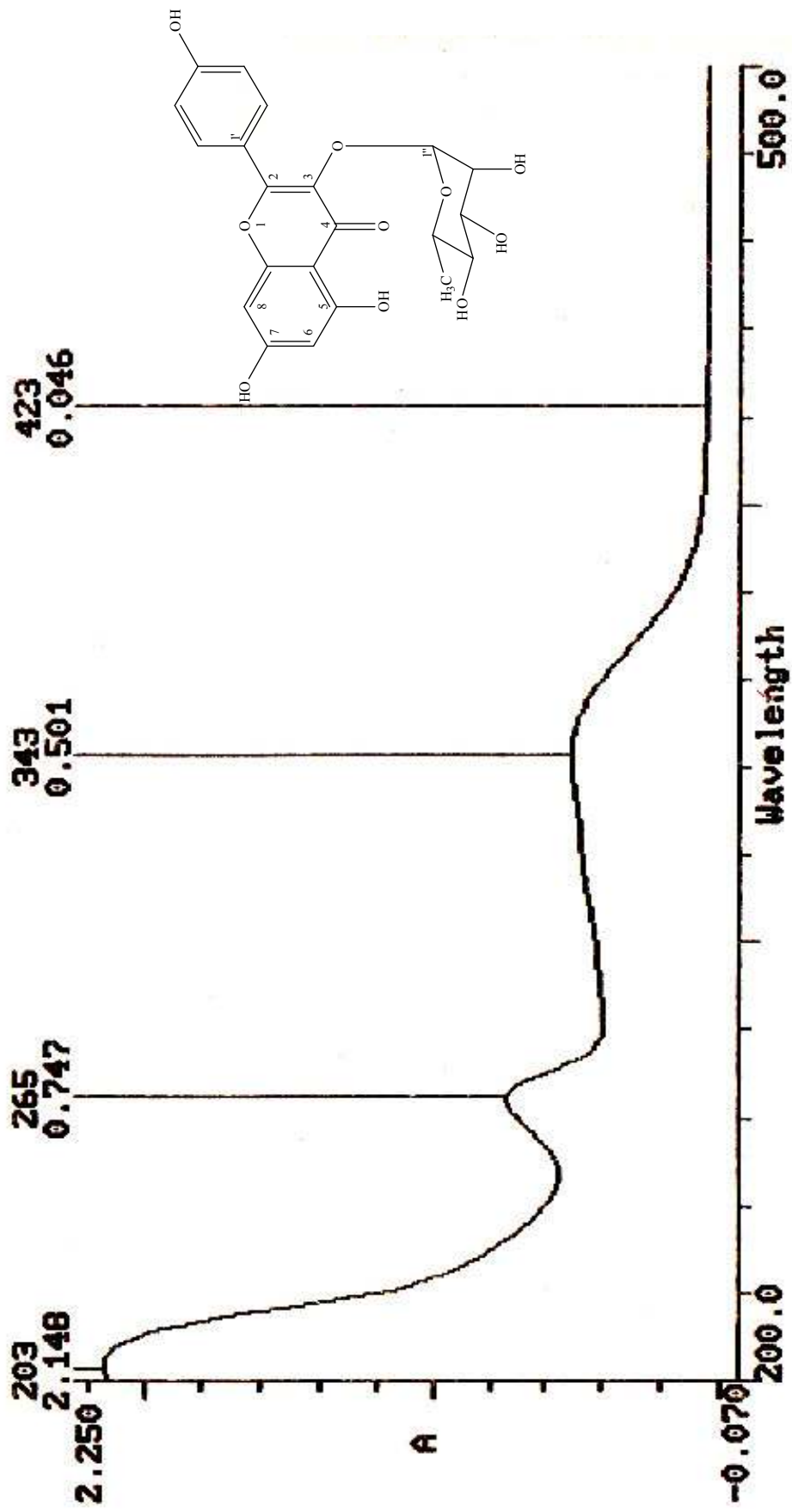
Figure 4-28 UV spectrum of compound **5** in methanol
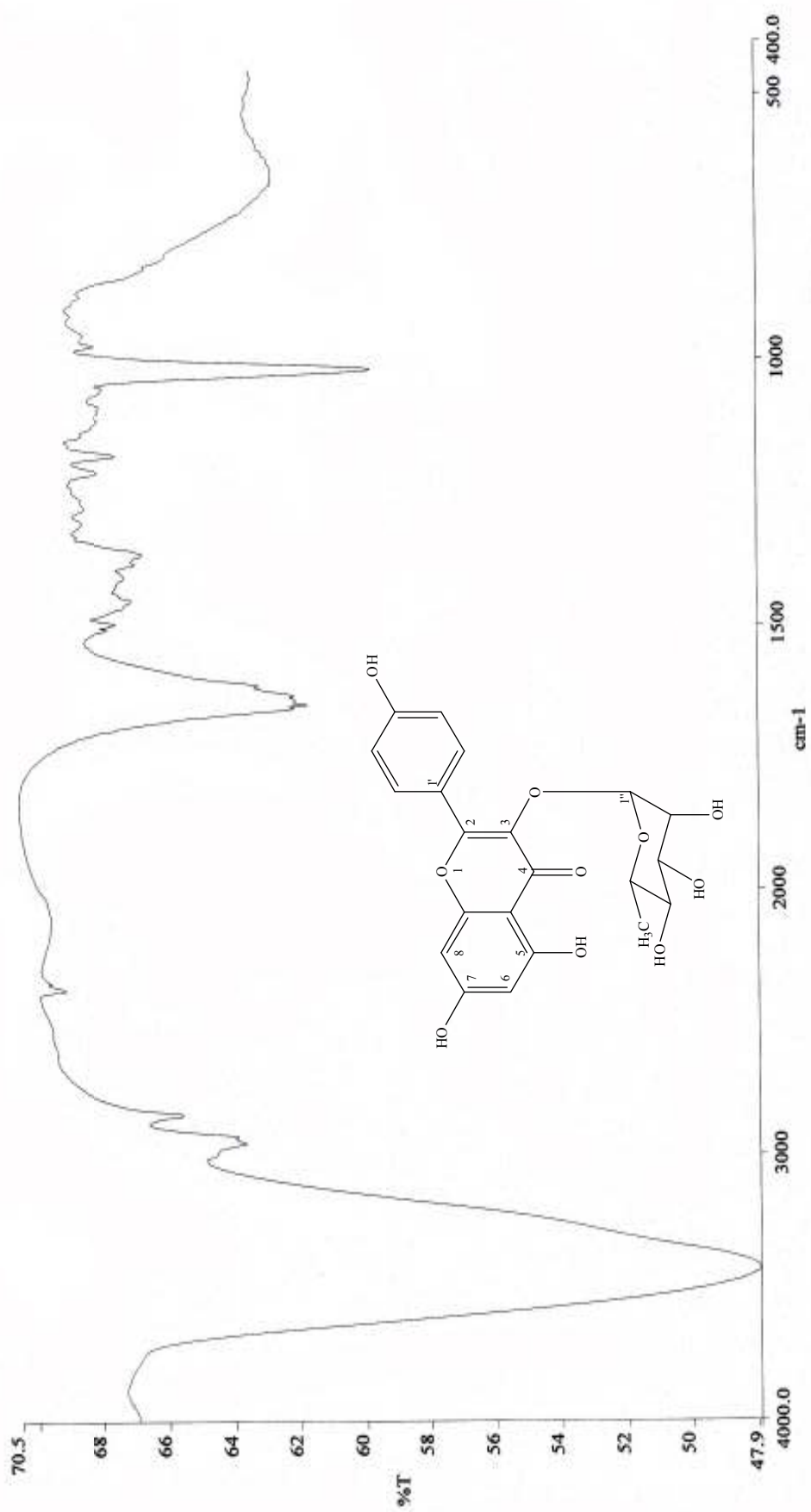
Figure 4-29 IR spectrum of compound **5**
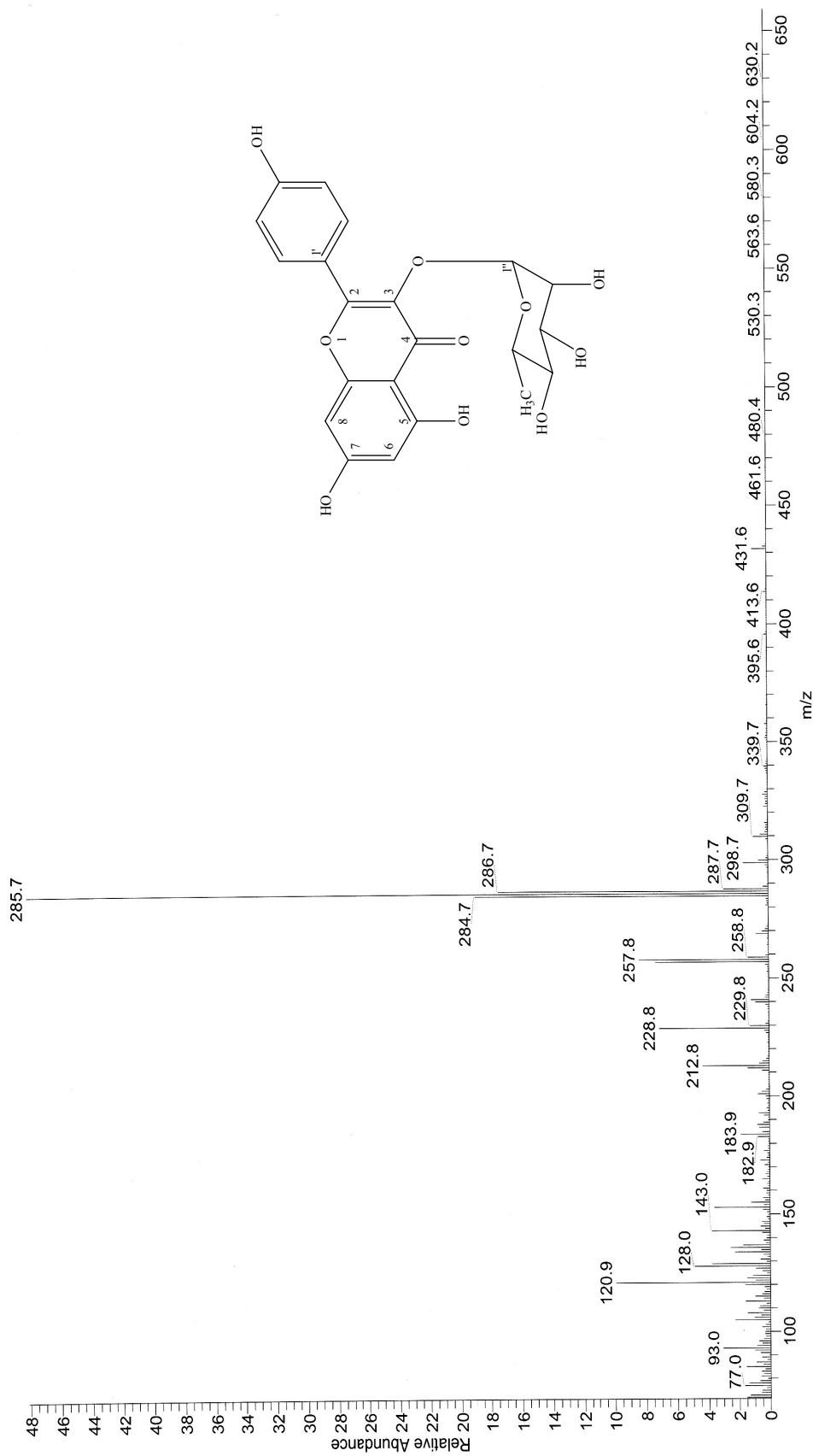
Figure 4-30 EI mass spectrum of compound **5**
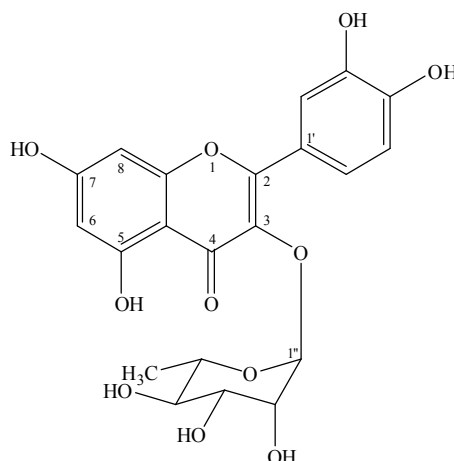
Figure 4-31 Chemical structure of quercetin-3-*O*-rhamnoside

Compound **6** was obtained as yellow amorphous powder (13 mg): mp 290-295 °C. The molecular formula of 6 was proposed to be $C_{21}H_{20}O_{11}$ determined by EI mass spectrum, which showed C_{15} flavonoid peak at m/z 301.7. UV spectrum showed absorption λ_{max} (MeOH) at 202, 255, 350 nm. IR spectrum showed absorption band for hydroxyl (3417 cm^{-1}) and C=C (1656 cm^{-1}). The ^{13}C NMR spectra data (Table 4-7) recorded in CD$_3$OD showed the existence of 21 signals for 21 carbon atoms in the molecule. This compound suggested the presence of 1 methyl (δ 17.65 ppm), 10 methine (δ 71.89, 72.03, 72.09, 73.23, 94.70, 99.81, 103.53, 116.36, 116.90, 122.86 ppm) and 10 quaternary carbons (δ 105.87, 122.94, 136.22, 146.41, 149.80, 158.52, 159.31, 163.21, 165.90, 179.63 ppm).

The ^{1}H NMR spectra data (Table 4-7) recorded in CD$_3$OD displayed a typical flavonol-rhamnopyranoside pattern having δ 0.95 ppm (*d*, *J* = 6.17 Hz, 3H-6″), 3.34 ppm (*dd*, *J* = 9.60, 6.86 Hz, 1H-4″), 3.43 ppm (*m*, 1H-5″), 3.74 ppm (*dd*, *J* = 3.20, 9.49 Hz, 1H-3″), 4.21 (*dd*, *J* = 1.83, 3.13 Hz, 1H-2″), and 5.34 ppm (*d*, *J* = 1.60 Hz, 1H-1″) and 5 aromatic protons at δ 6.19 ppm (*d*, *J* = 2.29 Hz, 1H-6), 6.34 ppm (*d*, *J* = 2.05 Hz, 1H-8), 6.90 ppm (*d*, *J* = 8.24 Hz, 1H-5′), 7.30 ppm (*dd*, *J* = 1.90, 8.35 Hz, 1H-6′) and 7.33 ppm (*d*, *J* = 2.28 Hz, 1H-2′) were observed in the ^{1}H NMR spectrum. This compound showed two peaks at δ 6.19 and 6.34 ppm corresponding to H-6 and H-8 on ring A. Similarly peaks at δ 6.90, 7.30 and 7.33 ppm were appeared due to the catechol protons on ring-B. Thus on the basis of its spectroscopic data and compare with the previously reported data (Chung, *et al*., 2004; Hanamura, *et al*., 2005 / Table 4-6). Compound **6** was assigned as quercetin-3-*O*-rhamnoside (Figure 4-31 and Figures 4-32 to 4-36).

Table 4-7 Spectral data of compound **6** (CD$_3$OD; 500 MHz for ^{1}H NMR, CD$_3$OD; 125 MHz for ^{13}C NMR) compare with quercetin-3-O-rhamnoside (CD$_3$OD; 500 MHz for ^{1}H NMR, CD$_3$OD; 125 MHz for ^{13}C NMR)

Position	Type of C	δ_C / ppm		δ_H / ppm	
		Compound **6**	quercetin-3-O-rhamnoside	Compound **6**	quercetin-3-O-rhamnoside
1	-	-	-	-	-
2	C	158.52	158.5	-	-
3	C	136.22	136.2	-	-
4	C	179.63	179.6	-	-
5	C	163.21	163.2	-	-
6	CH	99.81	99.8	6.19, 1H, *d*, J = 2.29 Hz	6.20, 1H, *d*, J = 2.1 Hz
7	C	165.90	165.9	-	-
8	CH	94.70	94.7	6.34, 1H, *d*, J = 2.05 Hz	6.37, 1H, *d*, J = 2.1 Hz
9	C	159.31	159.3	-	-
10	C	105.87	105.9		-
1′	C	122.94	123.0	-	-
2′	CH	116.9	116.9	7.33, 1H, *d*, J = 2.28 Hz	7.34, 1H, *d*, J = 2.1 Hz
3′	C	146.41	146.4	-	-
4′	C	149.80	150.1	-	-
5′	CH	116.36	116.4	6.90, 1H, *d*, J = 8.24 Hz	6.91, 1H, *d*, J = 8.2 Hz
6′	CH	122.86	122.9	7.30, 1H, *dd*, J = 1.9, 8.35 Hz	7.31, 1H, *dd*, J = 2.1, 8.2 Hz

Table 4-7 Spectral data of compound **6** (CD$_3$OD; 500 MHz for ^{1}H NMR, CD$_3$OD; 125 MHz for ^{13}C NMR) compare with the reference compound **R** (CD$_3$OD; 500 MHz for ^{1}H NMR, CD$_3$OD; 125 MHz for ^{13}C NMR) (continued)

Position	Type of C	δ_C / ppm		δ_H / ppm	
		Compound **6**	**R**	Compound **6**	**R**
1″	CH	103.58	103.6	5.34, 1H, *d*, $J = 1.60$ Hz	5.35, 1H, *d*, $J = 1.7$ Hz
2″	CH	72.09	72.1	4.21, 1H, *dd*, $J = 1.83, 3.13$ Hz	4.21, 1H, *dd*, $J = 1.7, 3.3$ Hz
3″	CH	72.03	72.0	3.74, 1H, *dd*, $J = 3.20, 9.49$ Hz	3.74, 1H, *dd*, $J = 3.3, 9.3$ Hz
4″	CH	73.23	73.3	3.34, 1H, *dd*, $J = 6.86, 9.60$ Hz	3.33, 1H, *dd*, $J = 6.1, 9.3$ Hz
5″	CH	71.89	71.90	3.43, 1H, *m*	3.41, 1H, *dd*, $J = 6.3, 9.5$ Hz
6″	CH$_3$	17.65	17.7	0.95, 3H, *d*, $J = 6.17$ Hz	0.94, 3H, *d*, $J = 6.1$ Hz
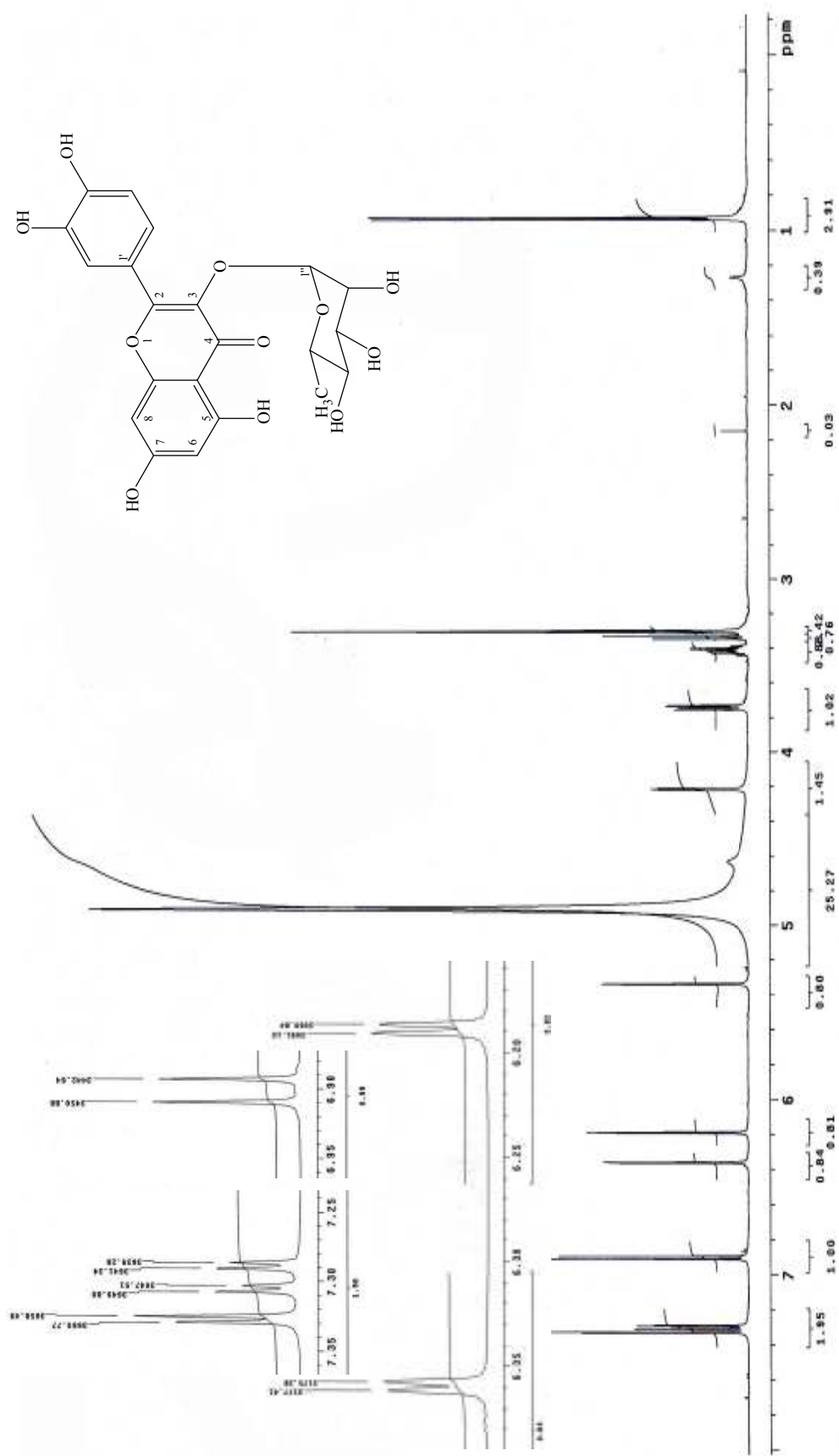
Figure 4-32 ^{1}H NMR spectrum of compound **6** in CD$_3$OD
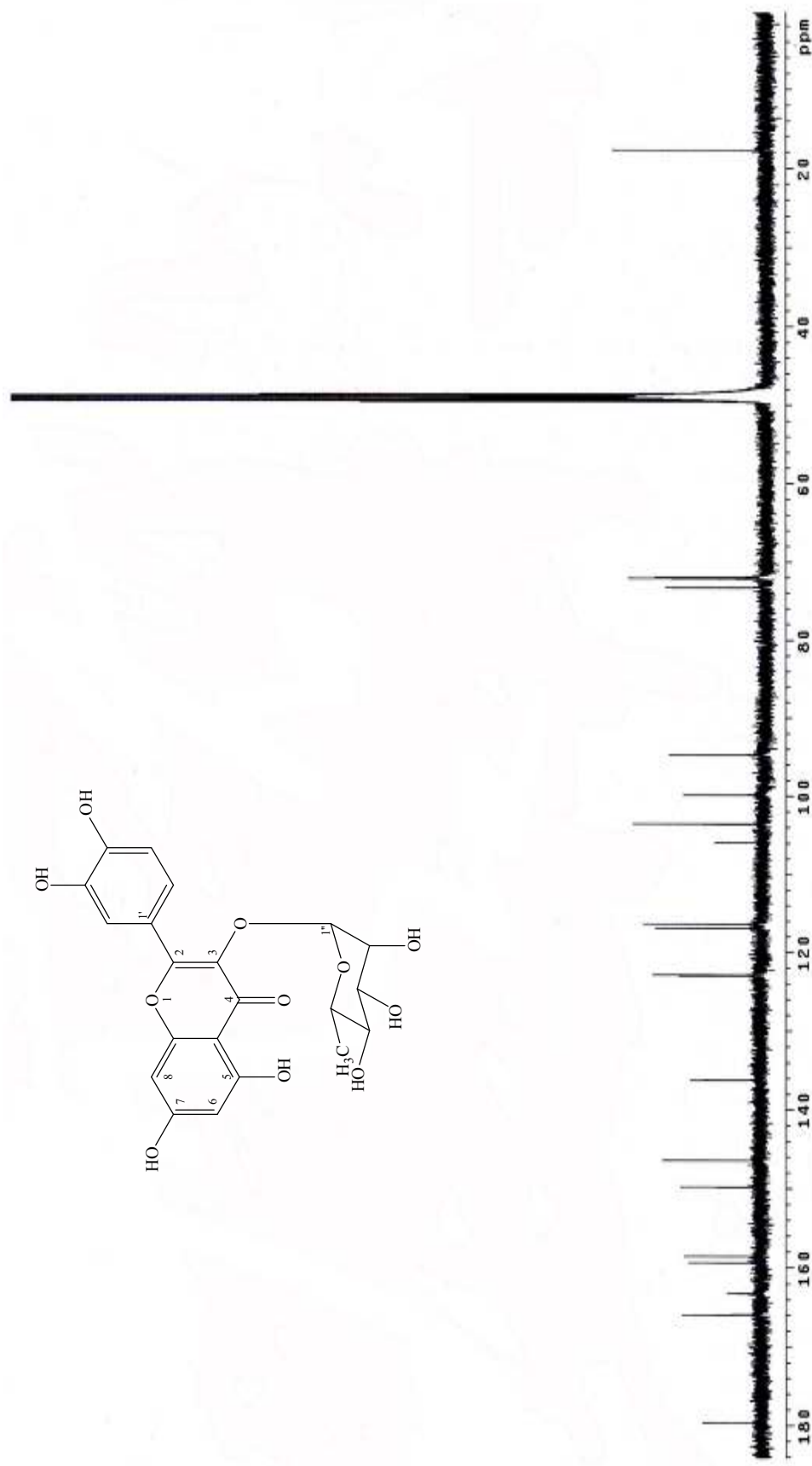
Figure 4-33 ^{13}C NMR spectrum of compound **6** in CD$_3$OD
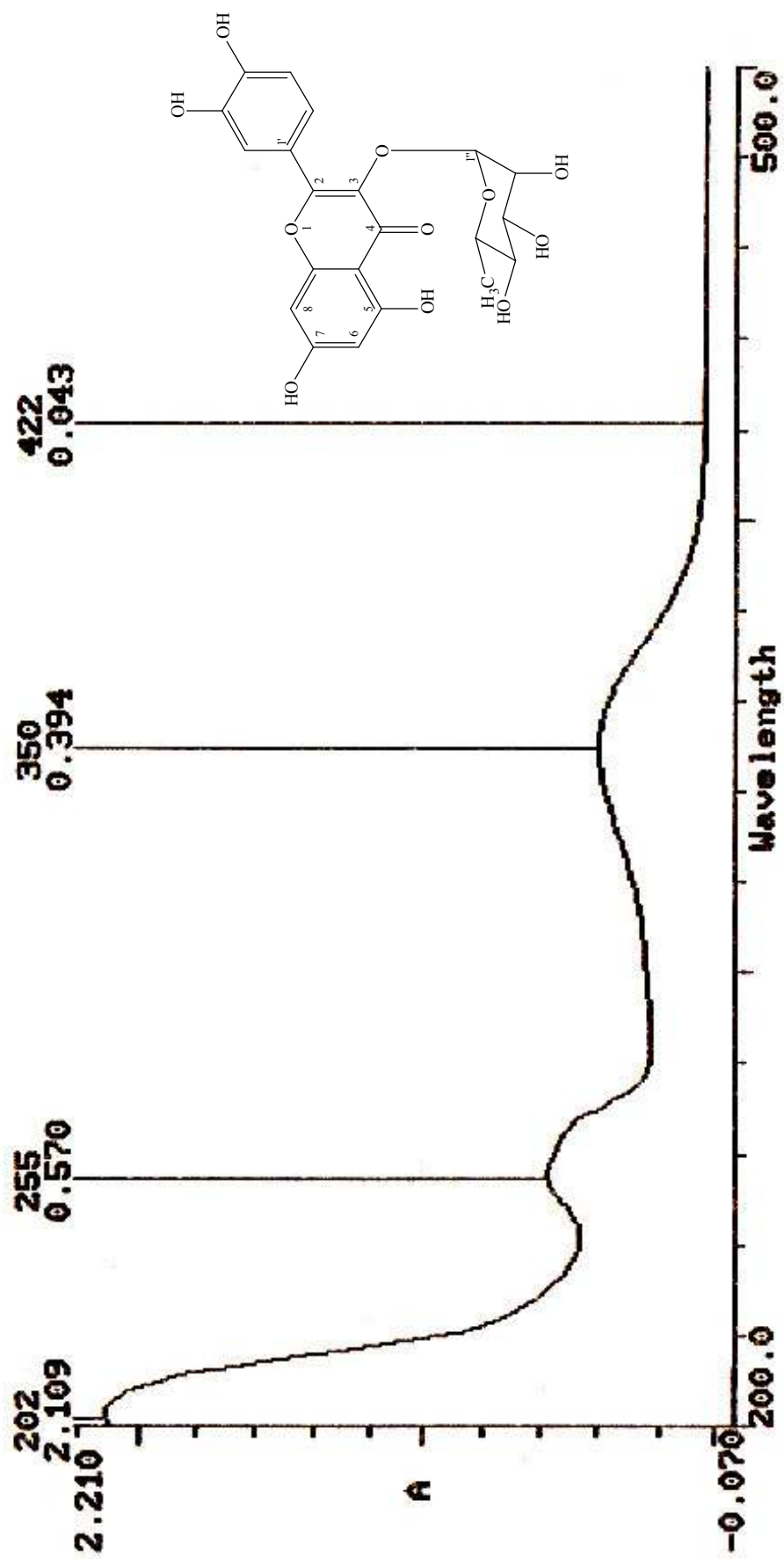
Figure 4-34 UV spectrum of compound **6** in methanol
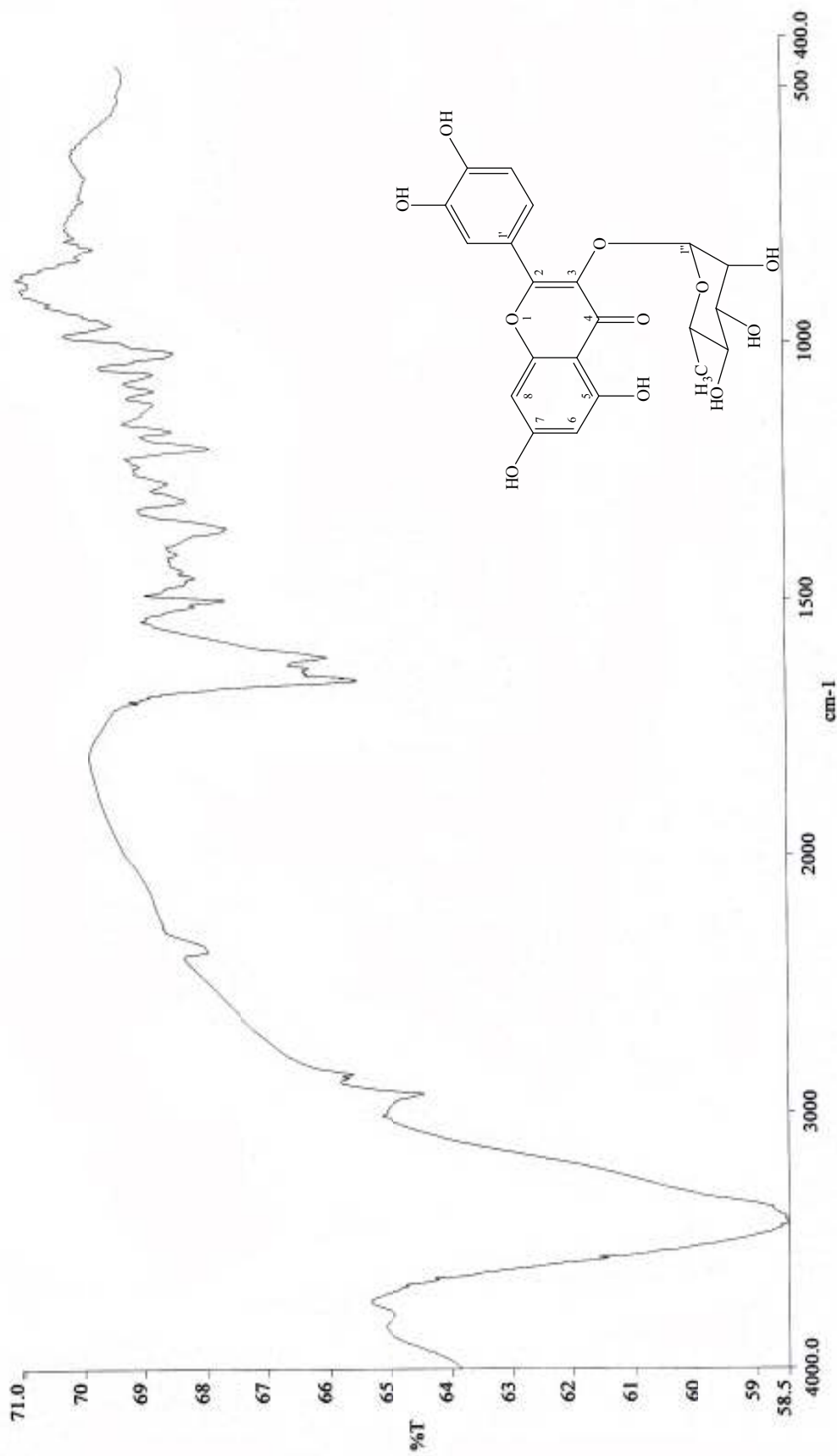
Figure 4-35 IR spectrum of compound **6**
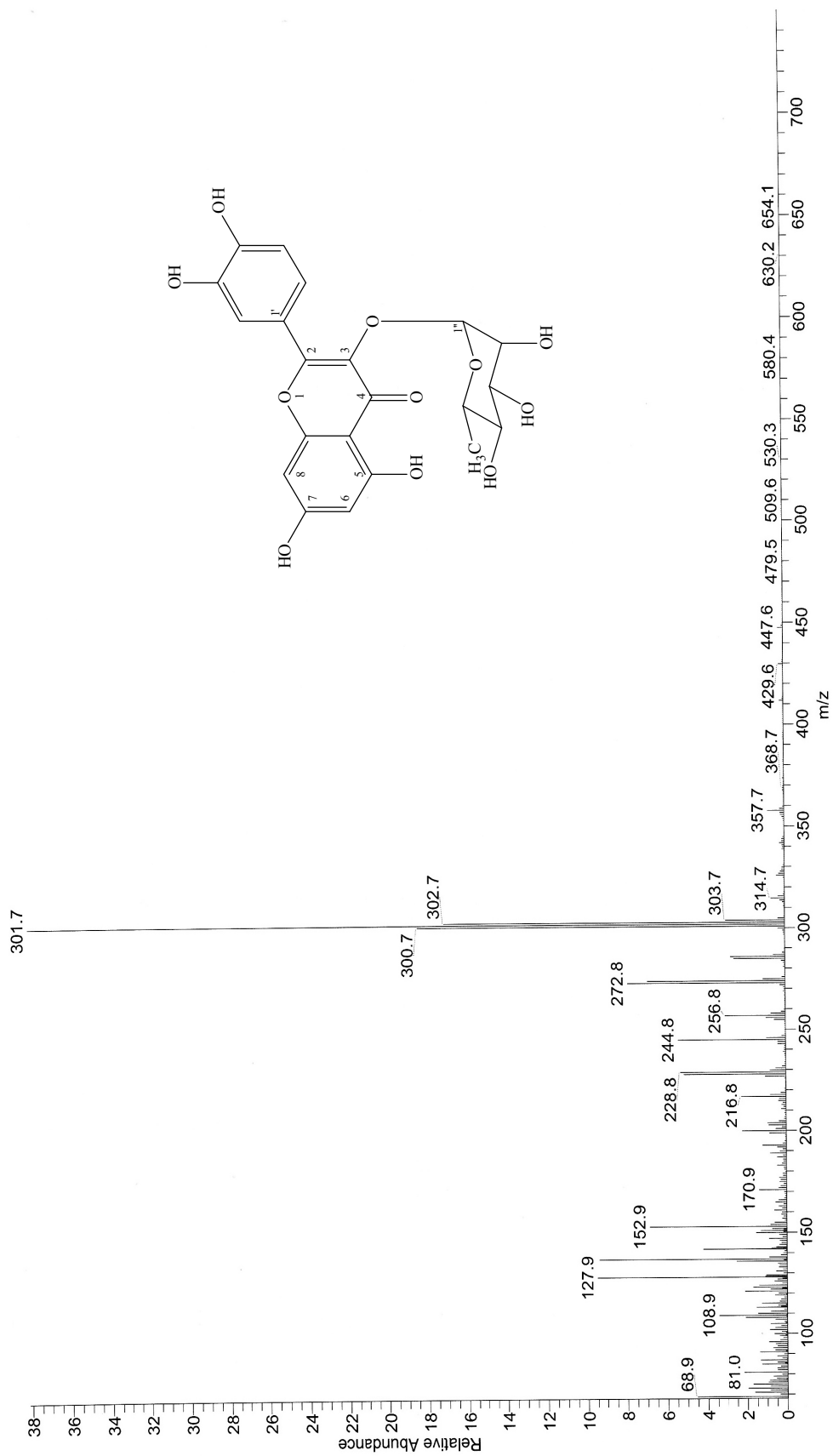
Figure 4-36 EI mass spectrum of compound **6**
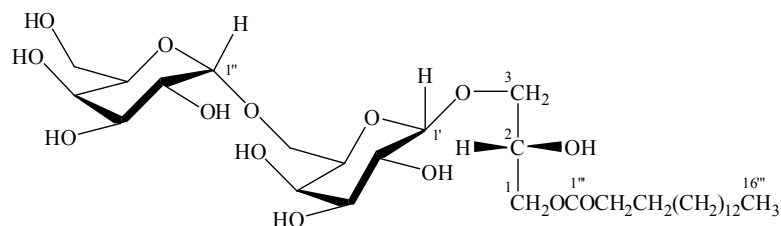
Figure 4-37 Chemical structure of 1-*O*-palmitoyl-3-*O*-[α-D-galactopyranosyl-(1⟶6)-β-D-galactopyranosyl]-*sn*-glycerol

Compound **7** was obtained as colourless semisolid (49 mg): mp 265-275 °C. The molecular formula of 6 was proposed to be $C_{31}H_{58}O_{14}$ determined by EI mass spectrum, which showed long-chain of glycolipids peak at m/z 340.9. IR spectrum showed absorption band for hydroxyl (3391 cm^{-1}), CH (2854 cm^{-1}), C=C (1733 cm^{-1}) and C-O (1068 cm^{-1}). The ^{13}C NMR spectra data (Table 4-8) recorded in CD_3OD showed the existence of 31 signals for 31 carbon atoms in the molecule. This compound suggested the presence of 1 methyl (δ 14.48 ppm), 18 methylene (δ 23.7-35.0 (12C), 26.03, 34.94, 62.84, 63.99, 67.78, 71.74 ppm), 11 methine (δ 68.74, 70.05, 70.21, 71.10, 71.45, 72.37, 72.54, 74.65, 74.57, 100.61, 105.30 ppm) and 1 quaternary carbons (δ 175.06 ppm).

The ^1H NMR spectra data (Table 4-8) recorded in CD_3OD displayed two galactopyranosides having δ 3.46 ppm (*dd*, *J* = 3.20, 10.06 Hz, 1H-3′), 3.57 ppm (*dd*, *J* = 7.32, 10.06 Hz, 1H-2′), 3.64 ppm (*dd*, *J* = 6.40, 10.52 Hz, 1H-6″α), 3.67 ppm (*dd*, *J* = 4.12, 10.06 Hz, 1H-6′α), 3.68 ppm (*dd*, *J* = 4.12, 10.20 Hz, 1H-6″β), 3.84 ppm (*t*, *J* = 5.94 Hz, 1H-4′, 1H-5″), 3.73 ppm (*m*, 1H-5′, 1H-2″), 3.74 ppm (*m*, 1H-3″), 3.85 ppm (*m*, 1H-4″), 3.88 ppm (*dd*, *J* = 6.40, 10.06 Hz, 1H-6′β), 4.31 ppm (*d*, *J* = 7.32 Hz, 1H-1′), 4.84 ppm (*d*, *J* = 3.65 Hz, 1H-1″). In its ^1H-NMR spectrum, there was a triplet methyl signal at δ 0.90 (*t*, *J* = 6.9 Hz, 3H-16″), a mass of oxymethylene and oxymethine hydrogen signals between δ 3.67 and 4.22 ppm and long-chain $(CH_2)_n$ signals at δ 1.30 ppm. No signals for olefenic protons were observed. These features are characteristic for glycolipids bearing saturated fatty acids. Signals at δ 4.22 (*dd*, *J* = 6.40, 11.85 Hz, 1H-1β) and 4.42 (*dd*, *J* = 3.21, 12.00 Hz, 1H-1α) indicated the presence of two β and α–glycosidic linkages, respectively. Furthermore the ^1H-NMR spectrum of **7** was characteristic of the 2S type, as indicated in Table 4-8 and the chemical shifts of H-1 methylene protons are very close (δ 4.22 and 4.42) and the coupling constant value between H-2 and H-3a is 4.12 Hz. Thus on the

basis of its spectroscopic data and compare with the previously reported data (Kim *et al*., 2004 / Table 4-8). Compound **7** was assigned as 1-*O*-palmitoyl-3-*O*-[α-D-galactopyranosyl-(1⟶6)-β-D-galactopyrano- syl]-*sn*-glycerol (Figure 4-37 and Figures 4-38 to 4-41).

Table 4-8 Spectral data of compound **7** (CD$_3$OD; 500 MHz for ^{1}H NMR, CD$_3$OD; 125 MHz for ^{13}C NMR) compare with 1-*O*-palmitoyl-3-*O*-[α-D-galactopyranosyl-(1⟶6)-β-D-galacto-pyranosyl]-*sn*-glycerol (CD$_3$OD; 500 MHz for ^{1}H NMR, CD$_3$OD; 125 MHz for ^{13}C NMR)

Position	Type of C	δ$_C$ / ppm		δ$_H$ / ppm	
		Compound **7**	1-*O*-palmitoyl-3-*O*-[α-D-galactopyra-nosyl-(1⟶6)-β-D-galactopyranosyl]-*sn*-glycerol	Compound **7**	1-*O*-palmitoyl-3-*O*-[α-D-galactopyra-nosyl-(1⟶6)-β-D-galactopyranosyl]-*sn*-glycerol
1α	CH	63.99	64.3	4.42, 1H, *dd*, *J* = 3.21, 12.0 Hz	4.42, 1H, *dd*, *J* = 3.0, 12.0 Hz
1β	CH	63.99	64.3	4.22, 1H, *dd*, *J* = 6.40, 11.85 Hz	4.22, 1H, *dd*, *J* = 6.5 12.0 Hz
2	CH	68.74	69.7	3.98, 1H, *m*	3.98, 1H, *m*
3α	CH	71.74	72.1	3.67, 1H, *dd*, *J* = 4.12, 10.06 Hz	3.66, 1H, *dd*, *J* = 4.5, 10.5 Hz
3β	CH	71.74	72.1	3.88, 1H, *dd*, *J* = 6.40, 10.06 Hz	3.87, 1H, *dd*, *J* = 6.3, 10.5 Hz
1′	CH	105.30	105.3	4.31, 1H, *d*, *J* = 7.32 Hz	4.24, 1H, *d*, *J* = 7.2 Hz
2′	CH	72.54	72.6	3.57, 1H, *dd*, *J* = 7.32, 10.06 Hz	3.56, 1H, *dd*, *J* = 7.2, 9.6 Hz
3′	CH	74.65	74.7	3.46, 1H, *dd*, *J* = 3.20, 10.06 Hz	3.48, 1H, *dd*, *J* = 3.3, 9.6 Hz

Table 4-8 Spectral data of compound **7** (CD₃OD; 500 MHz for ¹H NMR, CD₃OD; 125 MHz for ¹³C NMR) compare with 1-*O*-palmitoyl-3-*O*-[α-D-galactopyranosyl-(1⟶6)-β-D-galacto-pyranosyl]-*sn*-glycerol (CD₃OD; 500 MHz for ¹H NMR, CD₃OD; 125 MHz for ¹³C NMR) (continued)

Position	Type of C	δ_C / ppm		δ_H / ppm	
		Compound 7	1-*O*-palmitoyl-3-*O*-[α-D-galactopyra-nosyl-(1⟶6)-β-D-galactopyranosyl]-*sn*-glycerol	Compound 7	1-*O*-palmitoyl-3-*O*-[α-D-galactopyra-nosyl-(1⟶6)-β-D-galactopyranosyl]-*sn*-glycerol
4′	CH	70.05	70.1	3.84, 1H, *t*, *J* = 5.94 Hz	3.84, 1H, *m*
5′	CH	74.57	74.6	3.73, 1H, *m*	3.74, 1H, *m*
6′α	CH	67.78	67.8	3.67, 1H, *dd*, *J* = 4.12, 10.06 Hz	3.66, 1H, *dd*, *J* = 4.5, 10.5 Hz
6′β	CH	67.78	67.8	3.88, 1H, *dd*, *J* = 6.40, 10.06 Hz	3.87, 1H, *dd*, *J* = 6.3, 10.5 Hz
1″	CH	100.61	100.5	4.84, 1H, *d*, *J* = 3.65 Hz	4.86, 1H, *d*, *J* = 3.9 Hz
2″	CH	71.45	71.5	3.73, 1H, *m*	3.72, 1H, *m*
3″	CH	70.21	70.2	3.74, 1H, *m*	3.75, 1H, *m*
4″	CH	71.10	71.0	3.85, 1H, *m*	3.86, 1H, *m*
5″	CH	72.37	72.5	3.84, 1H, *t* *J* = 5.94 Hz	3.84, 1H, *m*
6″α	CH	62.84	62.7	3.64, 1H, *dd*, *J* = 6.40, 10.52 Hz	3.66, 1H, *dd*, *J* = 6.3, 10.2 Hz
6″β	CH	62.84	62.7	3.68, 1H, *dd*, *J* = 4.12, 10.2 Hz	3.70, 1H, *dd*, *J* = 4.5, 10.2 Hz

Table 4-8 Spectral data of compound **7** (CD$_3$OD; 500 MHz for ^{1}H NMR, CD$_3$OD; 125 MHz for ^{13}C NMR) compare with 1-*O*-palmitoyl-3-*O*-[α-D-galactopyranosyl-(1⟶6)-β-D-galacto-pyranosyl]-*sn*-glycerol (CD$_3$OD; 500 MHz for ^{1}H NMR, CD$_3$OD; 125 MHz for ^{13}C NMR) (continued)

Position	Type of C	δ$_C$ / ppm		δ$_H$ / ppm	
		Compound **7**	1-*O*-palmitoyl-3-*O*-[α-D-galactopyra-nosyl-(1⟶6)-β-D-galactopyranosyl]-*sn*-glycerol	Compound **7**	1-*O*-palmitoyl-3-*O*-[α-D-galactopyra-nosyl-(1⟶6)-β-D-galactopyranosyl]-*sn*-glycerol
1‴	CO	175.06	175.5	-	-
2‴	CH$_2$	34.94	34.9	2.35, 2H, *t*, J = 7.31 Hz	2.35, 1H, *t*, J = 7.5 Hz
3‴	CH$_2$	26.03	26.0	1.61, 2H, *d*, J = 5.49 Hz	1.61, 1H, *m*
4‴ - 15‴	CH$_2$	23.7 - 35.0	23.0 - 35.0	1.30, 2H, *br s*	1.28, 2H, *br s*
16‴	CH$_3$	14.48	14.4	0.90, 3H, *t*, J = 6.9 Hz	0.89, 3H, *t*, J = 6.9 Hz
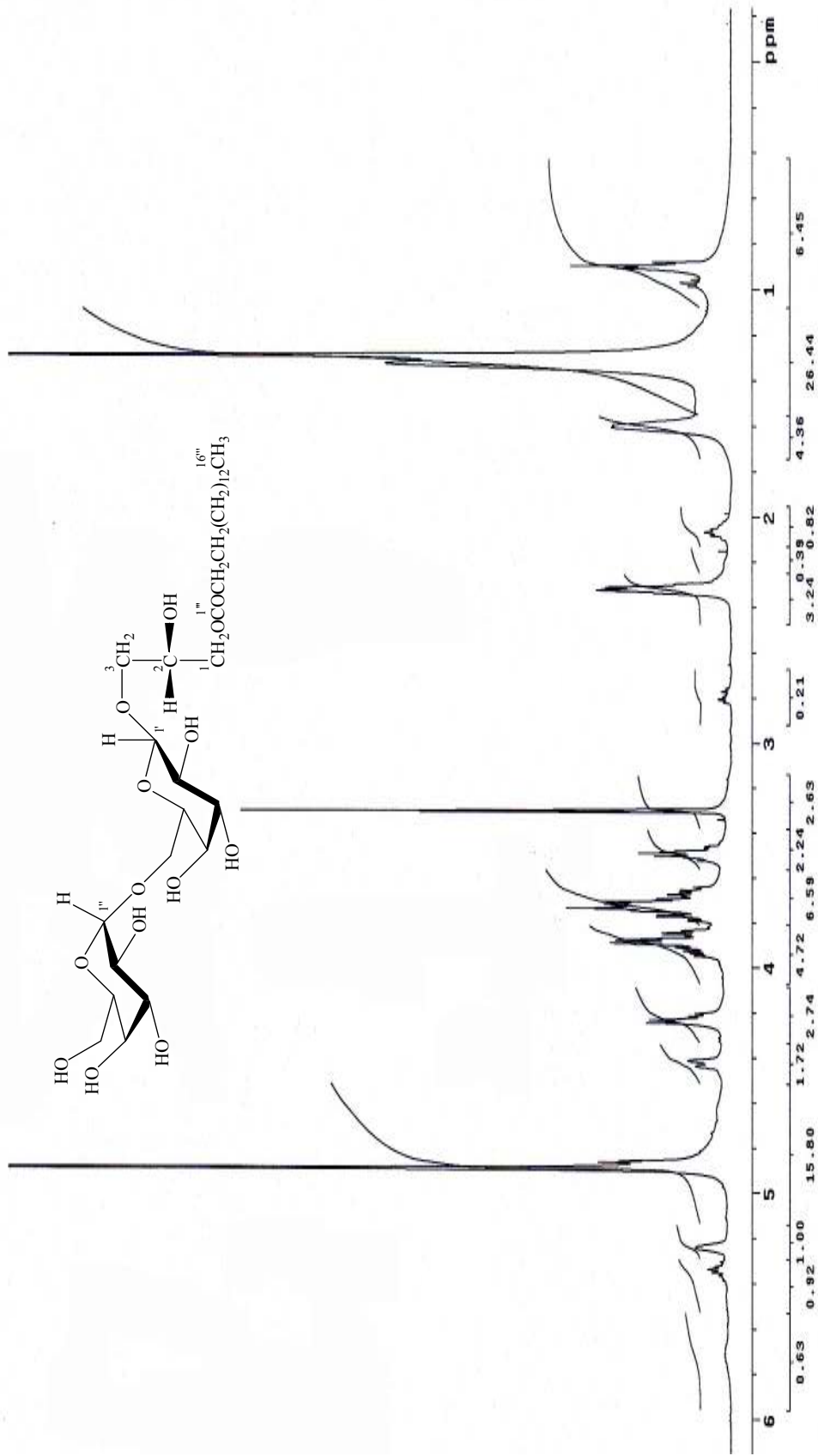
Figure 4-38 ^{1}H NMR spectrum of compound **7** in CD$_3$OD
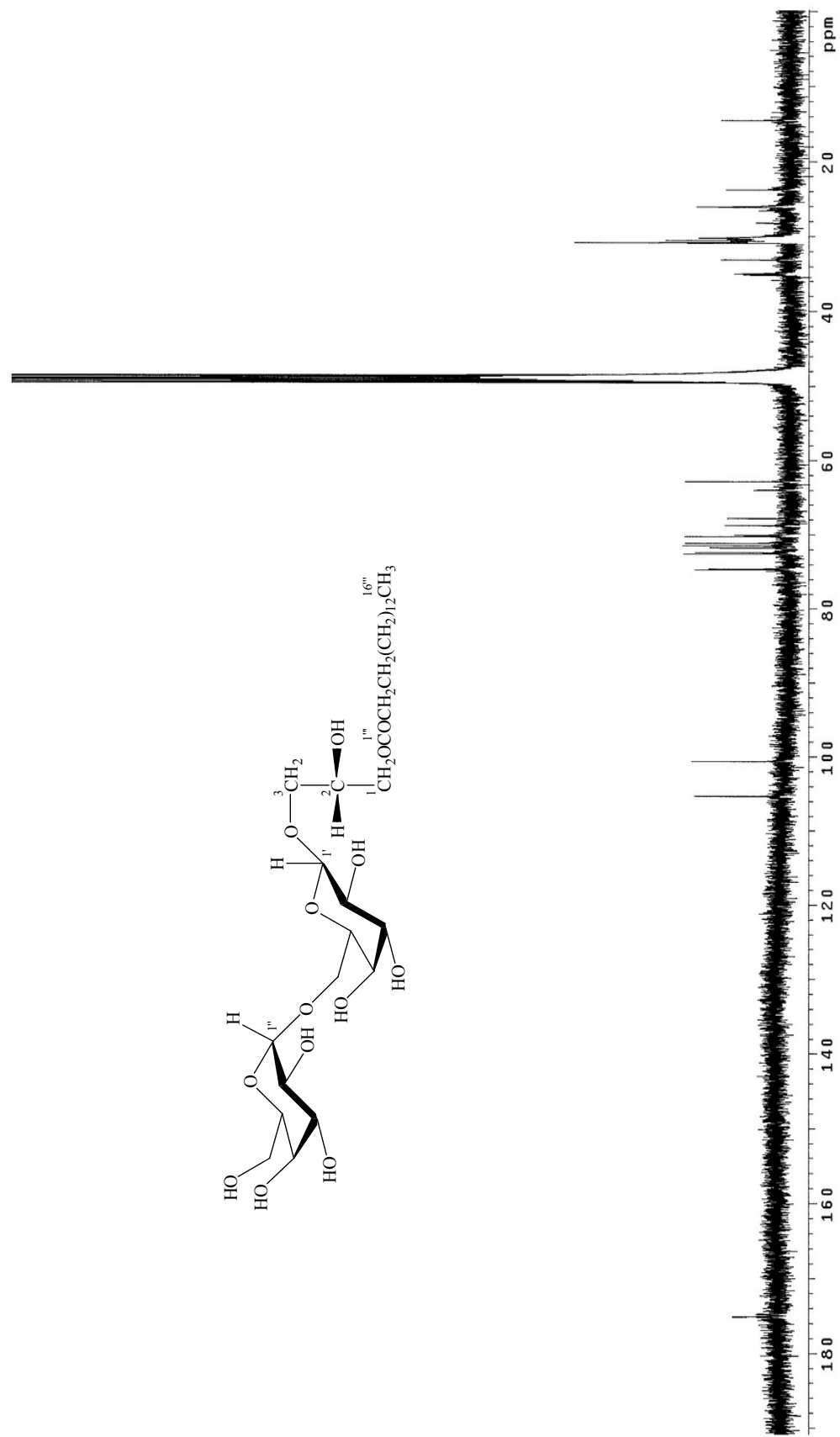
Figure 4-39 ^{13}C NMR spectrum of compound **7** in CD$_3$OD
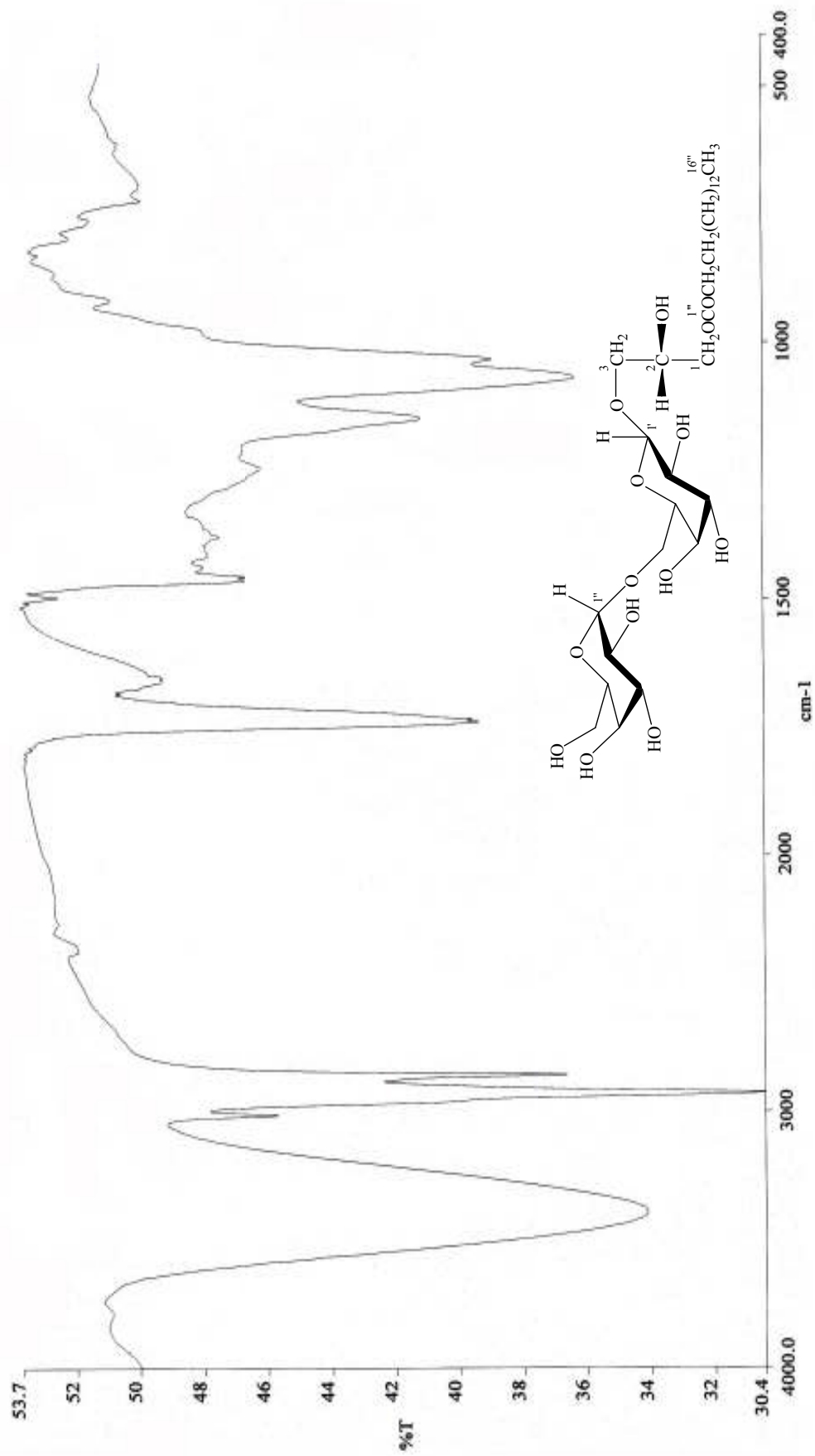
Figure 4-40 IR spectrum of compound 7
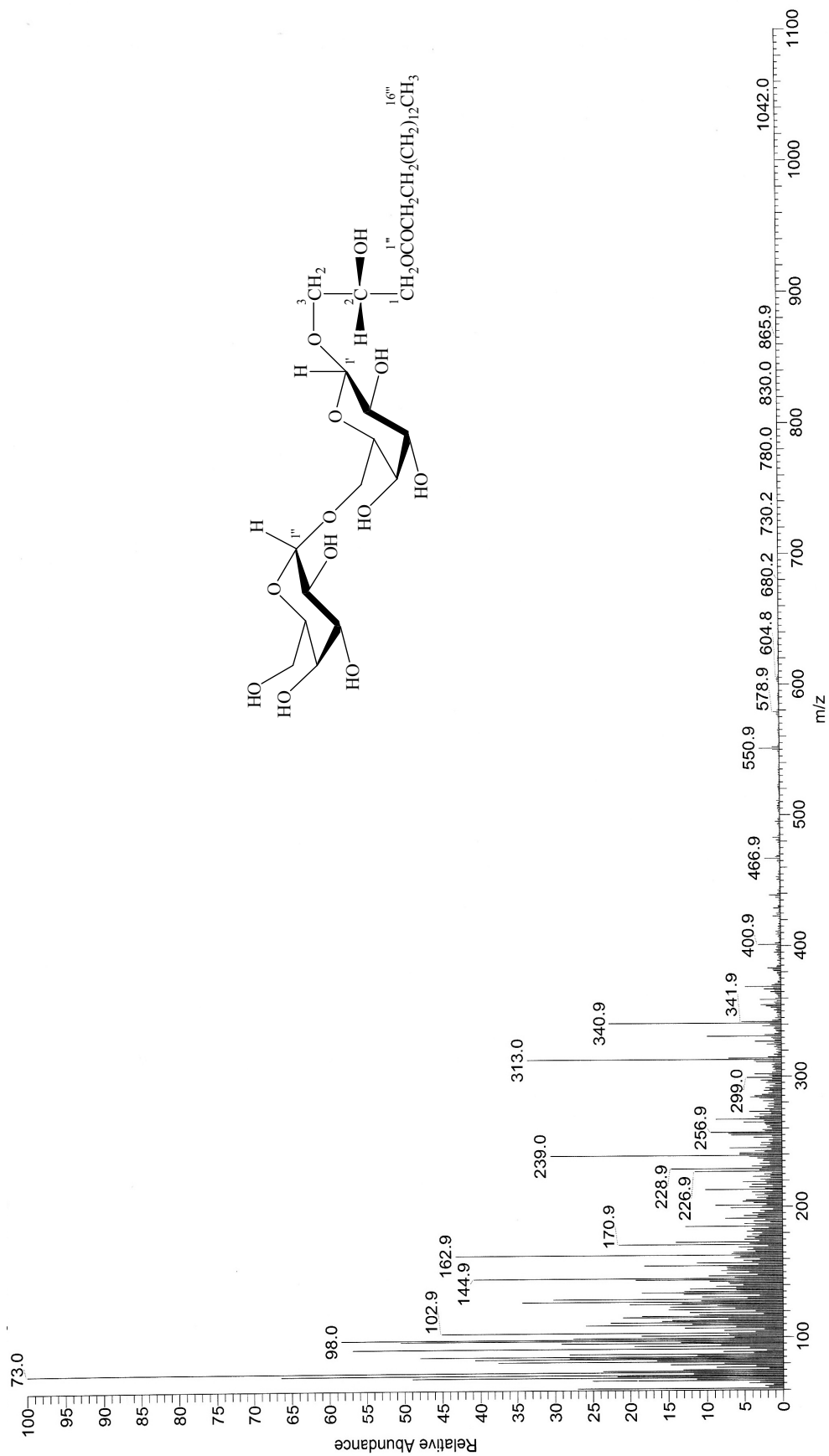
Figure 4-41 EI mass spectrum of compound **7**
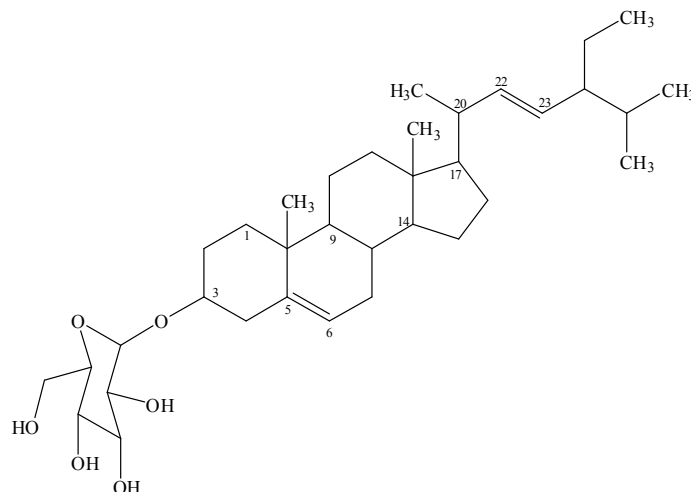
Figure 4-42 Chemical structure of stigmasterol-3-*O*-glucoside

Compound **8** was obtained as white amorphous powder (20 mg): mp 270-275 °C. The molecular formula of 8 was proposed to be $C_{35}H_{58}O_6$ determined by EI mass spectrum, which showed sterol peak at m/z 396.9. IR spectrum showed absorption band for hydroxyl (3436 cm^{-1}), C=C (1639 cm^{-1}) and C-O (1023 cm^{-1}). The ^{13}C NMR spectra data (Table 4-9) recorded in DMSO-d_6 showed the existence of 35 signals for 35 carbon atoms in the molecule. This compound suggested the presence of 6 methyl (δ 12.00, 12.25, 19.01, 19.25, 20.74, 21.26 ppm), 10 methylene (δ 21.07, 24.03, 25.00, 28.62, 29.43, 31.47, 36.99, 38.49, 40.30, 61.28 ppm), 15 methine (δ 31.95, 31.58, 40.20, 49.80, 50.74, 55.52, 56.67, 70.29, 73.64, 76.90, 76.94, 77.12, 121.30, 129.00, 138.17 ppm), including one anomeric carbon at δ 100.98 ppm and 3 quaternary carbons (δ 36.39, 41.91, 140.64 ppm).

The ^{1}H NMR spectra data (Table 4-9) recorded in DMSO-d_6 displayed characteristic signals of stigmasterol nucleus and a sugar unit. The stigmasterol unit was showed as two methyl singlet at δ 0.65 ppm (3H-18) and 0.94 ppm (3H-19), three methyl doublets at δ 0.79 ppm (*d*, *J* = 6.47 Hz, 3H-27), 0.81 ppm (*d*, *J* = 6.47 Hz, 3H-26) and 0.98 ppm (*d*, *J* = 6.73 Hz, 3H-21), one methyl triplet at δ 0.77 ppm (*t*, *J* = 7.25 Hz, 3H-29), 3 olefenic protons at δ 5.02 ppm (*dd*, *J* = 8.81, 15.03 Hz, 1H-23), 5.14 ppm (*dd*, *J* = 8.82, 15.28 Hz, 1H-22) and 5.31 ppm (*br d*, *J* = 4.92 Hz, 1H-6) and one oxymethaine protons at δ 3.36 ppm (*m*, 1H-3). The four methane protons in the sugar unit were shown as multiplet signals at δ 2.85 ppm (1H-2′), 3.35 ppm (1H-4′), 3.65 ppm (1H-5′) and 3.69 ppm (1H-3′), one anomeric proton at 4.89 ppm (*d*, *J* = 7.77 Hz, 1H-1′) and the oxymethylene protons were shown at δ 3.63 ppm (*m*, 1H-6′α) and 3.45 ppm (*m*, 1H-6′β) were observed in the ^{1}H NMR spectrum. Thus on the basis of its spectroscopic data and compare with

the previously reported data (Burdi, *et al*., 1991; Falodun, *et al*., 2008; Singh *et al*., 2005 / Table 4-9). Compound **8** was assigned as stigmasterol-3-*O*-glucoside (Figure 4-42 and Figures 4-43 to 4-46).

Table 4-9 Spectral data of compound **8** (DMSO-d_6; 500 MHz for ^{1}H NMR, DMSO-d_6; 125 MHz for ^{13}C NMR) compare with stigmasterol-3-*O*-glucoside (DMSO-d_6; 500 MHz for ^{1}H NMR, DMSO-d_6; 125 MHz for ^{13}C NMR)

Position	Type of C	δ_C / ppm		δ_H / ppm	
		Compound **8**	stigmasterol-3-*O*-glucoside	Compound **8**	stigmasterol-3-*O*-glucoside
1	CH$_2$	36.99	37.06	2.35, 2H, *m*	2.37, 1H, *m*
2	CH$_2$	31.58	32.00	1.23, 2H, *m*	1.29, 1H, *m*
3	CH	77.12	77.20	3.36, 1H, *m*	3.38, 1H, *m*
4	CH$_2$	40.30	40.50	1.14, 2H, *m*	1.15, 1H, *m*
5	C	140.64	140.23	-	-
6	CH	121.30	121.69	5.31, 1H, *br d*, $J = 4.92$ Hz	5.23, 1H, *br d*, $J = 5.4$ Hz
7	CH$_2$	31.47	31.72	1.48, 2H, *m*	1.48, 1H, *m*
8	CH	31.95	31.95	1.50, 1H, *m*	1.54, 1H, *br s*
9	CH	50.74	50.10	0.87, 1H, *m*	0.87, 1H, *br s*
10	C	36.39	36.72	-	-
11	CH$_2$	21.07	20.80	1.18, 2H, *m*	1.17, 1H, *m*
12	CH$_2$	38.49	39.59	1.35, 2H, *m*	1.31, 1H, *m*
13	C	41.91	42.50	-	-
14	CH	56.67	56.67	1.04, 1H, *m*	1.06, 1H, *m*
15	CH$_2$	24.03	24.01	1.02, 2H, *m*	1.03, 1H, *m*
16	CH$_2$	28.62	28.55	1.80, 2H, *m*	1.84, 1H, *m*
17	CH	55.52	55.85	1.12, 1H, *m*	1.13, 1H, *m*
18	CH$_3$	12.00	11.61	0.65, 3H, *s*	0.66, 3H, *s*
19	CH$_3$	19.25	19.23	0.94, 3H, *s*	1.01, 3H, *s*

Table 4-9 Spectral data of compound **8** (DMSO-d_6; 500 MHz for ^{1}H NMR, DMSO-d_6; 125 MHz for ^{13}C NMR) compare with stigmasterol-3-O-glucoside (DMSO-d_6; 500 MHz for ^{1}H NMR, DMSO-d_6; 125 MHz for ^{13}C NMR) (continued)

Position	Type of C	δ_C / ppm		δ_H / ppm	
		Compound **8**	stigmasterol-3-O-glucoside	Compound **8**	stigmasterol-3-O-glucoside
20	CH	40.20	40.13	1.21, 1H, *m*	1.26, 1H, *m*
21	CH$_3$	20.74	20.48	0.98, 3H, *d*, J = 6.73 Hz	0.90, 3H, *d*, J = 6.2 Hz
22	CH	138.17	138.04	5.14, 1H, *dd*, J = 8.82, 15.28 Hz	5.14, 1H, *dd*, J = 8.0, 15.2 Hz
23	CH	129.00	129.15	5.02, 1H, *dd*, J = 8.81, 15.03 Hz	5.02, 1H, *dd*, J = 8.0, 15.3 Hz
24	CH	49.80	50.06	0.90, 1H, *m*	0.91, 1H, *br s*
25	CH	29.43	28.70	1.52, 1H, *m*	1.56, 1H, *m*
26	CH$_3$	19.01	19.00	0.81, 3H, *d*, J = 6.47 Hz	0.83, 3H, *d*, J = 6.6 Hz
27	CH$_3$	21.26	21.21	0.79, 3H, *d*, J = 6.47 Hz	0.80, 3H, *d*, J = 6.5 Hz
28	CH$_2$	25.00	25.41	1.05, 2H, *m*	1.05, 1H, *m*
29	CH$_3$	12.25	12.00	0.77, 3H, *t*, J = 7.25 Hz	0.82, 3H, *t*, J = 7.0 Hz
1′	CH	100.98	100.74	4.89, 1H, *d*, J = 7.77 Hz	4.78, 1H, *d*, J = 7.5 Hz
2′	CH	73.64	73.22	2.85, 1H, *m*	2.80, 1H, *m*
3′	CH	76.90	76.50	3.61, 1H, *m*	3.58, 1H, *m*
4′	CH	70.29	69.95	3.35, 1H, *m*	3.35, 1H, *m*
5′	CH	76.94	76.19	3.65, 1H, *m*	3.76, 1H, *m*
6′α	CH$_2$	61.28	61.36	3.63, 2H, *m*	3.60, 1H, *m*
6′β	CH$_2$	61.28	61.36	3.45, 2H, *m*	3.39, 1H, *m*
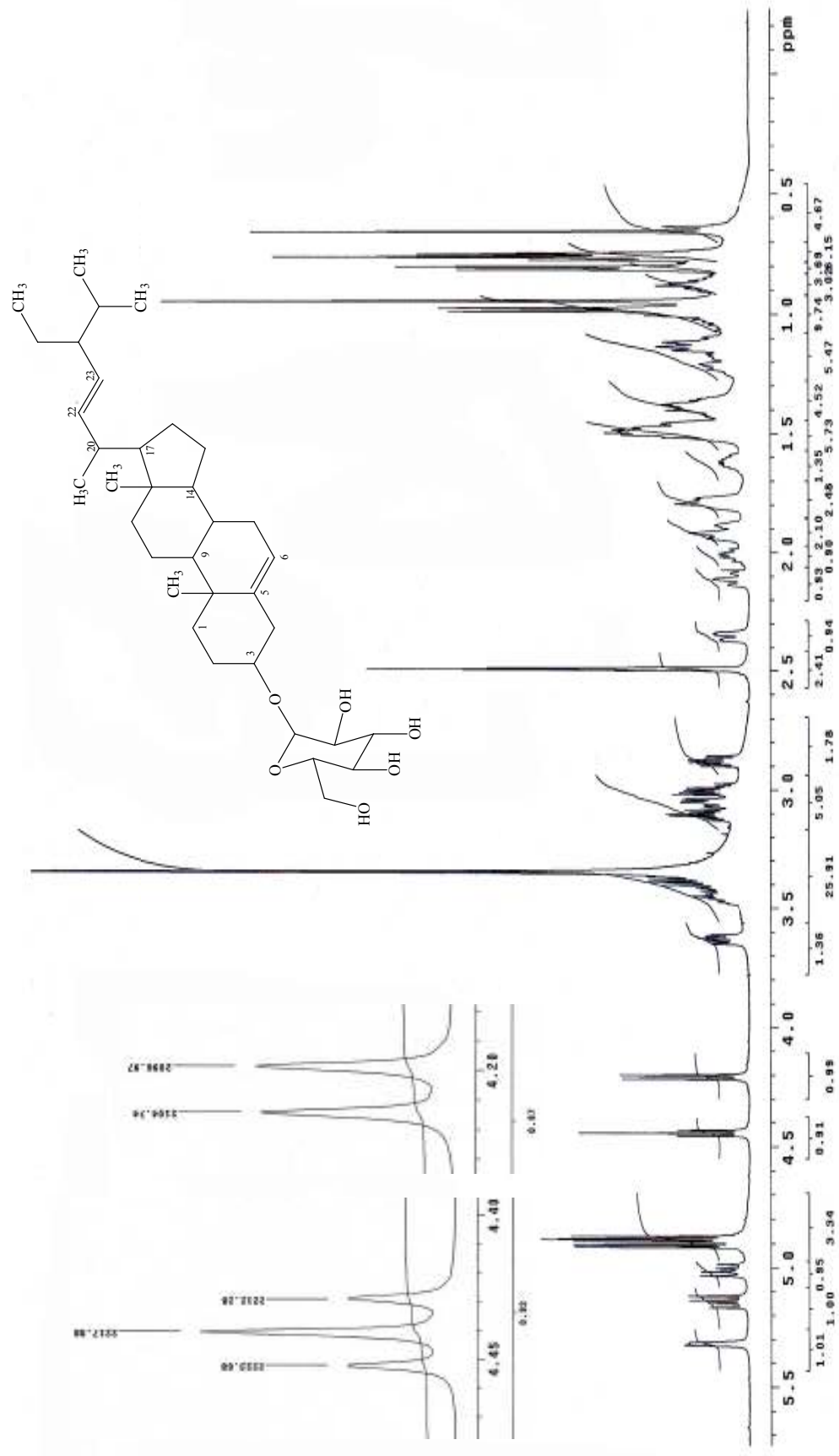
Figure 4-43 ^{1}H NMR spectrum of compound **8** in DMSO-d_6
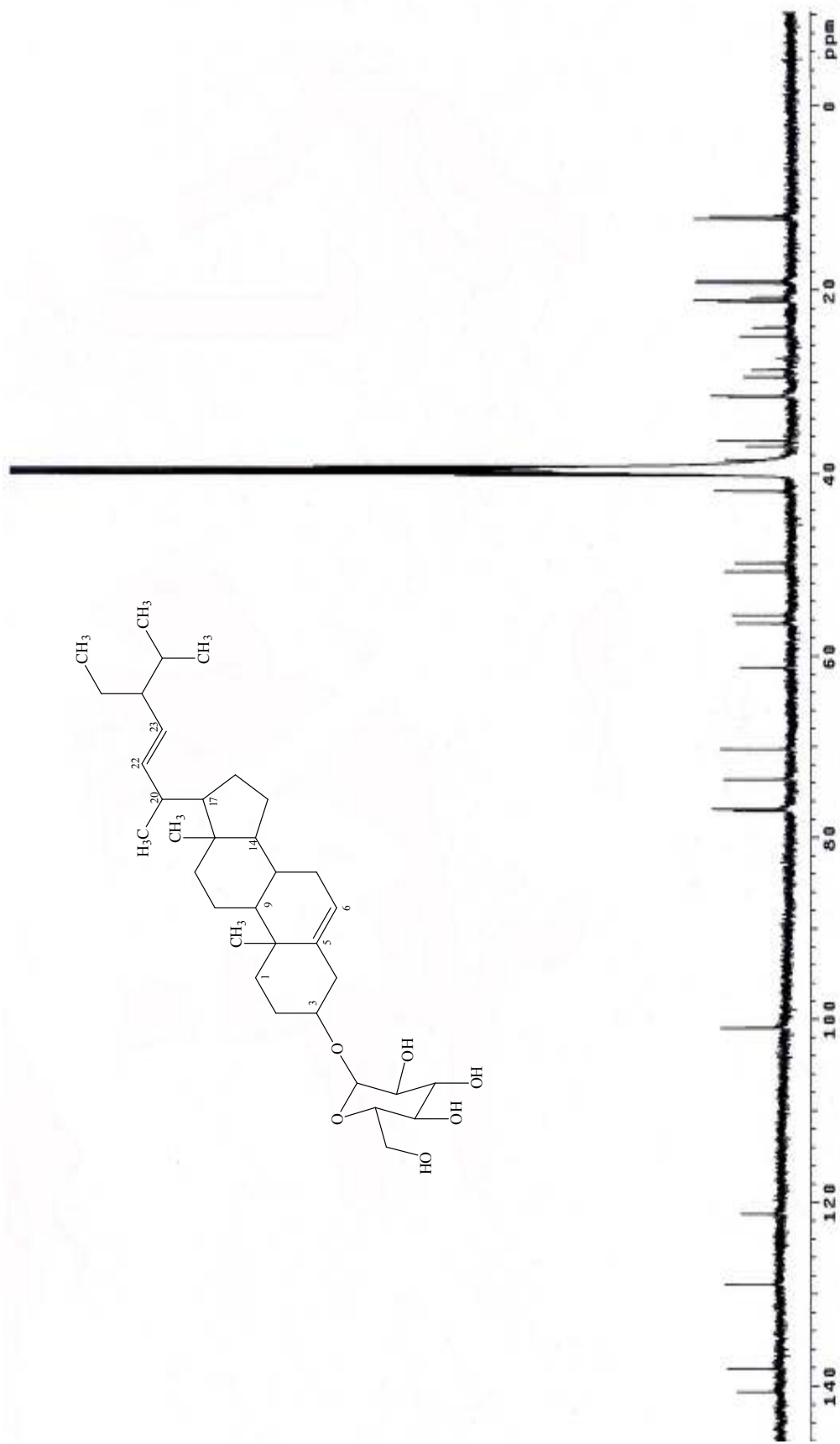
Figure 4-44 ^{13}C NMR spectrum of compound **8** in DMSO-d_6
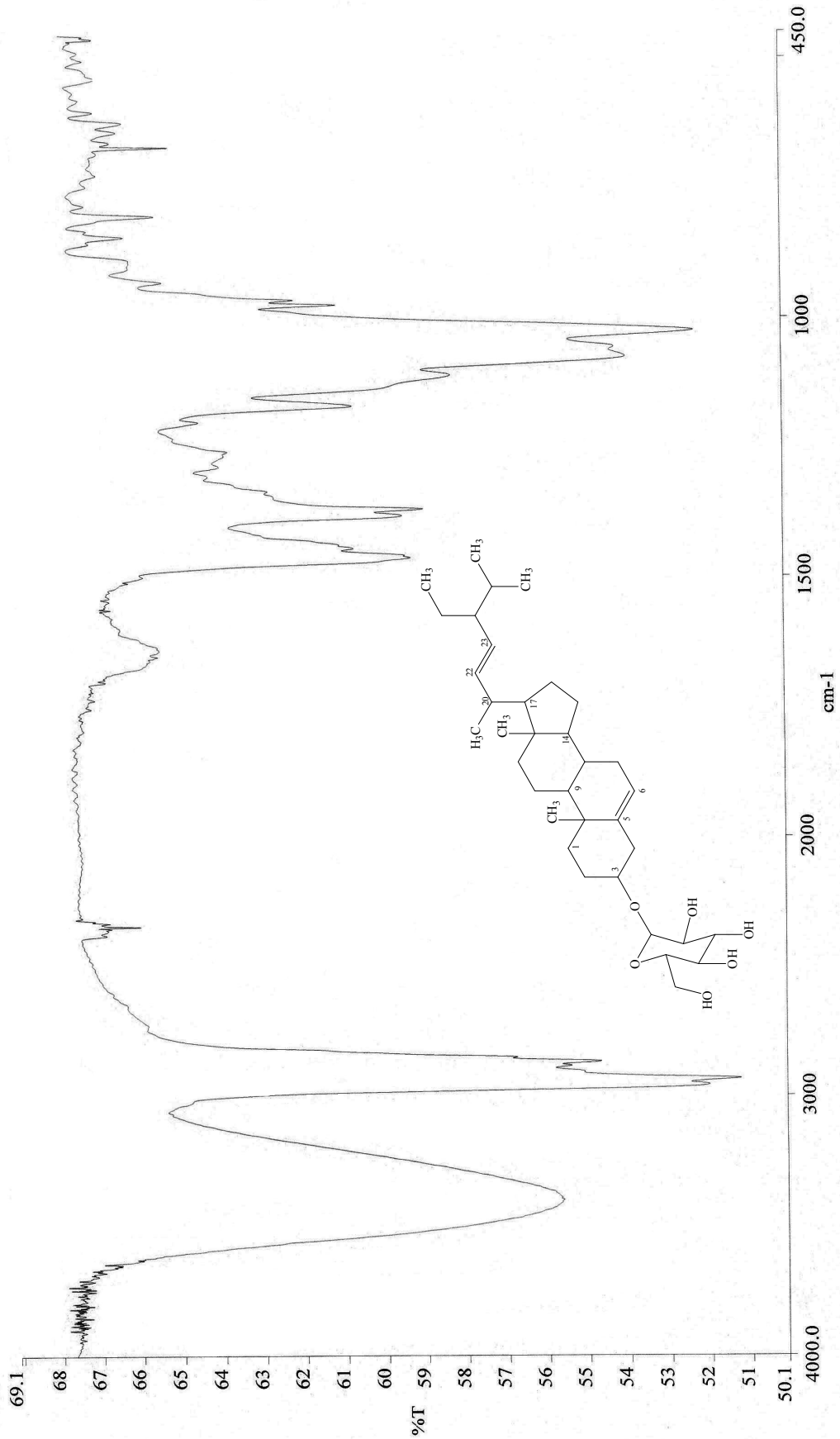
Figure 4-45 IR spectrum of compound **8**
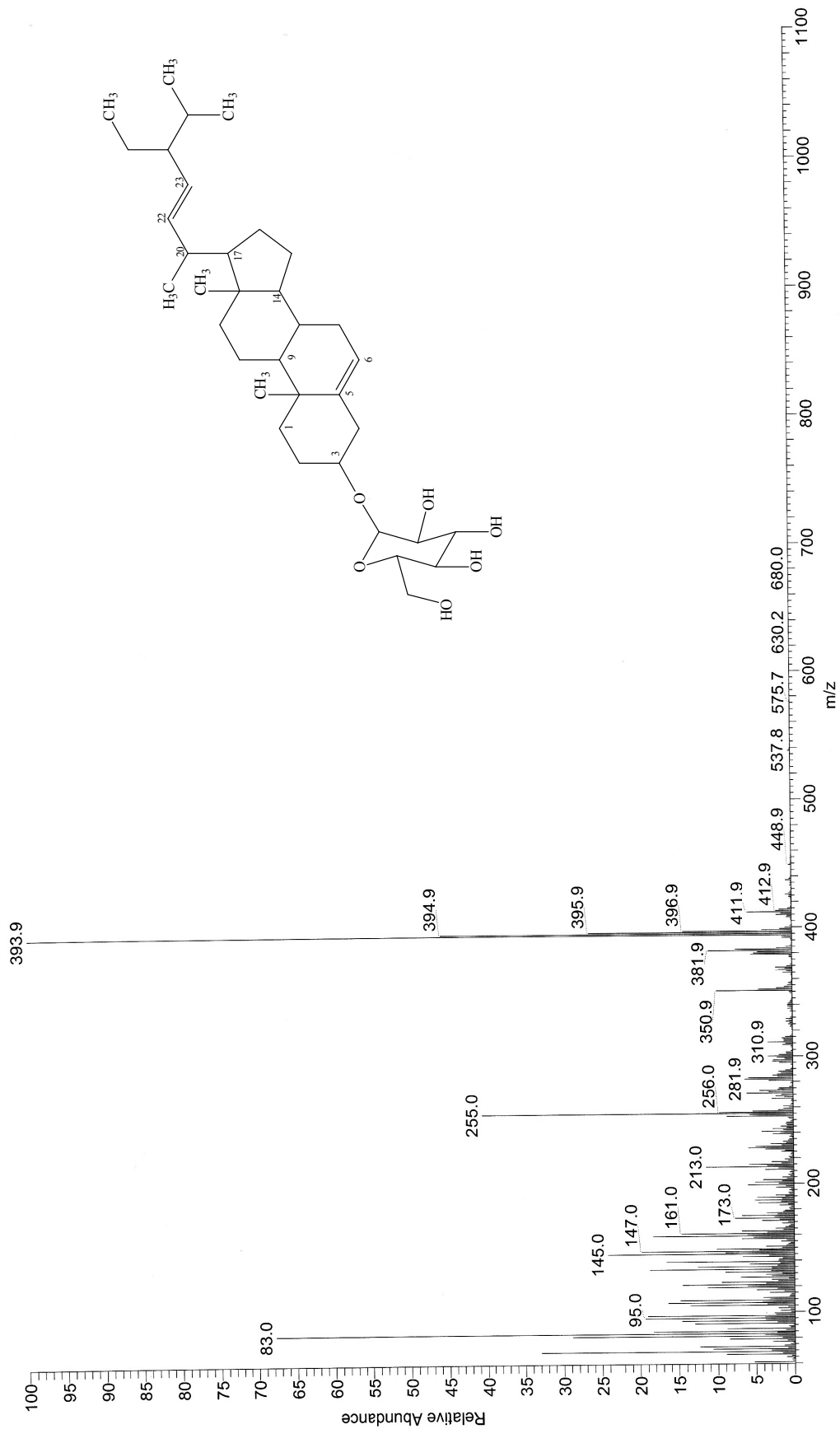
Figure 4-46 EI mass spectrum of compound **8**
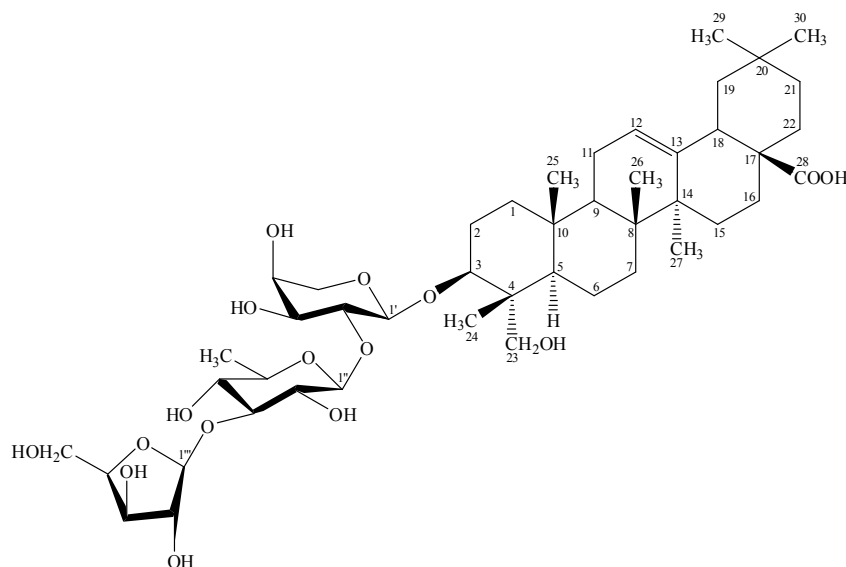
Figure 4-47 Chemical structure of 3-*O*-α-L-arabinofuranosyl-(1⟶3)-[α-L-rhamnopyranosyl-

(1⟶2)]-α-L-arabinopyranosyl hederagenin

Compound **9** was obtained as colourless needles (11 mg): mp 250-255 °C. The molecular

formula of 8 was proposed to be $C_{46}H_{74}O_{16}$ determined by EI mass spectrum, which showed

terpenoid peak at m/z 470.9. IR spectrum showed absorption band for hydroxyl (3413 cm^{-1}), C=C

(1659 cm^{-1}) and C-O (1017 cm^{-1}). The ^{13}C NMR spectra data (Table 4-10) recorded in CD$_3$OD

showed the existence of 46 signals for 46 carbon atoms in the molecule. This compound suggested

the presence of 7 methyl (δ 13.69, 16.39, 17.78, 18.03, 23.98, 26.63, 33.58 ppm), 13 methylene (δ

18.78, 24.06, 24.52, 26.46, 28.83, 33.39, 33.83, 34.89, 39.67, 47.24, 48.05, 64.42, 65.65 ppm), 18

methine (δ 42.74, 63.24, 69.51, 70.66, 71.53, 71.99, 73.73, 75.82, 79.04, 82.06, 82.40, 82.90,

86.90, 102.52, 105.04, 110.68, 123.60, 182.09 ppm) and 8 quaternary carbons (δ 31.61, 37.62,

40.50, 42.97, 43.97, 47.66, 49.63, 145.26 ppm). The anomeric carbon signals resonated at δ

102.52, 105.04 and 110.68 indicating the presence of three sugar moieties.

The ^{1}H NMR spectra data (Table 4-10) recorded in CD$_3$OD displayed characteristic

signals of terpenoid nucleus and a sugar unit. The terpenoid unit was showed as six methyls

singlet at δ 0.69 ppm (*s*, 3H-24), 0.80 ppm (*s*, 3H-26), 0.90 ppm (*s*, 3H-30), 0.94 ppm (*s*, 3H-29),

0.96 ppm (*s*, 3H-25) and 1.17 ppm (*s*, 3H-27) one methyl doublets at δ 1.23 ppm (*d*, *J* = 6.40 Hz,

3H-6″), one olefenic protons at δ 5.23 ppm (*t*, *J* = 3.66 Hz, 1H-12) and three oxymethaine protons

at δ 3.60 ppm (*dd*, *J* = 3.66, 9.63 Hz, 1H-3″), 3.62 ppm (*dd*, *J* = 5.49, 11.89 Hz, 1H-3) and 3.83

ppm (*m*, 1H-2′). The methane protons in the sugar unit were shown as signals at δ 3.38 ppm (*t*, *J* =

9.60 Hz, 1H-4″), 3.63 ppm (*dd*, *J* = 5.49, 11.89 Hz, 1H-4‴), 3.70 ppm (*dd*, *J* = 3.66, 7.50 Hz, 1H-3′), 3.85 ppm (*m*, 1H-3‴), 3.86 ppm (*m*, 1H-5″), 3.93 ppm (*dd*, *J* = 1.37, 3.20 Hz, 1H-2″), 3.98 ppm (*br s*, 1H-4′), 4.05 ppm (*br s*, 1H-2‴), 4.50 ppm (*d*, *J* = 6.41 Hz, 1H-1′), 5.05 ppm (*d*, *J* = 1.37 Hz, 1H-1‴), 5.10 ppm (*br s*, 1H-1″) and the oxymethylene protons were shown at δ 3.66 ppm (*d*, *J* = 3.70 Hz, 1H-5‴) were observed in the ^{1}H NMR spectrum. The ^{1}H NMR and ^{13}C NMR spectrum indicated the presence of a trisubstituted double bond δ_H 5.23 ppm (*t*, *J* = 3.66 Hz, 1H-12) and δ_c 123.60 and 145.26 ppm, characteristic of a 12 double bond in an oleanane skeleton. The appearance of signal at δ_c 182.09 is due to the presence of COOH group. The presence of hydroxyl group attached to C-23 was evidenced by signal in the downfield region of the ^{13}C NMR spectrum, δ 64.42 ppm. A comparision of the chemical shift of C-2′ of arabinose (C-2′, δ 75.82 ppm) with that of methyl rhamnose (C-5″, δ 70.66 ppm) allowed the assignment of a 1⟶2 linkage between arabinose and rhamnose. The downfield ^{13}C NMR chemical shift of C-3″ of rhamnose at 71.99 and small upfield shift of C-5″ of rhamnose of 70.66 indicated 1⟶3 linkage between rhamnose and the terminal arabinose. The nature of the interglycoside linkage was future confirmed by long-range connectivity information obtained from protons at δ 3.82 ppm (H-2′) and δ 3.60 (H-3″) with anomeric carbon at δ 102.52 (C-1″) and 110.68 (C-1‴) in agreement with presence of (1⟶2) and (1⟶3) linkages between arabinose and rhamnose and the terminal arabinose, respectively. The ^{1}H NMR and ^{13}C NMR chemical shifts were compared with the literature reports for triterpenoidal sapogenins/saponins, which confirmed the identity of the aglycone as hederagenin (Jayasinghe, *et al*., 1995; Adesegun, *et al*., 2008 / Table 4-10). Compound **9** was assigned as 3-*O*-α-L-arabinofuranosyl-(1⟶3)-[α-L-rhamnopyranosyl-(1⟶2)]-α-L-arabinopyranosyl hederagenin (Figure 4-47 and Figures 4-48 to 4-51).

Table 4-10 Spectral data of compound **9** (CD$_3$OD; 500 MHz for ^{1}H NMR, CD$_3$OD; 125 MHz for ^{13}C NMR) compare with 3-*O*-α-L-arabinofuranosyl-(1⟶3)-[α-L-rhamnopyranosyl-(1⟶2)]-α-L-arabinopyranosyl hederagenin (CD$_3$OD; 500 MHz for ^{1}H NMR, CD$_3$OD; 125 MHz for ^{13}C NMR)

Position	Type of C	δ$_C$ / ppm		δ$_H$ / ppm	
		Compound **9**	3-*O*-α-L-arabino-furanosyl-(1⟶3)-[α-L-rhamnopyra-nosyl-(1⟶2)]-α-L-arabinopyranosyl hederagenin	Compound **9**	3-*O*-α-L-arabino-furanosyl-(1⟶3)-[α-L-rhamnopyra-nosyl-(1⟶2)]-α-L-arabinopyranosyl hederagenin
1	CH$_2$	39.67	39.5	-	-
2	CH$_2$	26.46	26.3	-	-
3	CH	82.90	83.3	3.62, 1H, *dd*, *J* = 5.49, 11.89 Hz	3.62, 1H, *dd*, *J* = 5.5, 12.5 Hz
4	C	43.97	43.9	-	-
5	C	49.63	49.3	-	-
6	CH$_2$	18.78	18.8	-	-
7	CH$_2$	33.39	33.4	-	-
8	C	40.50	40.5	-	-
9	CH$_2$	48.05	48.1	-	-
10	C	37.62	37.7	-	-
11	CH$_2$	24.52	24.5	-	-
12	CH	123.60	123.6	5.23, 1H, *t*, *J* = 3.66 Hz	5.23, 1H, *t*, *J* = 3.5 Hz
13	C	145.26	145.3	-	-
14	C	42.97	43.0	-	-
15	CH$_2$	28.83	28.8	-	-
16	CH$_2$	24.06	24.0	-	-

Table 4-10   Spectral data of compound **9** (CD$_3$OD; 500 MHz for ^{1}H NMR, CD$_3$OD; 125 MHz for ^{13}C NMR) compare with 3-*O*-α-L-arabinofuranosyl-(1⟶3)-[α-L-rhamnopyranosyl-(1⟶2)]-α-L-arabinopyranosyl hederagenin (CD$_3$OD; 500 MHz for ^{1}H NMR, CD$_3$OD; 125 MHz for ^{13}C NMR) (continued)

Position	Type of C	δ$_C$ / ppm		δ$_H$ / ppm	
		Compound 9	3-*O*-α-L-arabino-furanosyl-(1⟶3)-[α-L-rhamnopyra-nosyl-(1⟶2)]-α-L-arabinopyranosyl hederagenin	Compound 9	3-*O*-α-L-arabino-furanosyl-(1⟶3)-[α-L-rhamnopyra-nosyl-(1⟶2)]-α-L-arabinopyranosyl hederagenin
17	C	47.66	47.6	-	-
18	CH	42.74	42.7	2.84, 1H, *dd*, *J* = 3.70, 13.94 Hz	2.84, 1H, *dd*, *J* = 3.7, 13.9 Hz
19	CH$_2$	47.24	47.2	-	-
20	C	31.61	31.6	-	-
21	CH$_2$	34.89	34.9	-	-
22	CH$_2$	33.83	33.8	-	-
23	CH$_2$	64.42	64.8	3.30, 2H, *m* 3.59, 2H, *d*, *J* = 10.0 Hz	3.30, 2H, *m* 3.59, 2H, *d*, *J* = 11 Hz
24	CH$_3$	13.69	13.4	0.69, 3H, *s*	0.69, 3H, s
25	CH$_3$	16.39	16.4	0.96, 3H, *s*	0.96, 3H, *s*
26	CH$_3$	17.78	17.8	0.80, 3H, *s*	0.80, 3H, *s*
27	CH$_3$	26.63	26.5	1.17, 3H, *s*	1.17, 3H, *s*
28	C	182.09	181.9	-	-
29	CH$_3$	33.58	33.6	0.94, 3H, *s*	0.94, 3H, *s*
30	CH$_3$	23.98	24.0	0.90, 3H, *s*	0.90, 3H, *s*

Table 4-10   Spectral data of compound **9** (CD$_3$OD; 500 MHz for ^{1}H NMR, CD$_3$OD; 125 MHz for ^{13}C NMR) compare with 3-*O*-α-L-arabinofuranosyl-(1⟶3)-[α-L-rhamnopyranosyl-(1⟶2)]-α-L-arabinopyranosyl hederagenin (CD$_3$OD; 500 MHz for ^{1}H NMR, CD$_3$OD; 125 MHz for ^{13}C NMR) (continued)

Position	Type of C	δ_C / ppm		δ_H / ppm	
		Compound **9**	3-*O*-α-L-arabino-furanosyl-(1⟶3)-[α-L-rhamnopyra-nosyl-(1⟶2)]-α-L-arabinopyranosyl hederagenin	Compound **9**	3-*O*-α-L-arabino-furanosyl-(1⟶3)-[α-L-rhamnopyra-nosyl-(1⟶2)]-α-L-arabinopyranosyl hederagenin
1′	CH	105.04	104.4	4.50, 1H, *d*, *J* = 6.41 Hz	4.51, 1H, *d*, *J* = 6.5 Hz
2′	CH	75.82	75.1	3.82, 1H, *m*	3.80, 1H, *m*
3′	CH	82.06	82.2	3.70, 1H, *dd*, *J* = 3.66, 7.50 Hz	3.77, 1H, *dd*, *J* = 3.6, 7.1 Hz
4′	CH	69.51	69.1	3.98, 1H, *br s*	3.95, 1H, *br s*
5′α	CH	65.65	65.2	3.84, 1H, *m*	3.82, 1H, *m*
5′β	CH	65.65	65.2	3.55, 1H, *dd*, *J* = 1.82, 11.43 Hz	3.55, 1H, *d*, *J* = 11.9 Hz
1″	CH	102.52	102.4	5.10, 1H, *br s*	5.08, 1H, *br s*
2″	CH	71.53	71.5	3.93, 1H, *dd*, *J* = 1.37, 3.2 Hz	3.94, 1H, *br s*
3″	CH	71.99	72.0	3.60, 1H, *dd*, *J* = 3.66, 9.63 Hz	3.71, 1H, *dd*, *J* = 3.7, 9.7 Hz
4″	CH	73.73	73.6	3.38, 1H, *t*, *J* = 9.6 Hz	3.32, 1H, *t*, *J* = 8.2 Hz
5″	CH	70.66	70.7	3.86, 1H, *m*	3.86, 1H, *m*
6″	CH$_3$	18.03	18.0	1.23, 3H, *d*, *J* = 6.40 Hz	1.23, 3H, *d*, *J* = 6.4 Hz

Table 4-10 Spectral data of compound **9** (CD$_3$OD; 500 MHz for ^{1}H NMR, CD$_3$OD; 125 MHz for ^{13}C NMR) compare with 3-*O*-α-L-arabinofuranosyl-(1⟶3)-[α-L-rhamnopyranosyl-(1⟶2)]-α-L-arabinopyranosyl hederagenin (CD$_3$OD; 500 MHz for ^{1}H NMR, CD$_3$OD; 125 MHz for ^{13}C NMR) (continued)

Position	Type of C	δ$_C$ / ppm		δ$_H$ / ppm	
		Compound **9**	3-*O*-α-L-arabino-furanosyl-(1⟶3)-[α-L-rhamnopyra-nosyl-(1⟶2)]-α-L-arabinopyranosyl hederagenin	Compound **9**	3-*O*-α-L-arabino-furanosyl-(1⟶3)-[α-L-rhamnopyra-nosyl-(1⟶2)]-α-L-arabinopyranosyl hederagenin
1‴	CH	110.68	110.0	5.05, 1H, *d*, *J* = 1.37 Hz	5.05, 1H, *d*, *J* = 1.8 Hz
2‴	CH	82.40	82.7	4.05, 1H, *br s*	4.04, 1H, *br s*
3‴	CH	79.04	78.9	3.85,1H, *m*	3.80, 1H, *m*
4‴	CH	86.90	86.9	3.63, 1H, *dd*, *J* = 5.49, 11.89 Hz	3.59, 1H, *d*, *J* = 11.9 Hz
5‴	CH$_2$	63.24	63.2	3.66, 2H, *d*, *J* = 3.70 Hz	3.66, 2H, *m*
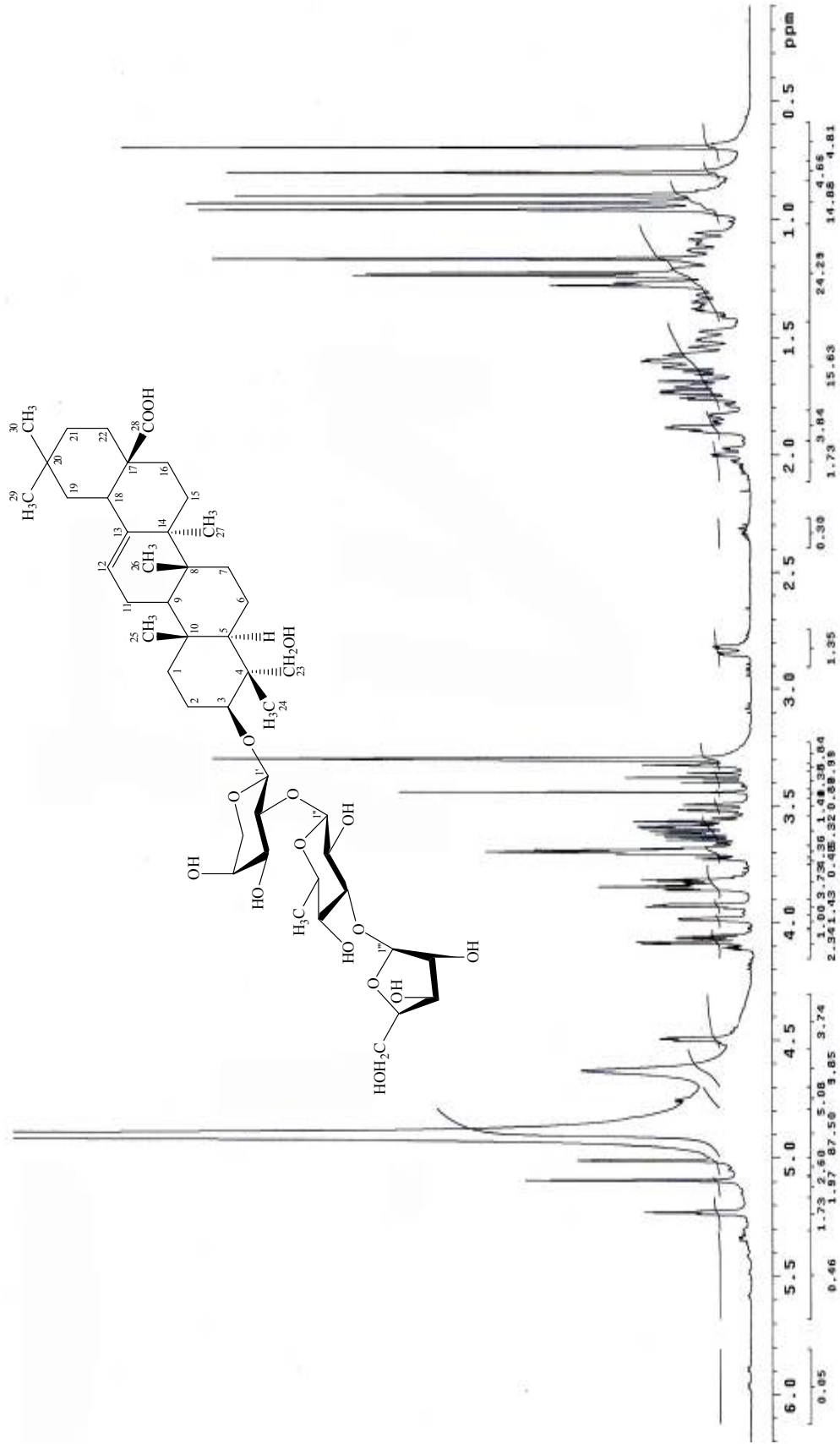
Figure 4-48 ^{1}H NMR spectrum of compound **9**
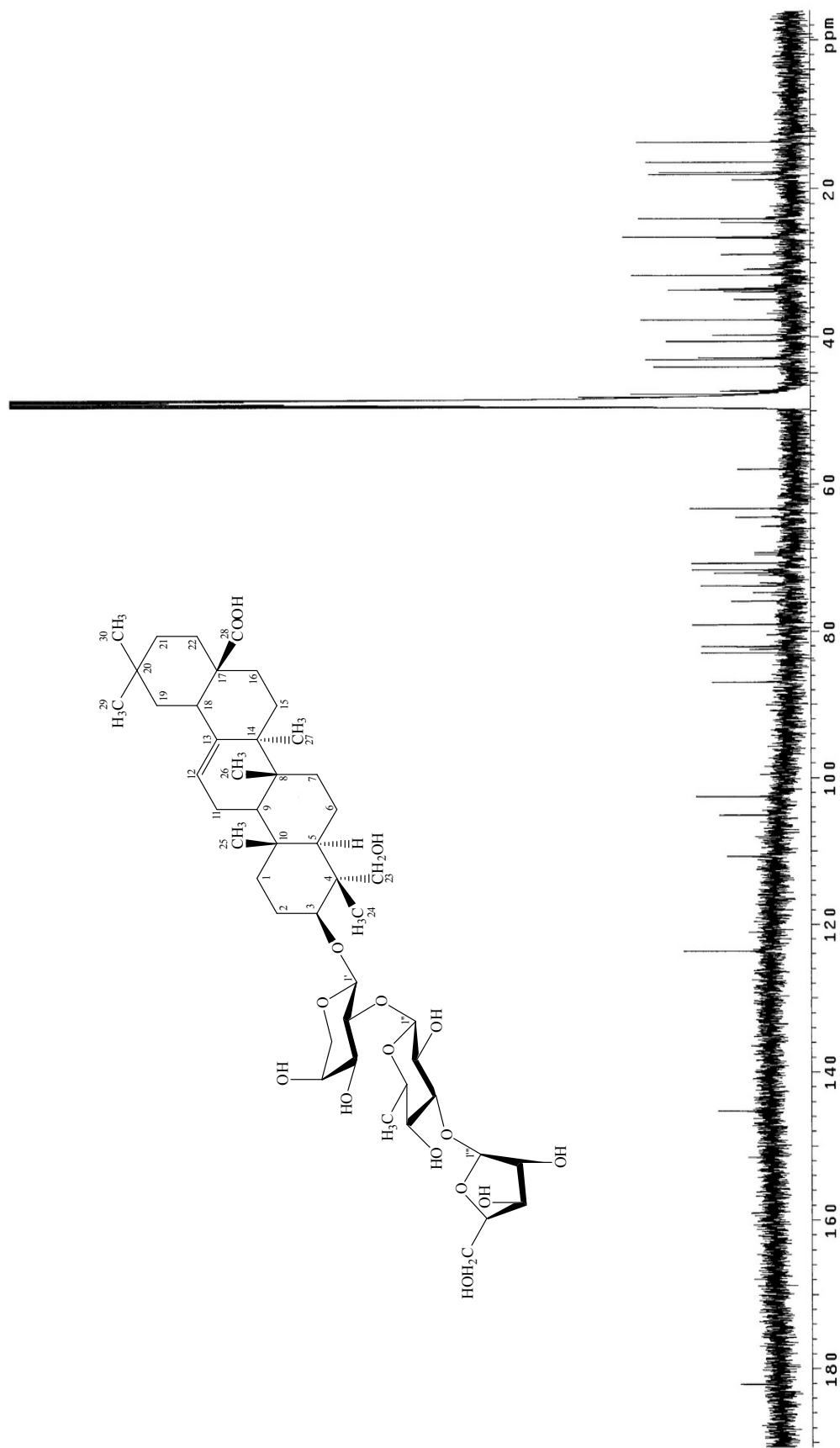
Figure 4-49 ^{13}C NMR spectrum of compound **9**

139
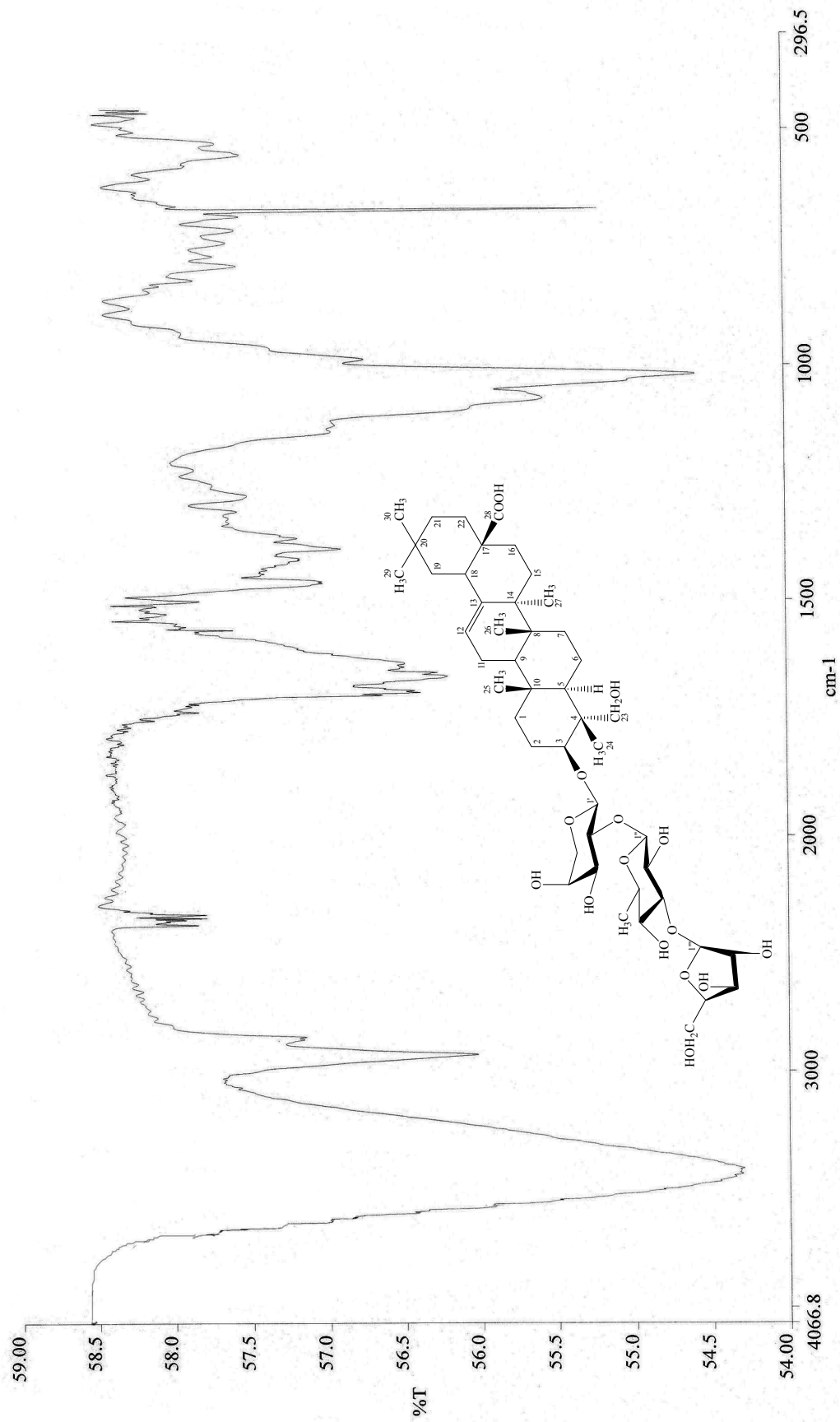
Figure 4-50 IR spectrum of compound **9**
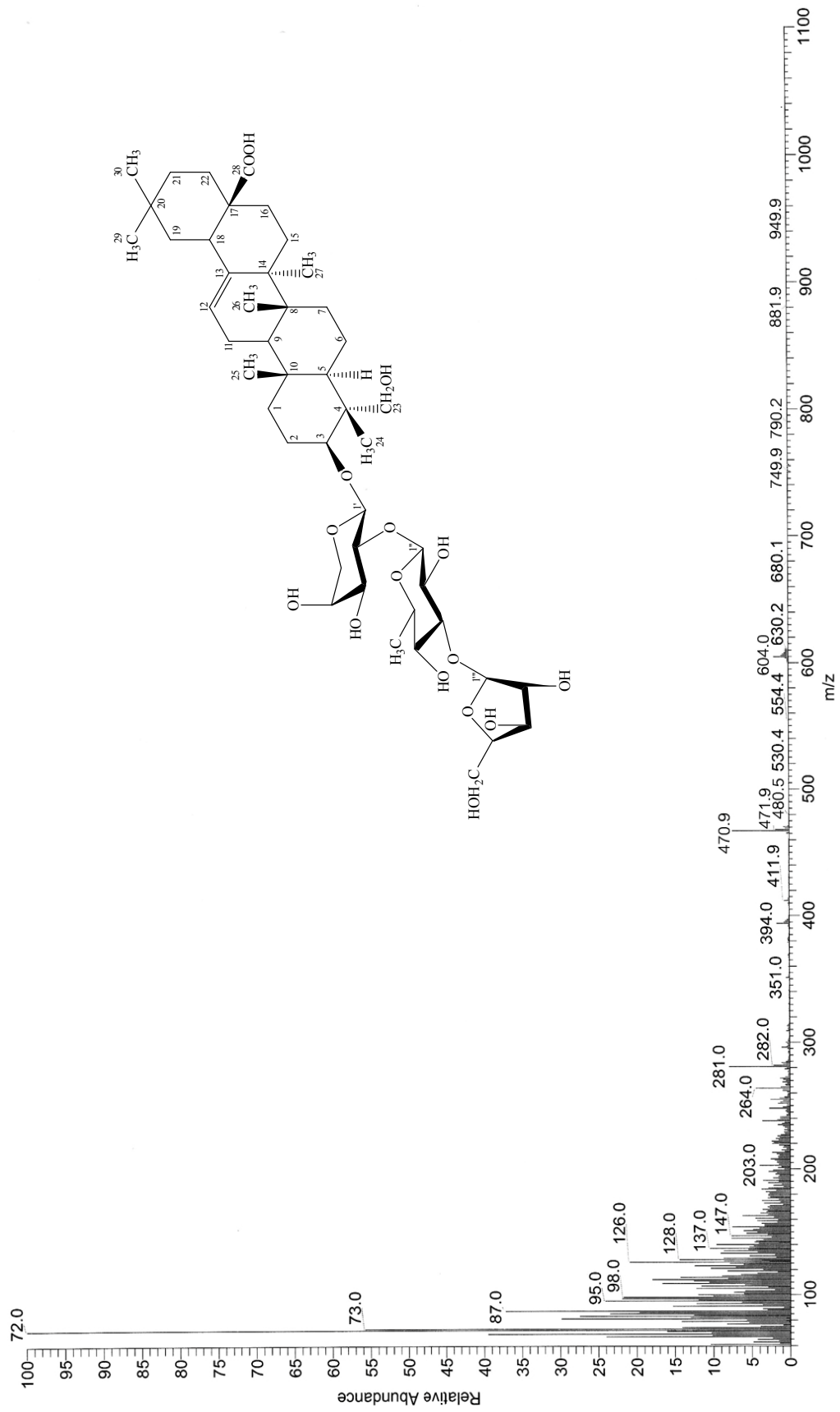
Figure 4-51 EI mass spectrum of compound **9**
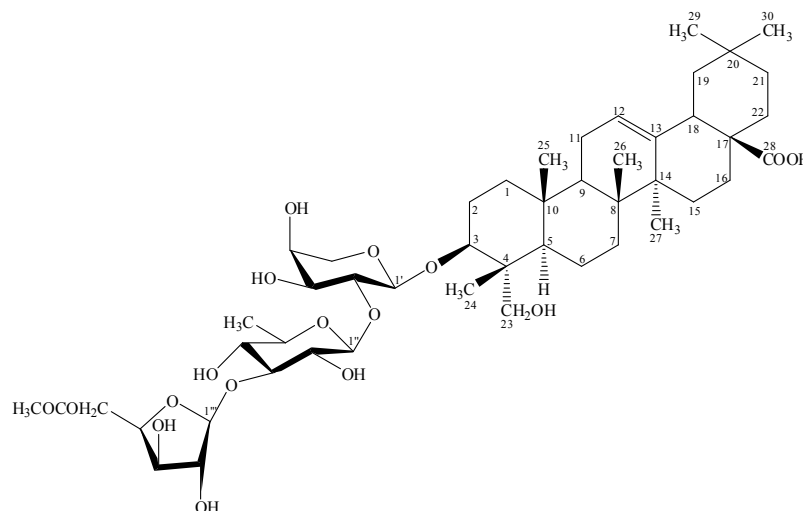
Figure 4-52 Chemical structure of 3-*O*-(5-*O*-Acetyl-α-L-arabinofuranosyl)-(1⟶3)-[α -L-
rhamnopyranosyl-(1⟶2)]-α -L-arabinopyranosyl hederagenin

Compound **10** was obtained as colourless crystals (97 mg): mp 250-260 °C. The molecular
formula of 8 was proposed to be $C_{48}H_{77}O_{17}$ determined by EI mass spectrum, which showed
terpenoid peak at m/z 470.4. IR spectrum showed absorption band for hydroxyl (3419 cm^{-1}), C=C
(1694 cm^{-1}) and C-O (1072 cm^{-1}). The ^{13}C NMR spectra data (Table 4-11) recorded in CD_3OD
showed the existence of 48 signals for 48 carbon atoms in the molecule. This compound suggested
the presence of 8 methyl (δ 13.68, 16.39, 17.77, 18.23, 20.68, 24.06, 26.46, 33.58 ppm), 13
methylene (δ 18.78, 23.98, 24.53, 26.64, 28.84, 33.83, 33.39, 34.90, 39.68, 47.24, 48.04, 64.42,
75.83 ppm), 18 methine (δ 42.74, 65.31, 65.64, 69.58, 70.69, 71.52, 72.00, 73.73, 75.82, 79.40,
82.06, 82.95, 83.73, 105.05, 102.54, 110.77, 123.62, 181.94 ppm) and 9 quaternary carbons (δ
37.63, 40.51, 42.98, 43.97, 47.64, 49.34, 145.25, 172.58 ppm). The anomeric carbon signals
resonated at δ 102.54, 105.05 and 110.77 indicating the presence of three sugar moieties.

The ^{1}H NMR spectra data (Table 4-11) recorded in CD_3OD displayed characteristic
signals of terpenoid nucleus and a sugar unit. The terpenoid unit was showed as six methyls
singlet at δ 0.70 ppm (*s*, 3H-24), 0.80 ppm (*s*, 3H-26), 0.90 ppm (*s*, 3H-30), 0.93 ppm (*s*, 3H-29),
0.96 ppm (*s*, 3H-25) and 1.17 ppm (*s*, 3H-27) one methyl doublets at δ 1.23 ppm (*d*, *J* = 6.40 Hz,
3H-6″), one olefenic protons at δ 5.23 ppm (*t*, *J* = 3.65 Hz, 1H-12) and three oxymethaine protons
at δ 3.60 ppm (*dd*, *J* = 4.58, 11.89 Hz, 1H-3) 3.68 ppm (*dd*, *J* = 3.20, 9.61 Hz, 1H-3″), and 3.83
ppm (*m*, 1H-2′). The methane protons in the sugar unit were shown as signals at δ 3.38 ppm (*t*, *J* =

9.60 Hz, 1H-4″), 3.59 ppm (*d*, *J* = 11.89 Hz, 1H-4‴), 3.70 ppm (*dd*, *J* = 3.66, 7.50 Hz, 1H-3′),
3.84 ppm (*m*, 1H-3‴), 3.85 ppm (*m*, 1H-5″), 3.93 ppm (*dd*, *J* = 1.83, 3.20 Hz, 1H-2″), 3.95 ppm
(*br s*, 1H-4′), 4.14 ppm (*t*, *J* = 6.4 Hz, 1H-2‴), 4.50 ppm (*d*, *J* = 5.94 Hz, 1H-1′), 5.05 ppm (*d*, *J* =
1.37 Hz, 1H-1‴) and 5.10 ppm (*br s*, 1H-1″) were observed in the ^{1}H NMR spectrum. The [1]H
NMR and ^{13}C NMR spectrum indicated the presence of a trisubstituted double bond δ_H 5.23 ppm
(*t*, *J* = 3.65 Hz, 1H-12) and δ_c 123.62 and 145.25 ppm, characteristic of a 12 double bond in an
oleanane skeleton. The appearance of signal at δ_c 181.94 is due to the presence of COOH group.
The presence of hydroxyl group attached to C-23 was evidenced by signal in the downfield region
of the ^{13}C NMR spectrum, δ 64.42 ppm. A comparision of the chemical shift of C-2′ of arabinose
(C-2′,δ 75.83 ppm) with that of methyl rhamnose (C-5″, δ 70.69 ppm) allowed the assignment of
a 1⟶2 linkage between arabinose and rhamnose. The downfield ^{13}C NMR chemical shift of C-3″
of rhamnose at 72.00 and small upfield shift of C-5″ of rhamnose of 70.69 indicated 1⟶3
linkage between rhamnose and the terminal arabinose. The nature of the interglycoside linkage
was future confirmed by long-range connectivity information obtained from protons at δ 3.83 ppm
(H-2′) and δ 3.68 (H-3″) with anomeric carbon at δ 102.54 (C-1″) and 110.77 (C-1‴) in
agreement with presence of (1⟶2) and (1⟶3) linkages between arabinose and rhamnose and
the terminal arabinose, respectively. Comparision of the ^{13}C NMR spectral data of compound **10**
with those of compound **9** showed the signal due to the same sugar moiety, indicating the present
of one acetyl group at 171.58 (C-5‴) of the arabinofuranosyl unit in compound **10**. The acetyl
group was assigned to attach at C-5‴, since the chemical shifts of C-5‴, C-4‴ changed by +1.9, -
1.2 ppm, respectively. The ^{1}H NMR and ^{13}C NMR chemical shifts were compared with the
literature reports for triterpenoidal sapogenins/saponins, which confirmed the identity of the
aglycone as hederagenin (Jayasinghe, *et al*., 1995; Kanchanapoom, *et al*., 2001; Adesegun, *et al*.,
2008; Sharma, *et al*., 2011 / Table 4-11). Compound **10** was assigned as 3-*O*-(5-*O*-acetyl-α-L-
arabinofuranosyl)-(1⟶3)-[α-L-rhamnopyranosyl-(1⟶2)]-α-L-arabinopyranosyl hederagenin
(Figure 4-52 and Figures 4-53 to 4-56).

Table 4-11 Spectral data of compound **10** (CD₃OD; 500 MHz for ¹H NMR, CD₃OD; 125 MHz for ¹³C NMR) compare with 3-*O*-(5-*O*-acetyl-α-L-arabinofuranosyl)-(1⟶3)-[α-L-rhamno-pyranosyl-(1⟶2)]-α-L-arabinopyranosyl hederagenin (CD₃OD; 500 MHz for ¹H NMR, CD₃OD; 125 MHz for ¹³C NMR)

Position	Type of C	δ_C / ppm		δ_H / ppm	
		Compound **10**	3-*O*-(5-*O*-Acetyl-α-L-arabinofurano-syl)-(1⟶3)-[α-L-rhamnopyra-nosyl-(1⟶2)]-α-L-arabinopyranosyl hederagenin	Compound **10**	3-*O*-(5-*O*-Acetyl-α-L-arabinofurano-syl)-(1⟶3)-[α-L-rhamnopyranosyl-(1⟶2)]-α-L-arabinopyranosyl hederagenin
1	CH₂	39.68	39.5	-	-
2	CH₂	26.64	26.3	-	-
3	CH	83.73	83.3	3.60, 1H, *dd*, J = 4.58, 11.89 Hz	3.62, 1H, *dd*, J = 5.5, 12.5 Hz
4	C	43.97	43.9	-	-
5	C	49.34	49.3	-	-
6	CH₂	18.78	18.8	-	-
7	CH₂	33.39	33.4	-	-
8	C	40.51	40.5	-	-
9	CH₂	48.04	48.1	-	-
10	C	37.63	37.7	-	-
11	CH₂	24.53	24.5	-	-
12	CH	123.62	123.6	5.23, 1H, *t*, J = 3.65 Hz	5.23, 1H, *t*, J = 3.5 Hz
13	C	145.25	145.3	-	-
14	C	42.98	43.0	-	-

Table 4-11 Spectral data of compound **10** (CD$_3$OD; 500 MHz for ^{1}H NMR, CD$_3$OD; 125 MHz for ^{13}C NMR) compare with 3-*O*-(5-*O*-acetyl-α-L-arabinofuranosyl)-(1⟶3)-[α-L-rhamno-pyranosyl-(1⟶2)]-α-L-arabinopyranosyl hederagenin (CD$_3$OD; 500 MHz for ^{1}H NMR, CD$_3$OD; 125 MHz for ^{13}C NMR) (continued)

Position	Type of C	δ$_C$ / ppm		δ$_H$ / ppm	
		Compound **10**	3-*O*-(5-*O*-Acetyl-α-L-arabinofurano-syl)-(1⟶3)-[α-L-rhamnopyra-nosyl-(1⟶2)]-α-L-arabinopyranosyl hederagenin	Compound **10**	3-*O*-(5-*O*-Acetyl-α-L-arabinofurano-syl)-(1⟶3)-[α-L-rhamnopyra-nosyl-(1⟶2)]-α-L-arabinopyranosyl hederagenin
15	CH$_2$	28.84	28.8	-	-
16	CH$_2$	24.06	24.0	-	-
17	C	47.64	47.6	-	-
18	CH	42.74	42.7	2.84, 1H, *dd*, *J* = 4.11, 13.72 Hz	2.84, 1H, *dd*, *J* = 3.7, 13.9 Hz
19	CH$_2$	47.24	47.2	-	-
20	C	31.62	31.6	-	-
21	CH$_2$	34.90	34.9	-	-
22	CH$_2$	33.83	33.8	-	-
23	CH$_2$	64.42	64.8	3.30, 2H, *m* 3.51, 2H, *d*, *J* = 12.35 Hz	3.30, 2H, *m* 3.59, 2H, *d*, *J* = 11 Hz
24	CH$_3$	13.68	13.4	0.70, 3H, *s*	0.69, 3H, *s*
25	CH$_3$	16.39	16.4	0.96, 3H, *s*	0.96, 3H, *s*
26	CH$_3$	17.77	17.8	0.80, 3H, *s*	0.80, 3H, *s*
27	CH$_3$	26.46	26.5	1.17, 3H, *s*	1.17, 3H, *s*
28	C	181.94	181.9	-	-

Table 4-11 Spectral data of compound **10** (CD$_3$OD; 500 MHz for ^{1}H NMR, CD$_3$OD; 125 MHz for ^{13}C NMR) compare with 3-*O*-(5-*O*-acetyl-α-L-arabinofuranosyl)-(1⟶3)-[α-L-rhamno-pyranosyl-(1⟶2)]-α-L-arabinopyranosyl hederagenin (CD$_3$OD; 500 MHz for ^{1}H NMR, CD$_3$OD; 125 MHz for ^{13}C NMR) (continued)

Position	Type of C	δ$_C$ / ppm		δ$_H$ / ppm	
		Compound **10**	3-*O*-(5-*O*-Acetyl-α-L-arabinofurano-syl)-(1⟶3)-[α-L-rhamnopyra-nosyl-(1⟶2)]-α-L-arabinopyranosyl hederagenin	Compound **10**	3-*O*-(5-*O*-Acetyl-α-L-arabinofurano-syl)-(1⟶3)-[α-L-rhamnopyra-nosyl-(1⟶2)]-α-L-arabinopyranosyl hederagenin
29	CH$_3$	33.58	33.6	0.93, 3H, *s*	0.94, 3H, *s*
30	CH$_3$	23.98	24.0	0.90, 3H, *s*	0.90, 3H, *s*
1′	CH	105.05	104.4	4.50, 1H, *d*, J = 5.94 Hz	4.51, 1H, *d*, J = 6.5 Hz
2′	CH	75.83	75.1	3.83, 1H, *m*	3.80, 1H, *m*
3′	CH	82.95	82.2	3.70, 1H, *dd*, J = 3.66, 7.50 Hz	3.77, 1H, *dd*, J = 3.6, 7.1 Hz
4′	CH	69.58	69.1	3.95, 1H, *br s*	3.95, 1H, *br s*
5′α	CH	65.64	65.2	3.82, 1H, *m*	3.82, 1H, *m*
5′β	CH	65.64	65.2	3.55, 1H, *dd*, J = 1.83, 12.35 Hz	3.55, 1H, *d*, J = 11.9 Hz
1″	CH	102.54	102.4	5.10, 1H, *br s*	5.08, 1H, *br s*
2″	CH	71.52	71.5	3.93, 1H, *dd*, J = 1.83, 3.20 Hz	3.94, 1H, *br s*
3″	CH	72.00	72.0	3.68, 1H, *dd*, J = 3.20, 9.61 Hz	3.71, 1H, *dd*, J = 3.7, 9.7 Hz

Table 4-11 Spectral data of compound **10** (CD$_3$OD; 500 MHz for ^{1}H NMR, CD$_3$OD; 125 MHz for ^{13}C NMR) compare with 3-*O*-(5-*O*-acetyl-α-L-arabinofuranosyl)-(1⟶3)-[α-L-rhamno-pyranosyl-(1⟶2)]-α-L-arabinopyranosyl hederagenin (CD$_3$OD; 500 MHz for ^{1}H NMR, CD$_3$OD; 125 MHz for ^{13}C NMR) (continued)

Position	Type of C	δ_C / ppm		δ_H / ppm	
		Compound **10**	3-*O*-(5-*O*-Acetyl-α-L-arabinofurano-syl)-(1⟶3)-[α-L-rhamnopyra-nosyl-(1⟶2)]-α-L-arabinopyranosyl hederagenin	Compound **10**	3-*O*-(5-*O*-Acetyl-α-L-arabinofurano-syl)-(1⟶3)-[α-L-rhamnopyra-nosyl-(1⟶2)]-α-L-arabinopyranosyl hederagenin
4″	CH	73.73	73.6	3.38, 1H, *t*, *J* = 9.6 Hz	3.32, 1H, *t*, *J* = 8.2 Hz
5″	CH	70.69	70.7	3.85, 1H, *m*	3.86, 1H, *m*
6″	CH$_3$	18.23	18.0	1.23, 3H, *d*, *J* = 5.95 Hz	1.23, 3H, *d*, *J* = 6.4 Hz
1‴	CH	110.77	110.9	5.05, 1H, *d*, *J* = 1.37 Hz	5.05, 1H, *d*, *J* = 1.8 Hz
2‴	CH	82.06	82.7	4.14, 1H, *t*, *J* = 6.40 Hz	4.07, 1H, *t*, *J* = 6.4 Hz
3‴	CH	79.40	79.9	3.84, 1H, *m*	3.89, 1H, *m*
4‴	CH	85.82	85.7	3.59, 1H, *d*, *J* = 11.89 Hz	3.79, 1H, *d*, *J* = 11.7 Hz
5‴	CH$_2$	65.31	66.0	4.60, 2H, *br s*	4.55, 2H, *br s*
COCH$_3$	CO	172.58	171.2	-	-
COCH$_3$	CH$_3$	20.68	20.8	2.15, 3H, *s*	2.05, 3H, *s*

Figure 4-53 ^{1}H NMR spectrum of compound **10** in CD$_3$OD
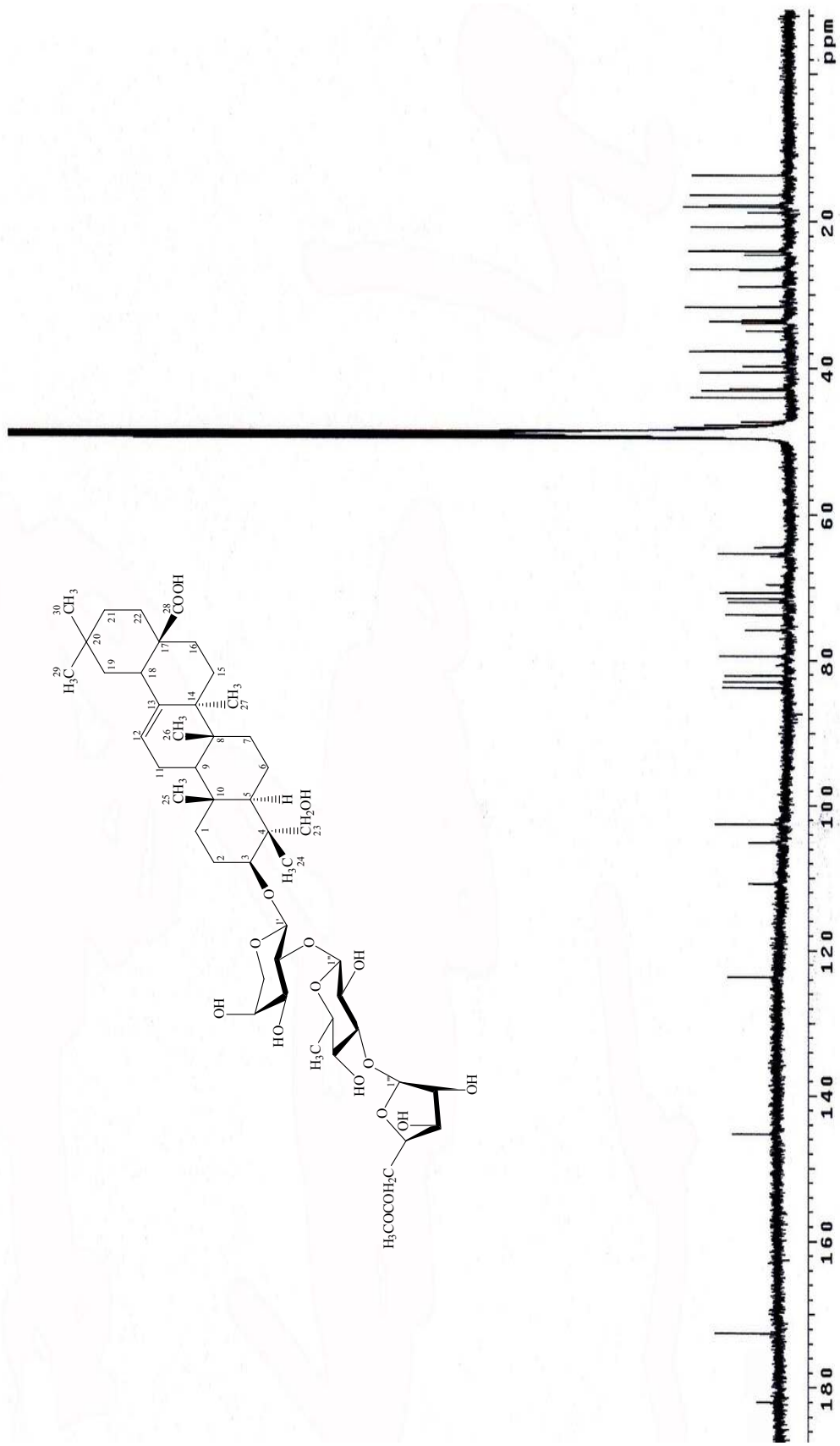
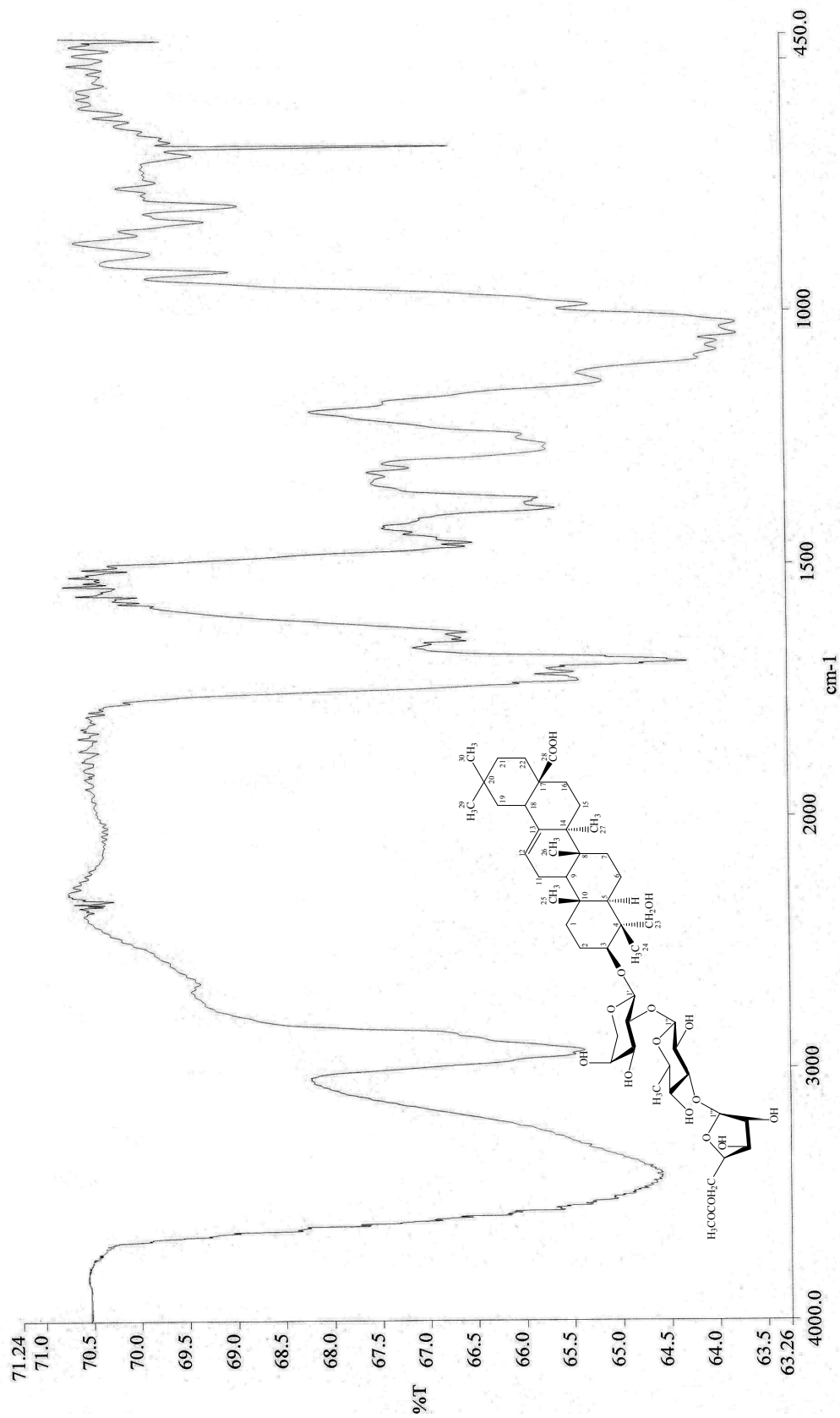**Figure 4-54** ^{13}C NMR spectrum of compound **10** in CD$_3$OD
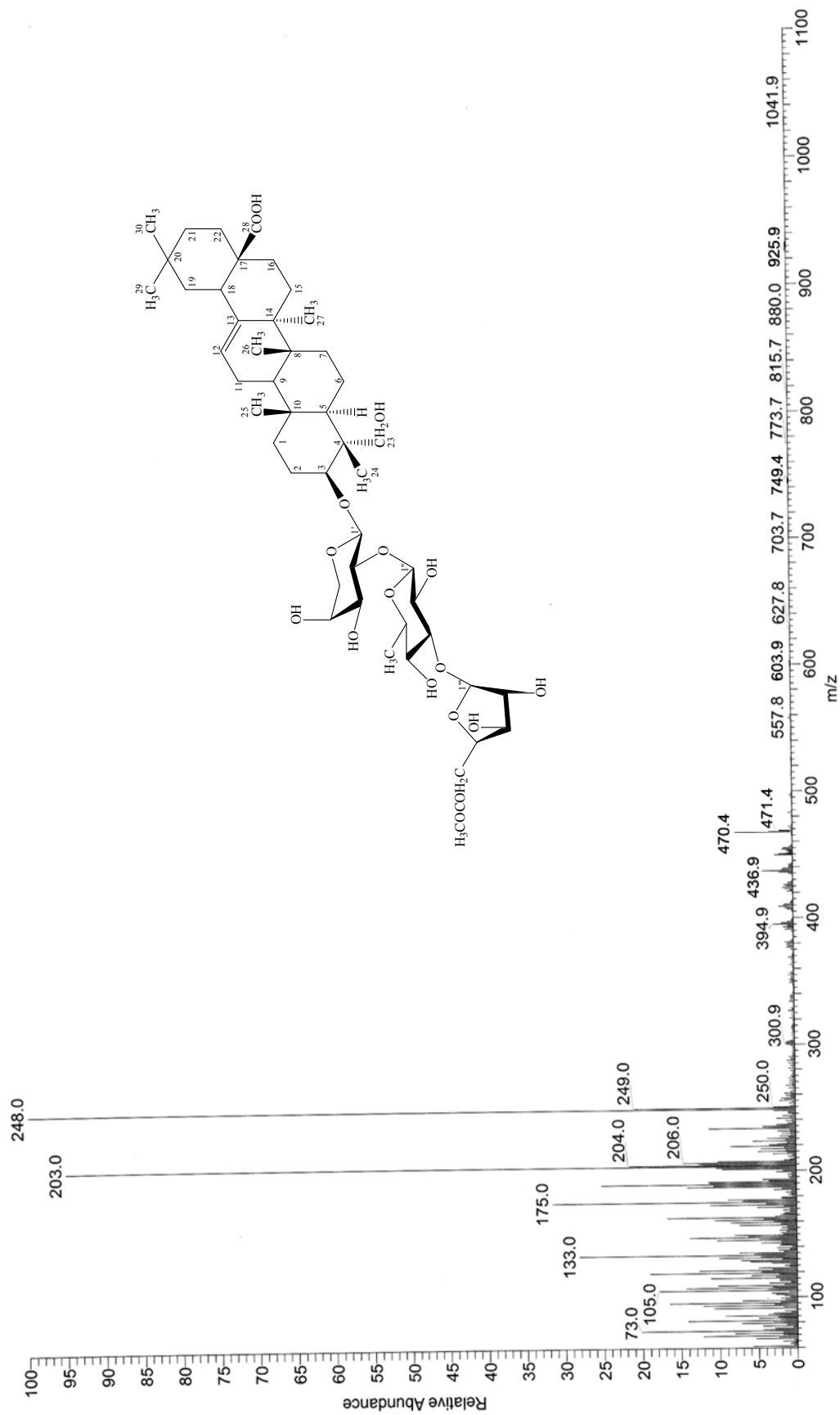
Figure 4-55 IR spectrum of compound **10**

Figure 4-56 EI mass spectrum of compound 10

4.2 Effect of isolated compounds on HIV-1 IN activity

Compounds **1-10** were isolated from the ethanol leaves extract of *Mimusops elengi* (Sapotaceae) and *Pometia pinnata* (Sapindaceae). They were carried out for testing on HIV-1 IN activity. The IC_{50} values are shown in Table 4-12. The result indicated that compound **1** (mixture of gallocatechin and epigallocatechin) shown activity against HIV-1 IN with IC_{50} value of 35.0 µM, followed by compound **3** (proanthocyanidin A2) with IC_{50} value of 30.1 µM; whereas other compounds (**2, 4-10**) were inactive. On the basis of anti-HIV-1 assay-guided purification of the crude ethanol extract of *M. elengi* leaves, compound **1** was isolated as anti-HIV-1 IN compounds, with an IC_{50} value of 35.0 µM. Recently, epigallocatechin gallate, a green tea catechin, has been shown to inhibit a broad spectrum of HIV-1 subtypes without harming human cells. Epigallocatechin gallate has been reported to inhibit HIV-1 replication by targeting several steps in the HIV-1 life cycle, such as interfering with the RT and protease activity, blocking gp120-CD4 interaction by binding to CD4, and inactivating virions (Nance *et al.*, 2009). In addition, four catechins with the galloyl moiety, including catechin gallate, epigallocatechin gallate, gallocatechin gallate, and epicatechin gallate, were found to inhibit HIV-1 IN effectively. These four catechins may reduce the activity of HIV-1 IN by disrupting its interaction with virus DNA (Jiang *et al.*, 2010). In this study, we report that other catechins, gallocatechin and epigallocatechin also possess significant anti-HIV-1 IN activity. This result confirms the potential of catechins with the galloyl moiety to act as novel and effective class of HIV-1 integrase inhibitors. In addition, a flavonol rhamnoside, mearnsitrin (**2**) (Fig. 4-2) were purified from the ethanol extract of *M. elengi* leaves. Mearnsitrin was firstly purified from the leaves of *Acacia mearnsii* (MacKenzie, 1967), and recognised as a rare flavonol glycoside (Nair *et al.*, 1999). This is the first report of mearnsitrin in *M. elengi* leaves. Unfortunately, mearnsitrin did not show any inhibitory activity against HIV-1 IN. However, some biological activities of mearnsitrin have been reported, including it having antioxidant and antithyroperoxidase activities (de Souza dos Santos *et al.*, 2011).

On the basis of anti-HIV-1 assay-guided purification of the crude ethanol extract of *P. pinnata* leaves, proanthocyanidin A2 (Fig. 4-3) was isolated as an anti-HIV-1 IN compounds, with an IC_{50} value of 30.1 μM. This is the first report of proanthocyanidin A2 in *P. pinnata* leaves. Proanthocyanidin A2 is a dimeric procyanidin resulting from the condensation of monomeric flavan-3-ols. At present, there are some reports on antiviral activity of proanthocyanidin A2 (Iwasawa *et al*., 2009; Gallina *et al*., 2011). Proanthocyanidin A2 also showed *in vitro* anti-HIV activity (Brinkworth *et al*., 1992; Shahat *et al*., 1998). Gallina *et al*. (2011) demonstrated one possible antiviral mechanism of proanthocyanidin A2 is reduction of viral RNA synthesis. In this study, we report the antiviral activity of proanthocyanidin A2 against HIV-1 *via* inhibitory effect on HIV-1 IN. In addition, three flavonoids, epicatechin, kaempferol-3-*O*-rhamnoside, quercetin-3-*O*-rhamnoside; a glycolipid, 1-*O*-palmitoyl-3-*O*-[α-D-galactopyranosyl-(1→6)-β-D-galactopyranosyl]-*sn*-glycerol; a steroidal glycoside; stigma-sterol-3-*O*-glucoside; and a pentacyclic triterpenoid saponin, 3-*O*-α-L-arabinofuranosyl-(1→3)-α-L-rhamnopyranosyl-(1→2)]-α-L-arabinopyranosyl hederagenin (Fig. 1) were firstly purified from the crude ethanol extract of *P. pinnata* leaves. There are some hederagenin glycosides, including 28-*O*-β-D-apiosyl(1→2)-β-D-glucopyranosyl hederagenin, 3-*O*-α-L-arabinofuranosyl(1→3)[α-L-rhamnopyranosyl(1→2)]-β-D-xylopyranosyl hederagenin, 3-*O*-β-D-apiosyl(1→3)[α-L-rhamnopyranosyl(1→2)]-β-D-glucopyranosyl hederagenin, 3-*O*-α-L-arabinofuranosyl(1→3) [α-L-rhamnopyranosyl(1→2)]-β-L-arabinopyranosyl hederagenin, 3-*O*-β-D-xylopyranosyl (1→3)[α-L-rhamnopyranosyl(1→2)]-α-L-arabinopyranosyl hedera-genin, 3-*O*-β-D-xylo-pyranosyl-(1→3)[α-L-rhamnopyranosyl(1→2)]-β-D-glucopyranosyl hederagenin, 3-*O*-β-D-galactopyranosyl(1→3)[α-L-rhamnopyranosyl(1→2)]-β-D-glucopyranosyl hederagenin were previously isolated from the stems of *Pometia eximia* (Jayasinghe *et al*., 1995).

Unfortunately, these compounds did not show any inhibitory activity against HIV-1 IN. However, some biological activities of the isolated compounds confirm the traditional use of *P. pinnata* leaves for the treatment of skin infection diseases. For examples; antioxidant and antibacterial activities of kaempferol-3-*O*-rhamnoside and quercetin-3-*O*-rhamnoside against

Bacillus subtilis, *Staphylococcus aureus* and *Escherichia coli* (Babaei *et al*., 2008; Ghaly *et al*., 2010); antifungal activity of 3-*O*-α-L-arabinofuranosyl-(1⟶3)-α-L-rhamnopyranosyl-(1⟶2)]-α-L-arabinopyranosyl hederagenin against *C. albican*s, *Cryptococcus neoformans* and *Aspergillus fumigatus* (Adesegun *et al*., 2008); and antimicrobial of stigmasterol-3-*O*-glucoside (Ahmed *et al*, 2011).

These active pure compounds (epigallocatechin and proanthocyanidin A2) used for standard markers to validated HPLC method.

Table 4-12 HIV-1 IN inhibitory activity of compounds isolated from the leaves of *Mimusops elengi* and *Pometia pinnata*

Compounds	HIV-1 IN inhibitory activity[IC_{50} (µM)]
Mixture of gallocatechin and epigallocatechin	35.0
Mearnsitrin	> 100
Proanthocyanidin A2	30.1
Epicatechin	> 100
Kaempferol-3-*O*-rhamnoside	> 100
Quercetin-3-*O*-rhamnoside	> 100
1-*O*-Acetyl-3-*O*-[α-D-galactopyranosyl-(1⟶6)-β-D-galactopyranosyl]-*sn*-glycerol	> 100
Stigmasterol-3-*O*-glucoside	> 100
3-*O*-α-L-Arabinofuranosyl-(1⟶3)-[α-L-rhamnopyranosyl-(1⟶2)]- α-L-arabinopyranosyl hederagenin	> 100
3-*O*-(5-*O*-acetyl-α-L-arabinofuranosyl)-(1⟶3)-[α-L-rhamnopyranosyl-(1⟶2)]-α-L-arabinopyranosyl hederagenin	> 100
Suramin (positive control)	3.4

4.3 HPLC quantitative analysis

4.3.1 HPLC conditions

The optimal conditions for simultaneous quantitative determination quantitative determination of compound **1** (epigallocatechin) and compound **3** (proanthocyanidin A2) were performed using reverse phase HPLC system on Agilent HPLC 1100 series with Agilent Chemstation for LC 3D software. The HPLC separation was achieved on a C18 Phenominex[®] Luna Hilic column (5 μm, 4.6 x 150 mm) using milli-Q water of mobile phase at a flow rate of 1.0 mL/min. Sample injection volumes were 20 μL, and detection was by UV at wavelength 210 nm with retention time eluted at 3.2 minute for epigallocatechin (Figure 4-57). Whilst, proanthocyanidin A2 using mixture of 2% acetic acid and acetonitrile (gradient elution as follows: 0-4 min, 5:95; 5-9 min, 10:90; 10-14 min, 20:80; 15-20 min, 0:100 v/v) as mobile phase at a flow rate of 1.0 mL/min. Sample injection volumes were 20 μL, and detection was by UV at wavelength 280 nm with retention time eluted at 6.3 minute (Figure 4-58).
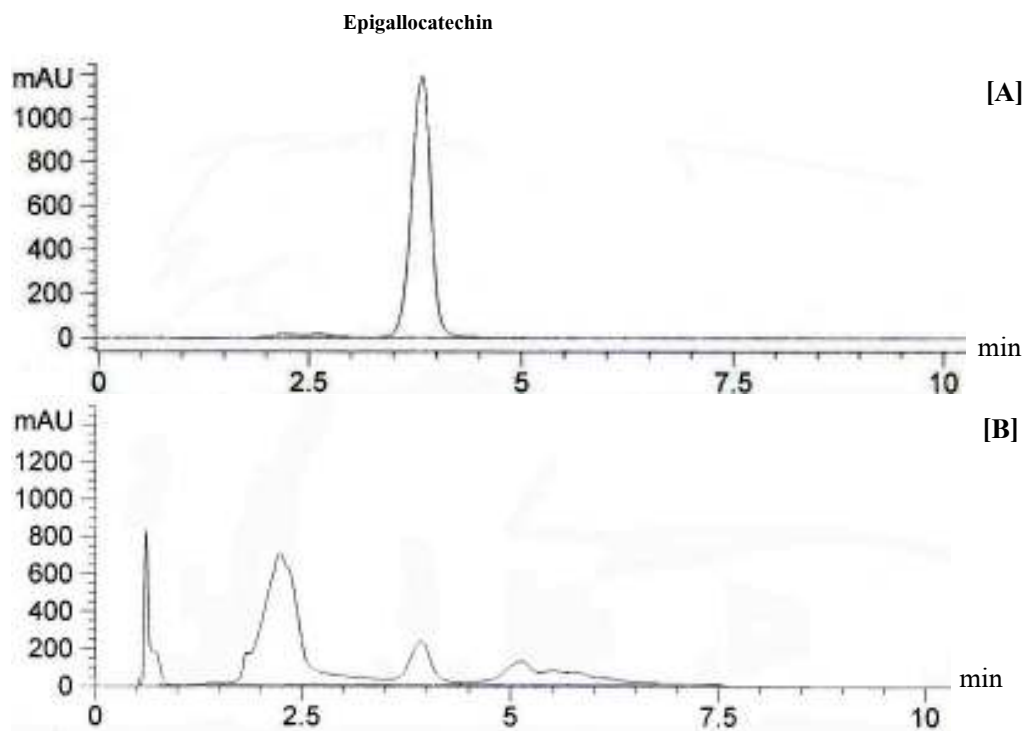
Figure 4-57 HPLC chromatogram of standard epigallocatechin **(A)** and epigallocatechin A2 in *M. elengi* leaf extracts **(B)**
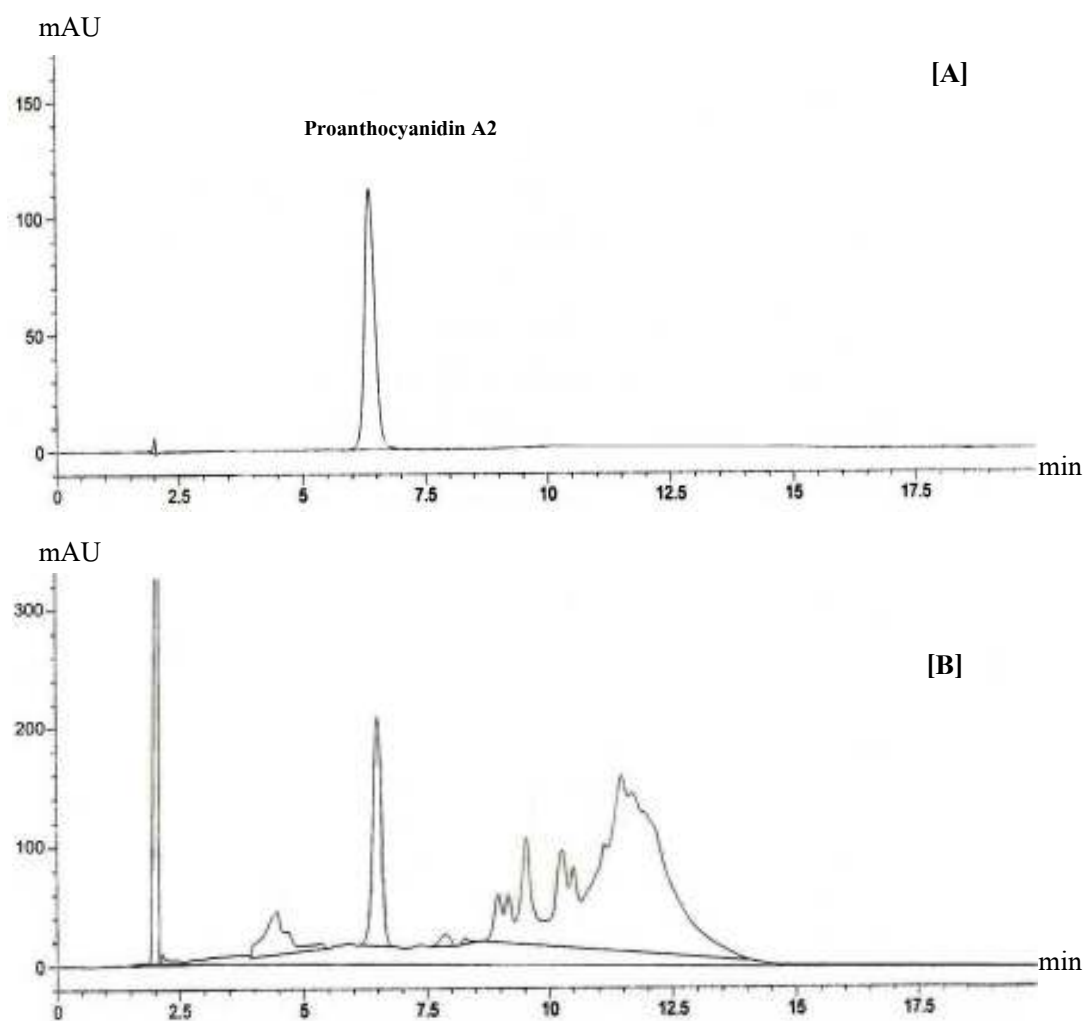
Figure 4-58 HPLC chromatogram of standard proanthocyanidin A2 **(A)** and proanthocyanidin

A2 in *P. pinnata* leaf extracts **(B)**

4.3.2 Method validation

The analytical method for epigallocatechin from *M. elengi* and proanthocyanidin A2 from *P. pinnata* leaf extracts were examined for linearity, accuracy, precision, specificity, LOD and LOQ, respectivly.

4.3.2.1 Limits of detection (LOD) and quantification (LOQ)

The limited of detection represents the lowest concentration that can be detected by the analytical method, whereas the limit of quantification represents the lowest concentration that can be determined with acceptable precision and accuracy. The LOD and LOQ for epigallocatechin

157

and proanthocyanidin A2 were exhibited (Table 4-13), indicated that the established HPLC method is sufficiently sensitive for determination of these compounds.

Table 4-13 LOD and LOQ of epigallocatechin from *M. elengi* and proanthocyanidin A2 from *P. pinnata* leaf extracts

Compounds	LOD[b] (µg/ml)	LOQ[c] (µg/ml)
Epigallocatechin	0.10	0.25
Proanthocyanidin A2	1.25	2.5

[a]Limit of detection (LOD): signal to noise ratio = 3

[b]Limit of quantification (LOQ): signal to noise ratio = 10

4.3.2.2 Calibration curve and linearity

Linearity were evaluated using standard samples over six calibration points (0.78, 1.56, 3.125, 6.25, 12.5, 25 µg/mL of epigallocatechin and 7.8, 15.6, 31.25, 62.5, 125, 250 µg/mL of proanthocyanidin A2). On a given day, the measurement was carried out with each concentration in triplicate, with a lot of nine measurements for each calibration point. Three separate calibration curves were obtained on three different days by plotting the mean peak area against concentration. Excellent linearity were observed for the analysts on the ranges 0.78-25 µg/mL of epigallocatechin and 7.8-250 µg/mL of proanthocyanidin A2, with correlation coefficients 0.9998 and 0.9999 for epigallocatechin and proanthocyanidin A2, respectively (Table 4-14).

Table 4-14 HPLC calibration data of epigallocatechin from *M. elengi* and proanthocyanidin A2 from *P. pinnata* leaf extracts

Compounds	Linear range (µg/ml)	t_R (min)	Equation[a]	Linearity (r^2)
Epigallocatechin	0.78-25	3.4	Y = 181.1549X-21.6110	0.9998
Proanthocyanidin A2	7.8-250	6.3	Y = 13.0551X-8.0995	0.9999

[a]Y = AX + B, where Y is peak area, X is the concentration of the analyzed material.

4.3.2.3 Accuracy

The accuracy of the analytical method were studied by spiking solution of epigallocatechin at concentration of 25, 12.5 and 6.25 µg/mL and proanthocyanidin A2 at concentration of 250, 125 and 62.5 µg/mL leave extracts to evaluated recoveries for this method. The recoveries near to 100% (Table 4-15) indicate a good accuracy of this method.

Table 4-15 Recoveries of of epigallocatechin from *M. elengi* and proanthocyanidin A2 from *P. pinnata* leaf extracts

Compounds	Spiked concentration (µg/ml)	Recovery (%)[a] (n = 3)
	25	103.21±0.27
Epigallocatechin	12.5	102.92±0.19
	6.125	99.09±0.87
	250	96.93±0.24
Proanthocyanidin A2	125	96.73±0.30
	61.25	97.97±0.38

[a]All values were mean ±S.D. obtained by triplicate analyzes.

4.3.2.4 Precision

The precision of the chromatographic method was tested by performing intra-day and inter-day multiple injections of a standard solution containing epigallocatechin and proanthocyanidin A2. The percentage relative standard deviation (%RSD) of the retention times and peak areas were calculated, and the values of intra- and inter-day for epigallocatechin and proanthocyanidin A2 were each less than 1% for both retention times and peak area (Table 33), indicating high precision of the developed HPLC method. The precision of the extraction procedure was similarly evaluated by determining intra- and inter-day %RSD data form repeated extraction of the same batch of leaves. The results (Table 4-16) suggest that the method is capable of quantification of epigallocatechin from *M. elengi* and proanthocyanidin A2 from *P. pinnata* leaf extracts with high precision.

Table 4-16 Intra-day and inter-day precision data of epigallocatechin from *M. elengi* and proanthocyanidin A2 from *P. pinnata* leaf extracts

| Compounds | Inter-day (n =3 per day) | | | | Intra-day (n = 6) | |
| | Content (% w/w of extract) | | | % RSD | Content (% w/w) | % RSD |
	Day 1	Day 2	Day 3			
Epigallocatechin	0.64	0.62	0.63	0.70	0.67	0.31
Proanthocyanidin A2	3.61	3.53	3.50	0.32	3.55	0.20

4.3.2.5 Specificity

The specificity of the method was evaluated using UV absorption spectra at three points of each of three peaks. Comparision of these spectra with those for authentic samples revealed that each peak was homogeneous and not overlapping with any impurity peaks (Figure 4-59 and Figure 4-60).
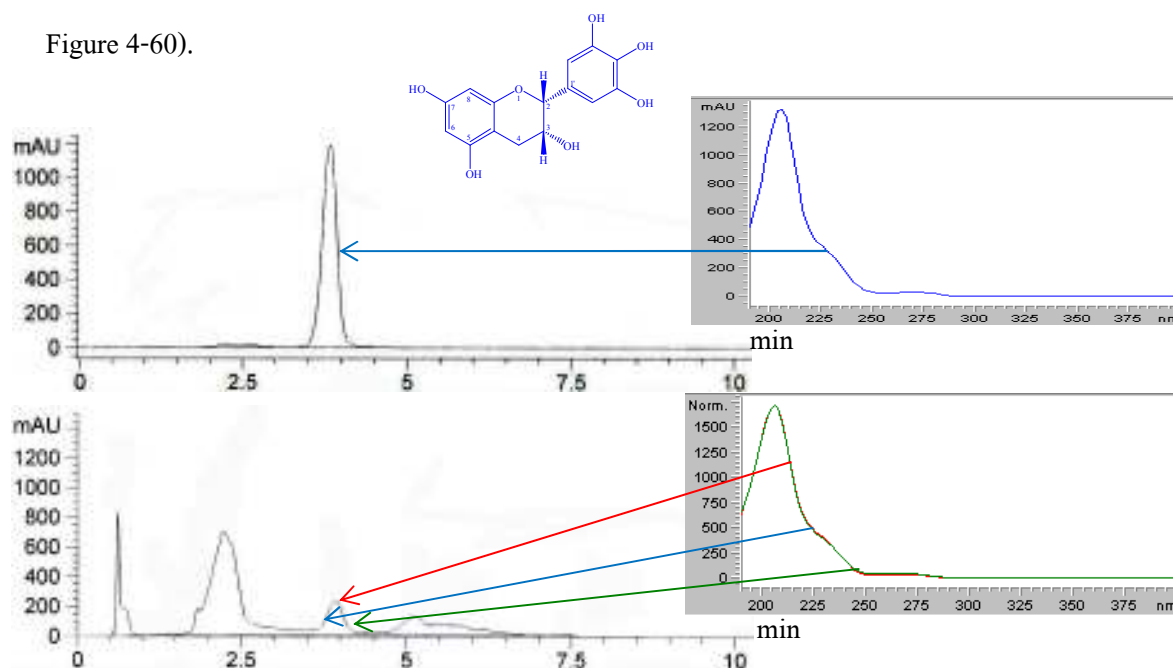
Figure 4-59 UV absorption spectra of epigallocatechin in *M. elengi* leaf extracts
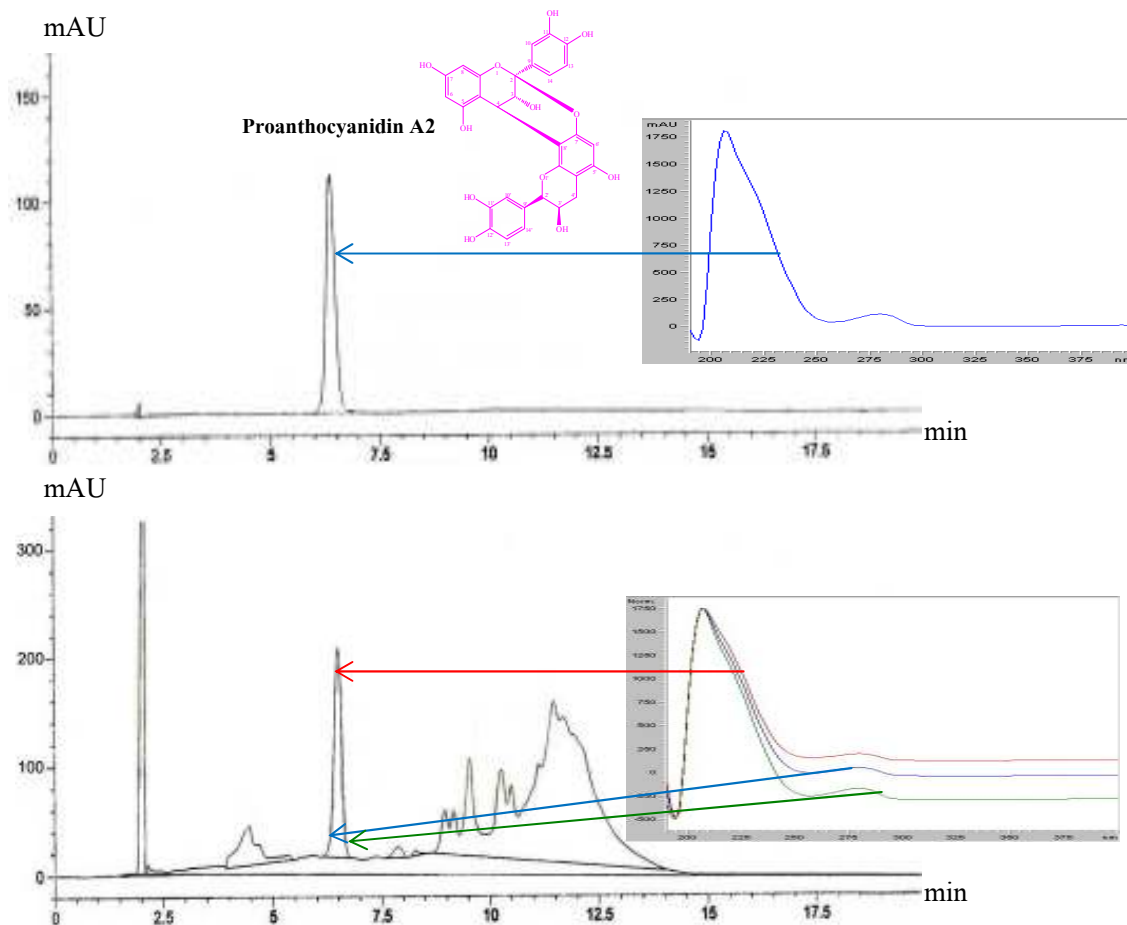
Figure 4-60 UV absorption spectra of proanthocyanidin A2 in *P. pinnata* leaf extracts

4.3.3 Determination of solvent for extraction

Different extraction solvents were used to determine the solvent that produced the maximum amount of epigallocatechin from the *M. elengi* leaves. Among the solvents that used for extraction, methanol gave both the highest extraction yield (19.6% w/w) and epigallocatechin content (0.64% w/w) and proanthocyanidin A2 from the *P. pinnata* leaves. Among the solvents that used for extraction, methanol gave both the highest extraction yield (23.3 % w/w) and proanthocyanidin A2 content (3.38% w/w) (Table 4-17 and 4-18). This indicates that methanol is a suitable solvent for extraction of epigallocatechin from the *M. elengi* and proanthocyanidin A2 from *P. pinnata* leaves.

Table 4-17 Yield and content of epigallocatechin in *M. elengi* leaf extracts

Solvents	Extraction yield (%w/w); Mean±S.D.	Epigallocatechin Contents[a] (%w/w of extract; Mean±S.D.)
Acetone	8.3 ± 0.90*	0.21 ± 0.01*
Ethyl acetate	11.6 ± 0.81*	0.31 ± 0.03*
Ethanol	19.4 ± 0.58	0.51 ± 0.08*
Methanol	19.6 ± 0.64	0.64 ± 0.04

[a]All values were mean ±S.D. obtained by triplicate analyzes.

*Significant difference ($P<0.05$) when compare with the methanol extract

Table 4-18 Yield and content of proanthocyanidin A2 in *P. pinnata* leaf extracts

Solvents	Extraction yield (%w/w); Mean±S.D.	Proanthocyanidin A2 Contents[a] (%w/w of extract; Mean±S.D.)
Hexane	6.2 ± 0.87*	0.13 ± 0.02*
Chloroform	7.2 ± 0.78*	0.11 ± 0.01*
Ethyl acetate	7.0 ± 0.12*	1.36 ± 0.02*
Methanol	23.3 ± 0.23	3.38 ± 0.04

[a]All values were mean ±S.D. obtained by triplicate analyzes.

*Significant difference ($P<0.05$) when compare with the methanol extract

4.3.4 Determination of extraction methods

The efficiency of RE, SAE and MAE methods for epigallocatechin from the *M. elengi* and proanthocyanidin A2 from *P. pinnata* leaves was evaluated. The content of epigallocatechin and proanthocyanidin A2 extracted by RE, SAE and MAE methods were not significantly different (Table 4-19). However, RE and SAE were much more time consuming (20 min) when compared to MAE (1 min). Recently, MAE has been accepted as a potential alternative to conventional techniques for extraction of active compounds from herbal materials. The MAE technique possesses many advantages compared to other extraction techniques, including a high extraction efficiency as well as a saving of the solvent used and the time required. This may be attributed to the fact that microwave energy is delivered efficiently to the target compounds

through molecular interaction with the electromagnetic field, which increases temperature inside the plant cells, resulting in the destruction of cell walls and the releasing of active compounds into the extraction solvent. Thus, MAE was the most suitable method for extraction of epigallocatechin from the *M. elengi* and proanthocyanidin A2 from *P. pinnata* leaves.

Table 4-19 Different extraction methods of epigallocatechin from *M. elengi* and proantho-cyanidin A2 from *P. pinnata* leaf extracts

Methods	Time consumed	Epigallocatechin contents[a]; Mean ± S.D. (% w/w)	Proanthocyanidin A2 contents[a]; Mean ± S.D. (% w/w)
Reflux	20 min	0.59 ± 0.03	3.42 ± 0.08
Sonication	20 min	0.53 ± 0.02	3.43 ± 0.06
Microwave assisted extraction	1 min	0.56 ± 0.02	3.41 ± 0.06

[a]All values were mean ±S.D. obtained by triplicate analyzes.

4.4 Optimization of MAE conditions

4.4.1 Effect of different irradiation period on the yield of plants

The variable factors for the MAE operating parameters included the time for microwave irradiation and the numbers of irradiation cycles (one cycle is 60 sec power on and 15 sec power off of epigallocatechin from the *M. elengi* and one cycle is 30 sec power on and 15 sec power off of proanthocyanidin A2 from *P. pinnata*) and cycles extracted were determined by single-factor experiments.

The effect of the irradiation period was first evaluated. Increasing the time of irradiation up to 60 sec resulted in an increase in the epigallocatechin content in the leaf extracts. However, increasing the irradiation period up to 120 sec caused no further increase. Therefore, the irradiation period was optimized at 60 sec. While, increasing the time of irradiation up to 30 sec resulted in an increase in the proanthocyanidin A2 content in the leaf extracts. However, increasing the irradiation period up to 60 sec caused no further increase. Therefore, the irradiation period was optimized at 30 sec (Table 4-20). These irradiation peroids were used for further study on the effect of irradiation cycles on extraction of the active compouds.

Table 4-20 Different irradiation periods of epigallocatechin from *M. elengi* and proantho-cyanidin A2 from *P. pinnata* leaf extracts

Irradiation periods (sec)	Epigallocatechin contents[a]; Mean ± S.D. (% w/w)	Proanthocyanidin A2 contents[a]; Mean ± S.D. (% w/w)
15	0.44 ± 0.008*	3.11 ± 0.07*
30	0.45 ± 0.010*	3.55 ± 0.10
60	0.53 ± 0.006	3.62 ± 0.08
120	0.52 ± 0.013	3.48 ± 0.07

[a]All values were mean ±S.D. obtained by triplicate analyzes.

* Significant difference ($P<0.05$) when compare with the methanol extract

4.4.2 Effect of irradiation cycles on the yield of plants

It is necessary to optimize a proper irradiation cycle to complete the extraction process. Different irradiation cycles (one cycle is 60 sec power on and 15 sec power off of epigallocatechin from the *M. elengi* and one cycle is 30 sec power on and 15 sec power off of proanthocyanidin A2 from *P. pinnata*) from 1 to 5 cycles were examined for the extraction of epigallocatechin and proanthocyanidin A2. The result revealed that increasing the irradiation cycles up to 3 cycles resulted in an increase in the epigallocatechin contents in the leaf extracts. While, increasing the irradiation cycles up to 4 cycles resulted in an increase in the proanthocyanidin A2 contents in the leaf extracts. Therefore, 3 cycles of epigallocatechin contents and 4 cycles of proanthocyanidin A2 contents of irradiation were used for further study on the effect of extraction cycles of *M. elengi* and *P. pinnata* leaf powder (Table 4-21).

Table 4-21 Different irradiation cycles of epigallocatechin from *M. elengi* and proanthocyanidin A2 from *P. pinnata* leaf extracts

Irradiation cycle (s)	Epigallocatechin contents[a]; Mean ± S.D. (% w/w)	Proanthocyanidin A2 contents[a]; Mean ± S.D. (% w/w)
1	0.46 ± 0.02*	2.43 ± 0.30*
2	0.49 ± 0.04*	3.04 ± 0.05*
3	0.58 ± 0.01	3.06 ± 0.04*
4	0.52 ± 0.02*	3.59 ± 0.09
5	0.49 ± 0.01*	3.22 ± 0.21

[a]All values were mean ±S.D. obtained by triplicate analyzes.

* Significant difference ($P<0.05$) when compare with the methanol extract

4.4.3 Effect of extraction times on the yield of plants

The effect of successive extractions of the residue such as extraction cycles was determined. The extraction residue was re-extracted using fresh solvent each time. After the first extraction, the yields of the extracts as well as epigallocatechin and proanthocyanidin A2 resulted in very low. In addition, the yield of epigallocatechin was 75% and proanthocyanidin A2 was 70% by the first extraction (Table 4-22). Thus, one extraction cycle was selected as the most suitable extraction cycles for epigallocatechin from *M. elengi* and proanthocyanidin A2 from *P. pinnata* leaves by MAE. These studies suggest that the optimal conditions of MAE of epigallocatechin from *M. elengi* leaf are: using methanol as the solvent, using an irradiation power of 90 W for 1 min, using three irradiation cycles and one extraction cycle. Whereas, the optimal conditions of MAE of proanthocyanidin A2 from *P. pinnata* leaf are: using methanol as the solvent, using an irradiation power of 90 W for 30 sec, using three irradiation cycles and one extraction cycle, respectively. These MAE conditions were used for further study on the effect of suitable ratio of plant powder to volume of the extracted solvent.

Table 4-22 Different extraction times of epigallocatechin from *M. elengi* and proanthocyanidin A2 from *P. pinnata* leaf extracts

Extraction times	Extraction yield (%w/w); Mean ± S.D.	Epigallocatechin contents[a]; Mean ± S.D. (%w/w)	Extraction yield (%w/w); Mean ± S.D.	Proanthocyanidin A2 contents[a]; Mean ± S.D. (%w/w)
1	12.43 ± 0.72	0.54 ± 0.02	12.36 ± 1.63	3.65 ± 0.18
2	1.67 ± 0.12*	0.12 ± 0.02*	4.00 ± 1.30*	1.10 ± 0.12*
3	0.67 ± 0.46*	0.064 ± 0.01*	2.13 ± 0.15*	0.49 ± 0.14*

[a]All values were mean ±S.D. obtained by triplicate analyzes.

* Significant difference ($P<0.05$) when compare with the methanol extract

4.5 Determination of suitable ratio of plants powder to solvent

The results revealed that increasing ratio of *M. elengi* and *P. pinnata* powders to the volume methanol resulted in an increase in the extraction yields with epigallocatechin and proanthocyanidin A2 contents. Increasing the ratios up to 1 g per 20 mL methanol resulted in the highest yields of both extract with epigallocatechin and proanthocyanidin A2 (Table 4-23, Figure 61-62). In addition, the content of epigallocatechin and proanthocyanidin A2 seems to become constant if further increase the ratio. The ratio of 1 g dry powder per 20 mL methanol is therefore the most suitable for extraction of epigallocatechin from *M. elengi* and proanthocyanidin A2 from *P. pinnata* leaves powder.

These results were consistent with mass transfer principles where the driving force for mass transfer is considered to be the concentration gradient between the plants powder and the solvent. A high plants powder to solvent ratio could promote an increasing concentration gradient, resulting in an increase of diffusion rate that allows greater extraction of plants powder by solvent. In addition, the chance of active components coming into contact with extracting solvent expanded with increase amount of extraction solvent, leading to higher leaching-out rates. However, active component yields will not continue to increase once equilibrium is reached stated that plants powder to solvent ratio could significantly affect the equilibrium constant and

characterized the relationship between yield and solvent use as a steep exponential increase followed by a steady state to give the maximum yield.

Table 4-23   Amount of dried leaf powders of epigallocatechin from *M. elengi* and proanthocyanidin A2 from *P. pinnata* leaf extracts

Amount of dry powder	Extraction yield (%w/w); Mean ± S.D.	Epigallocatechin contents[a] Mean ± S.D. (%w/w)	Extraction yield (%w/w); Mean ± S.D.	Proanthocyanidin A2 contents[a] Mean ± S.D. (%w/w)
100	11.60 ± 0.17	0.55 ± 0.02	13.03 ± 0.49	3.49 ± 0.04
300	32.17 ± 0.58*	1.58 ± 0.06*	35.97 ± 0.81*	10.61 ± 0.91*
500	60.13 ± 1.10*	2.55 ± 0.23*	53.47 ± 1.10*	18.76 ± 0.64*
700	71.23 ± 2.04*	4.21 ± 0.86*	65.93 ± 2.88*	29.75 ± 1.10*
1,000	106.63 ± 4.40*	5.15 ± 0.50*	99.23 ± 4.50*	36.58 ± 1.28*

[a]All values were mean ±S.D. obtained by triplicate analyzes.

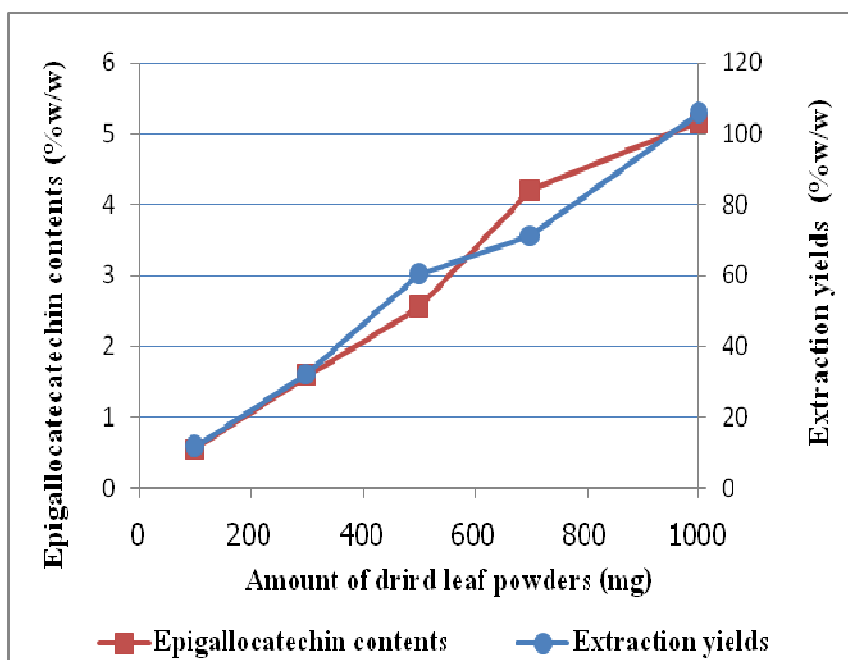* Significant difference ($P<0.05$) when compare with the methanol extract

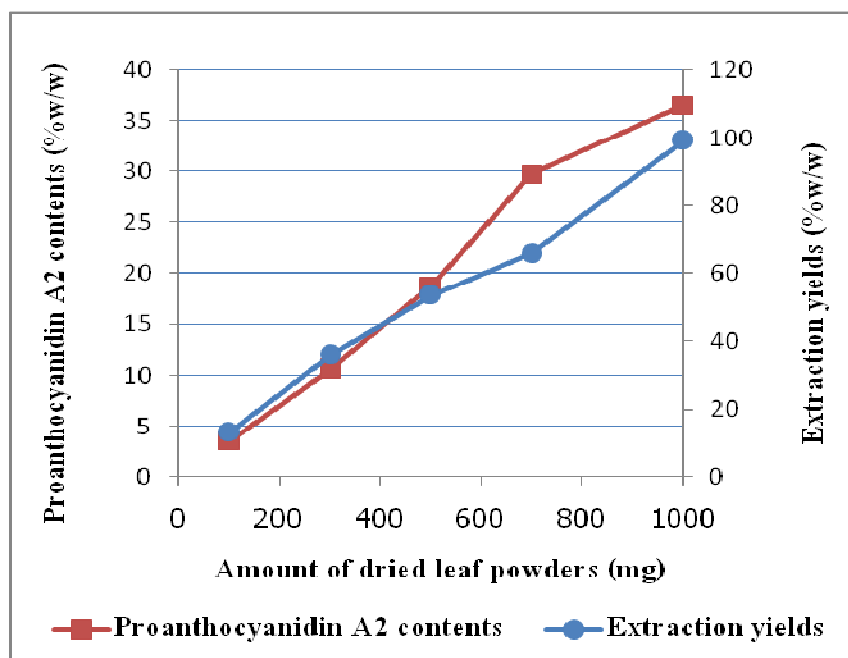**Figure 4-61**   Amount of dried leaf powders of epigallocatechin from *M. elengi* leaf extracts

Figure 4-62   Amount of dried leaf powders of proanthocyanidin A2 from *P. pinnata* leaf extracts

CHAPTER 5

CONCLUSION

1. An anti‑HIV‑1 IN assay‑guided isolation of the active compounds from *M. elengi* leaf extract resulted in the isolation of active compounds, identified as a mixture of gallocatechin and epigallocatechin. This mixture of gallocatechin and epigallocatechin showed satisfactory anti‑HIV‑1 IN activity with an IC_{50} value of 35.0 μM.

2. A flavanol glycoside, mearnsitrin was also isolated from *M. elengi* leaf extract. But it was not active against HIV‑1 IN, at a concentration of 100 μM.

3. An anti‑HIV‑1 IN assay‑guided isolation of the active compounds from a leaf extract of *P. pinnata* resulted in the isolation of an active compound, identified as proanthocyanidin A2. This compound showed satisfactory anti‑HIV‑1 IN activity with an IC_{50} value of 30.1 μM.

4. Three flavonoids, epicatechin, kaempferol‑3‑*O*‑rhamnoside, quercetin‑3‑*O*‑rhamnoside; a glycolipid, 1‑*O*‑palmitoyl‑3‑*O*‑[α‑D‑galactopyranosyl‑(1→6)‑β‑D‑galactopyranosyl]‑*sn*‑glycerol; a steroidal glycoside; stigmasterol‑3‑*O*‑glucoside; and two pentacyclic triterpenoid saponin, 3‑*O*‑α‑L‑arabinofuranosyl‑(1→3)‑α‑L‑rhamnopyranosyl‑(1→2)]‑α‑L‑arabinopyranosyl hederagenin, 3‑*O*‑(5‑*O*‑acetyl‑α‑L‑arabinofuranosyl‑(1→3)‑α‑L‑rhamnopyranosyl(1→2)]‑α‑L‑arabinopyranosyl hederagenin were also isolated from *P. pinnata* leaf extract. But they were not active against HIV‑1 IN, at a concentration of 100 μM.

5. A simple, specific, precise, accurate, rapid and reproducible HPLC method has been developed and validated for quantitative determination of epigallocatechin in *M. elengi* leaf extracts. The method utilized a Phenominex® Luna 5u Hilic column with 100% milli‑Q water as the mobile phase at a flow rate of 1.0 mL/min, and UV detection at 210 nm.

6. A specific, precise, accurate, rapid and reproducible HPLC method has been established and validated for quantitative determination of proanthocyanidin A2 in *P. pinnata* leaf extracts. The method utilized a Phenominex® Luna 5u Hilic column with the mixture of 2% acetic acid and acetonitrile (gradient elution as follows: 0‑4 min, 5:95; 5‑9 min, 10:90; 10‑14 min, 20:80; 15‑20 min, 0:100 v/v) as mobile phase at a flow rate of 1 mL/min and UV detection at 280 nm.

7.   These HPLC methods are considered to be suitable for routine quantitative determinations on either the dried *M. elengi* and *P. pinnata* leaves or their extracts, in a quality controlled protocols.

8. Microwave-assisted extraction (MAE) was selected as the best examination method for epigallocatechin. The optimal conditions of MAE are: using methanol as the solvent, using an irradiation power of 90 W for 1 min, using three irradiation cycles and one extraction cycle. This optimized MAE method was capable of increasing epigallocatechin in the dried leaf extract up to 5.15 %w/w.

9. MAE was also selected as the best examination method for proanthocyanidin A2. The optimal conditions of MAE are: using methanol as the solvent, using an irradiation power of 90 W for 1 min, using four irradiation cycles and one extraction cycle. This optimized MAE method was capable of increasing proanthocyanidin A2 in the dried leaf extract up to 36.58 %w/w.

REFERENCES

Thai

เย็นจิตร เตชะดำรงสิน และคณะ . รายงานการศึกษาวิจัยโครงการสมุนไพรต้านเอดส์: Project Herbs for AIDS (1) ฤทธิ์ของสมุนไพรไทยในการยับยั้งเชื้อเอชไอวีและเชื้อจุลินทรีย์ที่ก่อโรคติด เชื้อฉวยโอกาสและฤทธิ์เสริมภูมิคุ้มกัน.   โรงพิมพ์องค์การสงเคราะห์ผ่านศึก,   นนทบุรี. 2546, หน้า 1-170.

ศูนย์ข้อมูลทางระบาดวิทยา สำนักระบาดวิทยา กองควบคุมโรค . สถานการณ์ผู้ป่วยเอดส์ ณ วันที่ 24 มีนาคม พ.ศ. 2554. กระทรวงสาธารณสุข, นนทบุรี. 2554

English

Abd-Elazem, I.S., Chen, H.S., Bates, R.B., Huang, R.C., 2002. Isolation of two highly potent and non-toxic inhibitors of human immunodeficiency virus type 1 (HIV-1) integrase from *Salvia miltiorrhiza*. Antiviral Res. 55, 91–106.

Adesegun, S.A., Coker, H.A.B., Hamann, M.T., 2008. Antifungal triterpenoid saponin from *Lecaniodiscus cupanioides*. Res. J. Phytochem. 2, 93–99.

Ahmed, E., Sharif, A., Hussain, S., Malik, A., Hassan, M.U., Munawar, M.A., Nagra, S.A., Anwar, J., Ashraf, M., Afza, N., Athar, M., 2011. Phytochemical and antimicrobial studies of *Grewia tenax*. J. Chem. Soc. Pakistan 33, 676–681.

Akhtar, N., Ali, M., Alam, M.S., 2009. Pentacyclic triterpenes from the stem bark of *Mimusops elengi* L. Acta Pol. Pharm. 66, 549–552.

Ali, M.A., Mozid, M.A., Yeasmin, M.S., Khan, A.M., Sayeed, M.A., 2008. An evaluation of antimicrobial activities of *Mimusops elengi* Linn. Res. J. Agr. Biol. Sci. 4, 871–874.

Artan, M., Li. Y., Karadeniz, F., Lee, S.H., Kim, M.M., Kim, S.K., 2008. Anti‑HIV‑1 activity of phloroglucinol derivative, 6,60‑bieckol, from *Ecklonia cava*. Bioorg. Med. Chem. 16, 7921–7926.

Au, T.K., Lam, T.L., Ng, T.B., Fong, W.P., Wan, D.C.C., 2001. A comparision of HIV‑1 integrase inhibition by aqueous and methanol extracts of Chinese medicinal herbs. Life Sci. 68, 1687–1694.

Babaei, H., Sadeghpour, O., Nahar, L., Delazar, A., Nazemiyeh, H., Mansouri, M.R., Poursaeid, N., Asnaashari, S., Moghadam, S.B., Sarker, S.D., 2008. Antioxidant and vasorelaxant activities of flavonoids from *Amygdalus lycioides* var. *horrid*. Turkish J. Biol. 32, 203–208.

Baliga, M.S., Pai, R.J., Bhat, H.P., Palatty, P.L., Boloor, R., 2011. Chemistry and medicinal properties of the Bakul (*Mimusops elengi* Linn): A review. Food Res. Int. 44, 1823–1829.

Bedoya, L.M., Sanchez‑Palomino, S., Abad, M.J., Bermejo, P., Alcami, J., 2001. Anti‑HIV activity of medicinal plant extracts. J. Ethnopharmacol. 77, 113‑116.

Brinkworth, R.I., Stoermer, M.J., Fairlie D.P., 1992. Flavones are inhibitors of HIV‑1 proteinase. Biochem. Biophys. Res. Commun. 188, 631–637.

Briz, V., Poveda, E., Soriano, V., 2006. HIV entry inhibitors: mechanisms of action and resistance pathways. J. Antimicrob. Chemother. 57, 619–627.

Bunluepuech, K., 2010. Study on anti‑HIV‑1integrase activity of Thai medicinal plants. Master thesis of Science in Herb Sciences (International Program). Prince of Songkla University. pp.2–25.

Bunluepuech, K and Tewtrakul, S., 2011. Anti-HIV-1integrase activity of Thai medicinal plants in longevity preparations. Songklanakarin J. Sci. Technol. 33, 693–697.

Burdi, D.R., Hasan, M., Uddin, V., 1991. Sterols and a glycoside from the flowers of *Inula grantioides*. Pak. J. Pharm. Sci. 4, 131–136.

Chang, Y.C. Ching, T.T., Syn, W., 1996. Assaying the activity of HIV-1 integrase with DNA-coated plated. J. Virol. Methods 59, 135–140.

Chung, S.K., Kim, Y.C., Takaya, Y., Kenji , T., Niwa, M., 2004. Novel flavonol glycoside, 7-*O*-Methyl Mearnsitrin, from *Sageretia theezans* and its antioxidant effect. J. Agric. Food Chem. 52, 4664–4668.

Craigie, R., 2001. HIV integrase, a brief overview from chemistry to therapeutics. J. Biol. Chem. 276, 23213–23216.

de Souza dos Santos, M.C., Gonçalves, C.F.L., Vaisman, M., Ferreira, A.C.F., de Carvalho, D.P., 2011. Impact of flavonoids on thyroid function. Food Chem. Toxicol. 49, 2495–2502.

Eskander, J., Lavaud, C., Pouny, I., Soliman, H.S.M., Abdel-Khalik, S.M., Mahmoud, I.I., 2006. Saponins from the seeds of *Mimusops laurifolia*. Phytochemical 67, 1793–1799.

Falodun, A., Ali, S., Quadir, I.M., Choudhary, I.M.I., 2008. Phytochemical and biological investigation of chloroform and ethylacetate fractions of *Euphorbia heterophylla* leaf (Euphorbiaceae) J. Med. Plants Res. 2, 365–369.

Friedman, M., Levin, C.E., Choi, S.H., Kozukue, E., Kozukue, N., 2006. HPLC analysis of catechins, theaflavins, and alkaloids in commercial teas and green tea dietary supplements: comparison of water and 80% ethanol/water extracts. Food Chem. Toxicol. 71, c328–c337.

Gallina, L., Pozzoa, F. D., Galligionia, V., Bombardellib, E., Scagliarini, A., 2011. Inhibition of viral RNA synthesis in canine distemper virus infection by proanthocyanidin A2. Antiviral Res. 92: 447–452.

Gami, B., Pathak, S., Parabia, M., 2012. Ethnobotanical, phytochemical and pharmacological review of *Mimusops elengi* Linn. Asian Pac. J. Trop. Biomed. 743–748.

Ghaly, N.S., Melek, F.R., Abdelwahed, N.A.M., 2010. Flavonoids from *Albizia chinensis* of Egypt. Rev. Latinoam. Quím. 38, 153–158.

Goldgur, Y., Craigie, R., Cohen, G.H., Fujiwara, T., Yoshinaga, T., Fujishita, T., Sugimoto, H., Endo, T., Murai, H. and Daveis, R.D., 1999. Structure of the HIV-1 integrase catalytic domain complexed with an inhibitor: A platform for antiviral drug design. Proc. Natl. Acad. Sci. USA. 96, 13040–13043.

Hanamura, T., Hagiwara, T., Kawagishi, H., 2005. Structure and functional characterization of polyphenols isolated from Acerola (*Malpighia emarginata* DC.) fruit. Biosci. Biotechnol. Biochem. 69, 280–286.

Hazra, K.M., Roy1, R.N., Sen, S.K., Laskar, S., 2007. Isolation of antibacterial pentahydroxy flavones from the seeds of *Mimusops elengi* Linn. Afr. J. Biotechnol. 6, 1446–1449.

Hazuda, D.J., Hastings, J.C., Wolfe, A.C., Emini, E.A., 1994. A novel assay for the DNA stand-transfer reaction of HIV-1 integrase. Nucleic Acid Res. 2, 1121–1122.

Hsieh, M.C., Shen, Y.J., Kuo, Y.H. and Hwang, L.S., 2008. Antioxidative activity and active components of Longan (*Dimocarpus longan* Lour.) flower extracts. J. Agric. Food Chem. 56, 7010–7016.

Hupfeld, J. and Efferth, T., 2009. Drug resistance of human immunodeficiency virus and overcoming it by natural products. In Vivo 23, 1–6.

Ibrahim, S.A., Hong, S.C., Robert, B.B., Ru, C.C., 2002. Isolation of two highly potent and non-toxic inhibitors of human immunodeficiency virus type 1 (HIV-1) integrase from *Salvia miltiorrhiza*. Antiviral Res. 55, 91–106.

ICH (2005). Guideline Q2(R1)-Validation of analytical Procedures: Text and methodology. Geneva: ICH. p. 1–13.

Iwasawa, A., Niwano, Y., Mokudai, T., Kohno, M., 2009. Antiviral activity of proanthocyanidin against feline calicivirus used as a surrogate for noroviruses, and Coxsackievirus used as a representative enteric virus. Biocontrol Sci. 14, 107–111.

Jahan, N., Ahmed, W., Malik, A., 1995. A lupine-type triterpene from *Mimusops elengi*. Phytochemistry 39, 255–257.

Jayasinghe, L., Shimada, H., Hara, N., Fujimoto, Y., 1995. Hederagenin glycosides from *Pometia eximia*. Phytochemistry 40, 891–897.

Jenkins, T.M., Esposito, D., Engelman, A., Craigie, R., 1997. Critical contacts between HIV-1 integrase and viral DNA identified by structure-based analysis and photo-crosslinking. EMBO J. 16, 6849–6859.

Jiang, F., Chen, W., Yi, K., Wu, Z., Si, Y., Han, W., Zhao, Y., 2010. The evaluation of catechins that contain a galloyl moiety as potential HIV-1 integrase inhibitors. Clin. Immunol. 137, 347–356.

Kanchanapoom, T., Kasai, R., Yamasaki, Kazuo., 2001. Acetylated triterpene saponins from the Thai medicinal plant, *Sapindus emarginatus.* Chem. Pharm. Bull. 49, 1195–1197.

Katz, R.A. and Skalka, A.M., 1994. The retroviral enzymes. Annu. Rev. Biochem. 63, 133–173.

Kawamura, F., Shaharuddin, N.A., Sulaiman, O., Hashim, R., Ohara, S. 2010. Evaluation on antioxidant activity, antifungal activity and total phenols of 11 selected commercial malaysian timber species. Jpn. Agric. Res. Q. 44, 319–324.

Kejik, R., 2008. Study on antioxidant and HIV‑1 integrase inhibitory effect of *Smilax corbularia* Kunth. Master thesis of Pharmacy in Pharmaceutical Sciences. Prince of Songkla University. pp.7–12.

Kim, H.J., Lee, H.K., Shin, C.G., Huh, H., 1999. HIV integrase inhibitory activity of *Agastache rugosa*. Pharm. Res. 22, 420–523.

Kim, H.J., Woo, E.R., Shin, C.G., Park, H., 1998. A new flavonol glycoside gallate ester from *Acer okamotoanum* and its inhibitory activity against human immunodeficiency virus‑1 (HIV‑1) integrase. J. Nat. Prod. 61, 145–148.

Kim, J.S., Shim, S. H., Lee, S., Chae, S., Han, S.J., Kang, S.S., Lee, Y.S., Jung, S.H., Shin, K.H., 2004. A monoacyldigalactosyl glycerol from the green alga *Enteromorpha prolifera*. Nat. Prod. Sci. 10, 341–343.

Koerner, J.L., Hsu, V.L., Lee, J., Kennedya, J.A., 2009. Determination of proanthocyanidin A2 content in phenolic polymer isolates by reversed‑phase high-performance liquid chromatography. J. Chromatogr. A. 1216, 1403–1409.

Lavaud, C., Massiot, G., Becchi, M., Misra, G., Nigam, S.K., 1996. Saponins from three species of *Mimusops*. Phytochemistry 41, 887–893.

Lee-Huang, S., Huang, P.L., Huang, P.L., Bourinbaiar, A.S., Chen, H.C., Kung, H.F., 1995. Inhibition of the integrase of human immunodeficiency virus (HIV) type 1 by anti-HIV plant proteins MAP 30 and GAP 31. Biochemistry 92, 8818–8822.

Lee-Huang, S., Huang, P.L., Nara, P.L., Chen, H.C., Kung, H.F., Huang, P., Huang, H.I., Huang, P. L., 1990. MAP 30: a new inhibitor of HIV-l infection and replication. FEBS. Lett. 272, 12–18.

Lee, J.S., Kim, H.J., Lee, Y.S., 2003. A new anti-HIV flavonoid glucuronide from *Chysanthemum morifolium*. Planta Med. 69, 859–861.

Liang, N.N., He, F., Pan, Q.H., Wang, J., Reeves, M,J., Duan, C.Q., 2012. Optimization of sample preparation and phloroglucinol analysis of marselan grape skin proanthocyanidins using HPLC-DADESI-MS/MS. S. Afr. J. Enol. Vitic. 33, 122–131.

MacKenzie, A.M., 1967. Mearnsitrin: A new flavonol glycoside from the leaves of *Acacia mearnsii*. Tetrahedron Lett. 8, 2519–2520.

Matsuda, H., Morikawa, T., Toguchida, I., Yoshikawa, M., 2002. Structural requirements of flavonoids and related compounds for aldose reductase inhibitory activity. Chem. Pharm. Bull. 50, 788–795.

Mbisa, J. L., Martin, S. A., Cane, P. A., 2011. Patterns of resistance development with integrase inhibitors in HIV. Infect. Drug Resist. 4, 65–76.

McColl, D.J. and Chen, X., 2010. Strand transfer inhibitors of HIV-1 integrase: Bringing IN a new era of antiretroviral therapy. Antiviral Res. 85, 101–118.

Misra, G., Mitra, C.R., 1966. *Mimusops hexandra*-II. : constituents of bark and seed. Phytochemistry 5, 535–538.

Misra, G., Mitra, C.R., 1968. *Mimusops hexandra*-III. : constituents of root, leaves and mesocarp. Phytochemistry 7, 2173–2176.

Misra, G., Mitra, C.R., 1969. *Mimusops manilkara*, constituents of fruit and seed. Phytochemistry 8, 249–252.

Mohammad, F.V., Ahmad, V.U., Noorwala, M., Lajis, N.H., 2010. A new triterpenoid saponin from the stem bark of *Pometia pinnata*. Nat. Prod. Commun. 5, 191–195.

Nair, A.G.R., Krishnan, S., Ravikrishna, C., Madhusudanan K.P., 1999. New and rare flavonol glycosides from leaves of *Syzygium samarangense*. Fitoterapia 70, 148–151.

Nance, C.L., Siwak, E.B., Shearer, W.T., 2009. Preclinical development of the green tea catechin, epigallocatechin gallate, as an HIV‑1 therapy. J. Allergy Clin. Immunol. 123, 459–465.

Ng, T.B., Huang, B., Fong, W.P., Yeung, H.W., 1997. Anti‑human immunodeficiency virus (Anti‑HIV) natural products with special emphasis on HIV reverse transcriptase inhibitors. Life Sci. 61, 933–949.

Nittayananta, W., 2001 Oral manifestations of HIV infection : Current update with Asian focus. O.S. Printing house, Bangkok. pp. 23.

Ovenden, S.P.B., Yu.J., Wan, S.S., Sberna, G., Tait, R.M., Rhodes, D., Cox, S., Coates, J., Walsh, N.G. Meurer‑Grimes., B.M., 2004. Globoidnan A: a lignan from *Eucalyptus globoidea* inhibits HIV integrase. Phytochemistry 65, 3255–3259.

Pommier, Y., Johnson, A.A., Merchand, C., 2005. Integrase inhibitors to treat HV/AIDS : Examples of biochemical assays for integrase inhibitor screening. Nat. Rev. Drug Discov. 4, 236–248.

Proestos, C. and Komaitis, M., 2008. Application of microwave‑assisted extraction to the fast extraction of plant phenolic compounds. Food Sci. Technol. 41, 652–659.

Qi, S.H., Wu, D.G., Ma, Y.B., Luo, X.D., 2003. A novel flavones from *Carapa guianensis*. Acta Bot.Sin. 45, 1129–1133.

Rangaka, M.X., Wilkinson, K.A., Seldon, R., Van, C.G., Meintijes, G.A. Morrani, C., 2007. Effect of HIV‑1 infection on T‑cell based and skin test detection of tuberculosis infection. Am. J. Respir. Crit. Care Med. 175, 514–520.

Rauha, J.P. The search for biological activity in Finnish plant extracts containing phenolic compounds. Academic Dissertationon. Sipi Siintola Auditorium of Biocentre Viikki, Faculty of Science of the University of Helsinki. August 10th, 2001.

Rösch, D., Krumbein, A., Kroh, L.W., 2004. Antioxidant gallocatechins, dimeric and trimeric proantho‑ cyanidins from sea buckthorn (*Hippophaë rhamnoides*) pomace. Eur. Food Res. Technol. 219:605–613.

Saha, M.R., Hasan, S.M.R., Akter, R., Hossain, M.M., Alam, M.S., Alam, M.A., Mazumder, M.E.H., 2008. In vitro free radical scavenging activity of methanol extract of the leaves of *Mimusops elengi* Linn. BJVM. 6, 197–202.

Sahu, N.P., 1996. Triterpenoid saponins of *Mimosops elengi*. Phytochemistry 41, 883–886.

Sanches, A.C.C., Lopes, G.C., Nakamura, C.V., Filho, B.P.D., Mello, J.C.P., 2005. Antioxidant and antifungal activities of extracts and condensed tannins from Stryphnodendron obovatum Benth. RBCF. Braz. J. Pharm. Sci. 41, 1–7.

Santangelo, C., Varì, R., Scazzocchio, B., Benedetto, R., Filesi, R., Masella, R., 2007. Polyphenols, intracellular signaling and inflammation. Ann. Ist. Super Sanità. 43, 394–405.

Sehgal, S., Gupta, V., Gupta, R., Saraf, S.A., 2011. Analgesic and antipyretic activity of *Mimusops elengi* L. (Bakul) leaves. Pharmacologyonline 3, 1–6.

Sen, S., Sahu, N.P., Mahato, S.B., 1995. Pentacyclic triterpenoids from *Mimusops elengi*. Phytochemistry 38, 205–207.

Shahat, A.A., Ismail, S.I., Hammouda, F.M., Azzam, S.A., Lemière, G., De Bruyne, T., De Swaef, S., Pieters, L., Vlietinck, A., 1998. Anti-HIV activity of flavonoids and proanthocyanidins from *Crataegus sinaica*. Phytomedicine. 5, 133–136.

Shahwar, D. and Raza, M.A., 2012. Antioxidant potential of phenolic extracts of Mimusops elengi. Asian Pac. J. Trop. Biomed. 547–550.

Sharma, A., Sati, S.C., Sati, O.P., Sati, D.M., Kothiyal, S.K., 2011. Chemical constituents and bioactivity of genus *Sapindus*. IJRAP. 2, 403–409.

Singh, D.D., Chitra, G., Singh, I.P., Bhutani, K.K., 2005. Immunostimulatory compounds from *Vitex negundo*. Indian J. Chem. 44B, 1288–1290.

Singh, I.P., Bharate, S.B., Bhutani, K.K., 2005. Anti-HIV natural products. Current Science 89, 269–282.

Suedee A, Tewtrakul S, Panichayupakaranant P. Anti-HIV-1 integrase activity of Thai medicinal plants. RGJ Seminar Series LXXXIII: Natural resourses and management for sustainable utilization. 50, Seminar room, Faculty of science, Prince of Songkla University. 31st August, 2011.

Suprapta, D.N., Suwari, I.G.A.N.A., Arya, N., Ohsawa, K., 2002. *Pometia pinnata* leaves extract to control late blight disease in potato. ISSAAS. 8, 31–36.

Tan, P.W., Tan, C.P., Ho, C.W. 2011. Antioxidant properties: Effect of solid-to-solvent ratio in on antioxidant compounds and capacities of Pegaga (Centella asiatica). Int. Food Res. J. 18, 557–562.

Tewtrakul, S., Miyashiro, H., Hattori, M., Yoshinaga, T., Fujiwara, T., Tomimori, T., Kizu, H., Miyaichi, Y., 2001. Inhibitory effects of flavonoids on human immunodeficiency virus type‑1 integrase. J. Trad. Med. 18, 229–238.

Tewtrakul, S., Nakamura, N., Hattori, M., Fujiwara, T. Supavita, T., 2002. Flavanone and flavonol glycosides from the leaves of *Thevetia peruviana* and their HIV-1 reverse transcriptase and HIV‑1 integrase inhibitory activities. Chem. Pharm. Bull. 50, 630–635.

Tewtrakul, S., Miyashiro, H., Nakamura, N., Hattori, M., Kawahata, T., Otake, T., Yoshinaga, T., Fujiwara, T., Supavita, T., Yuenyongsawad, S., Rattanasuwan, P. Dej-Adisai, S., 2003. HIV‑1 integrase inhibitory substances from *Coleus parvifolius*. Phytother. Res. 17, 232–239.

Tewtrakul, S., Itharat, A. Rattanasuwan, P., 2006. Anti‑HIV-1 protease and HIV‑1 integrase activities of Thai medicinal plants known as Hua‑Khao‑Yen. J. Ethnopharmacol. 105, 312–315.

Tewtrakul, S., Subhadhirasakul, S., Kummee, S., 2006. Anti‑HIV-1 integrase activity of medicinal plants used as self medication by AIDS patients. Songklanakarin J. Sci.Technol. 31, 785–790.

Tewtrakul, S., Subhadhirasakul, S., Cheenpracha, S., Karalai, C., 2007. HIV-1 protease and HIV-1 integrase inhibitory substances from *Elipta prostrata*. Phytother. Res. 21, 1092–1095.

Thomson, L.A.J. and Thaman, R.R., 2006. *Pometia pinnata* (tava): Species Profiles for Pacific Island Agroforestry (www.traditionaltree.org) ver 2.1, 1–17.

U.S. Global Health Policy., 2011. The Global HIV/AIDS Epidemic. The Henry J. Kaiser Family Foundation. USA. pp. 1–2.

Vink, C., Banks, M., Bethell, R., Plasterk, R.H.A., 1994. A high-throughput non-radioactive plate assay for activity of human immunodeficiency virus integrase protein. Nucleic Acid Res. 22, 433–437.

Voutquenne, L., Guinot, P., Thoison, O., Sevenet, T., Lavaud, C., 2003. Olealonic glycoside from *Pometia ridleyi*. Phytochemistry 64, 781–789.

Weiss, R.A., 2003. HIV and AIDS in relation to other pandemics. EMBO. Rep. 4, S1–S14.

Xu, X., Xie, H., Wang, Y., Wei, X., 2010. A-Type proanthocyanidins from lychee seeds and their antioxidant and antiviral activities. J Agric Food Chem. 58, 11667–11672.

Yan, M.M., Liu, W., Fu, Y.J., Zu, Y.G., Chen, C.Y., Luo, M., 2010. Optimisation of the microwave-assisted extraction process for four main astragalosides in Radix Astragali. Food Chem. 119, 1663–1670.

Zhang, B., Yang, R., Liu, C.Z., 2008. Microwave-assisted extraction of chlorogenic acid from flower buds of Lonicera japonica Thunb. Sep. Purif. Technol. 62, 480–483.

Zhang, L.L. and Lin, Y.M., 2008. HPLC, NMR and MALDI-TOF MS Analysis of condensed tannins from *Lithocarpus glaber* leaves with potent free radical scavenging activity. Molecules. 13, 2986–2997.

Zuo, Y., Chen, H., Deng, Y., 2002. Simultaneous determination of catechins, caffeine and gallic acids in green, Oolong, black and pu-erh tea using HPLC with a photodiote array detector. Talanta. 57, 307–316.